TECHNICAL REPORT STANDARD TITLE PAGE

1. Report No.	2. Government Accession No.	3. Recipient's Catalog No.
FHWA/TX-87/404-1F		

4. Title and Subtitle	5. Report Date
DEVELOPMENT OF NEW GUARDRAIL END TREATMENTS	June 1988
	6. Performing Organization Code
7. Author(s) Dean L. Sicking, Asif B. Qureshy, Roger P. Bligh, Hayes E. Ross, Jr., and C. E. Buth	8. Performing Organization Report No. Research Report 404-1F
9. Performing Organization Name and Address Texas Transportation Institute Texas A&M University College Station, Texas 77843	10. Work Unit No. 11. Contract or Grant No. Research Study 2-8-86-404
12. Sponsoring Agency Name and Address Texas State Department of Highways and Public Transportation Transportation Planning Division P. O. Box 5051, Austin, Texas 78763	13. Type of Report and Period Covered Final Report Sept. 1985 - Aug. 1987 14. Sponsoring Agency Code

15. Supplementary Notes

Research performed in cooperation with FHWA.

16. Abstract

This report describes the development of two new end treatments for W-beam guardrail. The first design, called the "split rail end treatment," consists of weakened W-beam segments, with slots cut along the length of the rail to reduce the buckling strength of the rail. The end of the rail is flared and anchored with standard "breakaway-cable-terminal" hardware. The split rail design was crash tested and shown to be in compliance with nationally recognized impact performance standards. The second design, called the "guardrail extruder terminal," consists of a device that, when struck, causes the W-beam to be flattened and projected in front of the impacting vehicle and behind the guardrail. Vehicular energy is dissipated in the process, resulting in a uniform, controlled deceleration of the vehicle. The guardrail extruder terminal was crash tested and shown to be in compliance with nationally recognized impact performance standards.

Of the two designs, the guardrail extruder terminal offers the greatest improvement in comparison to present guardrail end treatments. It is advantageous in terms of cost, impact performance, and design.

17. Key Words	18. Distribution Statement
Guardrail, End, Treatment, Terminal, Crash, Test, Safety, Traffic, Barrier	No restriction. This document is available to the public through the National Technical Information Service 5285 Port Royal Road Springfield, VA 22161

19. Security Classif. (of this report)	20. Security Classif. (of this page)	21. No. of Pages	22. Price
Unclassified	Unclassified	244	

Form DOT F 1700.7 (8-69)

DEVELOPMENT OF NEW GUARDRAIL END TREATMENTS

by

Dean L. Sicking
Assistant Research Engineer

and

Asif B. Qureshy
Engineering Research Assistant

and

Roger P. Bligh
Engineering Research Assistant

and

Hayes E. Ross, Jr.
Research Engineer

and

C. E. Buth
Research Engineer

Research Report 404-1F

on

Research Study No. 2-8-86-404
New Guardrail End Treatment

Sponsored by

Texas State Department of Highways and Public Transportation

in cooperation with

The U.S. Department of Transportation
Federal Highway Administration

June 1988

Texas Transportation Institute
Texas A&M University
College Station, Texas

METRIC CONVERSION FACTORS

Approximate Conversions to Metric Measures

Symbol	When You Know	Multiply by	To Find	Symbol
		LENGTH		
in	inches	*2.5	centimeters	cm
ft	feet	30	centimeters	cm
yd	yards	0.9	meters	m
mi	miles	1.6	kilometers	km
		AREA		
in^2	square inches	6.5	square centimeters	cm^2
ft^2	square feet	0.09	square meters	m^2
yd^2	square yards	0.8	square meters	m^2
mi^2	square miles	2.6	square kilometers	km^2
	acres	0.4	hectares	ha
		MASS (weight)		
oz	ounces	28	grams	g
lb	pounds	0.45	kilograms	kg
	short tons (2000 lb)	0.9	tonnes	t
		VOLUME		
tsp	teaspoons	5	milliliters	ml
Tbsp	tablespoons	15	milliliters	ml
fl oz	fluid ounces	30	milliliters	ml
c	cups	0.24	liters	l
pt	pints	0.47	liters	l
qt	quarts	0.95	liters	l
gal	gallons	3.8	liters	l
ft^3	cubic feet	0.03	cubic meters	m^3
yd^3	cubic yards	0.76	cubic meters	m^3
		TEMPERATURE (exact)		
°F	Fahrenheit temperature	5/9 (after subtracting 32)	Celsius temperature	°C

*1 in = 2.54 (exactly). For other exact conversions and more detailed tables, see NBS Misc. Publ. 286, Units of Weights and Measures, Price $2.25, SD Catalog No. C13.10:286.

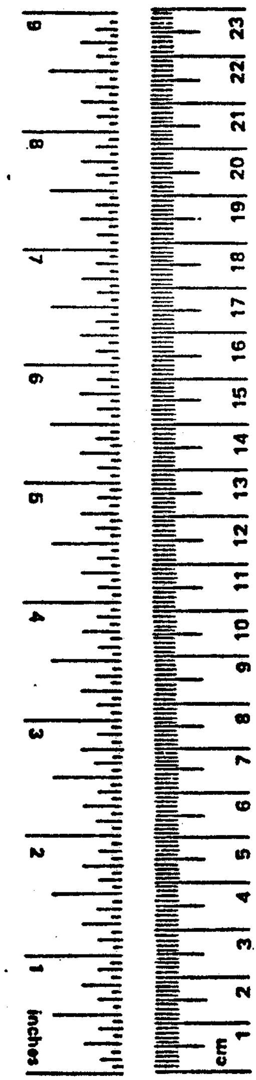

Approximate Conversions from Metric Measures

Symbol	When You Know	Multiply by	To Find	Symbol
		LENGTH		
mm	millimeters	0.04	inches	in
cm	centimeters	0.4	inches	in
m	meters	3.3	feet	ft
m	meters	1.1	yards	yd
km	kilometers	0.6	miles	mi
		AREA		
cm^2	square centimeters	0.16	square inches	in^2
m^2	square meters	1.2	square yards	yd^2
km^2	square kilometers	0.4	square miles	mi^2
ha	hectares (10,000 m^2)	2.5	acres	
		MASS (weight)		
g	grams	0.035	ounces	oz
kg	kilograms	2.2	pounds	lb
t	tonnes (1000 kg)	1.1	short tons	
		VOLUME		
ml	milliliters	0.03	fluid ounces	fl oz
l	liters	2.1	pints	pt
l	liters	1.06	quarts	qt
l	liters	0.26	gallons	gal
m^3	cubic meters	35	cubic feet	ft^3
m^3	cubic meters	1.3	cubic yards	yd^3
		TEMPERATURE (exact)		
°C	Celsius temperature	9/5 (then add 32)	Fahrenheit temperature	°F

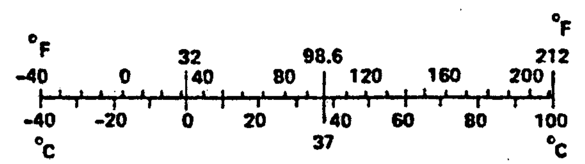

DISCLAIMER

The contents of this report reflect the views of the authors who are responsible for the opinions, findings, and conclusions presented herein. The comments do not necessarily reflect the official views or policies of the Federal Highway Administration. This report does not constitute a standard, specification, or regulation.

KEY WORDS

Guardrail, End, Treatment, Terminal, Crash, Test, Safety, Traffic, Barrier

ACKNOWLEDGEMENTS

This research study was conducted under a cooperative program between the Texas Transportation Institute (TTI), the Texas State Department of Highways and Public Transportation (SDHPT), and the Federal Highway Administration (FHWA). Harold Cooner and Mark Marek of the SDHPT worked closely with the researchers and their comments and suggestions are appreciated.

IMPLEMENTATION STATEMENT

The "guardrail extruder terminal" and "split rail terminal" developed in this study are recommended for immediate incorporation into the SDHPT standard specifications. Field performance of the new designs should be monitored to identify any potential problems with their construction or safety performance.

ABSTRACT

This report describes the development of two new end treatments for W-beam guardrail. The first design, called the "split rail end treatment," consists of weakened W-beam segments, with slots cut along the length of the rail to reduce the buckling strength of the rail. The end of the rail is flared and anchored with standard "breakaway-cable-terminal" hardware. The split rail design was crash tested and shown to be in compliance with nationally recognized impact performance standards. The second design, called the "guardrail extruder terminal," consists of a device that, when struck, causes the W-beam to be flattened and projected in front of the impacting vehicle and behind the guardrail. Vehicular energy is dissipated in the process, resulting in a uniform, controlled deceleration of the vehicle. The guardrail extruder terminal was crash tested and shown to be in compliance with nationally recognized impact performance standards.

Of the two designs, the guardrail extruder terminal offers the greatest improvement in comparison to present guardrail end treatments. It is advantageous in terms of cost, impact performance, and design.

TABLE OF CONTENTS

LIST OF FIGURES

Figure		Page
B-16	VEHICLE BEFORE AND AFTER TEST SR-2	B-19
B-17	SPLIT RAIL END TREATMENT BEFORE TEST SR-3	B-21
B-18	SPLIT RAIL END TREATMENT AFTER TEST SR-3	B-22
B-19	VEHICLE BEFORE AND AFTER TEST SR-3	B-23
B-20	SPLIT RAIL END TREATMENT BEFORE TEST SR-4	B-24
B-21	SPLIT RAIL END TREATMENT AFTER TEST SR-4	B-25
B-22	VEHICLE BEFORE AND AFTER TEST SR-4	B-26
B-23	SPLIT RAIL END TREATMENT BEFORE TEST SR-5	B-28
B-24	SPLIT RAIL END TREATMENT AFTER TEST SR-5	B-29
B-25	VEHICLE BEFORE AND AFTER TEST SR-5	B-30
B-26	SPLIT RAIL END TREATMENT BEFORE TEST SR-6	B-31
B-27	SPLIT RAIL END TREATMENT AFTER TEST SR-6	B-32
B-28	VEHICLE BEFORE AND AFTER TEST SR-6	B-33
C-1	VEHICLE ANGULAR DISPLACEMENTS FOR TEST MB-1	C-2
C-2	VEHICLE ANGULAR DISPLACEMENTS FOR TEST MB-2	C-3
C-3	VEHICLE ANGULAR DISPLACEMENTS FOR TEST MB-3	C-4
C-4	VEHICLE ANGULAR DISPLACEMENTS FOR TEST MB-4	C-5
C-5	VEHICLE ANGULAR DISPLACEMENTS FOR TEST MB-5	C-6
C-6	VEHICLE ANGULAR DISPLACEMENTS FOR TEST MB-6	C-7
C-7	VEHICLE ANGULAR DISPLACEMENTS FOR TEST MB-7	C-8
C-8	VEHICLE ANGULAR DISPLACEMENTS FOR TEST 9429A-1	C-9
C-9	VEHICLE ANGULAR DISPLACEMENTS FOR TEST 9429A-2	C-10
C-10	VEHICLE ANGULAR DISPLACEMENTS FOR TEST SR-1	C-11
C-11	VEHICLE ANGULAR DISPLACEMENTS FOR TEST SR-2	C-12
C-12	VEHICLE ANGULAR DISPLACEMENTS FOR TEST SR-3	C-13
C-13	VEHICLE ANGULAR DISPLACEMENTS FOR TEST SR-4	C-14
C-14	VEHICLE ANGULAR DISPLACEMENTS FOR TEST SR-5	C-15
C-15	VEHICLE ANGULAR DISPLACEMENTS FOR TEST SR-6	C-16
D-1	SEQUENTIAL PHOTOGRAPHS FOR TEST MB-1	D-2
D-2	SEQUENTIAL PHOTOGRAPHS FOR TEST MB-2	D-4
D-3	SEQUENTIAL PHOTOGRAPHS FOR TEST MB-3	D-6
D-4	SEQUENTIAL PHOTOGRAPHS FOR TEST MB-4	D-8
D-5	SEQUENTIAL PHOTOGRAPHS FOR TEST MB-5	D-10
D-6	SEQUENTIAL PHOTOGRAPHS FOR TEST MB-6	D-12
D-7	SEQUENTIAL PHOTOGRAPHS FOR TEST MB-7	D-15
D-8	SEQUENTIAL PHOTOGRAPHS FOR TEST 9429A-1	D-18
D-9	SEQUENTIAL PHOTOGRAPHS FOR TEST 9429A-2	D-20
D-10	SEQUENTIAL PHOTOGRAPHS FOR TEST SR-1	D-22
D-11	SEQUENTIAL PHOTOGRAPHS FOR TEST SR-2	D-25
D-12	SEQUENTIAL PHOTOGRAPHS FOR TEST SR-3	D-28
D-13	SEQUENTIAL PHOTOGRAPHS FOR TEST SR-4	D-30
D-14	SEQUENTIAL PHOTOGRAPHS FOR TEST SR-5	D-33
D-15	SEQUENTIAL PHOTOGRAPHS FOR TEST SR-6	D-36
E-1	GUARDRAIL EXTRUDER TERMINAL CONSTRUCTION DRAWINGS	E-2
E-2	INITIAL SPLIT RAIL END TREATMENT DESIGN	E-22
E-3	FINAL SPLIT RAIL END TREATMENT DESIGN	E-23

LIST OF TABLES

I. INTRODUCTION

Highway engineers have been searching for many years to find a safe and economical method to terminate strong post W-beam barriers. Early W-beam barriers were constructed with an untreated standup end. These untreated guardrail ends were found to be capable of piercing through impacting vehicles. In an effort to mitigate the hazard associated with guardrail ends, engineers with the Texas State Department of Highways and Public Transportation developed the "Texas Twist" whereby the guardrail end was twisted and sloped to the ground. Although this end treatment effectively solved the problem of guardrails spearing impacting vehicles, it has been shown to have the potential for causing some impacting vehicles to roll over (1,2).

In an effort to solve problems associated with the Texas Twist, researchers developed the "Floppy End", a sloped guardrail end treatment that was designed to be pushed down by vehicles impacting the sloped barrier section (3). Although this end treatment appeared to exhibit somewhat improved impact performance, it proved to be a maintenance problem since the barrier end was frequently knocked down by roadside mowing activities. Further efforts to refine the floppy end technique have solved some of its maintenance problems (4,5). However, the end treatment continues to exhibit a tendency to cause roll over during accidents involving small vehicles impacting the end of the barrier.

The Breakaway Cable Terminal (BCT) is a guardrail end treatment that has gained widespread acceptance across the country (6). BCT end treatments rely on the dynamic buckling of a flared section of guardrail to provide a mechanism for slowing impacting vehicles in a controlled manner. As a result the BCT is very sensitive to the way the barrier end is flared, and field experience has indicated that improper flare rates are frequently employed (7). Furthermore, even when installed correctly the BCT system has been shown to impart unacceptably high deceleration forces on mini-size vehicles (8).

An improved BCT design, the Eccentric Loader BCT (ELBCT), was recently developed and successfully crash tested with mini-size vehicles (9). Although this system should offer improved safety performance over the standard BCT, the flared barrier end remains a critical component of the design. Further, the ELBCT has several other important design details that may adversely affect end treatment performance if not installed correctly. Finally, the ELBCT requires significant new hardware that will raise the cost of this system.

The Sentre (10) and Vehicle Attenuator Terminal (VAT) (11) end treatments are proprietary guardrail terminals that have been introduced recently. While neither system has a great deal of service history, crash test results indicate that both terminals should perform well in the field. However, the proprietary nature and the complexity of the designs increase the cost of these end treatments to an unacceptable level. As a result, proprietary end treatment deployment has been limited to locations where impact probabilities are extremely high.

No economical guardrail end treatment system with adequate safety performance is currently available for use on a routine basis by highway agencies. The study reported herein was therefore undertaken to develop a new guardrail end treatment system that would provide adequate safety performance at a relatively low cost.

II. RESEARCH OBJECTIVES

Barrier end treatment safety standards (12) require that a guardrail terminal provide safe deceleration or controlled barrier penetration for vehicles impacting upstream from the beginning of the length of barrier need (LON) and barrier anchorage for redirecting vehicles impacting beyond the LON. Crash test experience has indicated that when a vehicle penetrates a barrier end at a high rate of speed, even small deceleration forces can throw the vehicle out of control, thereby increasing the probability of a rollover. Further, vehicles traveling behind a guardrail are likely to impact the hazard that the barrier was designed to shield. Thus it is desirable for an end treatment to provide impact attenuation to prevent high speed penetrations of the barrier end.

Experience with field installations of barrier end treatments has revealed that it is desirable to terminate guardrails along a tangent, thereby eliminating problems associated with terminating barriers on roadside slopes. Finally, if a guardrail terminal design is to be widely used it must be relatively inexpensive and simple to construct. Therefore, the primary objectives of the research report herein were to develop a guardrail end treatment design that could offer the following features; 1.) meet nationally recognized safety standards (12); 2.) inexpensive to install and maintain; 3.) perform safely when installed on a tangent section of guardrail; 4.) provide attenuation of vehicles impacting the end of the barrier; and 5.) simple to construct.

III. GUARDRAIL END TREATMENT DESIGN CONCEPTS

The primary design feature of a guardrail end treatment is the method for softening the hard point associated with the end of the longitudinal guardrail element. Some systems such as the Sentre and the VAT provide attenuation systems that redirect or stop impacting vehicles before reaching the hardpoint. This softening method is the most expensive approach to the end treatment problem and was therefore not strongly considered in the study described herein. Other systems slope the barrier end to the ground to eliminate all possibility of head-on impact with a guardrail end. This method of softening the barrier end was not considered due to the previously mentioned problems associated with rollovers resulting from sloped terminal designs. BCT end treatments utilize an unsupported, flared segment of guardrail to reduce the stiffness of the barrier hard point by reducing its dynamic buckling strength. Extensive testing and analysis of these systems has indicated that dynamic buckling of W-beam elements is very sensitive to a number of construction details and, therefore, this method of softening end impacts was rejected from consideration in the current development effort.

Primary emphasis was placed on the development of low cost end treatment concepts that would be simple to construct. In view of this emphasis, it was desirable to maintain a post and beam barrier system throughout the end treatment. Thus, the primary design feature of interest was a method for softening impacts with the end of a longitudinal rail element.

When a vehicle impacts the end of a longitudinal beam element, the beam must either fracture or buckle dynamically. The only method for inducing beam fracture is to incorporate a beam constructed from a brittle material such as a fiber reinforced plastic (FRP). Although this alternative may have some promise, the authors could not obtain the necessary cooperation from the FRP industry to properly evaluate its potential. Methods for reducing dynamic buckling of a beam element include increasing eccentricity in the beam, increasing the unsupported length of the element, and reducing the beam's section modulus. Extensive analysis of BCT designs has concentrated on the first two alternatives with little or no success. Therefore, concept development concentrated on methods for reducing the section modulus of the longitudinal rail element.

Flat-Plate

The simplest method for reducing a beam's section modulus is to reduce the depth of its cross-section. A flat steel plate has a very low section modulus and could be substituted for the W-beam in a stand-up BCT type end treatment. An 8 ga. high strength plate, 12 inches deep would offer the same tensile capacity as a 12 ga. W-beam. The buckling strength of such a flat plate would be less than 3 tenths of one percent of the buckling strength of standard W-beam guardrail. Thus, the buckling strength of a stand-up flat plate design would be too low and the end treatment would decelerate impacting vehicles at a very slow rate. As a result a flat plate end treatment would have to be flared off the roadway and allow vehicles impacting near the barrier end to penetrate the guardrail.

Split Rail

The section modulus of a standard W-beam guardrail can be greatly reduced by cutting longitudinal slots in the beam as illustrated in Figure 1. These slots would allow the W-beam to buckle as several small independent beam elements. A major advantage of this concept over the flat plate concept is that the buckling strength of the guardrail elements could be tuned to any desirable level by controlling the number and length of slots. Therefore, the concept could ideally be implemented in a straight terminal design, since the slotted guardrail elements could be designed to decelerate vehicles to a stop over a reasonable distance.

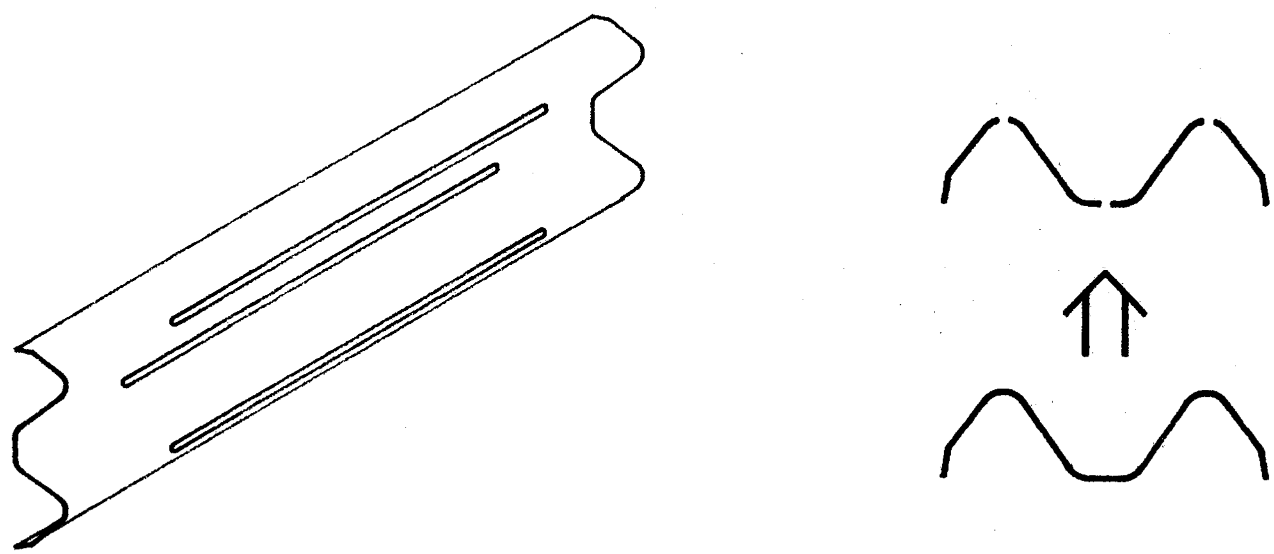

FIGURE 1. SPLIT RAIL CONCEPT.

Guardrail Extruder

The final concept for reducing guardrail hard point stiffness involved placing an extruder over the end of a straight W-beam guardrail section as shown in Figure 2. When struck by an automobile, the extruder would curl the W-beam around a circular arc away from the front of the impacting vehicle. Plastic deformation of the guardrail would dissipate impact energy and decelerate vehicles to a stop at an acceptable rate. The force required to bend the guardrail was estimated based on the energy required to form a plastic hinge in the W-beam and bend it approximately 90 deg. This preliminary analysis indicated that the extruder would require a minimum 7000 lb to extrude a 12 ga. W-beam. The guardrail element must not buckle in order for the extruder to perform as intended. The static buckling strength of a 12 ga. W-beam over a 6 ft. 3 in. post spacing was calculated to be 100 kips which was believed to be much more than the force necessary to extrude the W-beam.

Preliminary calculations indicated that all three of the concepts described above were mechanically feasible. However, unlike the flat plate design, both the split rail and guardrail extruder concepts have the potential for capturing impacting vehicles and could be used in a straight end treatment design. Therefore, since funding limitations precluded development of three different concepts, the latter two concepts were chosen for further development.

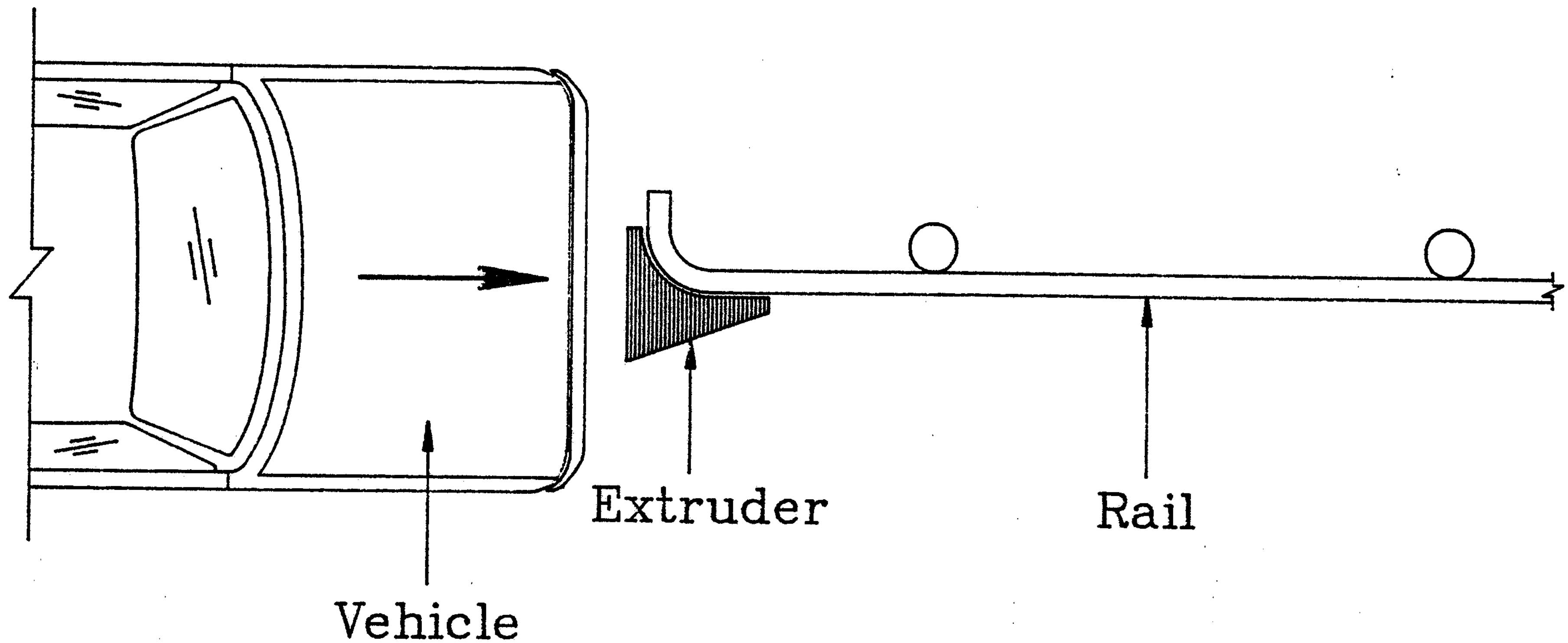

FIGURE 2. GUARDRAIL EXTRUDER CONCEPT.

IV. GUARDRAIL EXTRUDER TERMINAL DEVELOPMENT

Preliminary Development

As discussed above, the guardrail extruder must be designed to bend a W-beam element around a circular arc and direct the guardrail end away from the path of impacting vehicles. In addition, a method for developing the tensile strength of the W-beam guardrail had to be designed into the concept to provide redirection capacity. The BCT cable anchor system offers a standard hardware item that has been shown to be capable of developing adequate anchorage for a strong post W-beam guardrail system (6). However, this system involves bolting a heavy metal channel to the first guardrail element. If this anchoring system was to be employed, the metal channel would have to feed through the extruder.

The first extruder design, shown in Figure 3, involved an open chute with a plate bent into a circular arc to bend the guardrail away from the impacting vehicle. The back side of the extruder was left open to allow the BCT cable anchoring channel to feed through the device. Preliminary static testing revealed that, when a W-beam element was pushed into the extruder, it began to flatten on the edges and protrude out the open part of the extruder as shown in Figure 4. The deformed beam became a very deep channel with a highly increased section modulus and the force required to push the beam into the extruder rose rapidly. Constraint along the edges of the beam was believed to be a potential cause for this phenomenon and a second test was conducted after the sides of the channel had been removed. The W-beam deformed into the same deep channel section observed in previous testing and it was concluded that this concept could not be designed with an open extruder section.

The second extruder design, shown in Figure 5, involved two separate processes, a "squeezer" section and a "bender" section. The squeezer section was designed to flatten the W-beam section and thereby virtually eliminate any bending strength. The bender section would then bend the relatively flat W-beam around a small radius and direct it away from an impacting vehicle.

Static testing of the new concept was conducted in two phases. First a 24 in. long squeezer section was constructed that would reduce the depth of the W-beam from 3.25 in. to 1 in. A W-beam element was then forced through the squeezer in a static load - deflection test. As shown in Figure 6, a force of approximately 10,000 lb. was required to flatten the W-beam. A circular bender section with a 4.5 in radius was then added to the squeezer and the static test was repeated. Results of this test are also shown in Figure 6. As shown in this figure, the force required to extrude a 12 ga. W-beam varied from 9,000 to 13,000 lb. with an average value of 11,000 lb. These force levels were well below the maximum allowable constant

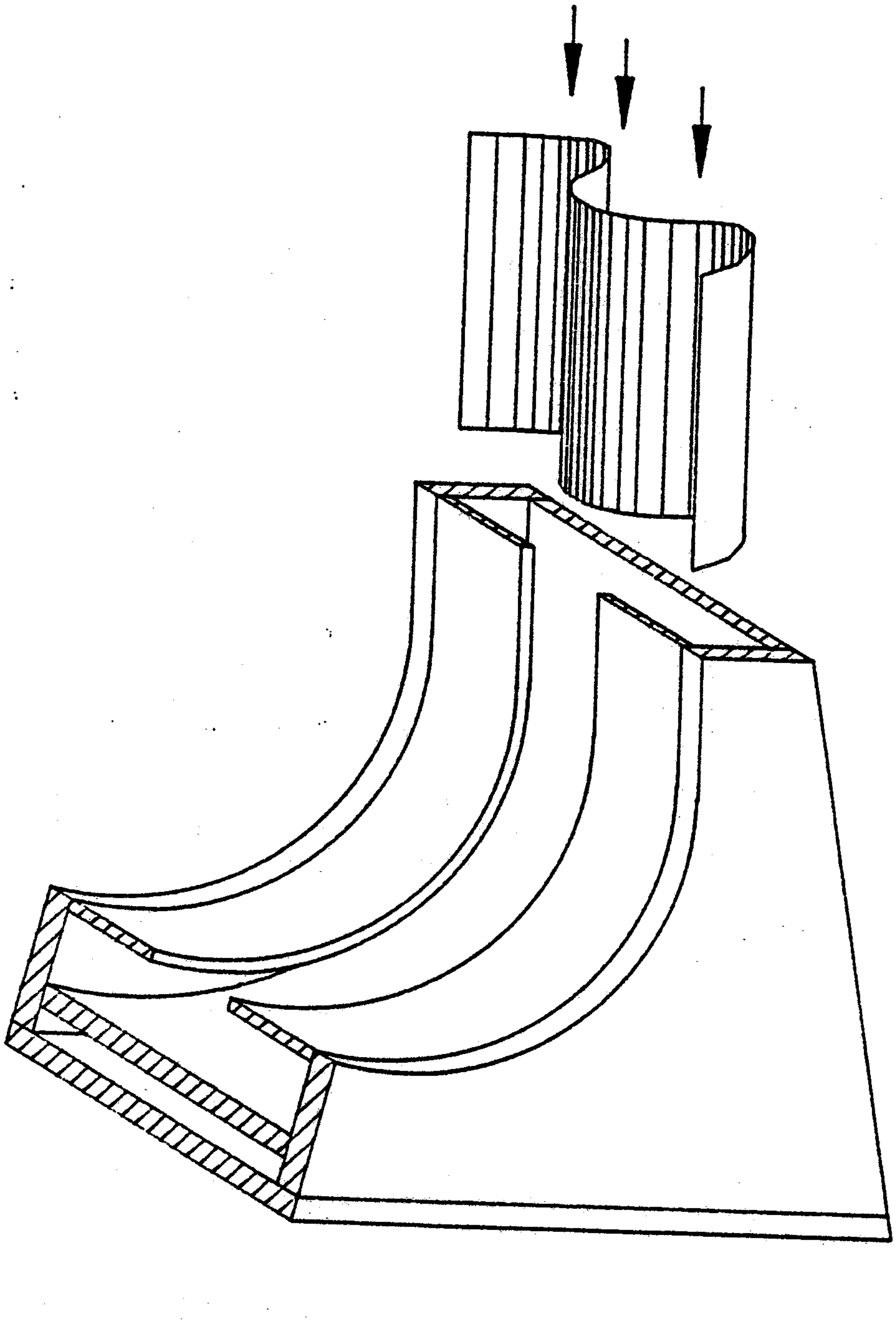

FIGURE 3. PRELIMINARY EXTRUDER DESIGN.

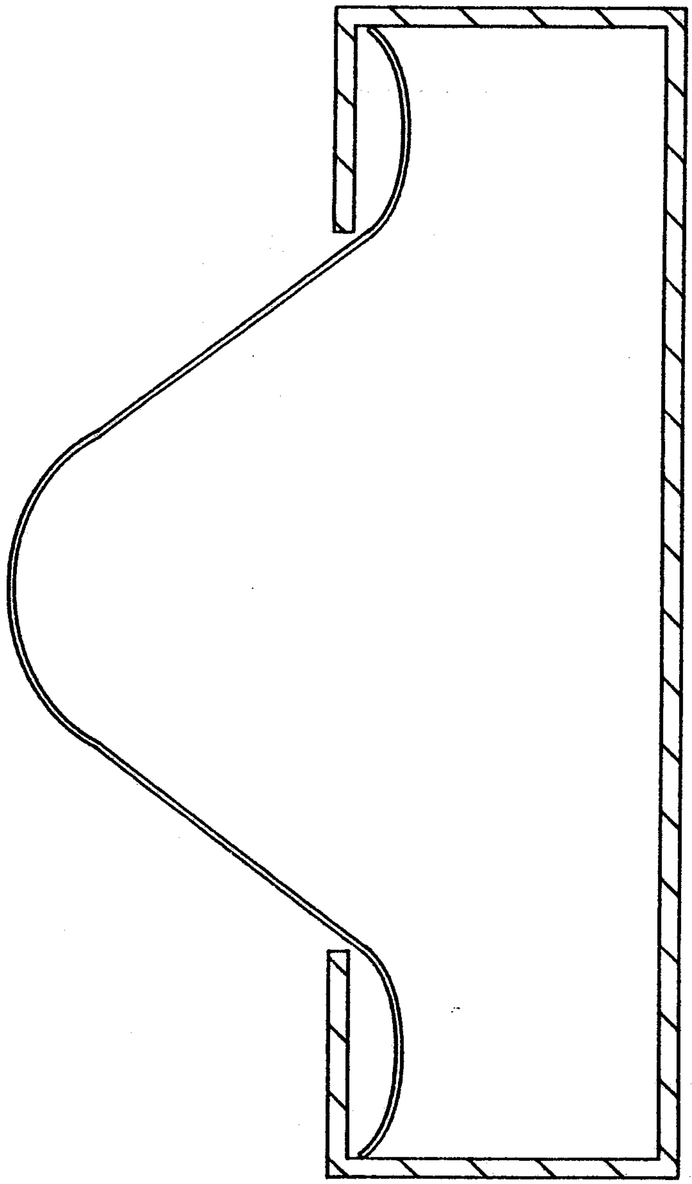

FIGURE 4. GUARDRAIL DEFORMATION PRELIMINARY EXTRUDER.

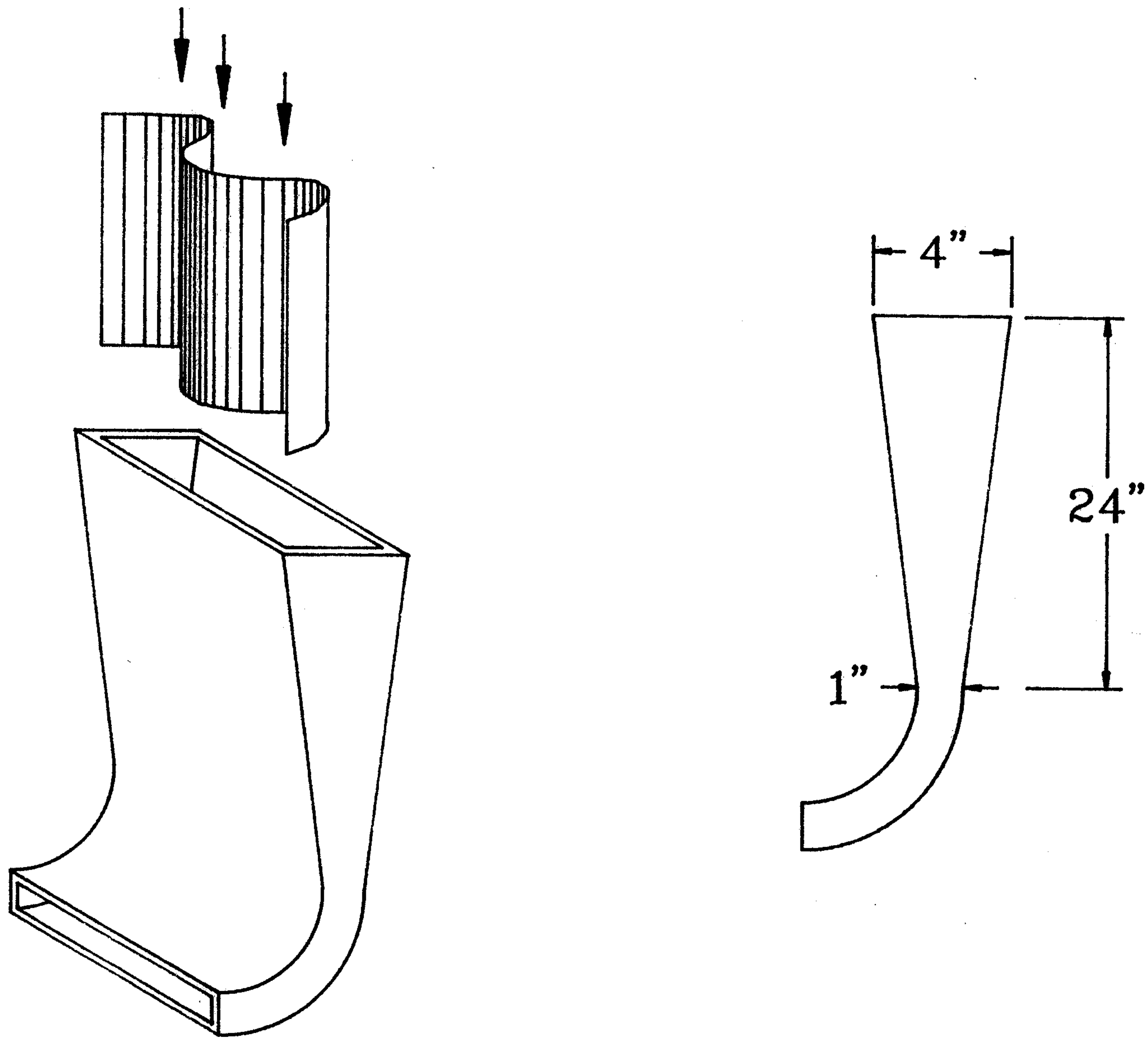

FIGURE 5. GUARDRAIL SQUEEZER AND BENDER

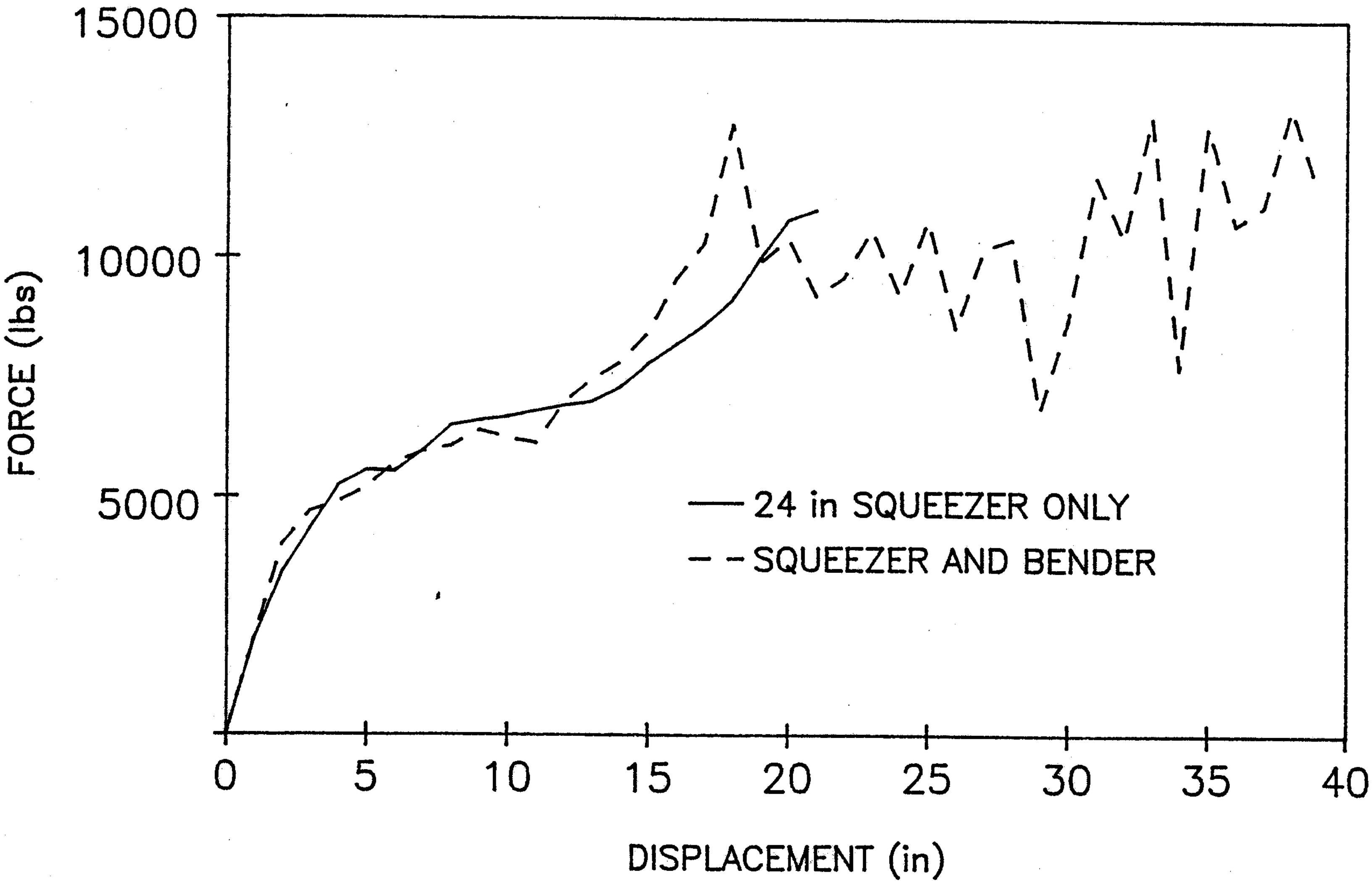

FIGURE 6. STATIC TESTS OF 24 INCH SQUEEZER AND BENDER.

deceleration force of 21,600 lb corresponding to 12 g's on an 1800 lb vehicle (12).

Preliminary Crash Tests

After determining that static extrusion forces were below maximum acceptable levels, a limited preliminary crash test program was undertaken to estimate dynamic extrusion forces. A heavy steel case was constructed around the extruder used in the static testing. A 20 in. x 24 in. steel plate was attached to the front of the extruder to distribute impact forces. Small steel angles were welded to the front of the impact plate to prevent impacting vehicles from sliding off the front of the extruder. The extruder was mounted on two thin wall steel tubes to support its weight and assure a proper mounting height.

The device was placed over the end of a standard Texas guardfence design as shown in Figure 7. Note that the extruder did not deform the end of the W-beam and the device was attached to the first post with 3/8 in. diameter lag screws. The W-beam rail was also attached to every second guardrail post with 3/8 in. diameter lag screws. Two crash tests were then conducted with full size automobiles impacting the extruder head-on at 35 and 45 mph. The extruder performed as intended and both vehicles were smoothly decelerated to a stop. Figure 8 shows the test vehicles and end treatments after the two tests.

Analysis of accelerometer data indicated that the extruder generated average deceleration forces of approximately 13,000 lb as it flattened the W-beam and curled it out of the vehicle's path. Figure 9 and Figure 10 show a plot of deceleration force versus vehicle travel for these two tests. Note that relatively high forces were generated when the extruder was initially impacted. Analysis of this phase of impact reveals that virtually all of the large initial impulse was attributable to the momentum transfer associated with accelerating the 350 lb. extruder from rest.

Secondary Extruder Development

Preliminary crash test results indicated that the guardrail extruder concept was mechanically feasible. Further development efforts then concentrated on optimizing the extruder design to enable it to perform adequately with both large and small vehicles. As noted above, the weight of the extruder used in the preliminary testing imparted a large momentum change on the test vehicles. Conservation of Momentum and Energy analyses indicated that a 350 lb. extruder, generating a constant force of 16,000 lb. would decelerate small vehicles at a rate slightly above the maximum recommended limit (12). Further, this analysis indicated that full size automobiles impacting at 60 mph might extrude as much as 50 feet of guardrail. Both of these problems could potentially be alleviated by reducing the weight of the extruder

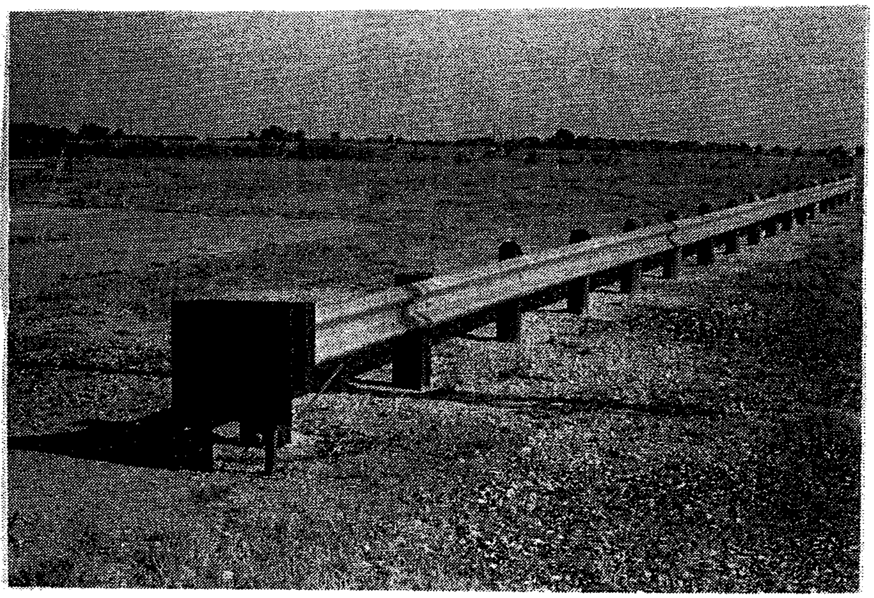

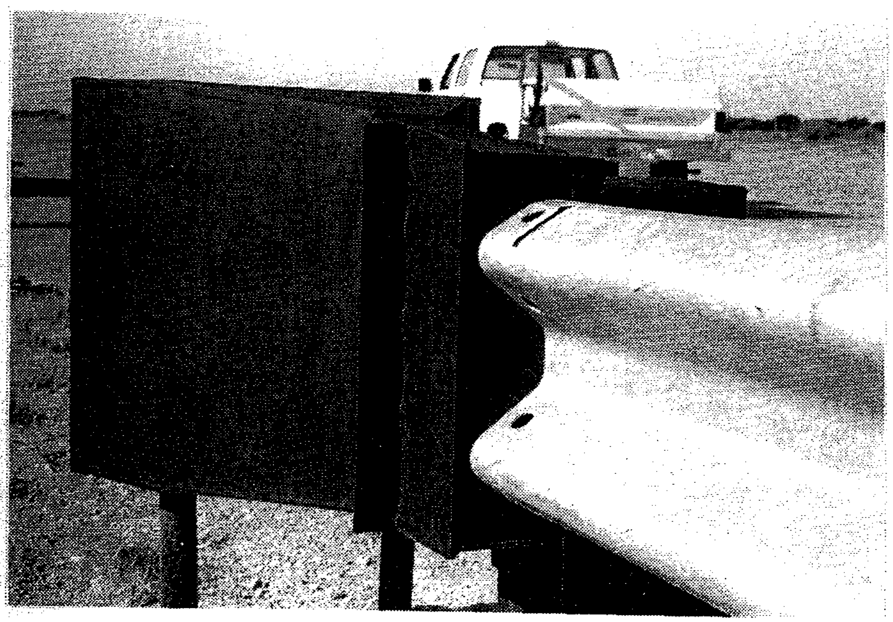

FIGURE 7. FIELD INSTALLATION OF GUARDRAIL EXTRUDER FOR PRELIMINARY TESTS.

FIGURE 8. VEHICLE AND INSTALLATION AFTER PRELIMINARY GUARDRAIL EXTRUDER TESTS.

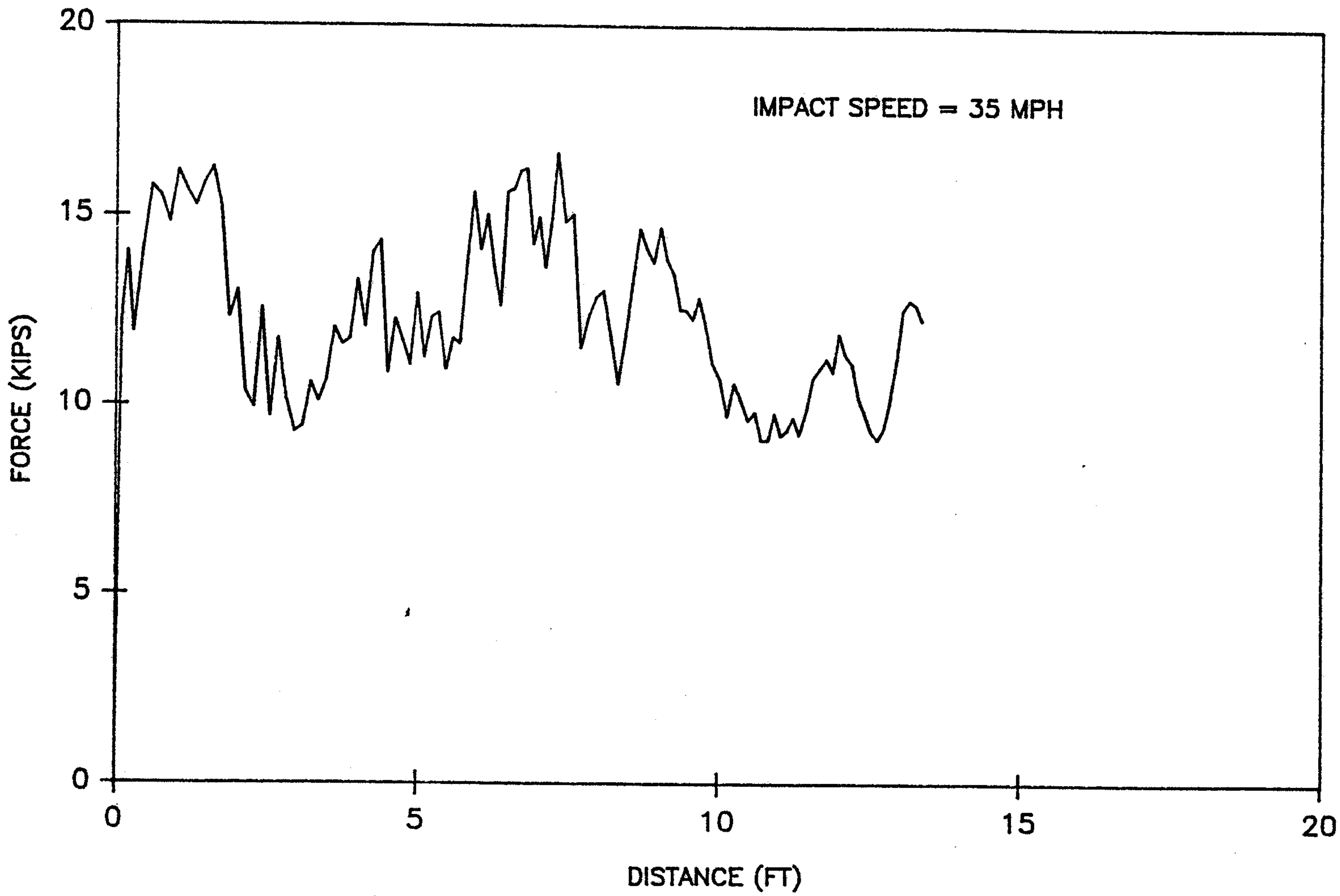

FIGURE 9. EXTRUDER FORCES MEASURED DURING TEST MBP-1

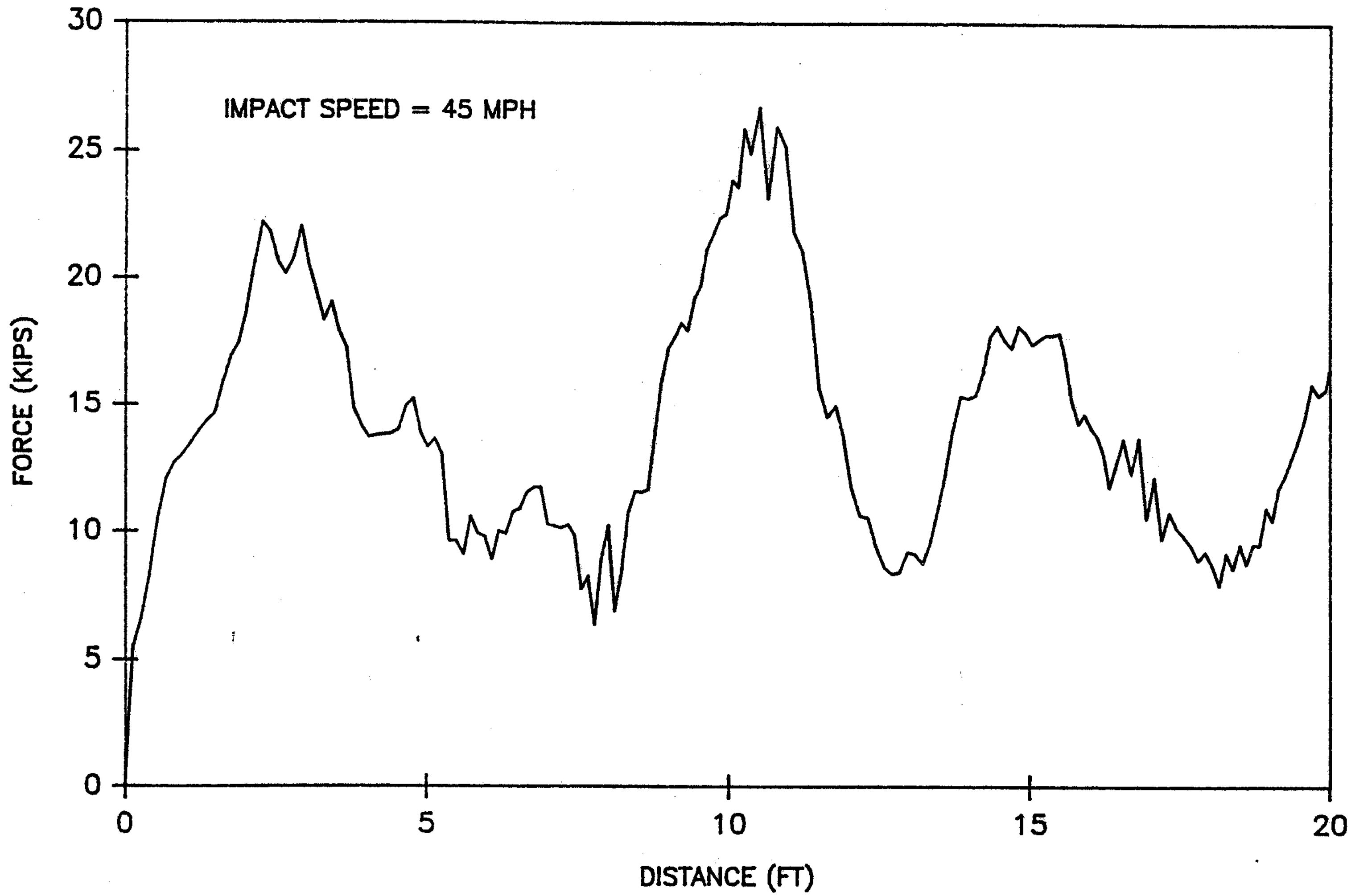

FIGURE 10. EXTRUDER FORCES MEASURED DURING TEST MBP-2

and increasing the extrusion force. Therefore, optimization efforts concentrated on these two design features.

Potential methods for increasing extrusion forces included reducing the length of the squeezer section and changing the radius of the bender section. Therefore a static testing program was undertaken to determine effects of reducing the squeezer section on static force - deflection characteristics. Squeezer sections of 18 in., 12 in., and 6 in. long were constructed. Tests of the 6 in. squeezer revealed that this squeezer design was unable to prevent large deformations of the squeezer. As a result, the 6 in long squeezer could not be tested successfully. The remaining devices were tested and results were plotted against previous squeezer tests as shown in Figure 11. Note that squeezer forces for all three devices fall into a very narrow band. This behavior was reinforced by visual observations that, after the W-beam started through a squeezer, it was only in contact with the device in the region near the bottom. Therefore it was concluded that the 12 in squeezer, the shortest squeezer successfully tested, would represent the best alternative for further development due to its light weight.

Note that forces generated during static squeezing tests were approximately 10,000 lb. This represents 90% of the 11 kip extrusion force measured during static extruder tests. Thus it was concluded that only a small percentage of the total extruder force could be attributed to the bender section and alternate bender radii were not investigated. However, further weight was cut out of the new extruder design by reducing the size of the striker plate to a 20 in. square. These modifications reduced the weight of the new extruder to 258 lb. Figure 12 shows the new extruder as it was first constructed.

Modified Cable Anchor

As discussed previously the BCT cable anchoring device requires a heavy steel channel to be bolted to the guardrail between the first and second posts. Since this device would not feed through the extruder, an alternate anchoring mechanism had to be developed. Any device firmly attached to the W-beam for anchoring purposes would likely jam the extruder under some conditions, thereby reducing the reliability of its performance. Therefore, an attachment mechanism had to be developed that would quickly release from the W-beam when impacted by the extruder.

A releasing cable attachment assembly was developed as shown in Figure 13. The releasing mechanism consisted of a 2x2x1/4 square structural steel tube with six wedge shaped lugs welded onto it. The wedge shaped lugs fit into small square holes cut into the W-beam and small protrusions on the front of the lugs lock the device onto the rail. When the guardrail is impacted on the side, the lugs transfer tensile forces into the steel tube which is attached to a standard BCT cable assembly. When the

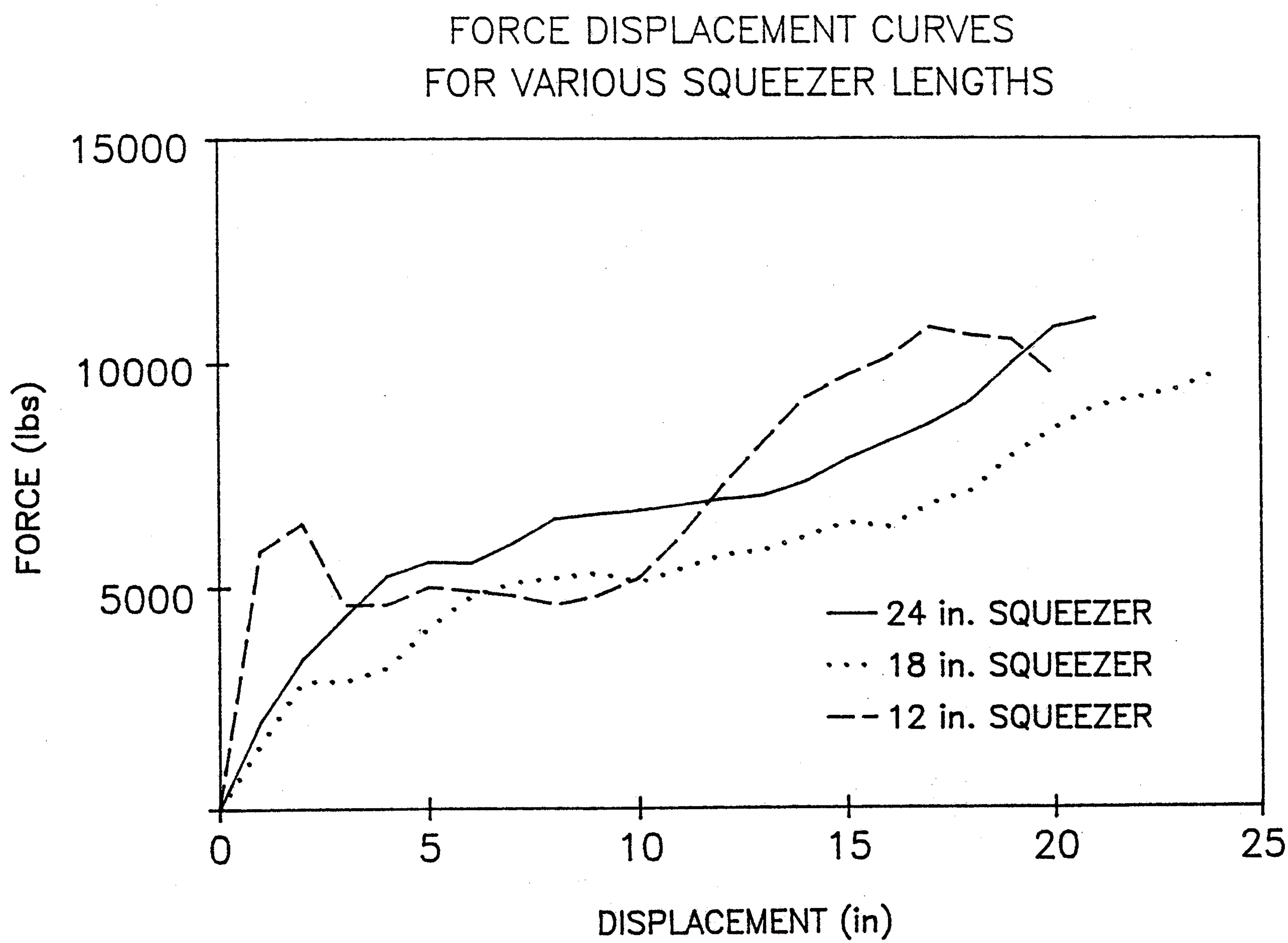

FIGURE 11. STATIC TESTS FOR VARIOUS SQUEEZER LENGTHS.

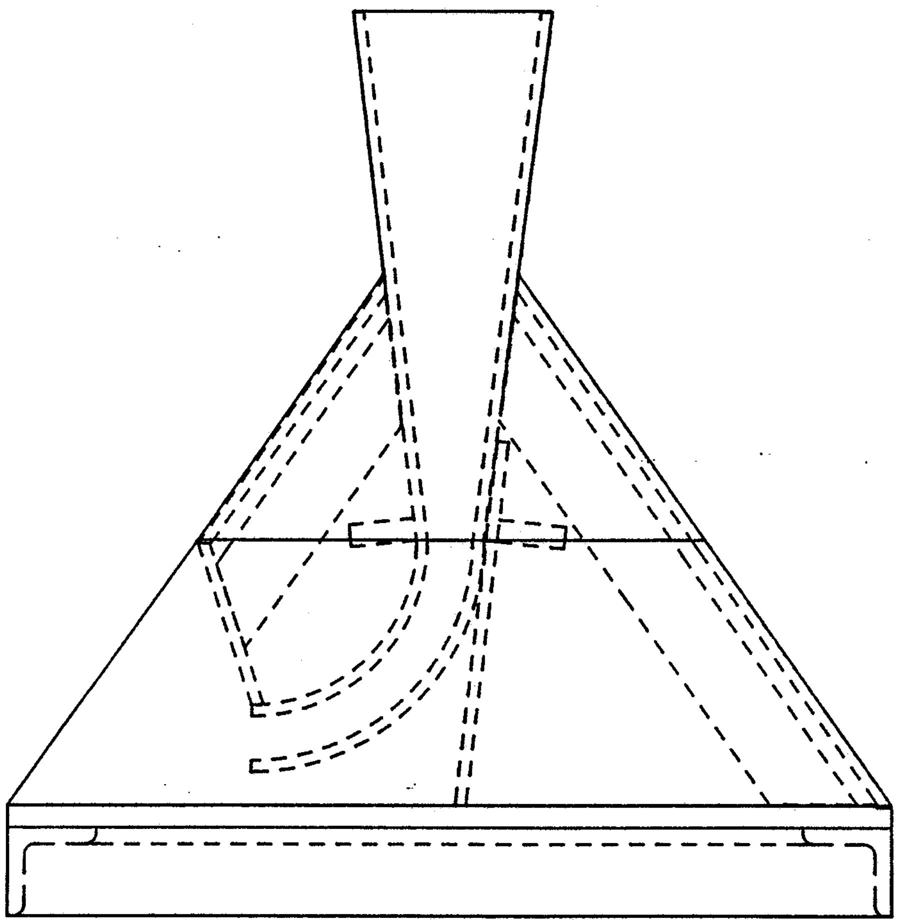

FIGURE 12. 12 INCH EXTRUDER DESIGN.

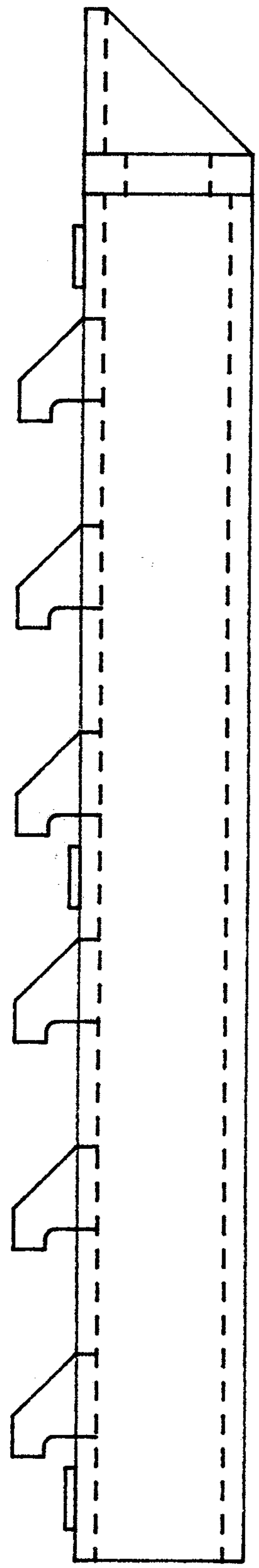

FIGURE 13. RELEASING CABLE ATTACHMENT
ASSEMBLY.

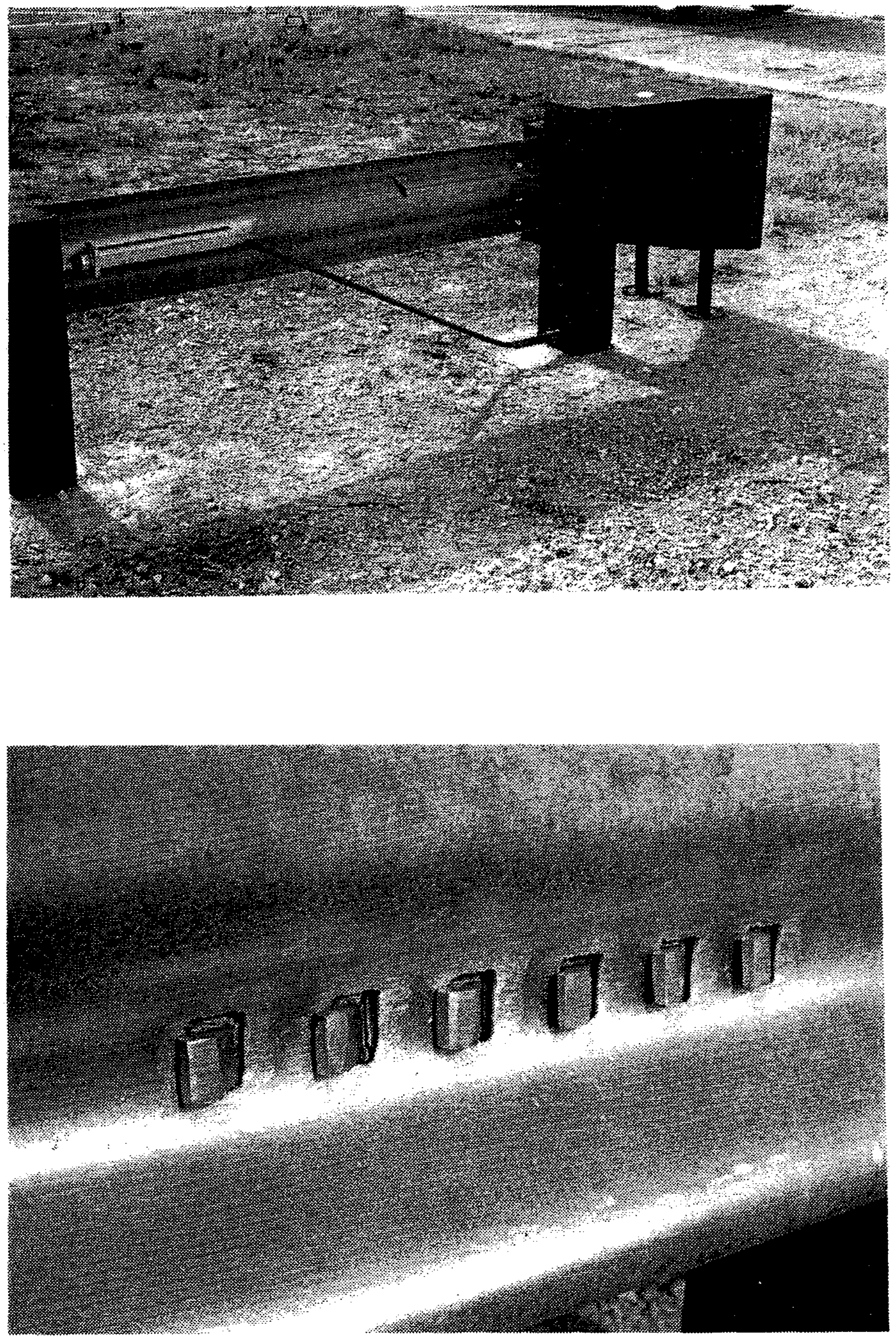

FIGURE 14. CABLE RELEASE MECHANISM.

extruder is impacted head-on, it breaks the first post and frees the upstream end of the cable assembly. When the extruder impacts the release mechanism, the wedge shaped lugs force it out of the holes in the W-beam. The W-beam can then continue to feed without any risk of jamming. Figure 14 shows the cable release mechanism.

Tests of the BCT cable anchor assembly indicated that it was capable of developing a 40 kip tensile load prior to failure (8). The new cable release mechanism was tested statically to determine its tensile capacity as shown in Figure 15. The release mechanism resisted a peak static load of 38 kips before the W-beam began to tear at the edges of the square holes. Observation of the holes in the test specimen revealed very jagged edges arising from torch cuts. Due to the small difference between the desired load capacity of 40 kips and the measured static load of 38 kips and the great reductions in stress concentration factors that could be achieved by punching the holes in the W-beam, it was concluded that the release mechanism would develop sufficient tensile capacity for redirection purposes.

Compliance Testing

Compliance testing of the guardrail extruder terminal was then undertaken. During the progress of the testing program, the prototype extruder exhibited a tendency to yaw or pitch to an extent that the guardrail would stop feeding into the device. A series of five full-scale crash tests, MB-1 through MB-5, and four design changes were completed before the problem was eliminated. A series of four successful compliance tests, MB-6, MB-7, 9429a-1, and 9429A-2, were then conducted. All nine crash tests are summarized in Table 1 and discussed briefly below. Each test is reported in greater detail in Appendix A. Angular displacement plots for each test are given in Appendix C, and sequential photographs are shown in Appendix D.

Test MB-1 - The basic design of the terminal at the start of testing is shown in Figure 16. Note that the first two posts were 6 in. x 8 in. wood posts set in a concrete foundation to facilitate break-away. The 12 in. extruder was mounted in such a way as to bend the guardrail away from the roadway and the new cable release assembly was installed to anchor the W-beam between the first and second posts. The splice between the first two guardrail segments was welded to prevent the extruder from becoming jammed on the splice bolts. All of the first nine posts, both rectangular and round, had 2 3/8 in. diameter holes drilled through their centers, parallel to the guardrail beam, both at the groundline and 18 in. below the surface. The holes at the ground line are intended to weaken the posts when embedded in stiff soils where the maximum bending moment during impact is near the ground surface. Holes drilled below the surface are intended to weaken the posts when embedded in soft soils where

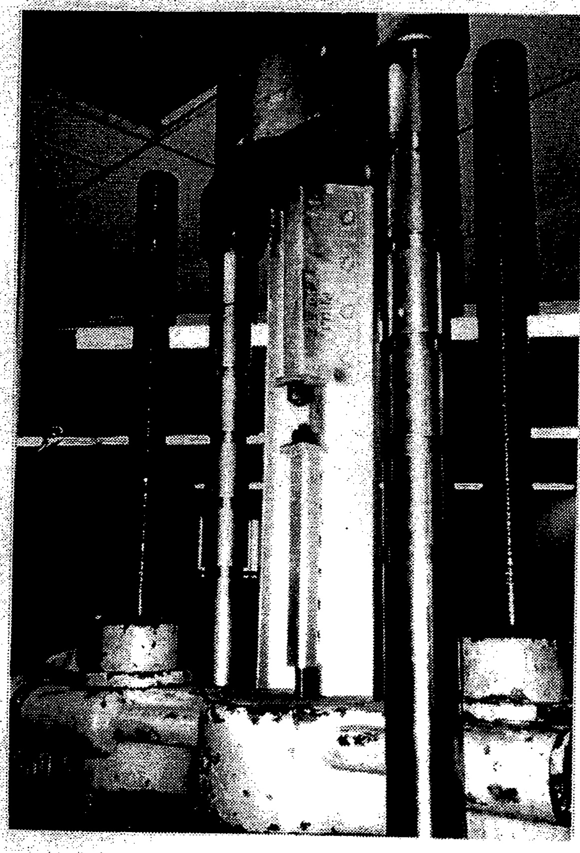

FIGURE 15. STATIC TEST SETUP FOR CABLE ATTACHMENT ASSEMBLY

TABLE 1. SUMMARY OF GUARDRAIL EXTRUDER TERMINAL CRASH TESTS.

TEST NO.	VEHICLE WEIGHT (lbs)	IMPACT CONDITIONS			INSTALLATION MODIFICATION	TEST RESULTS				COMMENTS
						OCCUPANT IMPACT VELOCITY		RIDEDOWN ACCELERATION		
		SPEED (mph)	ANGLE (deg)	OFFSET (in.)		LONG. (ft/sec)	LAT. (ft/sec)	LONG. (G's)	LAT. (G's)	
MB-1	4,500	60.6	0	0	Lag screws on posts 2,3,4; 12 in. Extruder	19.3	0	6.3	0	Vehicle penetrated behind barrier
MB-2	1,750	62.1	0	15	Bolted starting at post #2; 12 in. Extruder	35.1	0	14.2	0	Vehicle came close to rolling over
MB-3	1,955	59.8	0	15	No bolts till post #5; Extruder facing roadway; 12 in. Extruder	29.9	12.1	14.5	1.2	Vehicle rolled onto its side
MB-4	1,750	56.7	0	15	No bolts til post #5; 24 in. Extruder	32.3	0	11.9	0	Vehicle rolled onto its side
MB-5	1,800	59.0	0	15	Bolted starting at post #2; 24 in. Extruder with bearing angle	37.0	0	8.4	0	Vehicle rolled over through 180 degrees
MB-6	1,785	58.7	0	15	Fig. E1	29.0	12.5	15.5	2.1	Vehicle decelerated smoothly to a stop
MB-7	4,600	61.6	0	0	Fig. E1	19.8	0	8.2	0	Vehicle decelerated [illegible] stop
9429A-1	1,780	59.1	15.6	0	Fig. E1	15.9	17.0	1.4	10.3	Vehicle redirected smoothly
[illegible]	4,410	[illegible]	[illegible]	0	Fig. E1	[illegible]	[illegible]	[illegible]	[illegible]	[illegible]

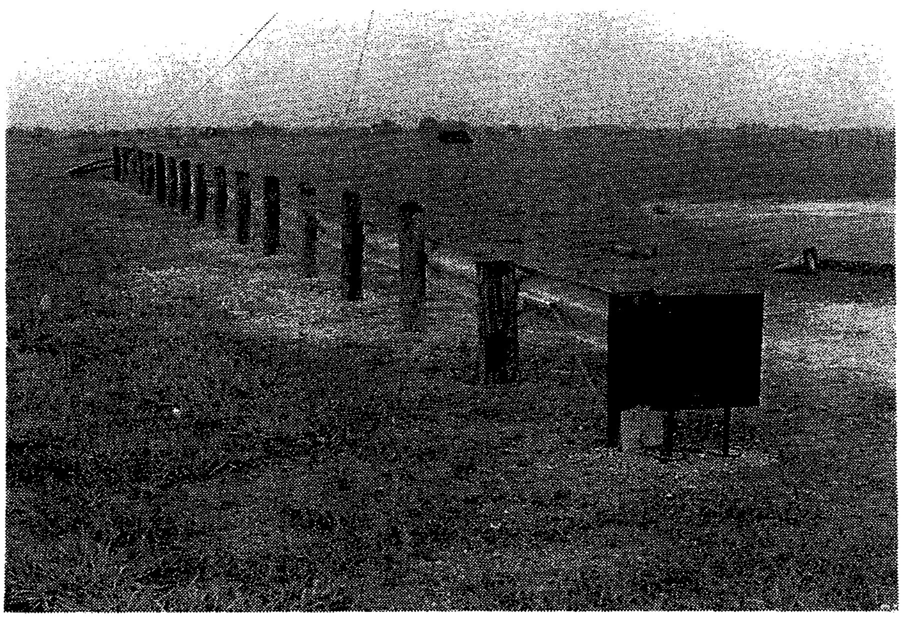

FIGURE 16. TEST INSTALLATION BEFORE
TEST MB-1.

the maximum bending moment during impact is approximately 18 in. below the groundline. These holes reduced the longitudinal bending strength by 54%, thereby reducing the impulse imparted to a vehicle impacting the terminal head-on. The holes do not significantly affect lateral bending strength and reduce it by only 6%. For the first test the guardrail was not attached to the first post and was attached to posts 2, 3, and 4 with 3/8 in. x 5 in. lag screws. All remaining posts had standard 5/8 in. diameter button head bolts with no washers.

One of the primary concerns about the extruder design was the distance that would be required to bring a full size automobile to a stop when impacted head-on at 60 mph. Test MB-1 examined this type of impact with the 12 in. extruder design. For this test, a 4500 lb. automobile impacted the extruder head-on at 60.6 mph. Upon impact the W-beam quickly popped off of the first 4 posts and the extruder and vehicle began to drift away from the guardrail posts. After extruding approximately 12 ft. of guardrail, the device yawed approximately 35 deg. and the W-beam stopped feeding properly. The test vehicle then pushed the extruder out of its path and continued along and behind the guardrail installation. High speed films indicated that the cable release mechanism performed very well in this test. Although the extruder was unable to stop the vehicle, all occupant severity measures were well within recommended limits and the test was considered a success. Figure 17 presents a summary of test MB-1.

Test MB-2 - The undesirable yawing of the extruder observed during test MB-1 was attributed to the long unsupported length of guardrail in front of the extruder at the time that the W-beam stopped feeding properly. Therefore the lag screws in posts 2, 3, and 4 were replaced with standard button head bolts. Furthermore, in an effort to simplify the design, the 6 in. x 8 in. wood post set in a concrete foundation was removed from the second post position. It was replaced with a standard 7 in. round wood post embedded in soil. The new post was weakened with 2 3/8 in. holes drilled at the ground line and 18 in. below the ground line as discussed previously.

Test MB-2 was then conducted to evaluate extruder performance for small car impacts. During this test a 1750 lb vehicle impacted the extruder head-on at 60 mph., offset 15 in. away from the roadway. It was believed that offsetting the vehicle in this manner would increase the probability of buckling the W-beam and the probability of the test vehicle yawing away from the guardrail end at a high rate and possibly rolling over.

Upon impact, the extruder began to yaw in a counterclockwise motion and the guardrail stopped feeding after approximately 6 ft. of extruder travel. The vehicle then impacted the second guardrail post which rotated in the soil without breaking. This rotation caused the right side of the vehicle to ride up the

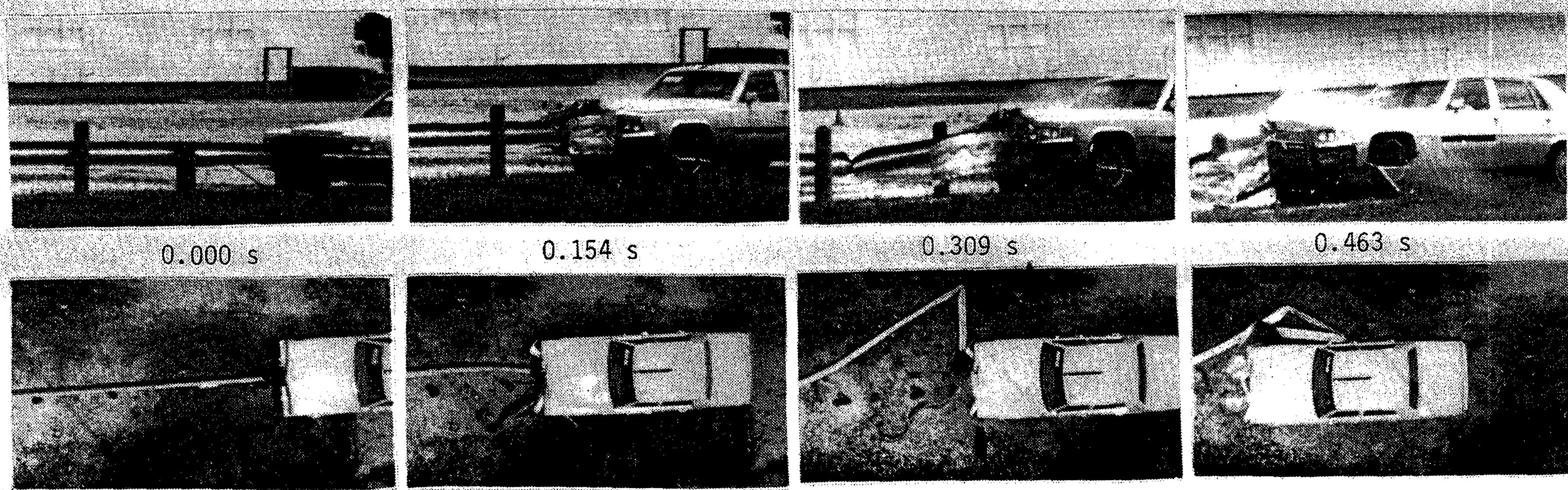

Test No.	2404-MB1
Date	5/12/87
Test Installation	Metal Bender End Treatment
Length of Installation	100 ft (3.5 m)
Vehicle	1978 Cadillac
Vehicle Weight	
Test Inertia	4,500 lb (2,043 kg)
Gross Static	4,670 lb (2,120 kg)
Vehicle Damage Classification	
TAD	12FR4
CDC	12FZEW2
Length of Rail Fed Through Bender	12.0 ft (3.7 m)

Impact Speed	60.6 mi/h (97.5 km/h)
Impact Angle	0 deg - center
Exit Speed	Not Available
Vehicle Accelerations (Max. 0.050-sec Avg)	
Longitudinal	-6.4 g
Lateral	2.1 g
Occupant Impact Velocity	
Longitudinal	19.3 ft/s (5.9 m/s)
Lateral	None
Occupant Ridedown Accelerations	
Longitudinal	-6.3 g
Lateral	No Contact

FIGURE 17. SUMMARY OF RESULTS FOR TEST MB-1.

inclined post, thereby inducing a high roll rate into the test vehicle. The vehicle then spun around the second post and rolled approximately 45 degrees before coming to rest behind the guardrail. Although occupant impact severity measures from this test were below maximum allowable limits (12), this test was considered to be only marginally successful due to the high roll angle achieved by the test vehicle. Further, the extruder was only effective for approximately 6 ft. and, therefore, the test vehicle was traveling at an undesirably high speed when it exited the terminal. A summary of test MB-2 is presented in Figure 18.

Test MB-3 - After the second test it became clear that the extruders effectiveness had to be improved. Degradation of extruder performance from the first to the second tests was attributed to a reduction in guardrail rotational flexibility associated with bolting the W-beam to posts 2, 3, and 4. Reduced rotational flexibility was hypothesized to be responsible for the formation of a plastic hinge at the mouth of the extruder at relatively low yaw angle. Formation of a plastic hinge in the guardrail increases beam depth to a point that the W-beam becomes wedged in the mouth of the extruder. Therefore, post bolts were again removed from the first 4 posts for subsequent testing. A wood block was bolted under the rail at the second post in order provide vertical support for the rail during side impacts. Further, a weakened 6 in x 8 in. rectangular wood post set in a concrete foundation was again placed at the second post position.

The extruder had exhibited a tendency to rotate counter-clockwise in all previous testing. It was believed that this tendency could be eliminated if the guardrail were bent toward the roadway rather than away from it. Thus, for test MB-3, the extruder was mounted to bend the W-beam toward the roadway. The terminal was tested under the same conditions as test MB-2. Figure 19 shows the test installation prior to test MB-3.

Upon impact the extruder immediately yawed counter-clockwise at a very high rate and the guardrail was extruded less than 2 ft. A high yaw moment was induced on the vehicle when the extruder stopped functioning properly and the test vehicle spun out and rolled over. Figure 20 gives a summary of test MB-3.

Preliminary analysis of test results indicated that forces required to extrude the W-beam were much higher than was observed in any previous testing. Static testing verified this finding and indicated that extrusion of the W-beam toward the roadway generated forces approximately 25% higher than extrusion away from the roadway. These results were somewhat surprising and are believed to be related to the manner in which the W-beam bears on the extruder plates.

Test MB-4 - Review of high speed test films indicated that the extruder appeared to stop functioning adequately when small plastic hinges formed in front of the extruder mouth. These

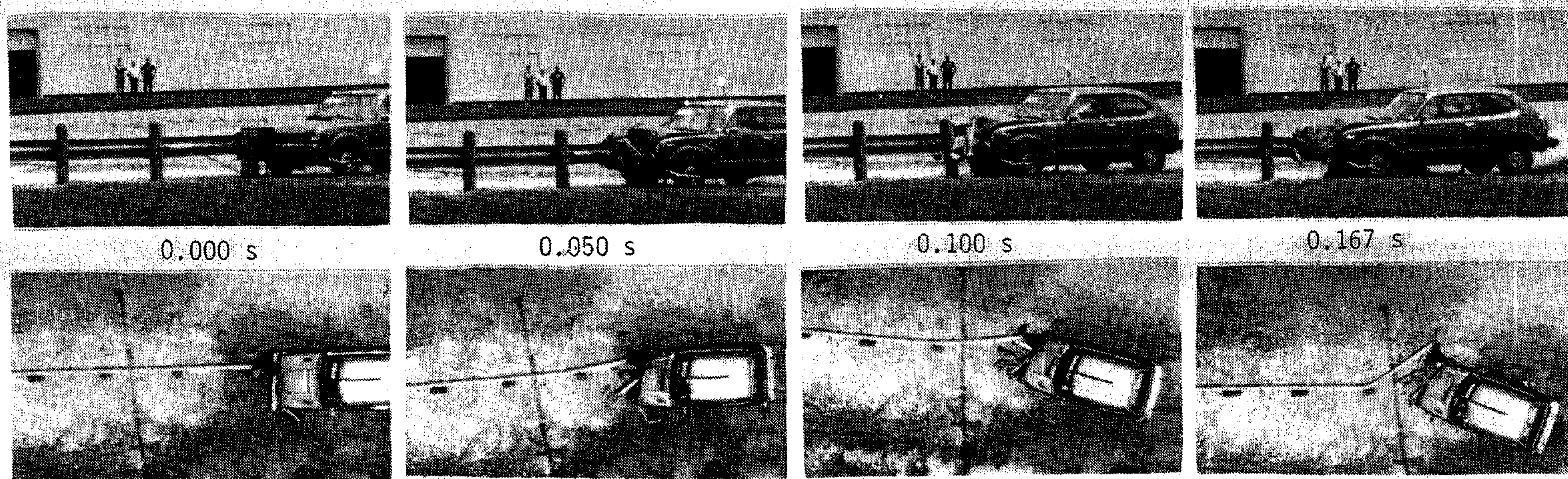

Test No	2404-MB2
Date.	5/21/87
Test Installation	Metal Bender End Treatment
Length of Installation. . . .	100 ft (3.5 m)
Vehicle	1979 Honda
Vehicle Weight	
Test Inertia.	1,750 lb (795 kg)
Gross Static.	1,924 lb (873 kg)
Vehicle Damage Classification	
TAD	12FR5
CDC	12FZEW3
Length of Rail Fed Through	
Bender.	6.1 ft (1.9 m)
Max. Rail Deformation	12.3 ft (3.7 m)

Impact Speed	62.1 mi/h (100.0 km/h)
Impact Angle	0 deg - 15" offset
Exit Speed	18.5 mi/h (29.8 km/h)
Vehicle Accelerations	
(Max. 0.050-sec Avg)	
Longitudinal	-15.2 g
Lateral.	2.9 g
Occupant Impact Velocity	
Longitudinal	35.1 ft/s (10.7 m/s)
Lateral.	None
Occupant Ridedown Accelerations	
Longitudinal	-14.2 g
Lateral.	No Contact

FIGURE 18. SUMMARY OF RESULTS FOR TEST MB-2.

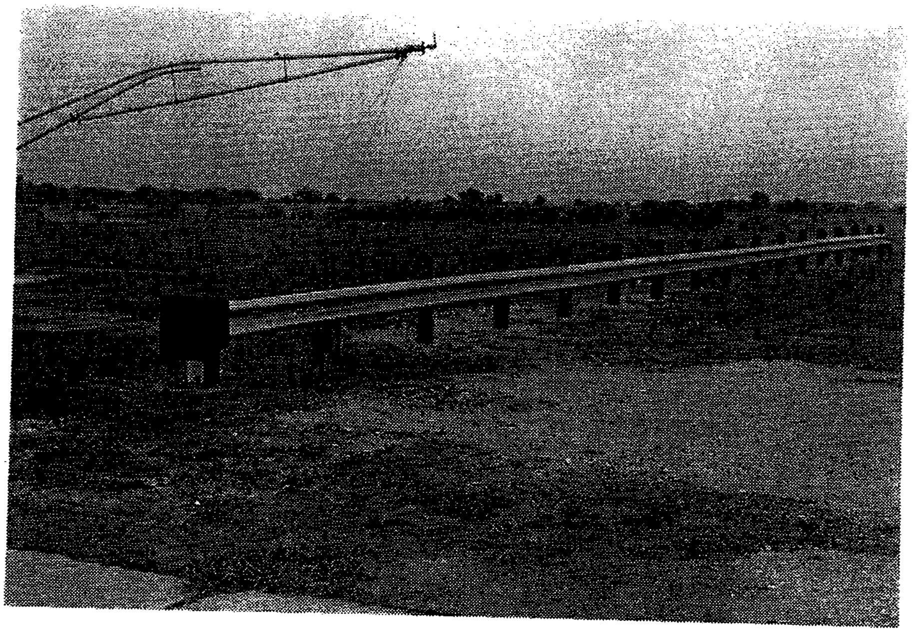

FIGURE 19. TEST INSTALLATION BEFORE TEST MB-3.

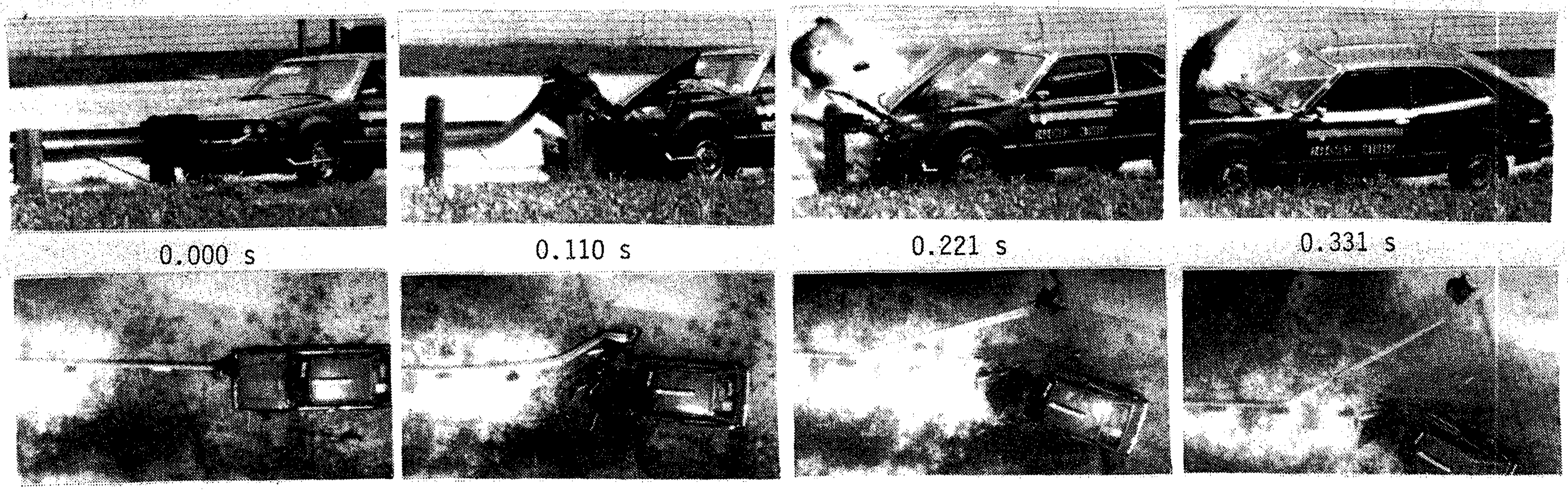

Test No	2404-MB3
Date	6/16/87
Test Installation	Metal Bender End Treatment
Length of Installation	100 ft (3.5 m)
Vehicle	1979 Honda
Vehicle Weight	
Test Inertia	1,955 lb (888 kg)
Vehicle Damage Classification	
TAD	12FR5
CDC	12FZEW3
Length of Rail Fed Through	
Bender	1.4 ft (0.4 m)
Max. Rail Deformation	22.8 ft (6.9 m)

Impact Speed	59.8 mi/h (96.2 km/h)
Impact Angle	0 deg - 15" offset
Exit Speed	35.1 mi/h (56.5 km/h)
Vehicle Accelerations (Max. 0.050-sec Avg)	
Longitudinal	-15.8 g
Lateral	-3.6 g
Occupant Impact Velocity	
Longitudinal	29.9 ft/s (9.1 m/s)
Lateral	12.1 ft/s (3.7 m/s)
Occupant Ridedown Accelerations	
Longitudinal	-14.5 g
Lateral	-1.2 g

FIGURE 20. SUMMARY OF RESULTS FOR TEST MB-3.

plastic hinges resulted from extruder rotations about its vertical axis and rotations about its lateral axis. The length of the squeezer section was believed to affect the extruders resistance to rotation. Therefore, the original prototype extruder with a 24 in. squeezer section was positioned to bend the guardrail away from the roadway in test MB-4. This extruder was further modified by adding a small funnel to its mouth in an effort to improve the capacity for plastic hinges to feed through the device.

In an effort to reduce costs associated with construction of the extruder terminal the concrete foundation under the second post was again removed. However, in order to facilitate break-away, a 3/4 in. diameter wire rope was looped around the concrete anchor at the first post and passed through holes in the base of posts 2, 3, and 4. Bearing plates were placed behind each post and cable clamps were attached to the cable to restrict the motion of the posts at the ground line. Thus, the ground line cable could eliminate virtually all post rotation observed in test MB-2 and standard 7 in. round wood posts could be used at all locations except at the first post. The first post must be placed in some type of rigid anchor to provide tensile capacity for the guardrail system. A rectangular post is used with the rigid anchor to simplify replacement after impacts since, unlike round posts, rectangular posts are cut to a consistent size. The modified terminal design prior to test MB-4 is shown in Figure 21. Test MB-4 involved the same impact conditions used in tests MB-2 and MB-3. Terminal performance for this test was very similar to results from MB-3. It was therefore concluded that increasing W-beam flexibility had no positive effect on extruder performance and, therefore, standard 5/8 in. diameter button head bolts should be used to attach the guardrail to all posts except the first. Further, it was concluded that the only way to improve impact performance was to reduce extruder rotations, especially counter-clockwise yaw rotation. Figure 22 summarizes test MB-4.

Test MB-5 - After review of high speed films from the first 4 tests, it was concluded that the first post imparted a lateral load on the extruder as it broke away. It was theorized that this behavior may have initiated the counter-clockwise rotation seen in the earlier tests. Therefore, a post deflector, shown in Figure 23, was added to the extruder in an attempt to impart a clockwise moment to the extruder as the first post was broken away. Test MB-5 was then conducted under the same conditions as the previous three tests. Extruder performance was not significantly improved by the addition of the post deflector. Figure 24 summarizes test MB-5.

A large pitch angle was induced in the extruder during this test. Measurement of the test vehicle indicated that the front bumper was significantly lower (17 in.) than any others used in the testing. After reviewing films of test MB-5, it was

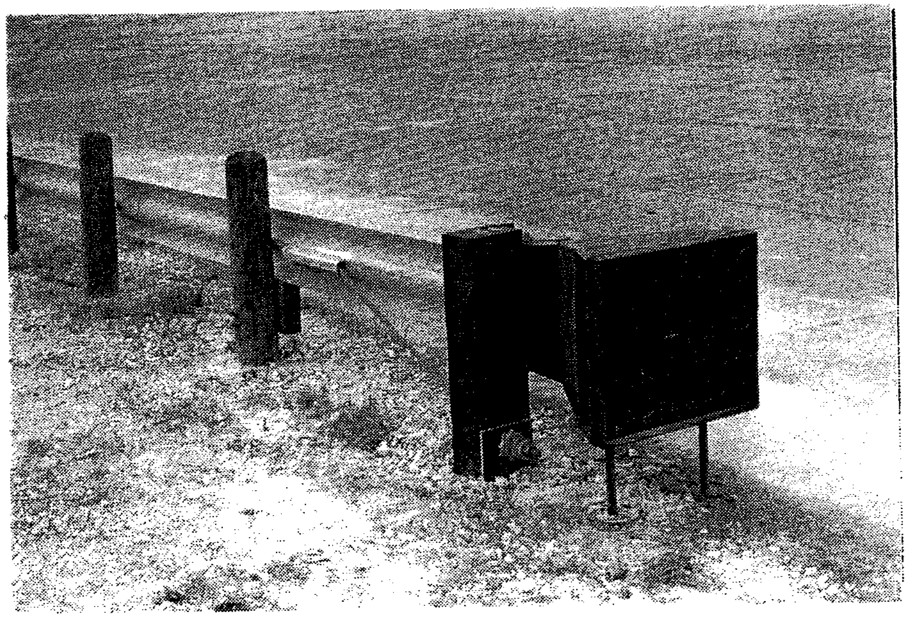

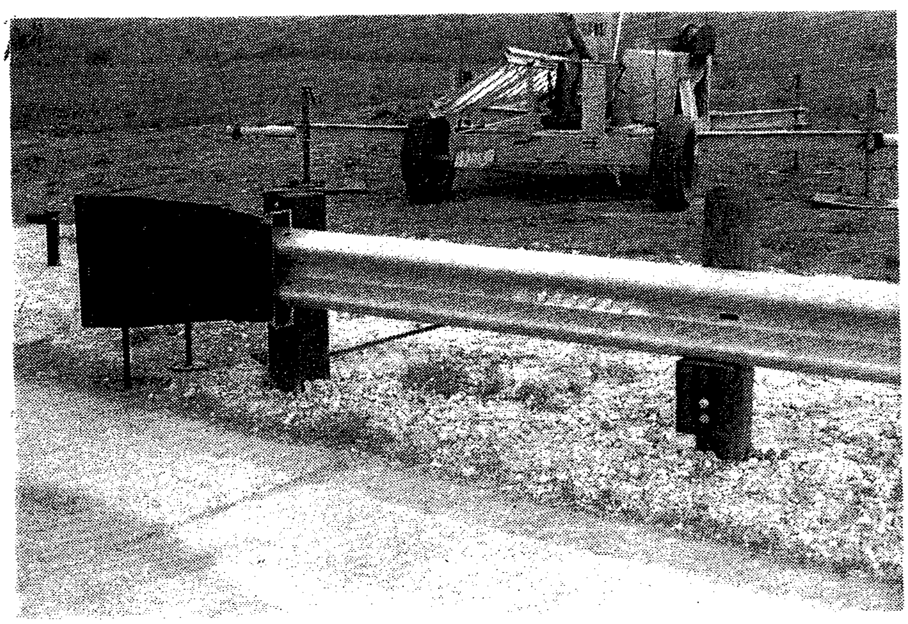

FIGURE 21. TEST INSTALLATION BEFORE
TEST MB-4.

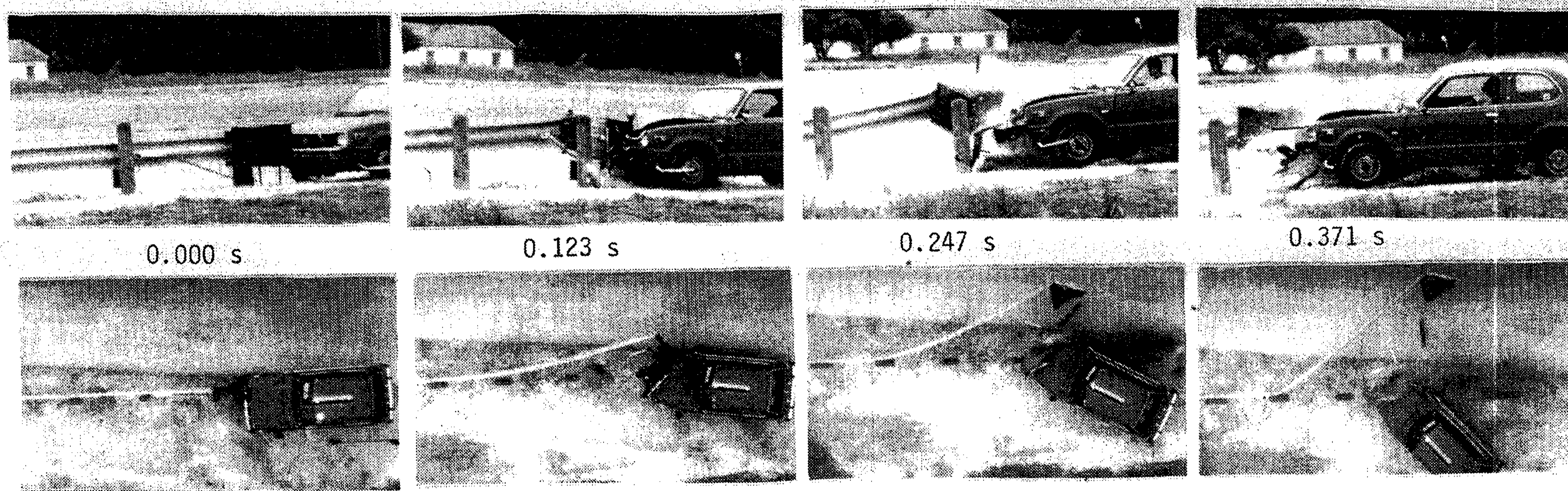

Test No	2404-MB4
Date	7/17/87
Test Installation	Metal Bender End Treatment
Length of Installation	100 ft (3.5 m)
Vehicle	1979 Honda
Vehicle Weight	
Test Inertia	1,750 lb (795 kg)
Gross Static	1,927 lb (875 kg)
Vehicle Damage Classification	
TAD	12FR4/9L&T2
CDC	12FZEW3/00RDA02
Length of Rail Fed Through Bender	4.9 ft (1.5 m)
Max. Rail Deformation	24.0 ft (7.3 m)

Impact Speed	56.7 mi/h (91.2 km/h)
Impact Angle	0 deg - 15" offset
Exit Speed	27.4 mi/h (44.1 km/h)
Vehicle Accelerations (Max. 0.050-sec Avg)	
Longitudinal	-13.8 g
Lateral	-3.3 g
Occupant Impact Velocity	
Longitudinal	32.3 ft/s (9.8 m/s)
Lateral	None
Occupant Ridedown Accelerations	
Longitudinal	-11.9 g
Lateral	No Contact

FIGURE 22. SUMMARY OF RESULTS FOR TEST MB-4.

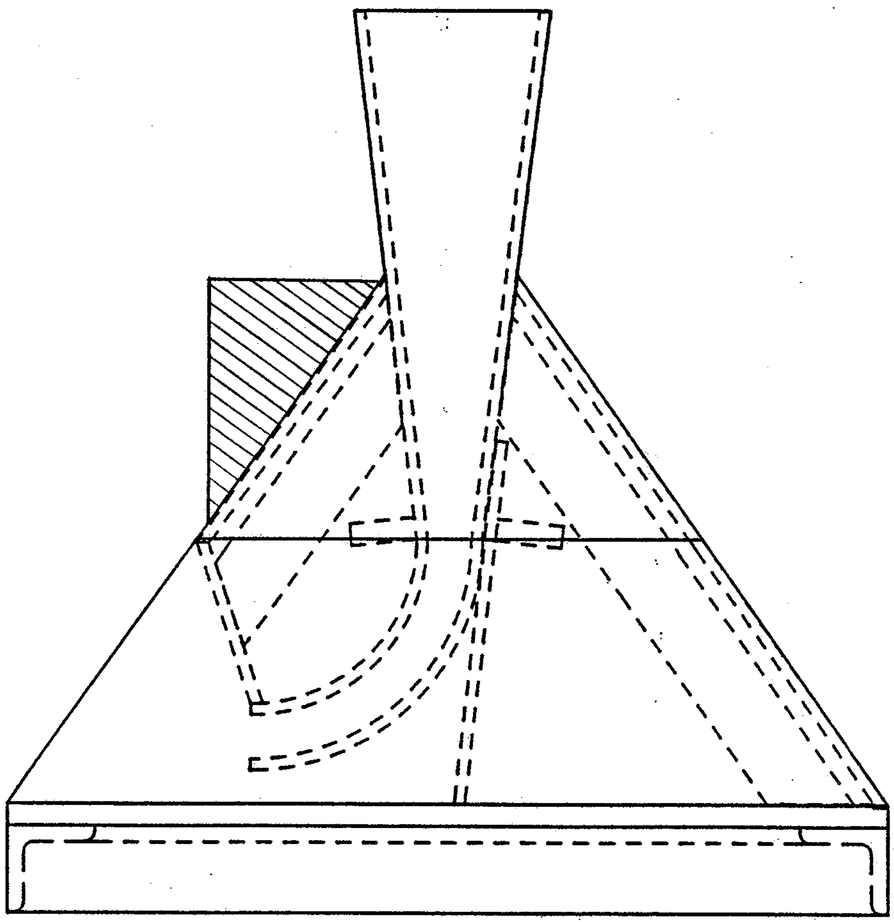

FIGURE 23. POST DEFLECTOR ATTACHMENT.

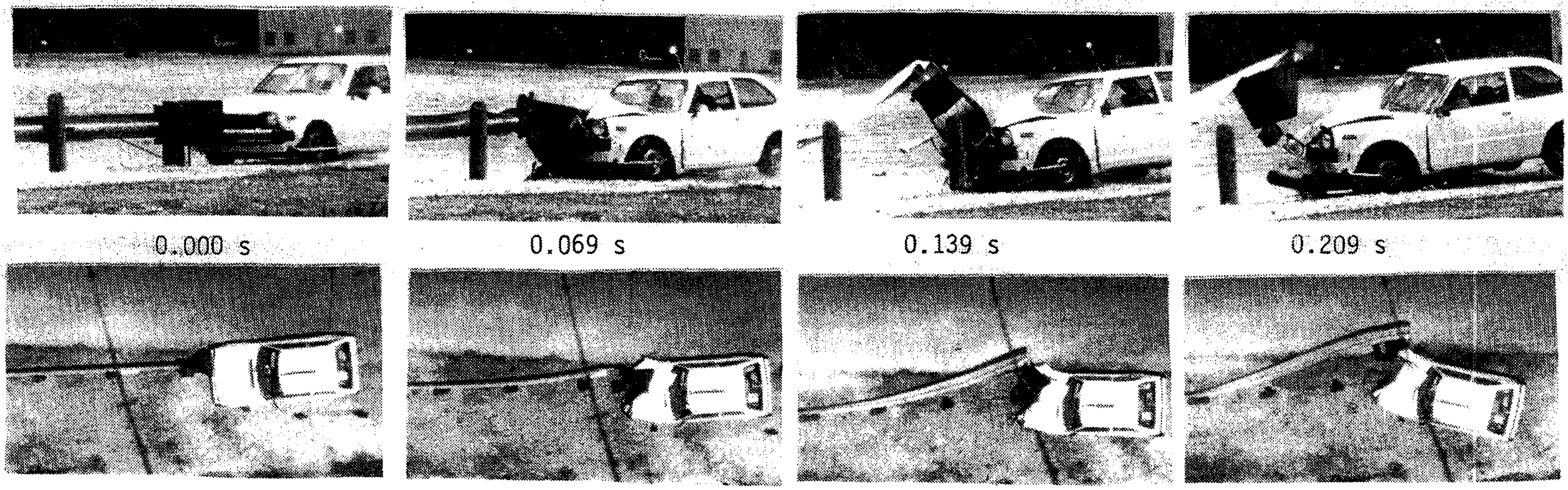

Test No	2404-MB5	Impact Speed	59.0 mi/h (94.9 km/h)
Date	7/22/87	Impact Angle	15 deg
Test Installation	Metal Bender End Treatment	Exit Speed	30.1 mi/h (48.4 km/h)
Length of Installation	100 ft (3.5 m)	Vehicle Accelerations (Max. 0.050-sec Avg)	
Vehicle	1980 Honda	Longitudinal	-15.5 g
Vehicle Weight		Lateral	-3.4 g
Test Inertia	1,800 lb (817 kg)	Occupant Impact Velocity	
Gross Static	1,965 lb (892 kg)	Longitudinal	37.0 ft/s (11.3 m/s)
Vehicle Damage Classification		Lateral	None
TAD	12FR3/9L&T4	Occupant Ridedown Accelerations	
CDC	12FZEW3/00TDD04	Longitudinal	-8.4 g
Length of Rail Fed Through Bender	3.8 ft (1.2 m)	Lateral	No Contact

FIGURE 24. SUMMARY OF RESULTS FOR TEST MB-5.

concluded that some method for resisting applied moments had to be developed if the extruder was to perform effectively over a wide range of impact conditions and vehicles. One method for providing moment resistance was to extend the extruder's feeder section. Therefore a 36 in. feeder chute was added to the light weight extruder. The chute was constructed from two steel channels and steel stabilizer plates as shown in Figure 25.

In addition, two cylindrical rubber bumpers were added to the front of the extruder in an effort to reduce the eccentric pitch load observed in test MB-5. The rubber bumpers were designed to contact the front of an impacting vehicle above the bumperline, thereby raising the effective point of load application to the extruder. The modified extruder is shown in Figure 26. Detailed construction drawings of the final terminal design are shown in Appendix E.

Test MB-6 - The modified extruder was tested with a small vehicle under the same conditions as the previous four tests. The extruder exhibited no tendency to rotate during this test and the impacting vehicle was decelerated smoothly as the first 12.5 ft. of guardrail was forced through the device. The extruder was still in a position to perform effectively when the forward motion of the front of the test vehicle was stopped. The test vehicle then slowly yawed clockwise and came to a safe stop within a few feet of the guardrail. The maximum roll angle during this test was less than 5 degrees. All occupant severity measures for this test were within recommended limits (12). This test was considered to be very successful. Figure 27 summarizes results of test MB-6.

Test MB-7 - Performance of the modified guardrail extruder terminal was evaluated for head-on impacts with full-size automobiles. Test MB-7 involved a 4600 lb. vehicle impacting the extruder at 61.6 mph and 0 deg. The terminal performed very well and decelerated the test vehicle to a smooth stop over 45 ft. The test vehicle exhibited no tendency to ride over the end treatment and all occupant impact severity measures were well below recommended limits. A summary of this test is presented in Figure 28.

Note that, as discussed previously, the splice between the first and second 25 ft. segments of guardrail was welded to eliminate bolts that would restrict the extrusion process. As shown in Figure 29, the test vehicle was traveling approximately 38 mph when the extruder encountered the welded splice. At this point the test vehicle would have been brought to an abrupt stop and a very high deceleration force would have developed. Thus, the extruder terminal system cannot be expected to perform acceptably with a bolted splice at this point in the guardrail system. However, the test vehicle was decelerated to 25 mph after extruding 37.5 ft. of guardrail. Further, if the test vehicle had weighed 4500 lb and impacted at 60 mph, as required

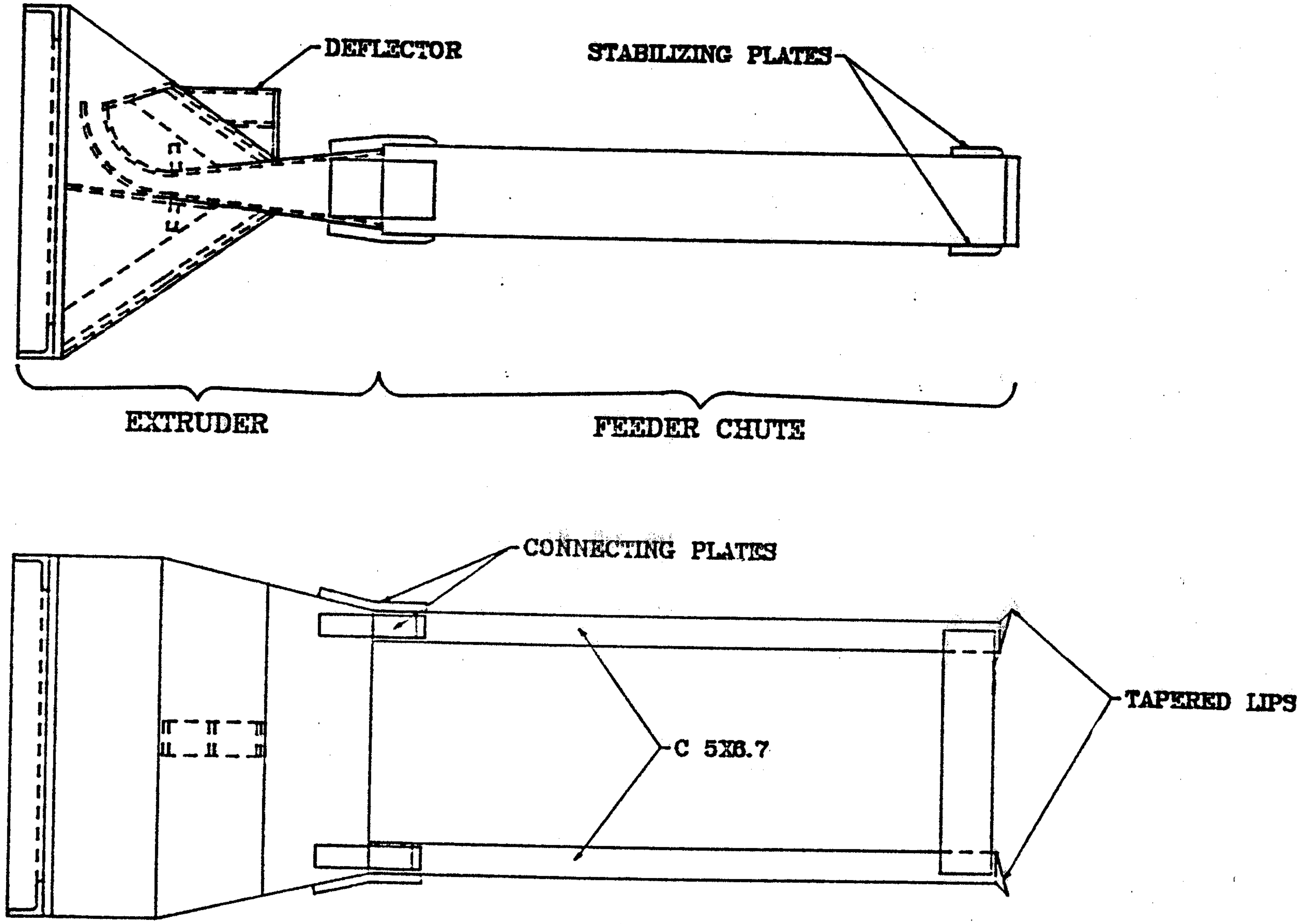

FIGURE 25. EXTENDED FEEDER CHUTE ATTACHMENT.

FIGURE 26. MODIFIED EXTRUDER.

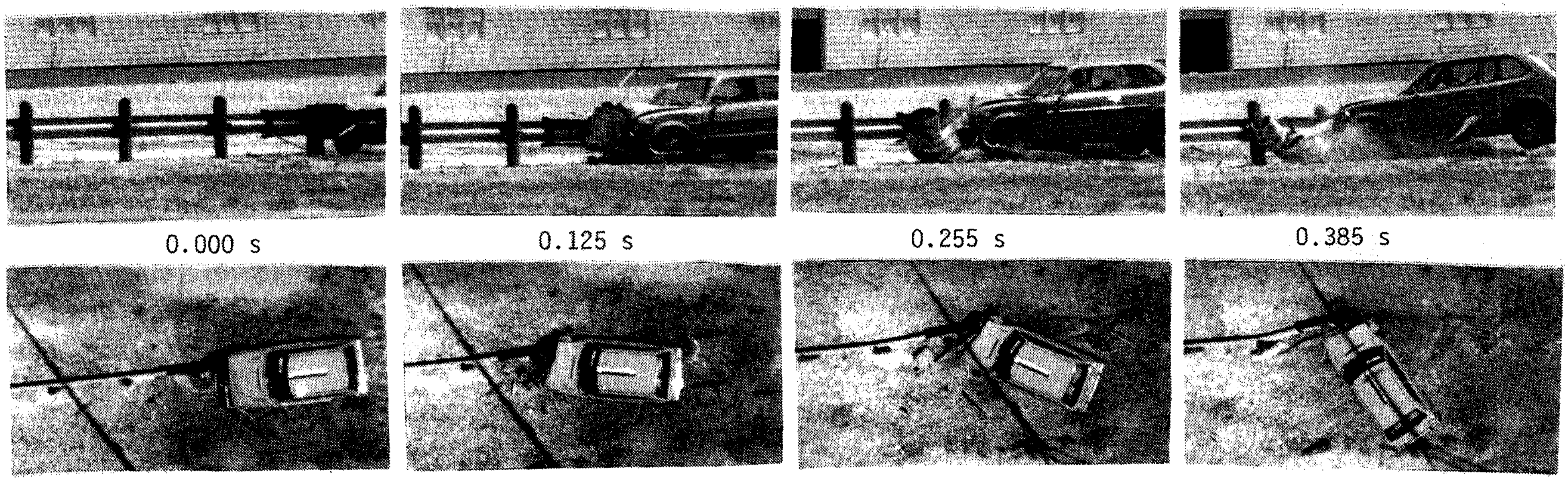

Test No	2404-MB6	Impact Speed	58.7 mi/h (94.4 km/h)
Date	8/18/87	Impact Angle	0 deg - 15" offset
Test Installation	Metal Bender End Treatment	Exit Speed	13.1 mi/h (21.1 km/h)
Length of Installation	100 ft (3.5 m)	Vehicle Accelerations (Max. 0.050-sec Avg)	
Vehicle	1979 Honda	Longitudinal	-13.8 g
Vehicle Weight		Lateral	-4.8 g
Test Inertia	1,785 lb (810 kg)	Occupant Impact Velocity	
Gross Static	1,957 lb (888 kg)	Longitudinal	29.0 ft/s (8.8 m/s)
Vehicle Damage Classification		Lateral	12.5 ft/s (3.8 m/s)
TAD	12FR4	Occupant Ridedown Accelerations	
CDC	12FZEW2	Longitudinal	-15.5 g
Length of Rail Fed Through Bender	13.2 ft (4.0 m)	Lateral	2.1 g

FIGURE 27. SUMMARY OF RESULTS FOR TEST MB-6.

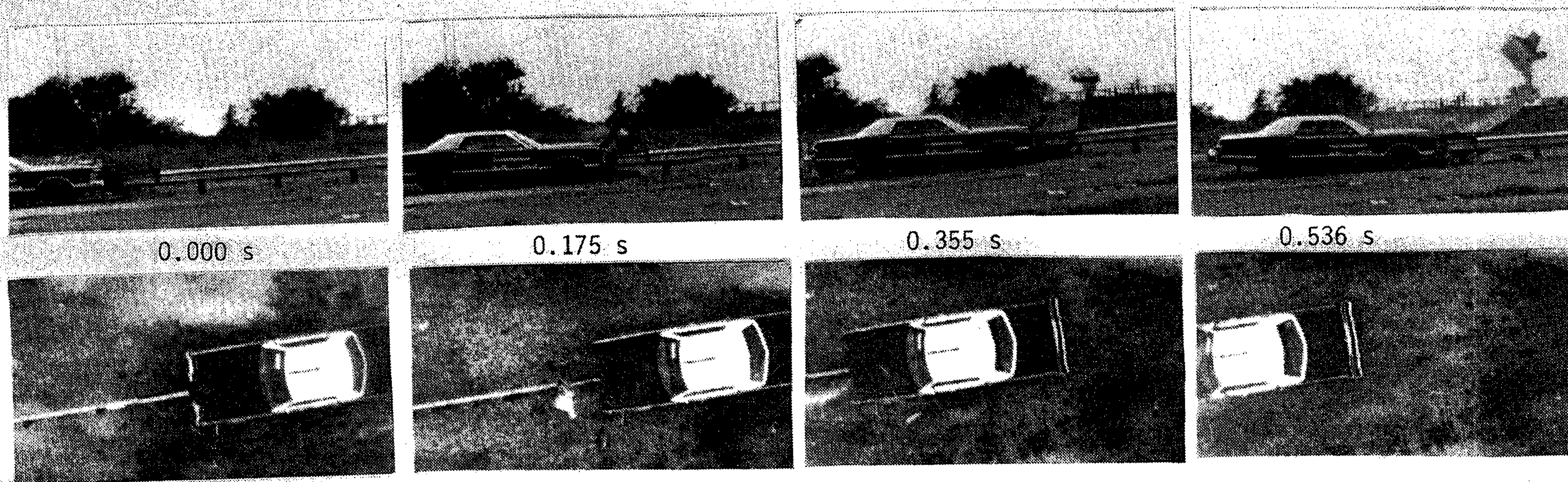

Test No	2404-MB7	Impact Speed	61.6 mi/h (99.1 km/h)
Date	8/27/87	Impact Angle	0 deg - center
Test Installation	Metal Bender End Treatment	Exit Speed	Not available
Length of Installation	100 ft (3.5 m)	Vehicle Accelerations (Max. 0.050-sec Avg)	
Vehicle	1978 Mercury	Longitudinal	-6.8 g
Vehicle Weight Test Inertia	4,600 lb (2,088 kg)	Lateral	-0.7 g
Vehicle Damage Classification		Occupant Impact Velocity	
TAD	12FC4	Longitudinal	19.8 ft/s (6.0 m/s)
CDC	12FCEW2	Lateral	None
Length of Rail Fed Through Bender	45 ft (14 m)	Occupant Ridedown Accelerations	
		Longitudinal	-8.2 g
		Lateral	No Contact

FIGURE 28. SUMMARY OF RESULTS FOR TEST MB-7.

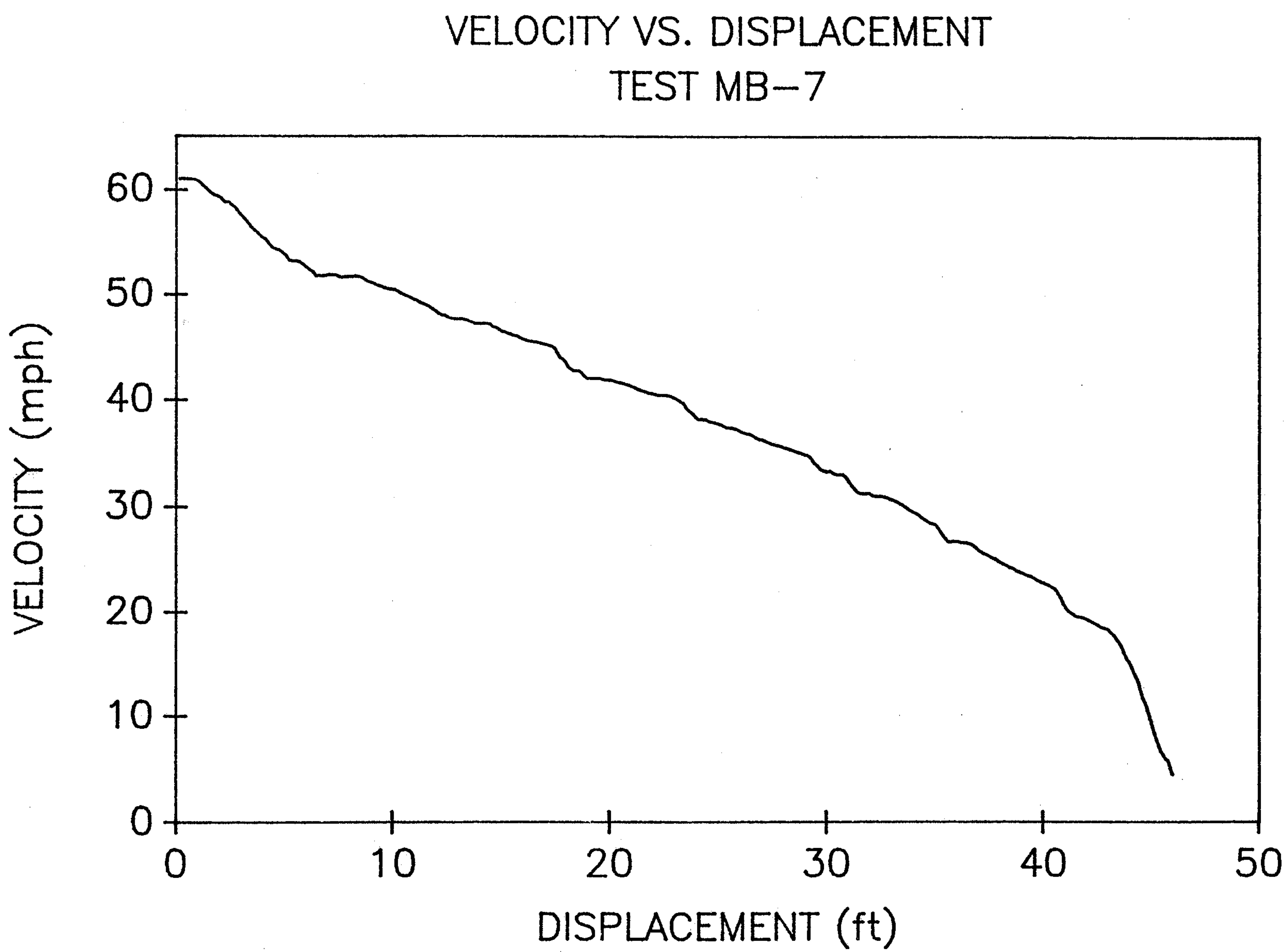

FIGURE 29. VELOCITY VS. DISPLACEMENT CURVE FOR TEST MB-7.

by NCHRP 230 test standards, it would have decelerated to less than 20 mph after extruding 37.5 ft. of guardrail. Although the extruding process would be restricted by a bolted splice connection, it is the authors' opinion that severe deceleration forces would not develop when the impacting vehicle is travelling at speeds less than 20 mph. A full scale crash test should be conducted to verify the safety performance of a GET with a bolted splice 37.5 ft. from the end. A leading guardrail manufacturer has indicated that a 37.5 length of guardrail could be purchased at a cost only modestly more than the cost of 37.5 ft. of guardrail cut to shorter lengths (13). Therefore, the terminal could be constructed without field welding guardrail segments together.

Test 9429A-1- The capacity of the modified terminal design for redirecting vehicles impacting along the side was then tested with a mini-size automobile. During this test an 1800 lb vehicle impacted the barrier 6.25 ft. from the end at a speed of 59.5 mph and an angle of 15 deg. The test vehicle was redirected very smoothly and, although there was some contact between the test vehicle's tires and the guardrail posts, no significant snagging was observed. All occupant severity measures were well within recommended safety limits and the test was considered to be very successful. Furthermore, no signs of distress were observed in the guardrail where the cable release mechanism was attached. Figure 30 presents a summary of test 9429A-1.

Test 9429A-2 - The final test in this series involved a full size vehicle impacting the end treatment 12.5 ft from the end at 60 mph and 25 deg. The end treatment again performed very well, even though the guardrail deflected sufficiently to allow significant wheel contact with the guardrail posts. Tensile forces generated in the rail during the test caused the concrete footing at the first post to move 3 inches. This anchor movement resulted in an approximate 12 in. (48 %) increase in maximum barrier deflection. Excessive barrier deflection allowed the rear wheels of the vehicle to ride up on the base of a guardrail post. Figure 31 presents a summary of test 9429A-2.

Although no large deceleration forces, indicative of snagging, were observed, the exit velocity for this test was somewhat lower than recommended by NCHRP Report 230 Evaluation Criteria I (12). This criteria is based on the concept that a vehicle should not be redirected into the traveled way at a speed less than 75 % of its impact speed. Thus, test evalutation is based on a subjective judgement of whether the test vehicle has been redirected back to the traveled way. During test 9429A-2, the test vehicle exited the guardrail at an angle of less than 6 degrees and then quickly steered back to the barrier. In the authors' opinion, this test vehicle would not have encroached significantly onto adjacent traffic lanes.

Further, although meeting Evalutation Criteria I is desirable, strict compliance with this factor has never been required for many of the longitudinal barriers now in use. As

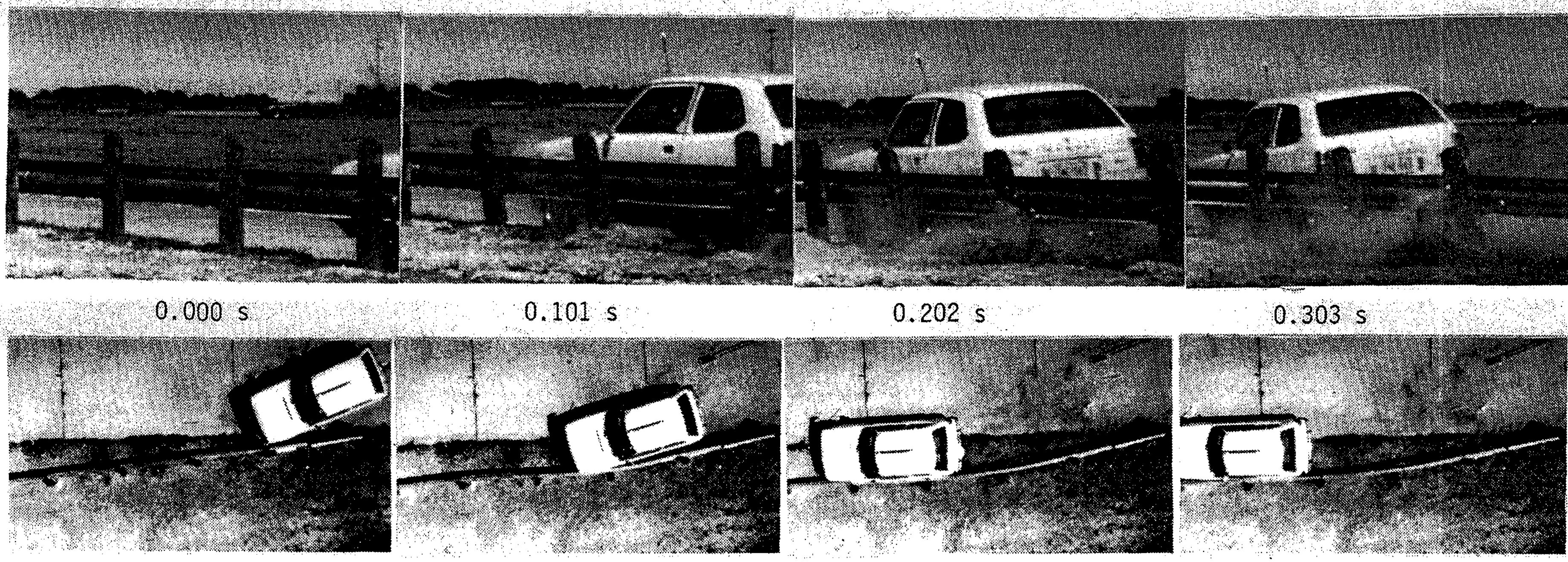

Test No	9429A-1
Date.	9/30/87
Test Installation	Metal Bender End Treatment
Length of Installation. . . .	100 ft (3.5 m)
Vehicle	1979 Honda Civic
Vehicle Weight	
Test Inertia.	1,780 lb (808 kg)
Gross Static.	1,945 lb (883 kg)
Vehicle Damage Classification	
TAD	11LFQ3
CDC	11LFES2
Maximum Vehicle Crush	4.0 in (10.2 cm)
Rail Deformation.	19.8 ft (6.0 m)
Maximum Rail Deflection . . .	2.4 ft (0.7 m)

Impact Speed	59.1 mi/h (95.1 km/h)
Impact Angle	15.6 deg
Exit Speed	52.3 mi/h (84.2 km/h)
Exit Angle	7.7 deg
Vehicle Accelerations (Max. 0.050-sec Avg)	
Longitudinal	-3.8 g
Lateral	-7.2 g
Occupant Impact Velocity	
Longitudinal	15.9 ft/s (4.8 m/s)
Lateral.	17.0 ft/s (5.2 m/s)
Occupant Ridedown Accelerations	
Longitudinal	-1.4 g
Lateral.	-10.3 g

FIGURE 30. SUMMARY OF RESULTS FOR

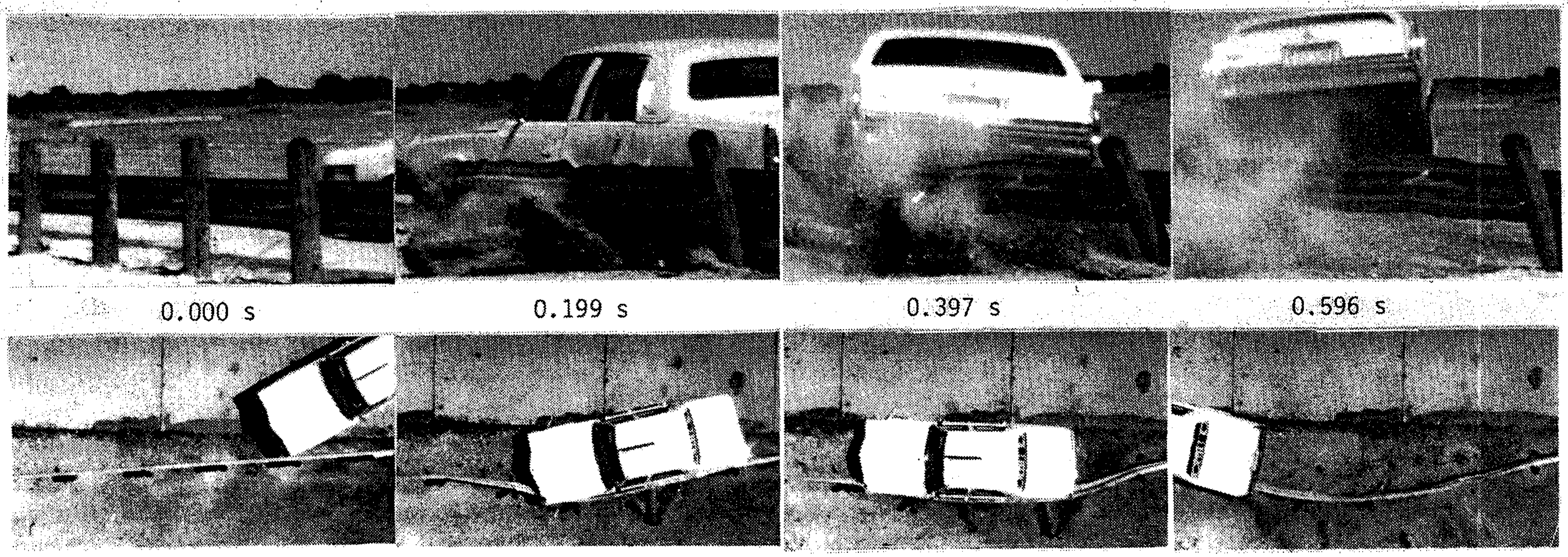

Test No	9429A-2	Impact Speed	58.9 mi/h (94.8 km/h)
Date	10/02/87	Impact Angle	24.9 deg
Test Installation	Metal Bender End Treatment	Exit Speed	38.1 mi/h (61.3 km/h)
		Exit Angle	5.3 deg
Length of Installation	100 ft (3.5 m)	Vehicle Accelerations (Max. 0.050-sec Avg)	
Vehicle	1979 Cadillac		
Vehicle Weight		Longitudinal	-4.9 g
Test Inertia	4,410 lb (2,002 kg)	Lateral	-6.4 g
Vehicle Damage Classification		Occupant Impact Velocity	
TAD	11LFQ5	Longitudinal	23.2 ft/s (7.1 m/s)
CDC	11LFES3	Lateral	16.5 ft/s (5.0 m/s)
Maximum Vehicle Crush	7.0 in (17.8 cm)	Occupant Ridedown Accelerations	
Rail Deformation	28.5 ft (8.7 m)	Longitudinal	-6.2 g
Maximum Rail Deflection	3.6 ft (1.1 m)	Lateral	-8.5 g

FIGURE 31. SUMMARY OF RESULTS FOR TEST 9429A-2.

shown in Table 2 many guardrails and guardrail end treatment systems now in wide use have failed to meet the velocity change requirements in the evaluation criteria. Based on results of tests 1 and 2 from this table, it can be concluded that the widely used G4(1S) barriers would not pass this evaluation criteria. Further as shown in Table 2, even tests of rigid vertical barriers, where vehicle snagging is completely eliminated, have failed this evaluation criteria. Finally, there is little or no evidence that secondary rear end collisions represent a significant fraction of all serious secondary impacts after a successful barrier redirection. Based on the discussion presented above, it is the authors' opinion that this evaluation criteria should be evaluated when current test standards are revised.

Summary

The guardrail extruder terminal (GET) has been fully tested and was shown to meet nationally recognized safety standards (12). The extruder captures a vehicle impacting the end of the barrier and safely decelerates it to a stop rather than allowing the vehicle to penetrate the barrier at a high rate of speed. The new terminal has only a 12.5 ft. length upstream of the beginning of the length of need. This distance is significantly shorter than some other end treatment designs, such as the twisted and buried end. Furthermore, the extruder terminal can be placed within 43.75 ft of a transition to another barrier, unlike the turned down design which requires over 100 ft. This terminal is installed on a tangent section of guardfence and, therefore, can be used at sites where flared treatments are unappropriate.

The cost of this system should be relatively low. Extruders used in the testing described herein were originally constructed for approximately $500 each. The cable release mechanism was constructed for approximately $250. Remaining hardware items should cost less than $250 and installation of this system is no more difficult than the twisted and buried end now used widely across Texas. Therefore, the entire cost of the guardrail extruder terminal should be approximately $1200. Finally, key components of the GET are very durable. No significant damage was sustained by the extruders or the cable release mechanism during any of the eleven full-scale crash tests described herein.

TABLE 2. Velocity Changes During Longitudinal Barrier Impacts

	Vehicle Weight (lbs)	Impact Velocity (mph)	Impact Angle (Deg)	Service	Velocity Change (mph)
1)	4450	61.8	25.3	G4 (1S) on Box Culvert	24.6
2)	4500	58.2	25	G4 (1S) at Turned Down End	29.4
3)	4490	58.7	25	TSDHPT Guard Fence at Turn Down End	22.6
4)	4490	58.5	23	TSDHPT Guard Fence at Turn Down End	19.2
5)	4740	59.9	24	Rigid Vertical Wall	17.5
6)	4490	61.8	25.6	Rigid Vertical Wall	15.9

V. SPLIT RAIL TERMINAL DEVELOPMENT

Preliminary Development

The split rail concept involves cutting longitudinal slots in the W-beam to reduce its dynamic buckling strength. The number and length of slots must be selected in order to reduce the rail's buckling strength sufficiently to safely accommodate small car impacts while maintaining sufficient capacity to stop full size vehicles within a reasonable distance. As shown in Figure 32, the W-beam cross-section can be cut into three relatively flat segments by placing a longitudinal slot at each peak and valley in the cross-section. A three slot configuration as described above is believed to represent a functionally minimum moment of inertia configuration.

The first step in evaluating the feasibility of the split rail concept was to conduct static testing to determine if the strips of W-beam in the slotted region could be expected to act independently, thereby reducing the buckling strength as expected. Results of several preliminary static tests on specimens with saw cut slots indicated that the individual metal strips began to buckle but quickly contacted other strips. This behavior greatly increased the buckling strength of the slotted guardrail sections. Subsequently, specimens with 0.5 in. wide slots were tested and the individual strips were found to act more independently.

If three 0.5 in. wide longitudinal slots are cut into the W-beam, the total cross-sectional area of the slotted region will be reduced to 1.83 $in.^2$ compared to a total area of 1.61 $in.^2$ at a section through the four bolt holes at a splice. Thus, the tensile capacity of the slotted segment is higher than the capacity of the beam at a splice point. The moment of inertia of an unslotted 12 ga. W-beam element is approximately 2.33 $in.^4$ The combined moments of inertia of the four strips of the cross-section is approximately 0.02 $in.^4$ Thus the buckling strength of a slotted W-beam cross-section is approximately 1% of that of an unmodified cross-section. The static buckling force could be adjusted by controlling the length of the slotted section.

Static testing was conducted on a number of specimens with three 0.5 in. wide slots and lengths of 36, 48, 60, and a combination specimen having slot lengths of 30 and 24 in. Table 3 summarizes results from this static testing. Note that the predicted values shown in this table are based on the assumption that the end conditions of the slotted segments were fixed-pinned. This assumption seemed to yield the best possible predictions of maximum buckling load. Figure 33 shows typical static test specimens.

Although static test results were believed to give some indication of energy dissipation associated with dynamic

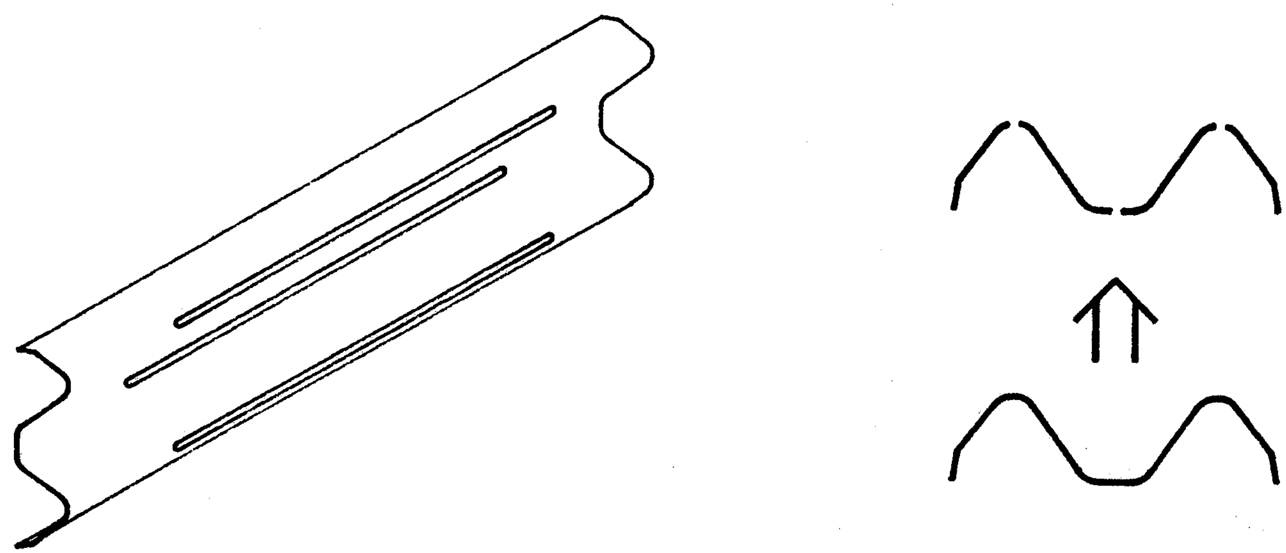

FIGURE 32. SLOT LOCATIONS FOR SPLIT RAIL DESIGN.

TABLE 3. STATIC SPLIT RAIL BUCKLING TEST RESULTS.

SLOT LENGTH (inches)	FAILURE LOAD (lbs)	EULER BUCKLING LOAD (lbs)
36	23,700	18,000
48	8,200	10,000
60	4,900	6,400
24 & 30	19,500	26,000

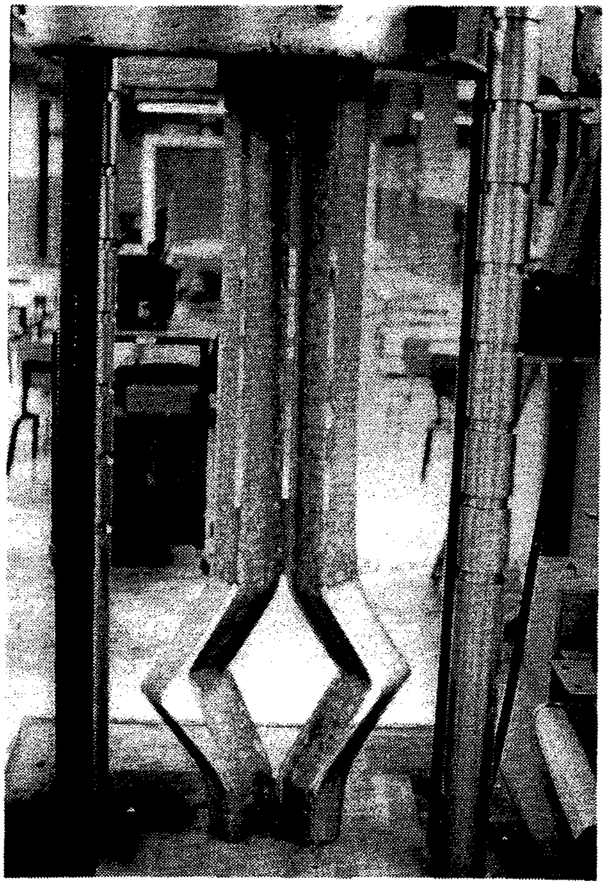

FIGURE 33. STATIC SPLIT RAIL BUCKLING SPECIMEN.

buckling, there is really no method for quantifying this relationship. Therefore, dynamic testing was undertaken in two phases. The first phase, designed to determine the effect of slot length on dynamic energy dissipation, involved pendulum testing specimens similar to those used in the static tests. Figure 34 shows the test configuration for the pendulum testing. Specimens used in this testing were 12.5 ft. long and had two slotted segments. A standard guardrail post supported the test specimen between the two slotted segments. The pendulum first struck a slotted segment of W-beam, collapsed it, and then struck the guardrail post. Accelerometers mounted on the pendulum were used to measure impact forces. Pendulum test results are presented in Figures 35 and 36. Note that the initial impulse was approximately the same for all slot lengths tested. This behavior was attributed to the slotted segments buckling in the second and higher modes, thereby virtually eliminating effects of slot length.

The second phase of dynamic testing, designed to determine effects of impact speed on dynamic energy dissipation, involved three full scale crash tests, (SRP-1, SRP-2, and SRP-3), of a single specimen design at impact speeds of 20, 30, and 40 mph. The test vehicles were instrumented with accelerometers to measure impact forces. A 60 in. slot length was selected for this phase of testing. Figure 37 shows the test installation used in Test SRP-3. Energy dissipation during these three tests was plotted as a function of displacement as shown in Figure 38. Note that the energy dissipation for test SRP-3, a 40 mph impact, was 25 kip-ft after collapsing the first set of 60 in. long slots. This energy dissipation rate corresponds to an 8 ft/sec velocity change in a mini-size vehicle during a 60 mph impact. For a 5 ft slotted section, the relationship between vehicle speed and energy absorbed is approximately linear. This is illustrated in Figure 39.

Based on results of this testing, it was concluded that the dynamic buckling strength of a W-beam could be reduced sufficiently with the split rail concept to accommodate high speed impacts of mini-size vehicles. Thereafter, the most pressing concern about the split rail concept was with its capacity for redirecting a full-size automobile impacting at a high speed and angle. Therefore, one more preliminary test was conducted to investigate the split rail's performance during angular impacts.

After reviewing results of all dynamic tests of the split rail concept, it was decided that an end treatment with 27 in. slot lengths might be designed to perform well for head-on impacts. Smaller slot lengths could result in significant rail support at the top of the post and prevent clean breakaway of the post during head on impacts. Conversely longer slot lengths would reduce the redirective capability of the barrier. Therefore, the installation constructed for test SRP-4 involved 27 in. slotted

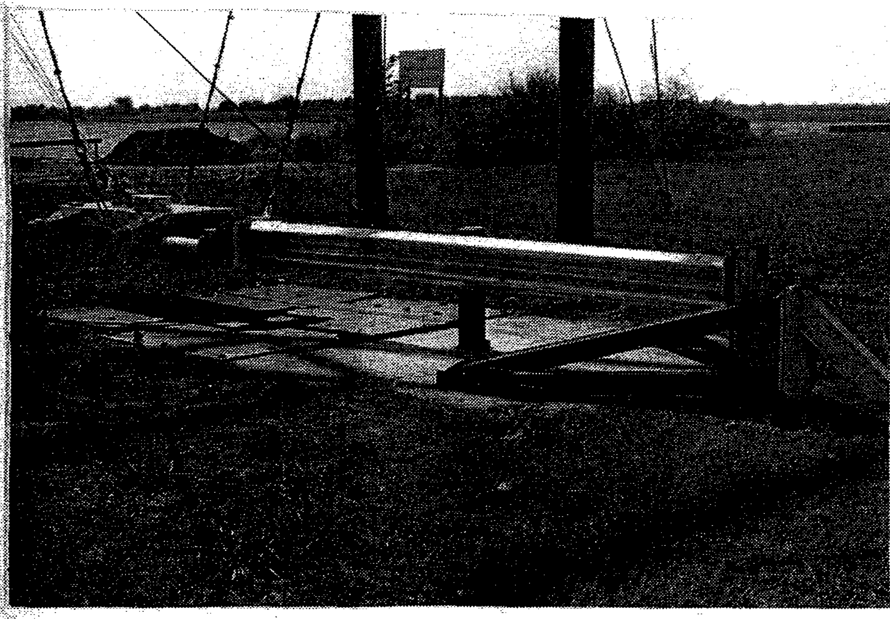

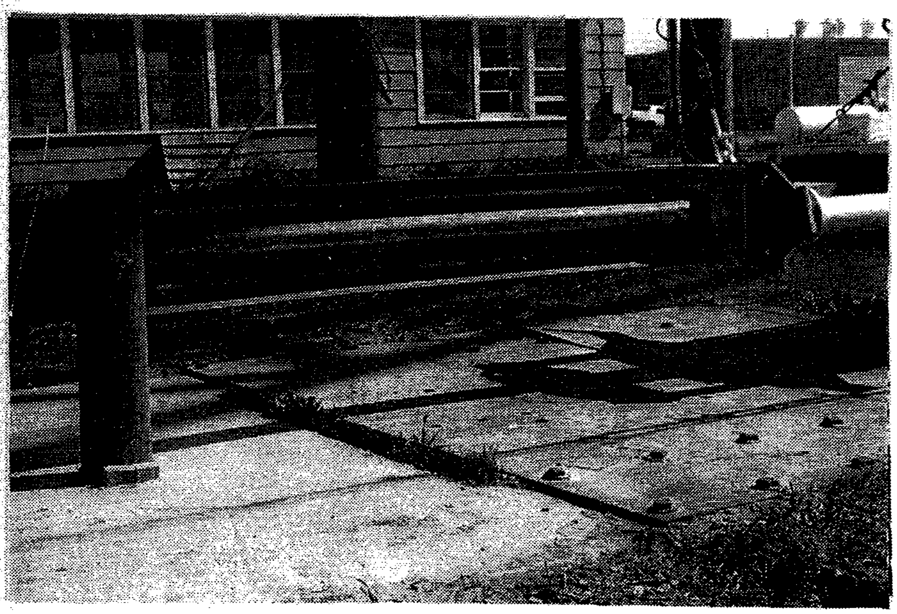

FIGURE 34. PENDULUM TEST CONFIGURATION.

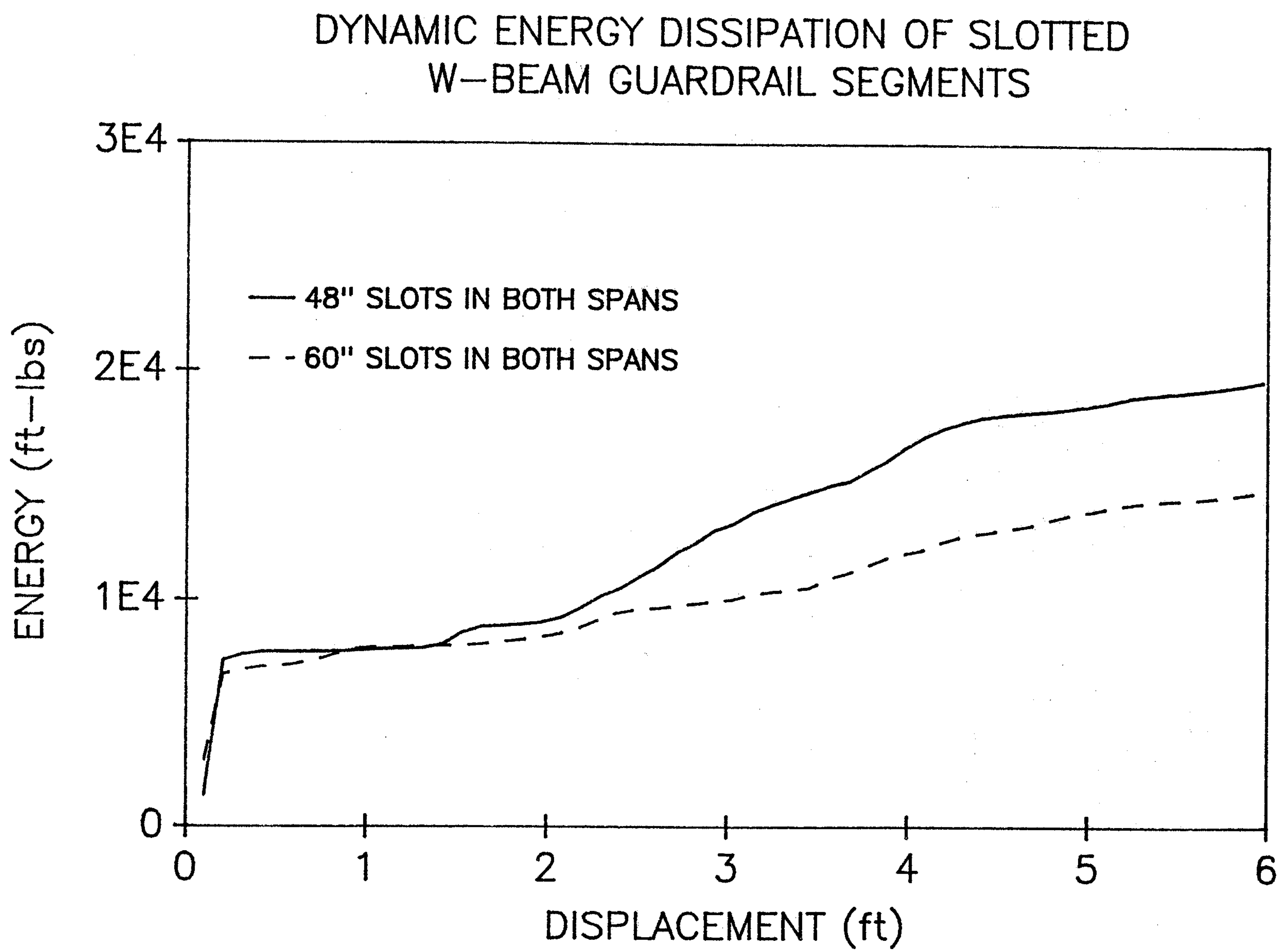

FIGURE 35. PENDULUM TEST RESULTS.

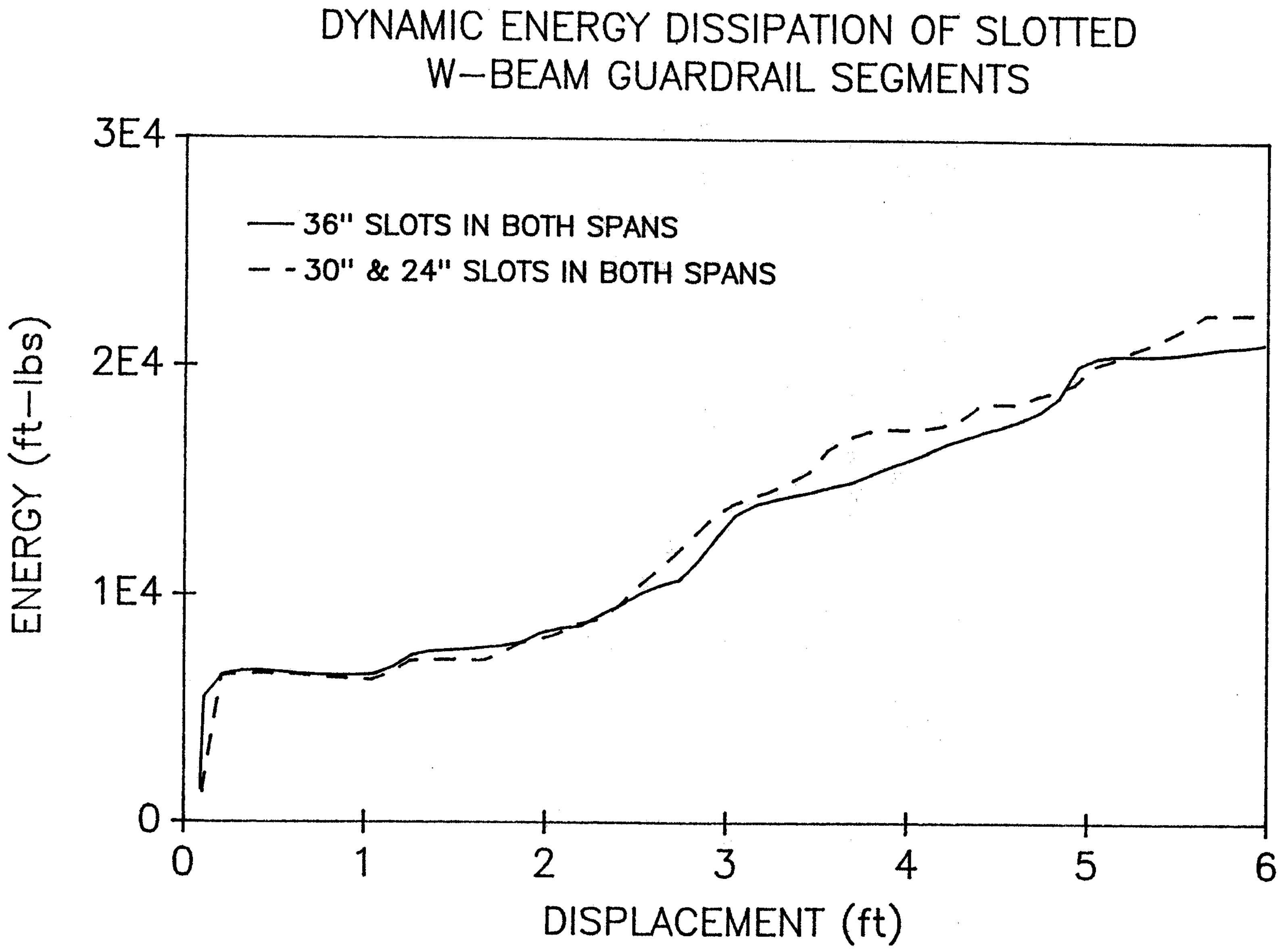

FIGURE 36. PENDULUM TEST RESULTS.

FIGURE 37. INSTALLATION FOR TEST SRP-3.

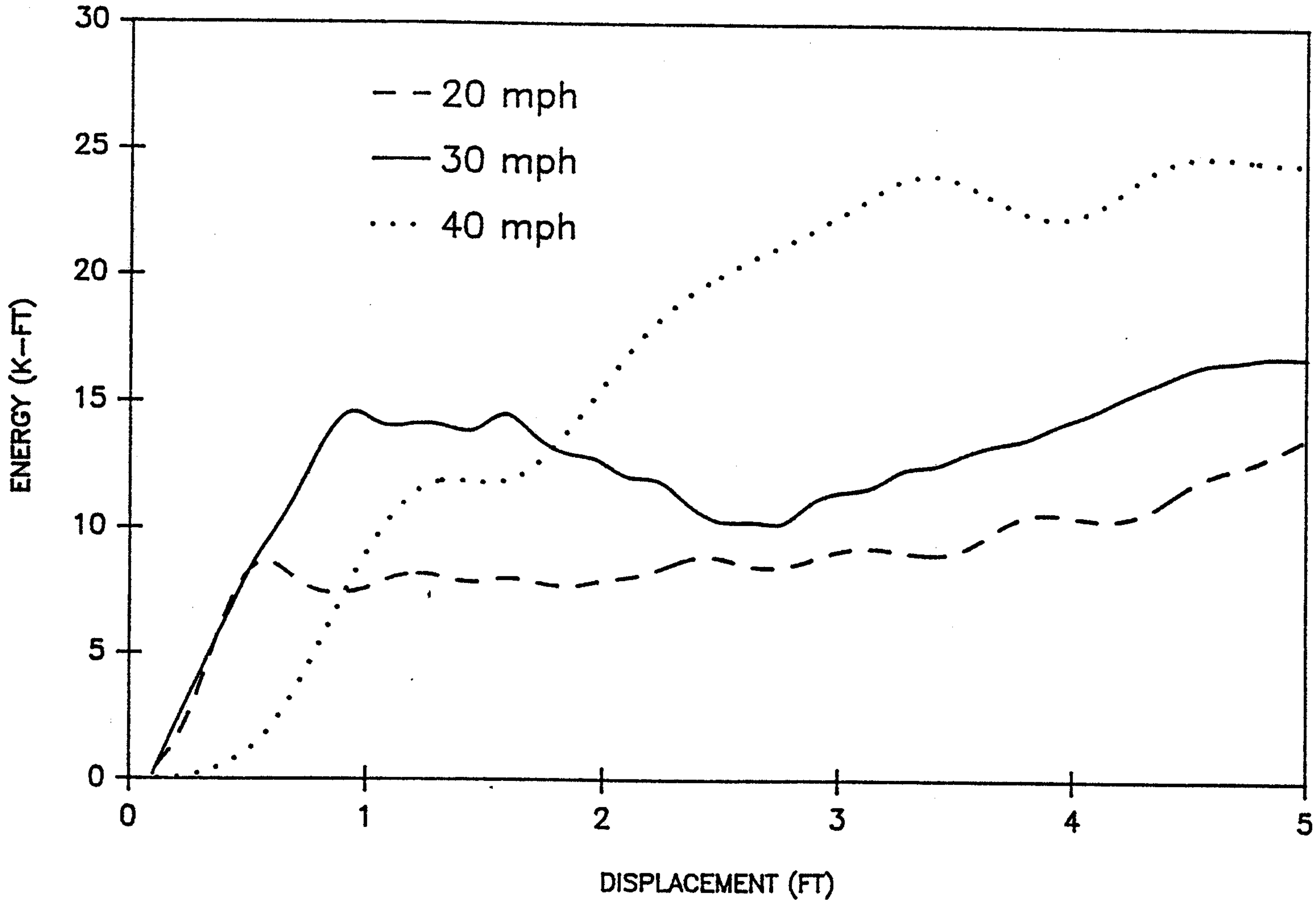

FIGURE 38. ENERGY DISSIPATION FOR PRELIMINARY SPLIT RAIL CRASH TESTS

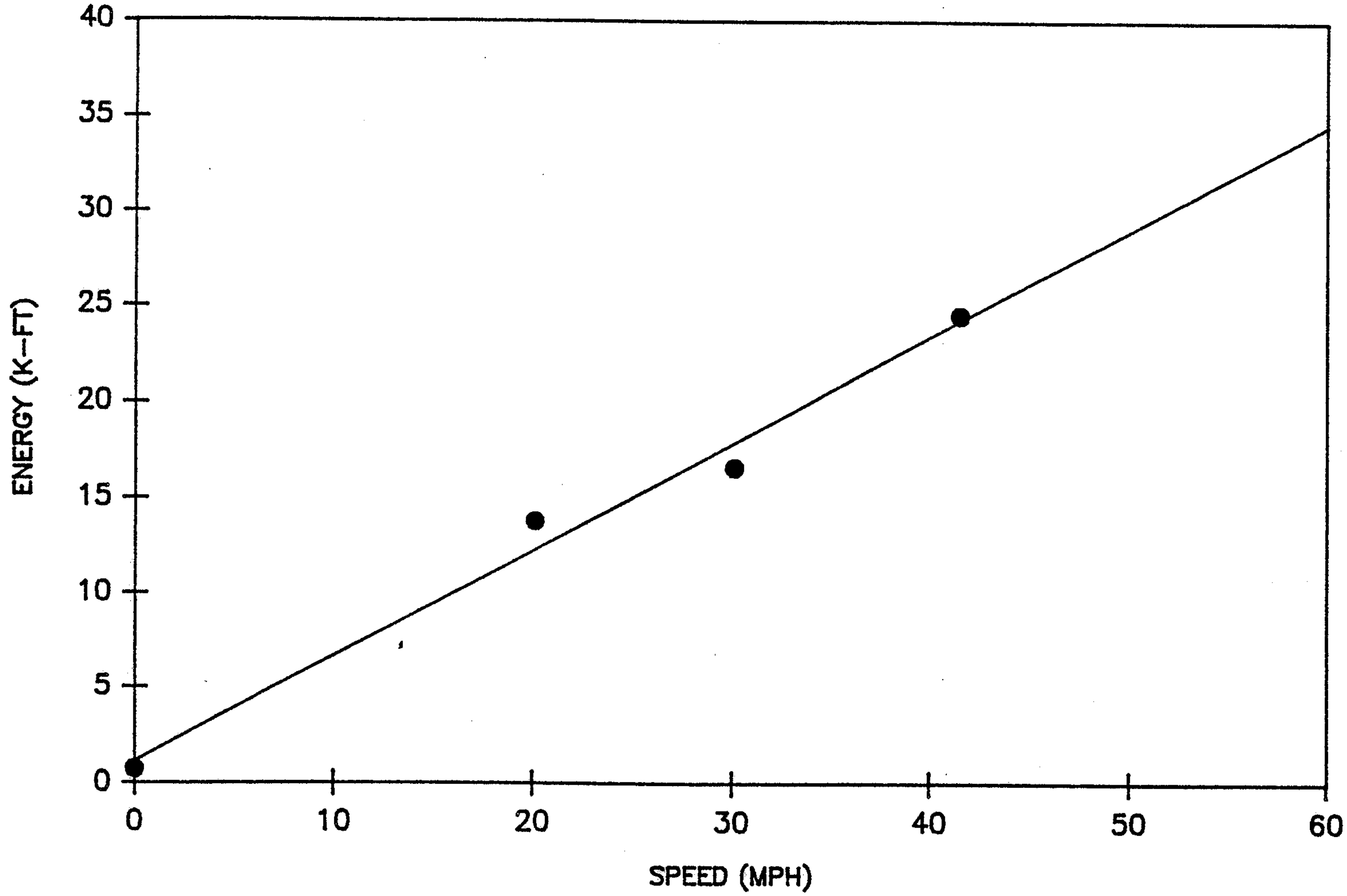

FIGURE 39. RELATIONSHIP BETWEEN ENERGY DISSIPATION AND IMPACT SPEED FOR 5FT SLOTTED RAIL SECTIONS

segments in each of the first 8 guardrail spans. Guardrail post spacing was a standard 6.25 ft. and the first post was placed in a concrete footing. A standard BCT cable anchor was incorporated to develop tensile strength in the W-beam. The test installation is shown in Figure 40. Test SRP-4 involved a full size automobile impacting the guardrail at 50 mph and 25 degrees. Upon impact with the barrier, the test vehicle's bumper pushed through a slotted section of rail and began to extend the slot. The W-beam then fractured when the slot was extended into a splice, and the test vehicle penetrated the barrier and rolled onto its top.

Thus, it was concluded that the split rail concept was not feasible in its original form. The problem with the original concept arises when a vehicle impacts the side of the rail and protrudes through a slotted section. No forces are generated to push the vehicle out of the slot and when the vehicle reaches the end of a slotted region, one of the slots will be extended until the beam breaks. Thus the only solution to this problem was to shield the slotted sections from vehicle penetration. This was accomplished with a cover plate as shown in Figure 41. The cover plate is firmly attached to one end of the slotted segment through welds or bolts. The other end of the cover plate is attached to the guardrail with clips that can slide relative to the W-beam, thereby allowing the slots to collapse under axially compressive loading. The clips are designed to prevent cover plate snagging on vehicles impacting the guardrail from the opposite direction. Although this design is considered adequate to prevent the aforementioned snagging, and the consequences of such snagging are not believed to be severe, the performance of this system when impacted from the opposite direction can only be verified through full scale crash testing.

Additional static and pendulum testing of slotted W-beam specimens was then undertaken to determine effects of the cover plates on buckling characteristics. Static testing was conducted with both welded and bolted cover plates and results are presented in Table 4. Note that measured maximum buckling loads were much less uniform than previous test results. Thus it was concluded that cover plates made static buckling of slotted W-beam a much less controlled event. Specimens tested with welded cover plates had longer slot lengths and generally high buckling loads. Thus, welded cover plates were believed to have more effect on buckling behavior than bolted cover plates. Further, bolting the cover plates was believed to be a less expensive alternative and therefore bolted cover plates were used for all remaining development efforts.

Pendulum testing was conducted on three cover plated specimens with 27 in. slot lengths. As shown in Figure 42, dynamic energy dissipation of cover plated specimens appeared to be much more controlled than corresponding static buckling loads. When these results are compared with results from the previous pendulum tests, shown in Figures 35 and 36, the cover plates can

FIGURE 40. INSTALLATION FOR TEST SRP-4.

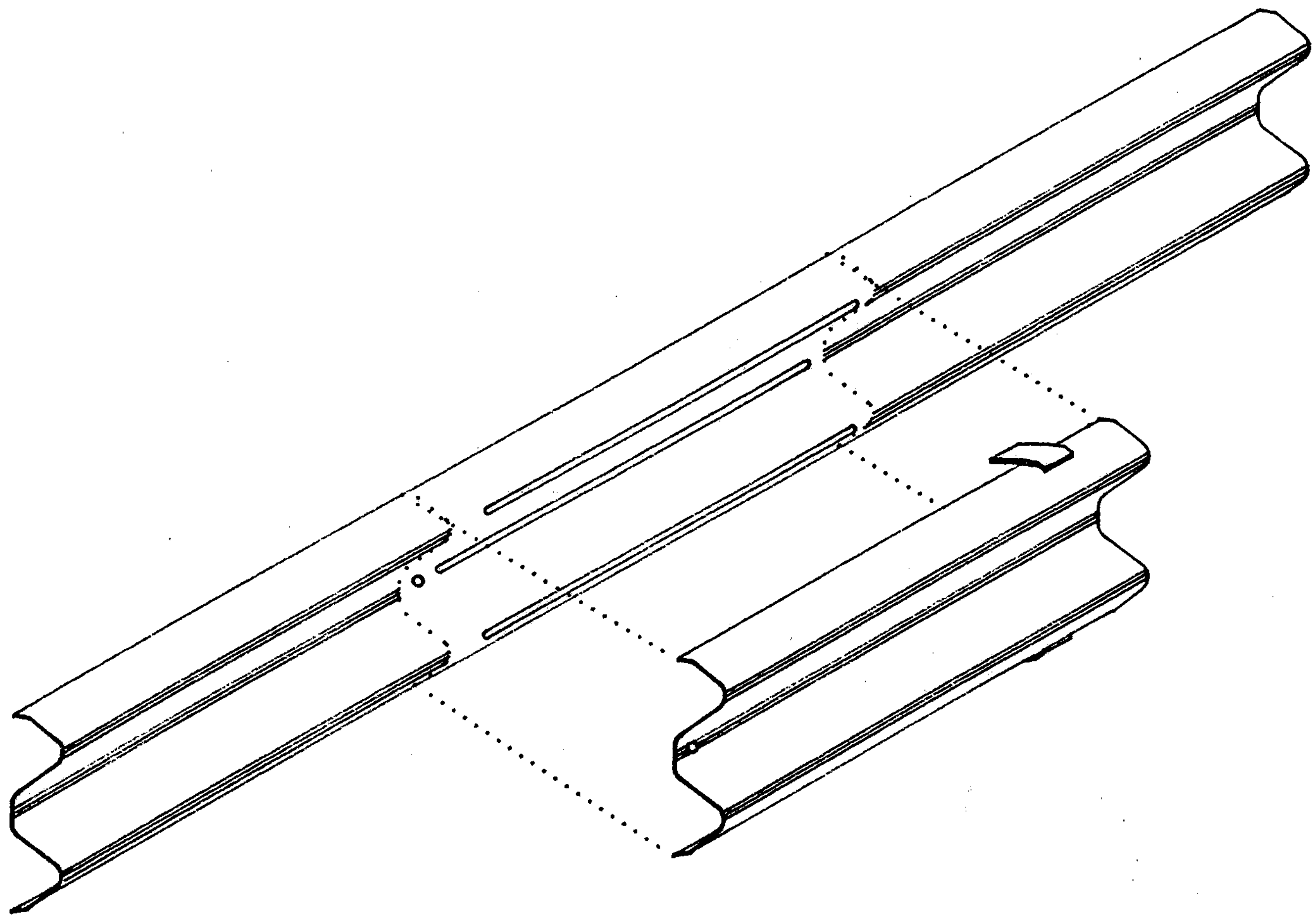

FIGURE 41. COVER PLATE CONCEPT.

TABLE 4. STATIC TESTS OF COVER PLATED SPLIT RAIL

SLOT LENGTH (inches)	COVER PLATE ATTACHMENT	BUCKLING LOAD (lbs)
36	welded	32,000
30	welded	24,000
30	welded	25,000
27	bolted	28,500
27	bolted	35,500
27	bolted	32,000
27	bolted	28,500
27	bolted	22,500
27	bolted	24,600

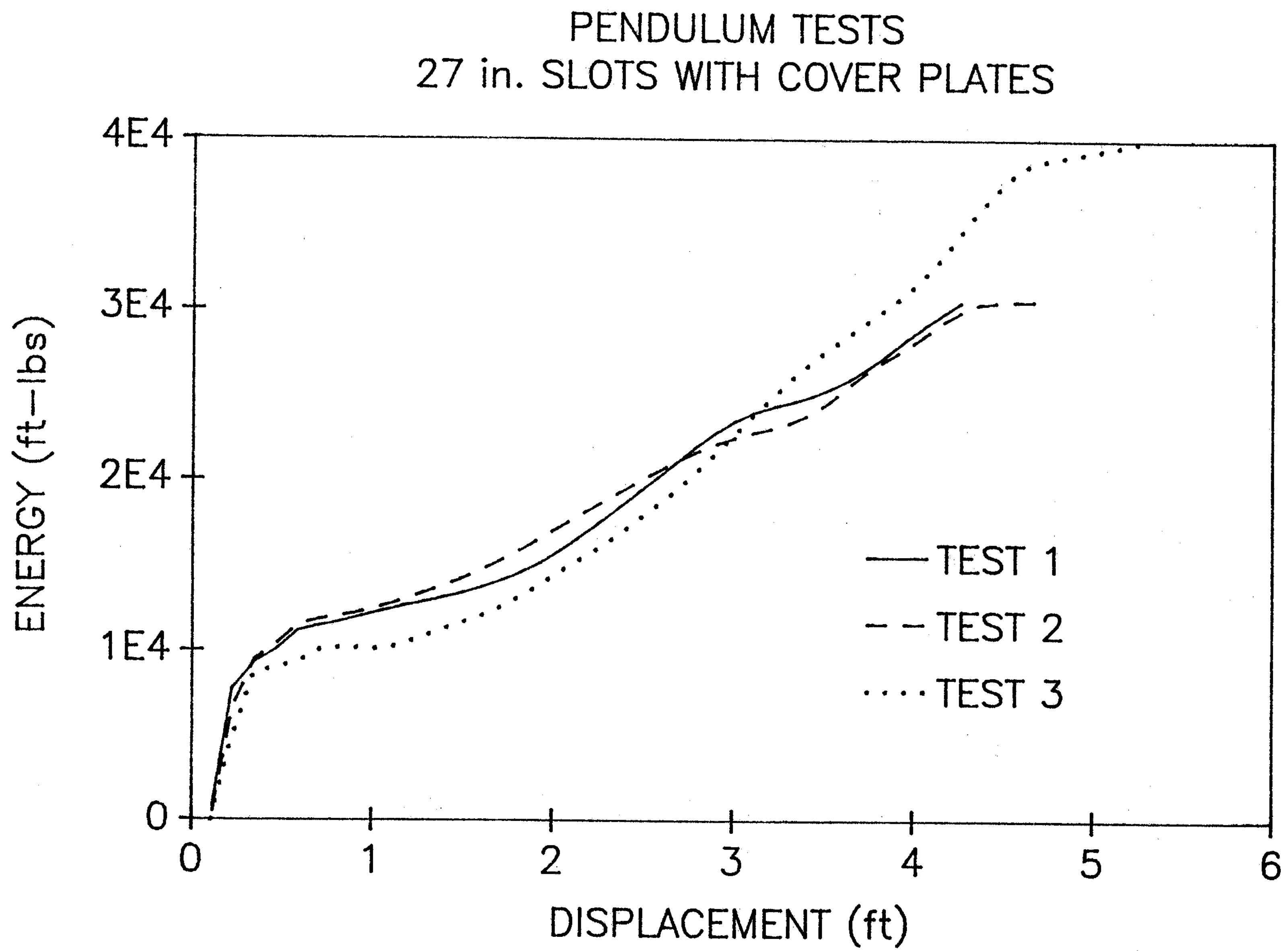

FIGURE 42. PENDULUM TEST RESULTS OF COVER PLATED SPECIMENS.

be shown to increase the dynamic energy dissipation of the split rail by approximately 30 percent.

Terminal Design

Based on results of static and dynamic testing, it was concluded that a mini-size automobile impacting at 60 mph. could safely collapse a W-beam rail with 27 in. slots and a bolted cover plate. Therefore a tangent terminal design was developed utilizing 27 in. slotted segments with bolted cover plates over the first 8 guardrail spans. A BCT cable anchor system attached to a 6 in. x 8 in. rectangular wood post set in a concrete foundation was used to provide tensile capacity for the W-beam. A BCT buffer section was wrapped around the end of the terminal to distribute impact forces over the front of the impacting vehicles. Round wood posts, weakened in the same manner as those used in the guardrail extruder terminal were used over the first 50 ft. of the barrier. The ground line cable developed for use with the GET was also employed to prevent rotations of posts 2, 3, and 4. The tangent terminal design is shown in Figure 43.

Test SR-1 - There was some concern over the capability of the split rail to fail sequentially as designed, without allowing impacting vehicles to dive under or ramp over the end treatment. Therefore head-on impact characteristics of the tangent terminal were investigated with a full-size vehicle impacting at 60 mph. Upon impact the end of the guardrail was pushed down and the test vehicle ramped over the top of the end treatment. Figure 44 summarizes this test.

A review of test films indicated that the cover plated slotted sections formed a hinge point to allow the guardrail to rotate down. An unslotted segment of guardrail that was bolted to a post then formed a ramp with sufficient strength to launch the impacting vehicle. The only possible method of preventing this type of behavior is to improve the moment capacity of the slotted segments of rail. Moment capacity in the slotted region might be improved by using three bolts to attach the cover plates rather than one. However, due to time and funding constraints, this potential solution could not be properly evaluated.

A flared terminal design was then developed to eliminate problems associated with vehicle ramping over the tangent terminal. The flared design incorporated a parabolic flare over the last 37.5 ft. of guardrail. The end of the barrier was offset 4 ft. laterally from the tangent guardrail section. Slotted W-beam sections, with 27 in. long slots, were placed between each of the first five posts. Weakened round wood posts were used in post positions 2 through 5. The first five posts were blocked out with standard 6 in. blockouts. The sixth post was fitted with a 3 in. blockout to facilitate the transition from the blocked-out system to the standard Texas guardfence. All other features of the terminal were the same as the tangent

FIGURE 43. INSTALLATION FOR TEST SR-1.

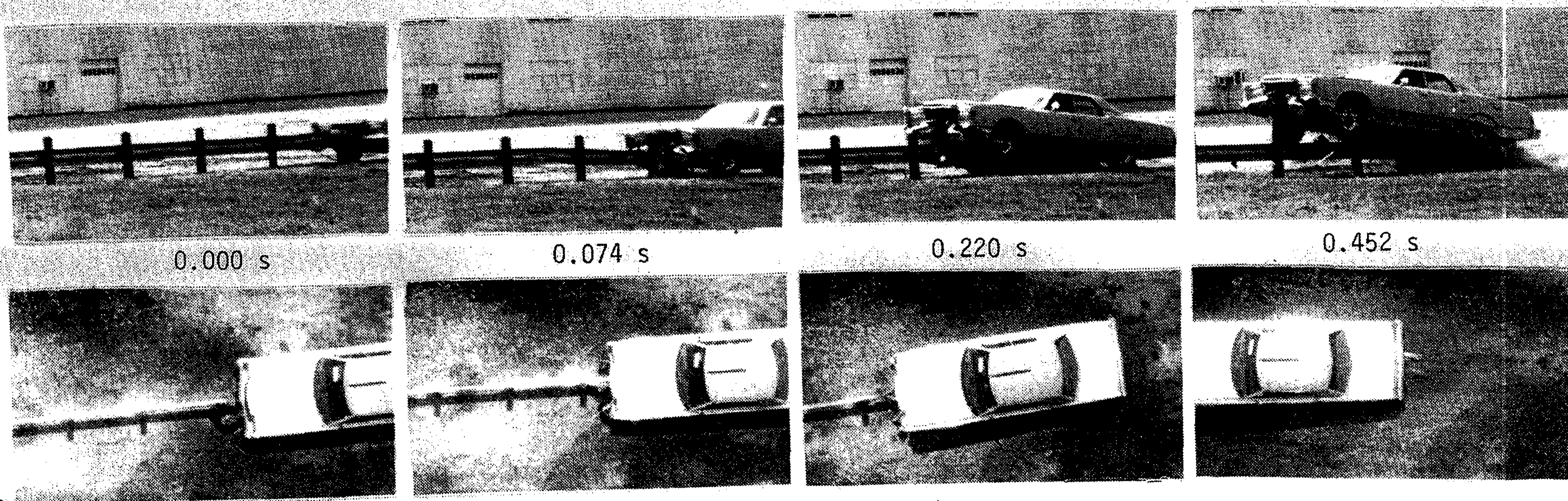

Test No	2404-SR1	Impact Speed	61.2 mi/h (98.5 km/h)
Date.	7/2/87	Impact Angle	0 deg - center
Test Installation	Split Rail End Treatment	Exit Speed	Not available
Length of Installation. . . .	100 ft (3.5 m)	Vehicle Accelerations (Max. 0.050-sec Avg)	
Vehicle	1978 Mercury	Longitudinal	-4.7 g
Vehicle Weight		Lateral.	-1.2 g
Test Inertia.	4,600 lb (2,088 kg)	Occupant Impact Velocity	
Gross Static.	4,765 lb (2,163 kg)	Longitudinal	19.2 ft/s (5.8 m/s)
Vehicle Damage Classification		Lateral.	None
TAD	12FC3	Occupant Ridedown Accelerations	
CDC	12FCEW2	Longitudinal	-9.4 g
Max. Rail Deformation	16.7 ft (5.1 m)	Lateral.	No Contact

FIGURE 44. SUMMARY OF RESULTS FOR TEST SR-1.

terminal. The flared split rail design is shown in Figure 45 Detailed construction drawings of the first flared split rail design are presented in Figure E-2, in appendix E.

Compliance Testing

Four compliance tests are required by NCHRP 230 for evaluation of safety performance of a barrier end treatment (12). Due to one test failure, a total of five compliance tests of the split rail terminal were conducted. These tests are summarized in Table 5 and discussed briefly below. Each test is reported in greater detail in appendix A. Angular displacement plots from the tests are presented in appendix C and sequential photos are shown in appendix D.

Test SR-2 - The flared split rail terminal was first tested with a mini-size automobile impacting the end treatment head-on at 60 mph. The vehicle was offset 15 in. from the center of the end treatment toward the traffic side of the barrier. This offset was intended to investigate the propensity for the test vehicle to yaw clockwise and strike the unmodified guardrail section. The test vehicle penetrated through the end of the terminal at a relatively low speed after fracturing the first and second posts. The slotted rail segments performed as intended and although the longitudinal occupant impact velocity was somewhat above recommended limits (12), it was well below the maximum allowable limit. Since very few end treatments can meet recommended occupant impact velocity limits and the post impact trajectory of the vehicle was good, this test was considered to be a success. Figure 46 summarizes this test.

Test SR-3 - The capacity of the split rail terminal for redirecting vehicles impacting at the LON was then examined. In an effort to reduce the potential for wheel snag, the blocked-out rail section was extended to include the first eight posts. For this test a full-size sedan impacted the barrier 12.5 ft. from the end at 60 mph and 25 deg. Upon impact, the test vehicle began to redirect and was traveling parallel to the barrier when an unmodified guardrail section fractured at a splice. The test vehicle then yawed away from the barrier and the driver's side was impaled on the broken guardrail end. Test SR-3 is summarized in Figure 47.

Tensile forces generated in a flared guardrail section are known to be near the ultimate strength of 12 ga. W-beam. The additional deflection allowed by the slotted rail segment may have been sufficient to overload downstream guardrail segments. The lateral strength of the terminal was therefore improved by adding two additional posts between posts 3 and 5. The modified split rail terminal is shown in Figure 48. Figure E-3 in appendix E shows construction drawings for the modified flared terminal design.

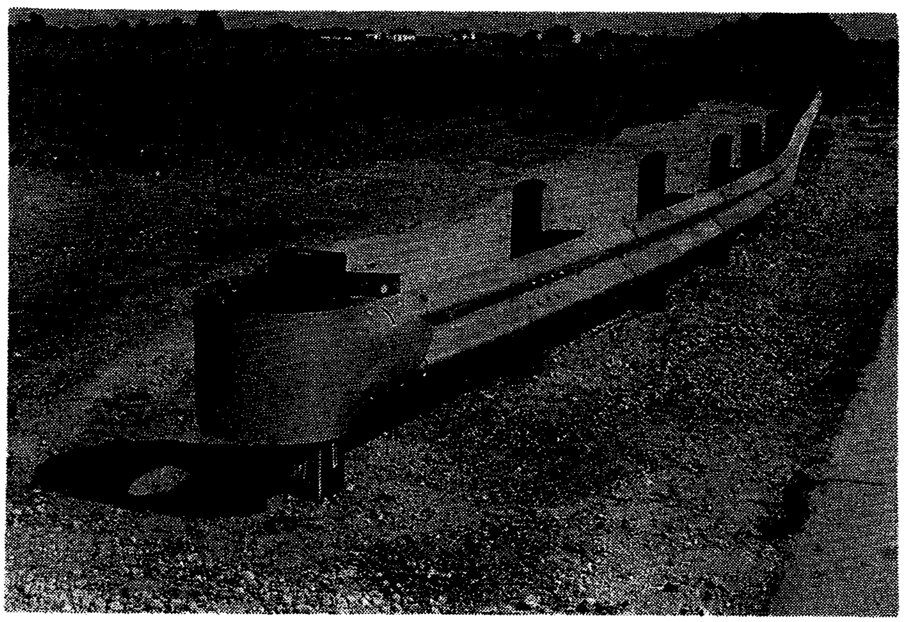

FIGURE 45. INITIAL SPLIT RAIL END TREATMENT.

TABLE 5. SUMMARY OF SPLIT RAIL TERMINAL CRASH TESTS.

TEST NO.	VEHICLE WEIGHT (lbs)	IMPACT CONDITIONS			INSTALLATION	TEST RESULTS				COMMENTS
						OCCUPANT IMPACT		RIDEDOWN ACCELERATION		
		SPEED (mph)	ANGLE (deg)	OFFSET (in.)		LONG. (ft/sec)	LAT. (ft/sec)	LONG. (G's)	LAT. (G's)	
SR-1	4,600	61.2	0	0	Tangent Terminal	19.2	0	9.4	0	Vehicle launched over rail
SR-2	1,750	58.2	0	15	Fig. E2	35.1	9.8	10.7	4.5	Vehicle decelerated to a stop
SR-3	4,508	61.3	25	0	Fig. E2	21.1	13.4	11.3	14.5	Vehicle penetrated the barrier
SR-4	4,463	60.3	25	0	Fig. E3	20.9	17.2	6.3	9.1	Vehicle redirected smoothly
SR-5	1,810	63.3	15	0	Fig. E3	19.2	23.7	1.8	13.8	Vehicle redirected smoothly
SR-6	4,470	60.0	0	0	Fig. E3	17.4	5.3	5.8	3.1	Controlled penetration of the end

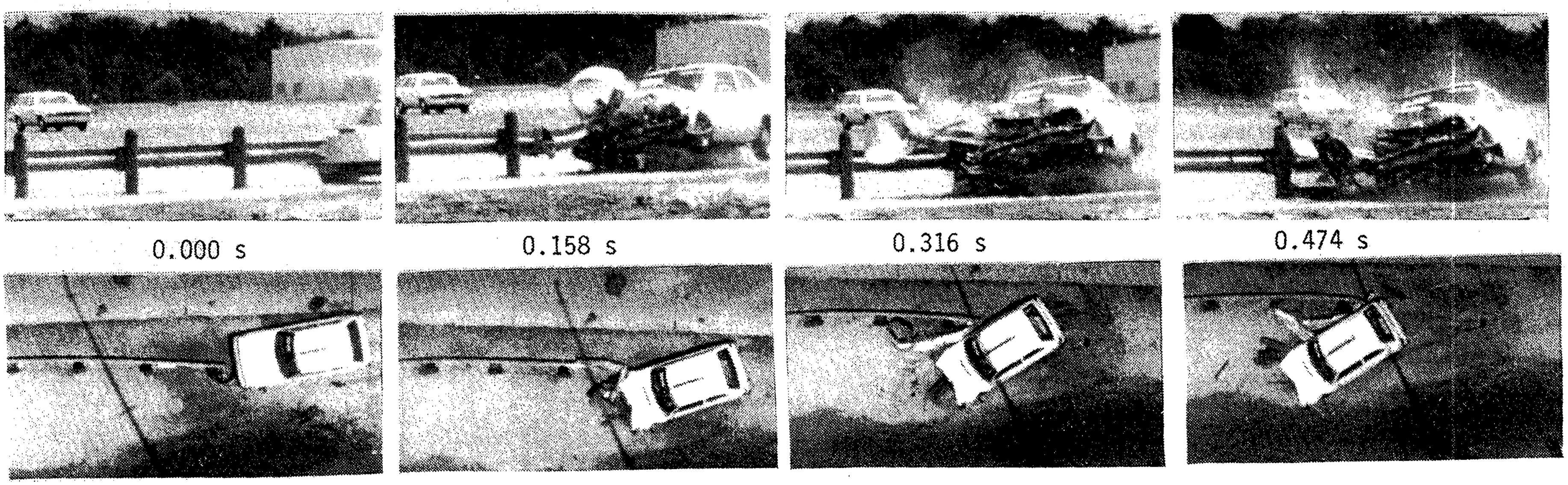

Test No	2404-SR2
Date	8/4/87
Test Installation	Split Rail End Treatment
Length of Installation	100 ft (3.5 m)
Vehicle	1979 Honda
Vehicle Weight	
Test Inertia	1,750 lb (795 kg)
Gross Static	1,917 lb (870 kg)
Vehicle Damage Classification	
TAD	12FR4
CDC	12FZEW3
Max. Rail Deformation	12.4 ft (3.8 m)

Impact Speed	58.2 mi/h (93.6 km/h)
Impact Angle	0 deg - 15" offset
Exit Speed	19.1 mi/h (30.7 km/h)
Vehicle Accelerations (Max. 0.050-sec Avg)	
Longitudinal	-15.4 g
Lateral	4.0 g
Occupant Impact Velocity	
Longitudinal	35.1 ft/s (10.7 m/s)
Lateral	9.8 ft/s (3.0 m/s)
Occupant Ridedown Accelerations	
Longitudinal	-10.7 g
Lateral	4.5 g

FIGURE 46. SUMMARY OF RESULTS FOR TEST SR-2.

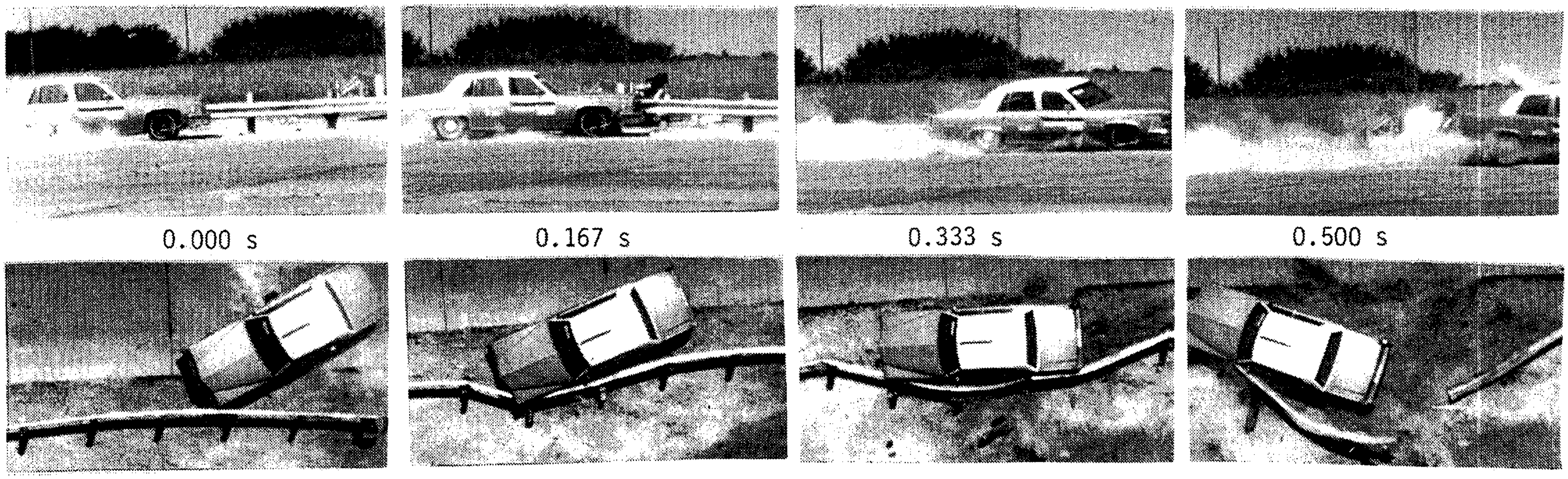

Test No	2404-SR3	Impact Speed	61.3 mi/h (98.6 km/h)
Date.	8/11/87	Impact Angle	25 deg
Test Installation	Split Rail End Treatment	Exit Speed	Not available
		Vehicle Accelerations (Max. 0.050-sec Avg)	
Length of Installation. . . .	100 ft (3.5 m)	Longitudinal	-7.9 g
Vehicle	1977 Cadillac	Lateral.	-5.0 g
Vehicle Weight		Occupant Impact Velocity	
Test Inertia.	4,508 lb (2,047 kg)	Longitudinal	21.1 ft/s (6.4 m/s)
Vehicle Damage Classification		Lateral.	13.4 ft/s (4.1 m/s)
TAD	11LFQ5	Occupant Ridedown Accelerations	
CDC	11FLEK2/11LYAS3	Longitudinal	-11.3 g
Max. Rail Deformation	29.0 ft (8.8 m)	Lateral.	-14.5 g

FIGURE 47. SUMMARY OF RESULTS FOR TEST SR-3.

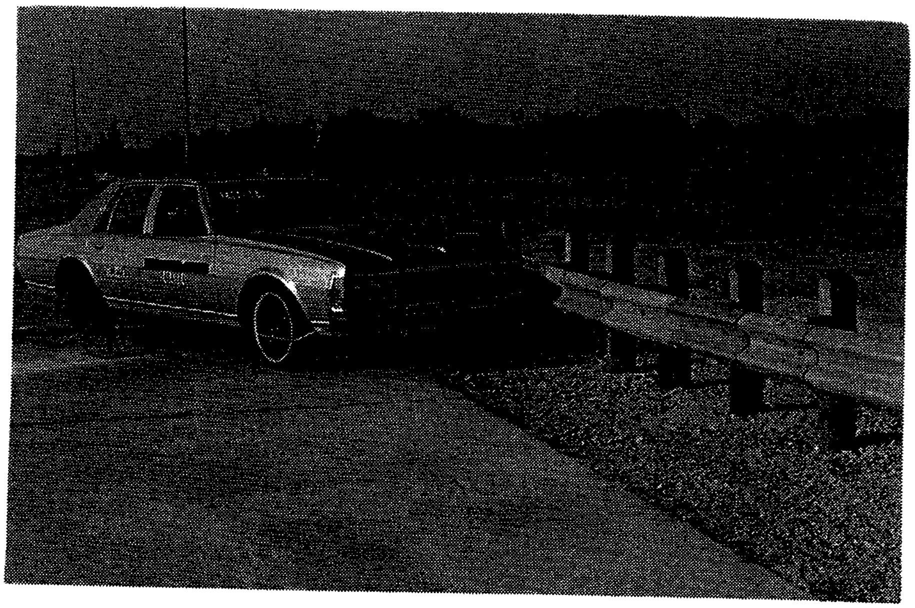

FIGURE 48. FINAL SPLIT RAIL END TREATMENT.

Test SR-4 - The previous test was then repeated on the modified flared split rail terminal. The test vehicle was smoothly redirected and all occupant impact severity measures were within recommended limits. Although the velocity change during this test was somewhat higher than safety standard recommendations, the performance of this barrier was similar to most other guardrail systems (14, 15, 16). Therefore this test was considered to be a success. Figure 49 summarizes test SR-4.

Test SR-5 - Test SR-5 investigated the performance of the terminal for mini-size vehicles impacting the side of the barrier upstream from the beginning of the length of need. This test involved a mini-size vehicle impacting the terminal near the second post at 60 mph and 15 deg. The test vehicle was smoothly redirected with no tendency for wheel snag. Although the lateral occupant impact velocity was higher than the recommended limit, it was below the maximum allowable limit and the test was still considered to be a success. This test is summarized in Figure 50.

Test SR-6 - The final compliance test involved a full-size vehicle impacting the end of the terminal head-on at 60 mph. Upon impact the first three posts were fractured and the test vehicle penetrated the barrier in a controlled manner. The vehicle then traveled parallel to the barrier for approximately 100 ft. before coming to rest. All measures of end treatment performance were within recommended limits and the test was a success. Figure 51 summarizes test SR-6.

Summary

The split rail terminal (SRT) has been fully tested and was shown to meet nationally recognized safety standards (12). This end treatment should be very inexpensive to construct. Major costs associated with the device include cutting longitudinal slots in the W-beam, steel W-beam cover plates, BCT cable anchor assembly, and a 6 in. x 8 in. rectangular post with a concrete footing. The total costs of these materials should not be more than $500. Further, installation costs should be only moderately more than costs associated with the BCT end treatment and the total cost of the system should not be more than $750. Thus, whenever sufficient space is available for a 4 ft. flared end treatment, this design should offer an inexpensive and safe alternative to the BCT. Finally, the design is quite similar to standard BCT designs and retrofit of an existing BCT installation would be very inexpensive.

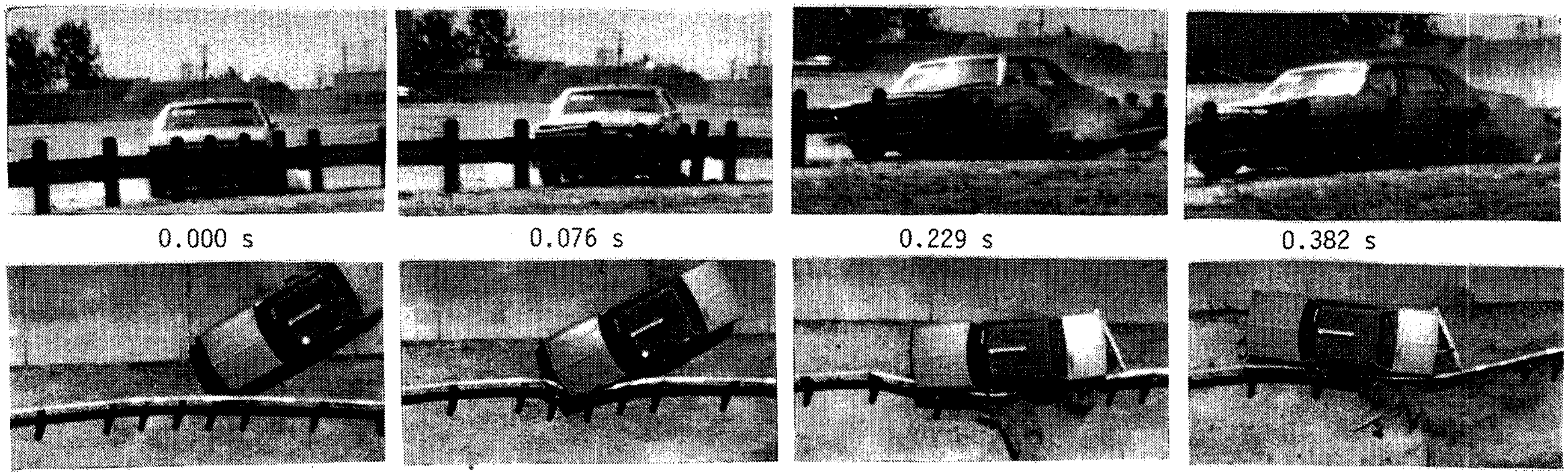

Test No	2404-SR4
Date	8/14/87
Test Installation	Split Rail End Treatment
Length of Installation	100 ft (3.5 m)
Vehicle	1977 Chevrolet
Vehicle Weight	
Test Inertia	4,463 lb (2,206 kg)
Vehicle Damage Classification	
TAD	11LFQ4
CDC	11FLEK2/11LYES2
Max. Rail Deformation	26.2 ft (8.0 m)

Impact Speed	60.3 mi/h (97.0 km/h)
Impact Angle	25 deg
Exit Speed	39.4 mi/h (63.4 km/h)
Vehicle Accelerations (Max. 0.050-sec Avg)	
Longitudinal	-4.6 g
Lateral	-6.4 g
Occupant Impact Velocity	
Longitudinal	20.9 ft/s (6.4 m/s)
Lateral	17.2 ft/s (5.2 m/s)
Occupant Ridedown Accelerations	
Longitudinal	-6.3 g
Lateral	-9.1 g

FIGURE 49. SUMMARY OF RESULTS FOR TEST SR-4.

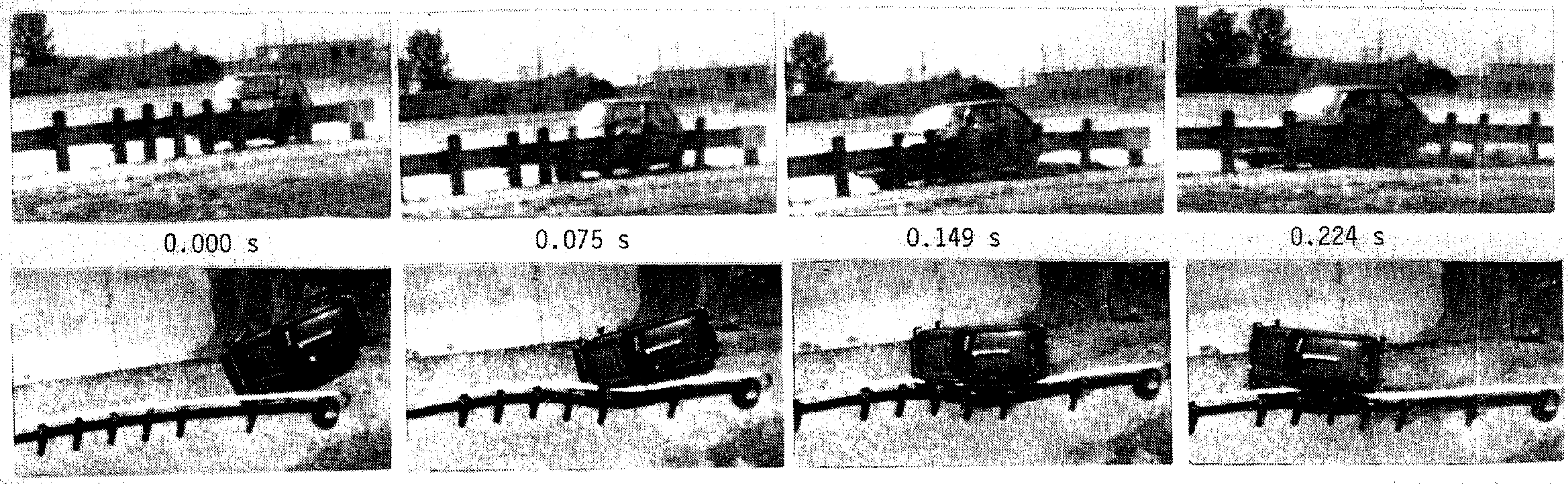

Test No	2404-SR5
Date.	8/20/87
Test Installation	Split Rail End Treatment
Length of Installation. . . .	100 ft (3.5 m)
Vehicle	1979 Honda
Vehicle Weight	
Test Inertia.	1,810 lb (822 kg)
Gross Static.	1,981 lb (899 kg)
Vehicle Damage Classification	
TAD	11LFQ4
CDC	11FLEK2/11LFES3
Max. Rail Deformation	13.9 ft (4.2 m)

Impact Speed	63.3 mi/h (101.8 km/h)
Impact Angle	15 deg
Exit Speed	53.1 mi/h (85.4 km/h)
Vehicle Accelerations (Max. 0.050-sec Avg)	
Longitudinal	-6.2 g
Lateral.	-9.9 g
Occupant Impact Velocity	
Longitudinal	19.2 ft/s (5.9 m/s)
Lateral.	23.7 ft/s (7.2 m/s)
Occupant Ridedown Accelerations	
Longitudinal	-1.8 g
Lateral.	-13.8 g

FIGURE 50. SUMMARY OF RESULTS FOR TEST SR-5.

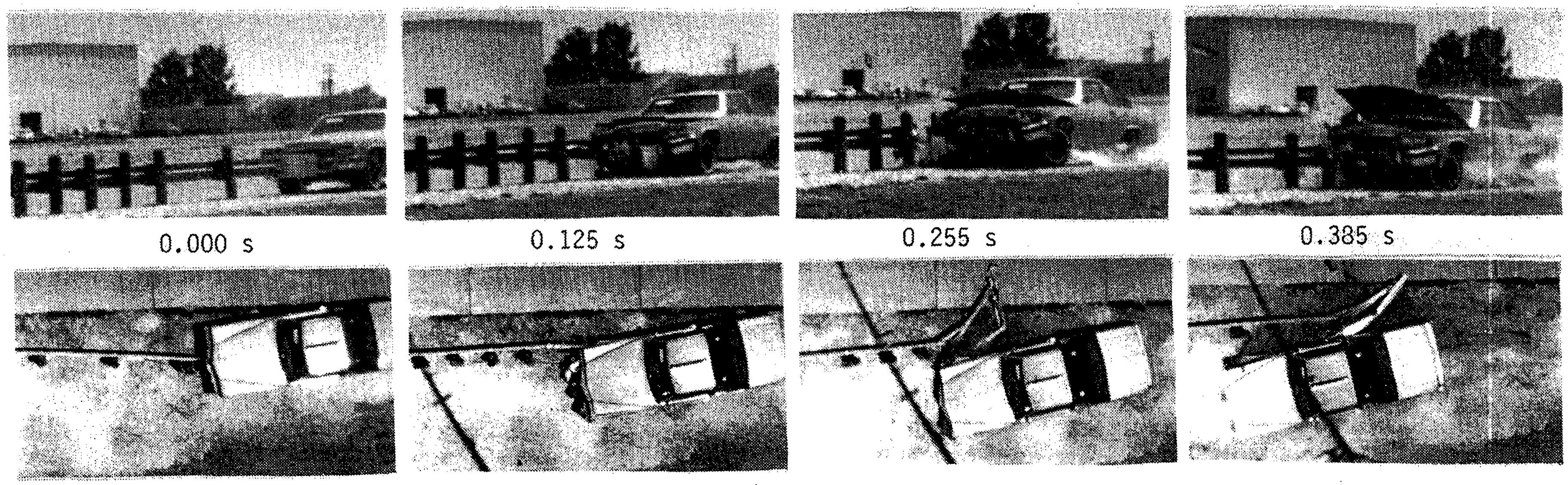

Test No	2404-SR6
Date	8/25/87
Test Installation	Split Rail End Treatment
Length of Installation	100 ft (3.5 m)
Vehicle	1979 Cadillac
Vehicle Weight	
Test Inertia	4,470 lb (2,029 kg)
Vehicle Damage Classification	
TAD	12FR4
CDC	12FYEW3
Max. Rail Deformation	18.9 ft (5.8 m)

Impact Speed	60.0 mi/h (96.5 km/h)
Impact Angle	0 deg - center
Exit Speed	44.3 mi/h (71.3 km/h)
Vehicle Accelerations (Max. 0.050-sec Avg)	
Longitudinal	-5.5 g
Lateral	-2.5 g
Occupant Impact Velocity	
Longitudinal	17.4 ft/s (5.3 m/s)
Lateral	5.3 ft/s (1.6 m/s)
Occupant Ridedown Accelerations	
Longitudinal	-5.8 g
Lateral	-3.1 g

FIGURE 51. SUMMARY OF RESULTS FOR TEST SR-6.

VI. CONCLUSIONS AND RECOMMENDATIONS

The guardrail extruder terminal and the split rail terminal described herein represent major improvements over existing end treatment alternatives. Both terminal designs have been added to the relatively short list of guardrail end treatments that have met nationally recognized safety standards. Further, at approximately $1200 for the GET and $750 for the SRT, these systems should be among the most inexpensive of the "safe" end treatments. Both systems should be simple to construct and relatively insensitive to installation details. The GET is the first inexpensive terminal that can be safely installed on a tangent and attenuate vehicles impacting head-on. Finally, key elements of the GET have been shown to be extremely durable and the system should therefore be inexpensive to maintain and repair.

In addition, individual components of the terminals described herein will reduce costs associated with other safety devices. For example the groundline cable used to weaken wooden posts will eliminate the need for concrete foundations used in many end treatment designs. Both the split rail and extruder concepts should find other applications in highway safety area.

Both the guardrail extruder terminal and the split rail terminal should be approved for installation in the field on an experimental basis. Construction activities and accident histories should be monitored to quickly identify any remaining construction, maintenance, or safety problems. Subject to acceptable field experience, these systems should be approved as operational terminals.

REFERENCES

1. Michie, Jarvis D. and Bronstad, M. E, "Guardrail Performance: End Treatments," Report of Southwest Research Institute, August 1969.

2. Nordlin, Eric F., Field, Robert N., and Folsom, J. J., "Dynamic Tests of Short Sections of Corrugated Metal Beam Guardrail," Highway Research Record No. 259, Highway Research Board, 1969.

3. Buth, C. E., and Hirsch, T. J., "Improved End Treatment for Metal Beam Guardrail," Research Report 189-1 Texas Transportation Institute, Texas A&M University, College Station, Texas, Aug. 1977.

4. Hirsch, T. J., Dolf, T. J., and Arnold, Althea, "Maryland Turned-Down Guardrail Terminal," Research Report FHWA/RD 83/02, Texas Transportation Institute, Texas A&M University, College Station, Texas, August 1982.

5. Hinch, J. A., Owings, R. P., Manhard, G. A., "Safety Modifications of Turned-Down Guardrail Terminals," Research Report FHWA/RD-84/035, ENSCO, Inc., Springfield, VA., June 1984.

6. Michie, J. D., and Bronstad, M. E., "Guardrail Crash Test Evaluation - New Concepts and End Designs," NCHRP REPORT 129, Highway Research Board, 1972.

7. Pigman, Jerry G., and Agent, Kenneth R., "Performance Evaluation of Breakaway-Cable-Terminal End Treatments," Transportation Research Record, Transportation Research Board, Washington D. C., (in publication).

8. Kimball Jr., C. E., Bronstad, M. E., Meczkowski, L., "Evaluation of Guardrail Breakaway Cable Terminals," Research Report FHWA/RD-82/057, Southwest Research Institute, San Antonio, Texas, May 1982.

9. Bronstad, M. E., et al., "Crash Test Evaluation of Eccentric Loader Guardrail Terminals," Transportation Research Record No. 1065, Transportation Research Board, Washington D.C., 1986.

10. "SENTRE (Safety Barrier End Treatment)," NCHRP 230 Certification Report, Energy Absorption Systems, Inc., One East Wacker Drive, Suite 2500, Chicago, Illinois, May 1983.

11. Bronstad, M. E., et al., "Crash Test Evaluation of the Vehicle Attenuating Terminal (V-A-T)," Transportation Research Record, Transportation Research Board, Washington

D. C., (in publication).

12. Michie, Jarvis D., "Recommended Procedures for the Safety Performance Evaluation of Highway Appurtenances," NCHRP REPORT 230, Transportation Research Board, March 1981.

13. Syro Steel Co., 1170 N. State Street, Girard, Ohio.

14. Hirsch, T. J., Beggs, Dale, "Use of Guardrails on Low Fill Bridge Length Culverts," Transportation Research Record, Transportation Research Board, Washington D. C., (in publication).

15. Bronstad, M. E., Calcote, L. R., Ray, M. H., Mayer, J. B., "Guardrail-Bridge Rail Transition Designs," Research Report FHWA/RD-86/178, Southwest Research Institute, San Antonio, Texas, June 1986.

16. Bligh, Roger P., Sicking, Dean L., Ross Jr., Hayes E., "Development of a Strong Beam Guardrail to Bridge Rail Transition," Transportation Research Record, Transportation Research Board, Washington D. C., (in publication).

APPENDIX A.

GUARDRAIL EXTRUDER TERMINAL CRASH TESTS

TEST MB-1

This test was run to evaluate the performance of the extruder during a head-on impact with a big car. The first two posts were rectangular 6 in. x 8 in. wood posts, set in concrete. Both posts had a 2 3/8 inch diameter hole at ground level, parallel to the barrier. Posts 2 to 9 were 7 inch diameter weakened round posts. These posts also had a 2 3/8 inch diameter hole at ground level parallel to the barrier. All the remaining posts were 7 inch diameter wooden posts. The first post was not connected to the rail. Posts 2, 3 and 4 were connected to the rail with 5 inch lag screws. The extruder was mounted such that the rail was extruded away from the roadway. A modified cable anchor was used in conjunction with the extruder and is shown in Figure A-1. Figure A-2 shows the completed test installation.

A 4500 lb, 1978 Cadillac impacted at 0 degrees (centerline of vehicle) and 60.6 m.p.h. Upon impact, approximately 12 ft. of rail fed through the extruder. The vehicle then pushed the extruder out of its path and towards the roadside. The rail caught in the front right fender of the vehicle as it traveled parallel to, and behind of, the barrier - breaking a total of 12 posts. The weld on one side of the extruder failed during the test. Figure A-3 shows the barrier and extruder after Test MB-1. The vehicle before and after impact is shown in Figure A-4.

TEST MB-2

This test was run to evaluate the performance of the extruder during a head-on impact with a small car. The leading post was not connected to the rail. All other posts were bolted to the rail. Figure A-5 shows the 12 in. extruder and modified cable anchor.

A 1750 lb, 1979 Honda impacted the extruder at 0.0 degrees and 62.1 m.p.h. The centerline of the vehicle was offset 15 in. towards the roadway. Upon impact, the vehicle and extruder began to yaw. After approximately 6 ft. of rail feed, the yaw angle became large enough that a plastic hinge formed in the rail and caused it to stop feeding. The vehicle then bounced off the extruder and the second post and came to a stop behind the barrier. Barrier damage after the test is shown in Figure A-6. Figure A-7 shows the test vehicle before and after impact. The occupant impact velocity and the ridedown acceleration were 35.1 ft/sec and 14.2 g's respectively.

TEST MB-3

The first four posts were not connected to the rail in any manner. The extruder was mounted in such a way that the rail would be extruded towards the roadway. Both the first and the second posts were rectangular and set in concrete. The second post had a 2 3/8 inch diameter hole at ground level, parallel to the direction of the rail. To maintain the vertical stability of

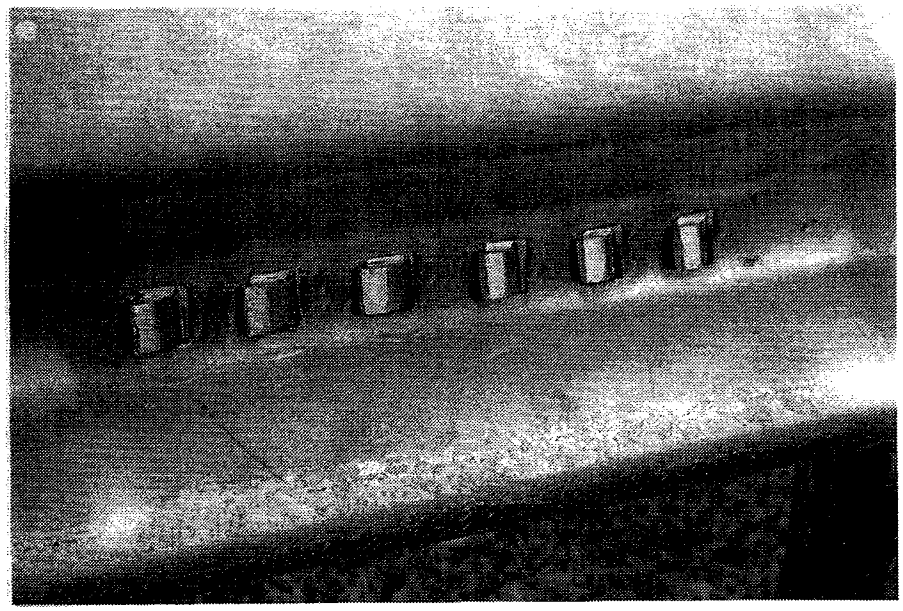

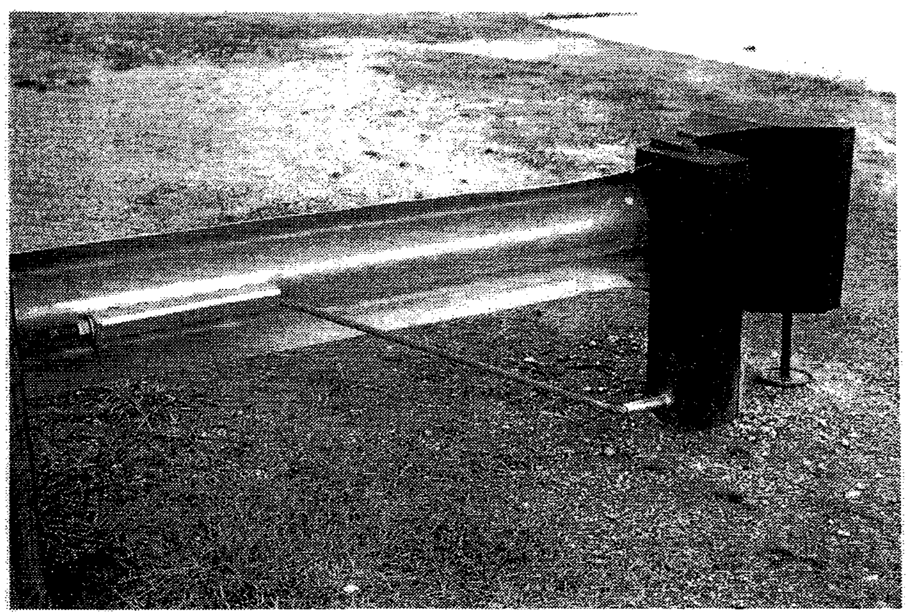

Fig. 45. Modified Cable Anchor Mounted on Guardrail (Test MB-1)

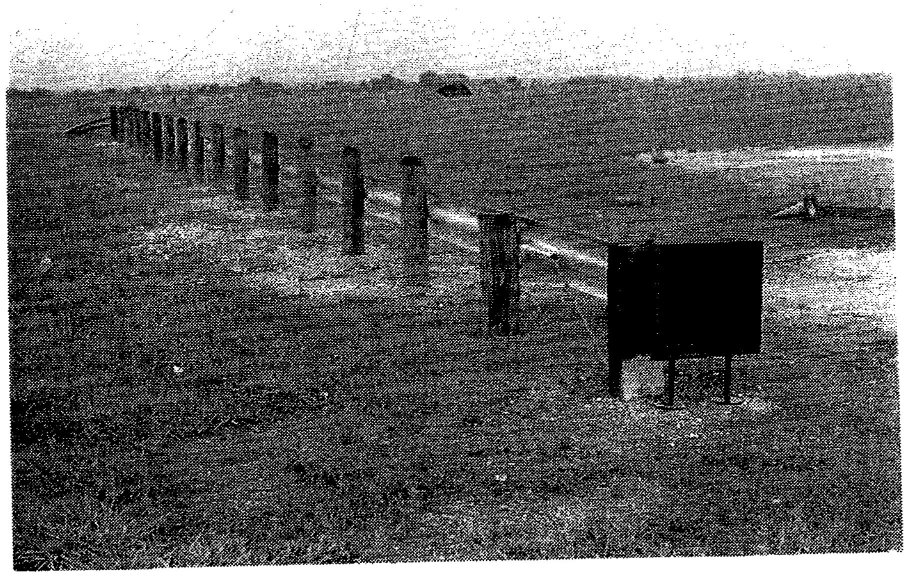

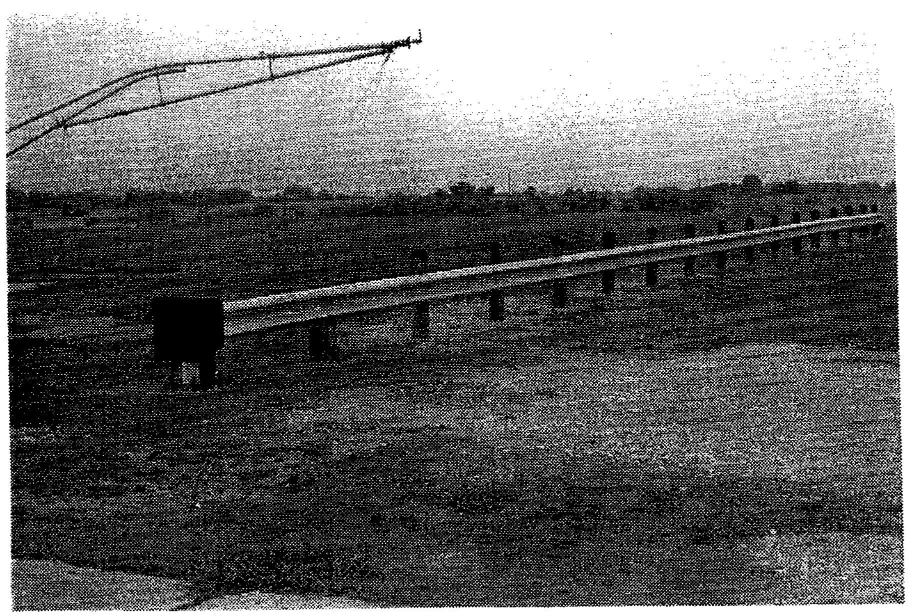

Fig. 46. Guardrail Extruder End Treatment Before Test MB-1

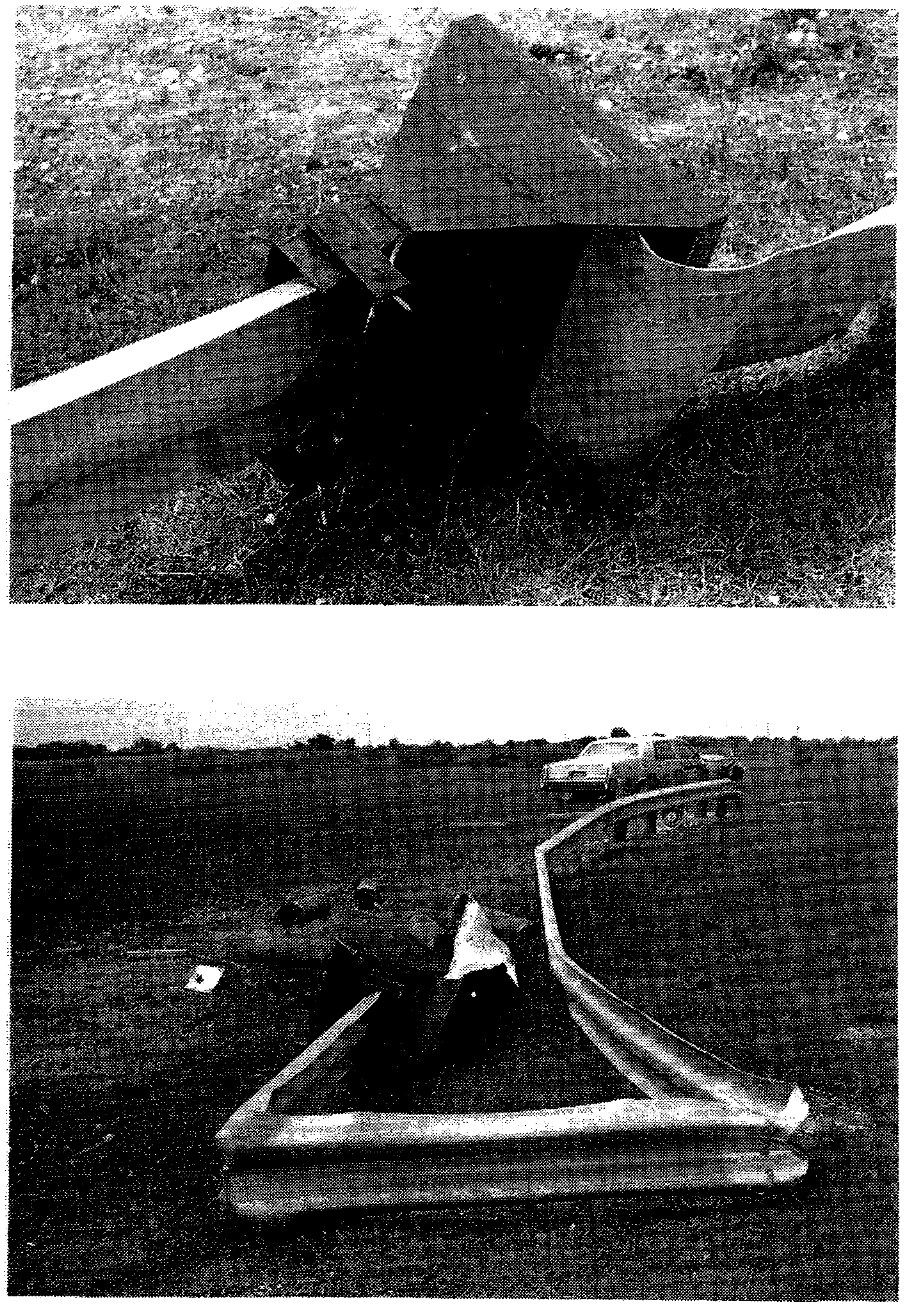

Fig. 47. Guardrail Extruder End Treatment After Test MB-1

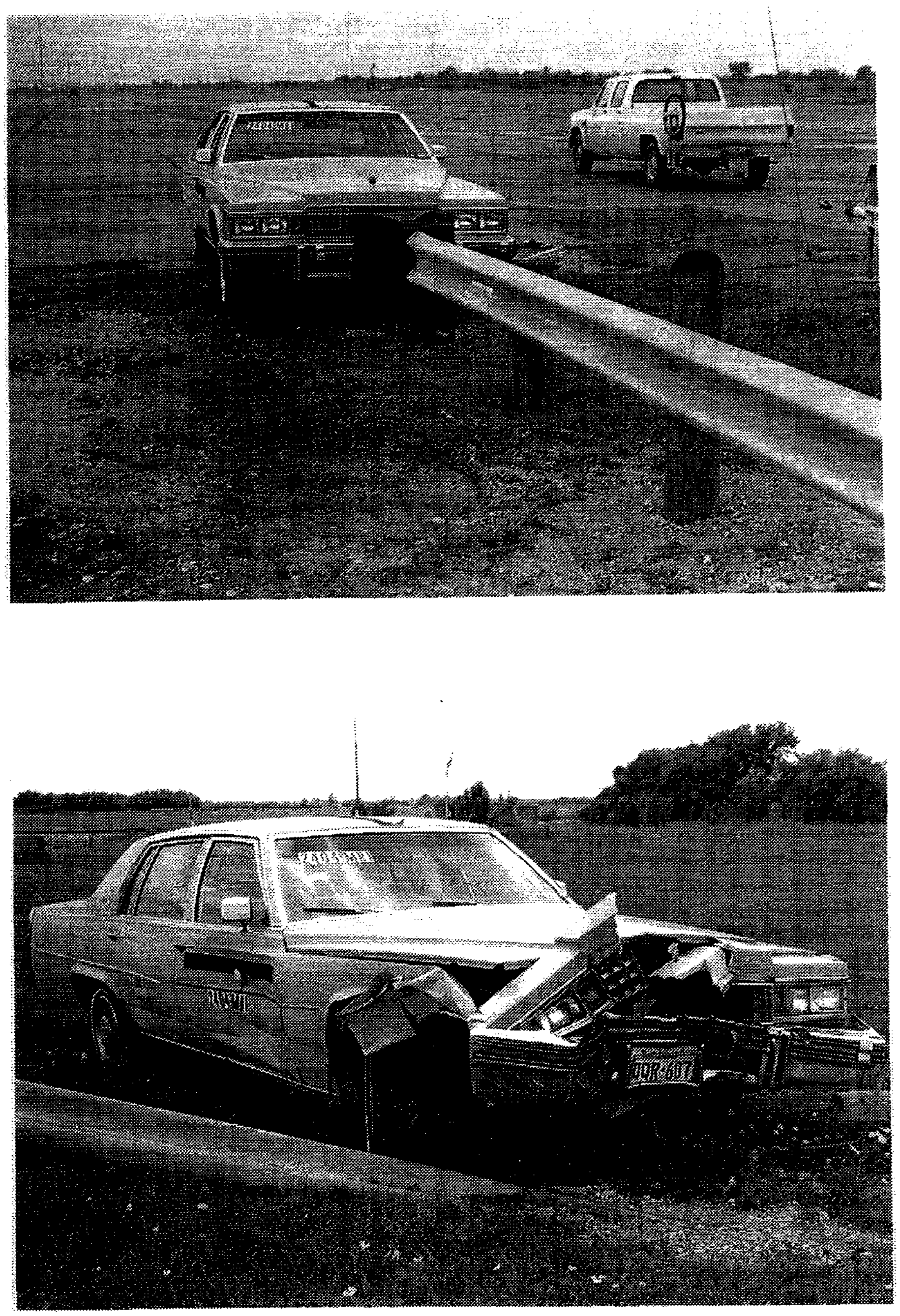

Fig. 48. Vehicle Before And After Test MB-1

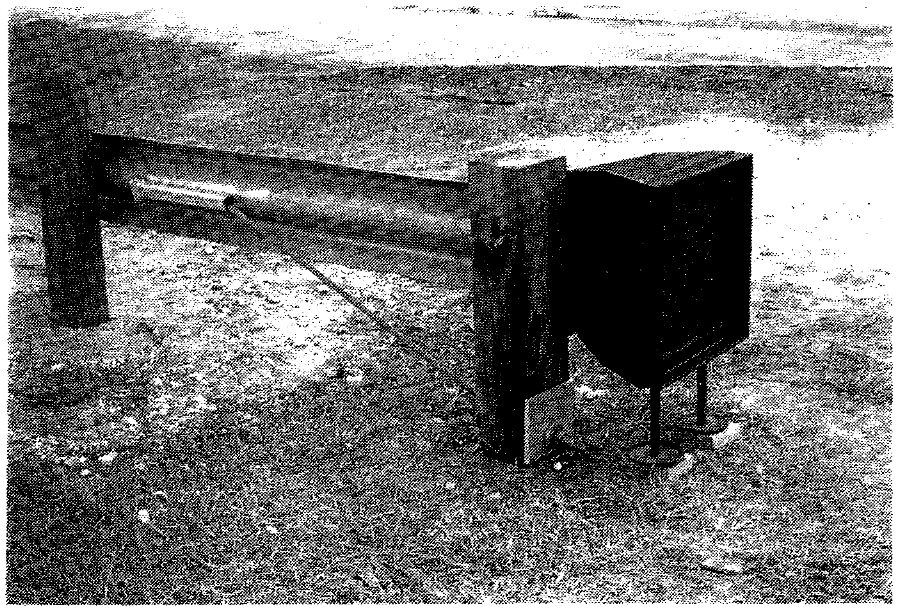

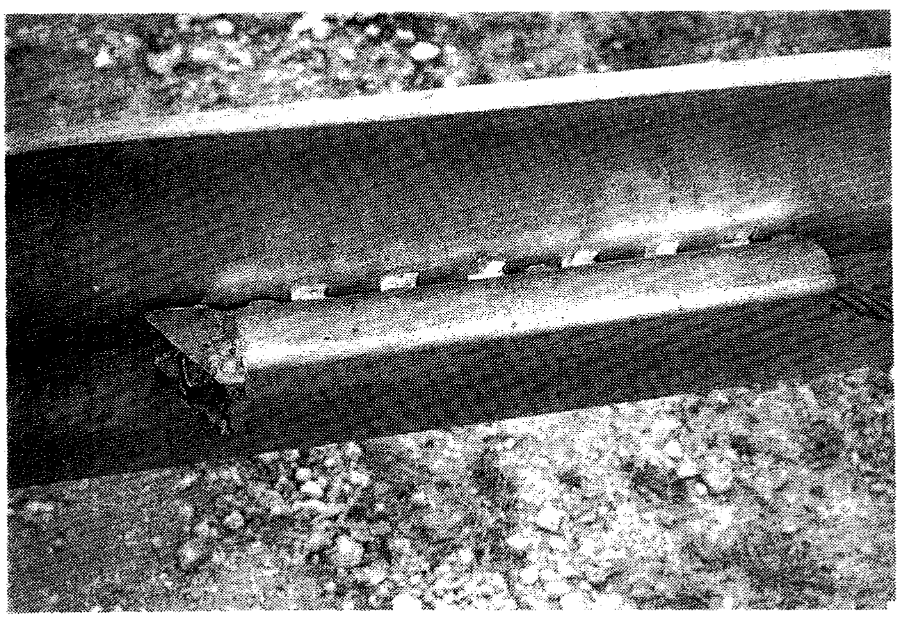

Fig. 49. Guardrail Extruder And Modified Cable Anchor (Test MB-2)

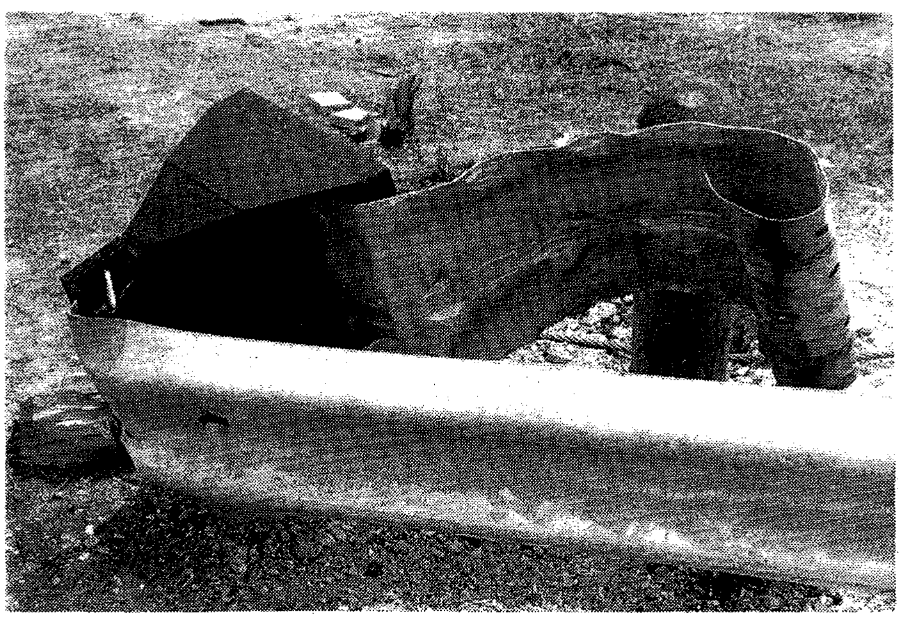

Fig. 50. Guardrail Extruder End Treatment After Test MB-2

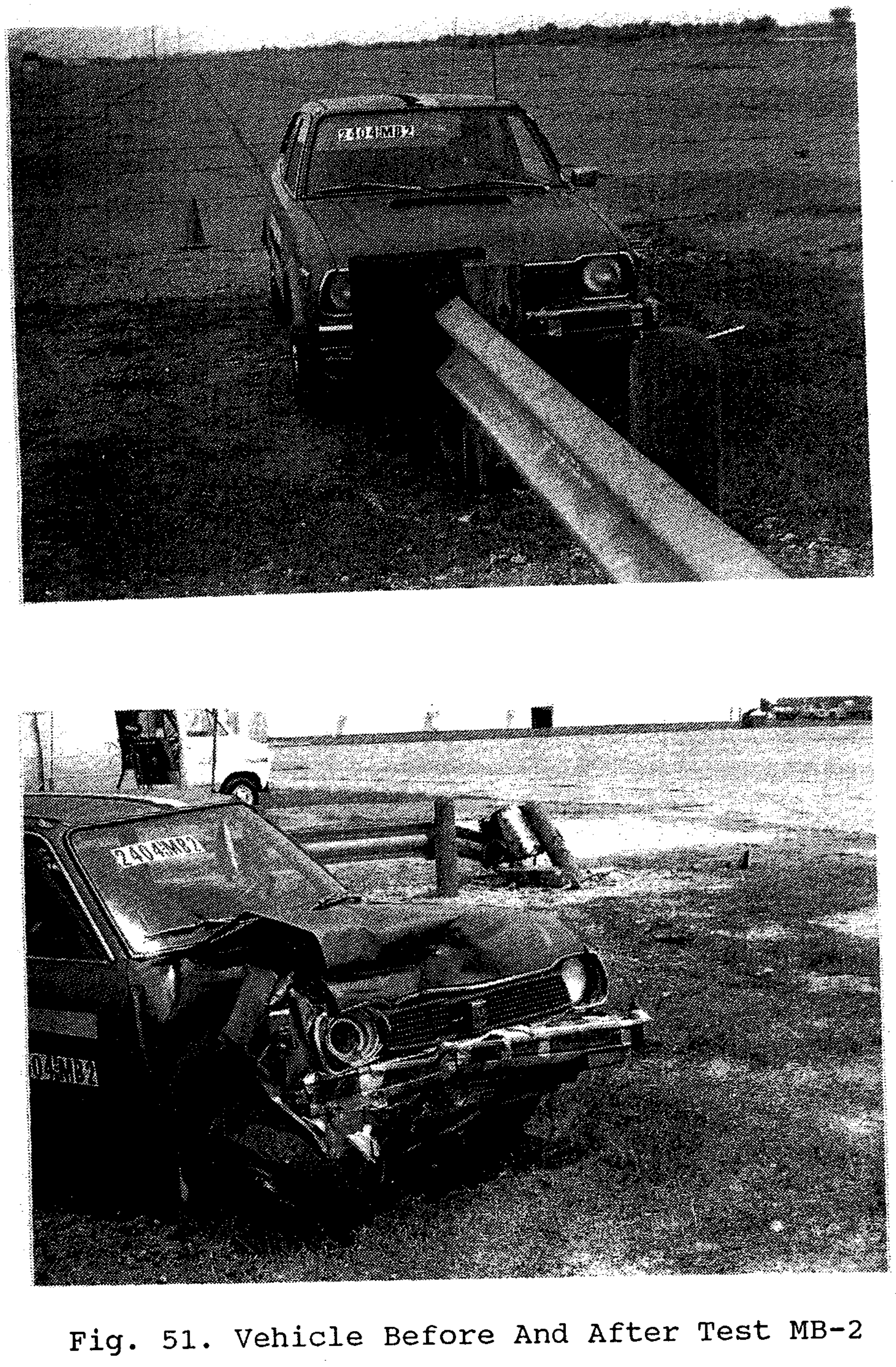

Fig. 51. Vehicle Before And After Test MB-2

the rail during a down stream hit, a rectangular block of wood was bolted to the second post. The rail rested on this block without any type of connection. The first and second 25 ft sections of the rail were welded together. This was required for the case when the vehicle would push the extruder past this point. A bolted rail splice would not feed through the extruder. Figure A-8 shows the stabilizing block at the second post and the welded rail splice. The rail was bolted to the posts starting at the fifth post.

A 1979 Honda weighing 1955 lbs. impacted the extruder at 59.8 m.p.h. and 0.0 degrees with a 15 inch offset. Upon impact the extruder yawed immediately, similar to test MB-2, forming the plastic hinge in the rail and causing the rail feed to stop abruptly. The resulting impulse caused the rail and the extruder to rotate about the fifth post. The vehicle underwent the same translation and yaw as in test MB-2. In addition, it rolled over on to the driver's side before straightening up and coming to rest on its wheels. The occupant impact velocity and the ridedown acceleration were 29.9 ft/sec and 14.5 g's. Figure A-9 shows the test installation and the third post after the test. The vehicle, before and after the test, is shown in figure A-10.

TEST MB-4

For this test, the 24 inch extruder was substituted for the 12 inch extruder, and the vertical ends of the extruder intake chute were tapered. The extruder was mounted so that the rail would be extruded away from the roadway, as in tests MB-1 and MB-2. The installation was the same as for test MB-3 except for the first four posts. The second post in concrete was replaced by a weakened 7 in. diameter round wood post in soil. A 3/4 inch diameter wire rope was looped around the concrete footing at the first post and threaded through the ground level holes in the 2nd, 3rd and 4th posts. The wire rope was braced snugly against these three posts with a bearing plate and three cable clamps at each post. This configuration prevents the leaning of the posts in weak soil and ensures clean breaks at ground level. Figure A-11 shows the modified installation for Test MB-4.

The test vehicle was a 1979 Honda weighing 1750 lbs. The impact was at 56.7 m.p.h. at 0 degrees with a 15 inch offset towards the roadway. The result of this test was almost identical to MB-3. The rail feed was blocked because of the formation of the plastic hinge created due to excessive yaw. The extruder and rail then rotated about the fifth post, and the vehicle overturned and stayed on its side. The installation after the test is shown in Figure A-12. Figure A-13 shows the vehicle before and after the test. The occupant impact velocity and the ridedown acceleration were 32.3 ft/sec and 11.9 g's respectively.

TEST MB-5

For this test all the posts, except for the leading post, were bolted to the rail. To resist the yawing of the extruder, a

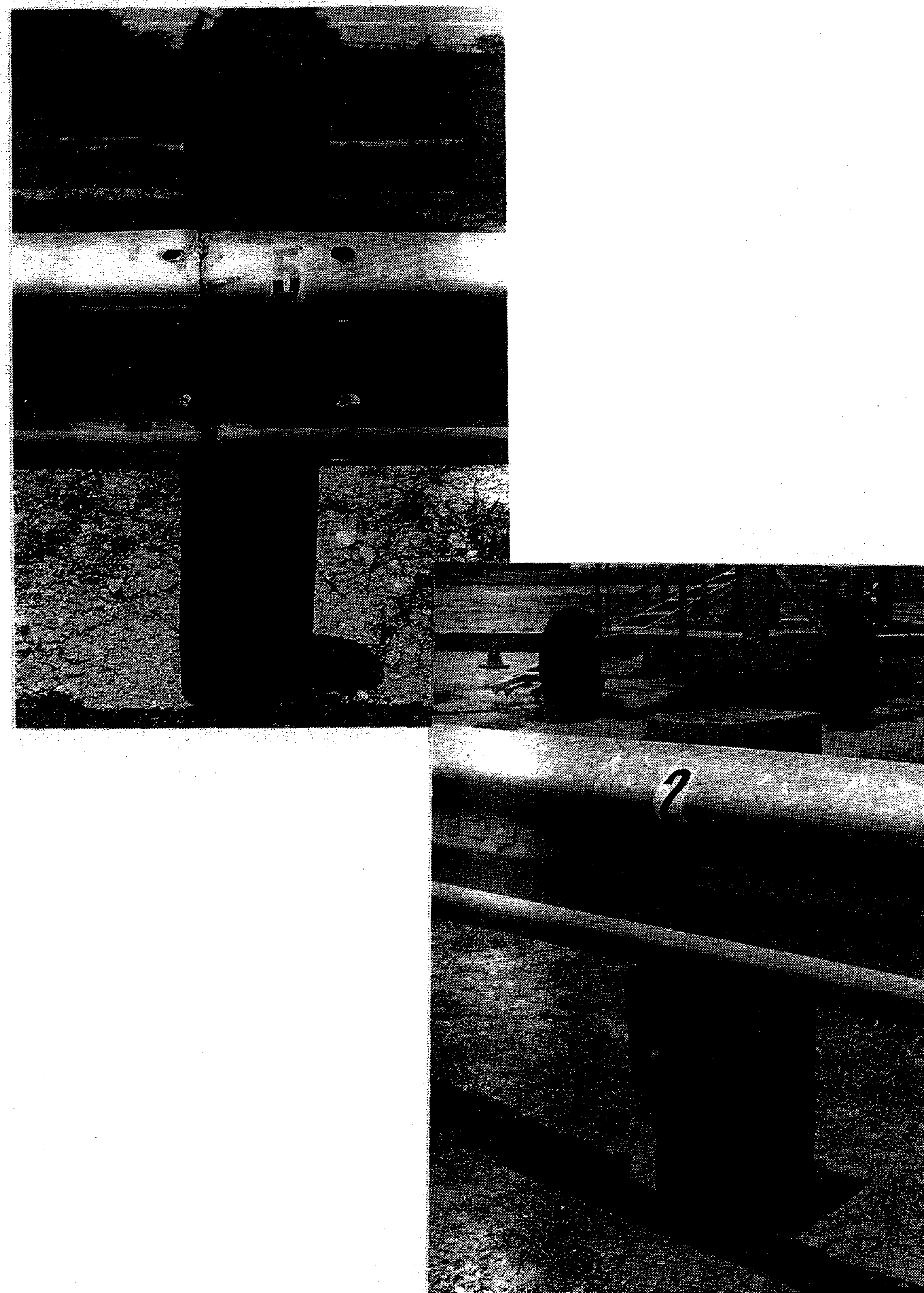

Fig. 52. Post Details Before Test MB-3

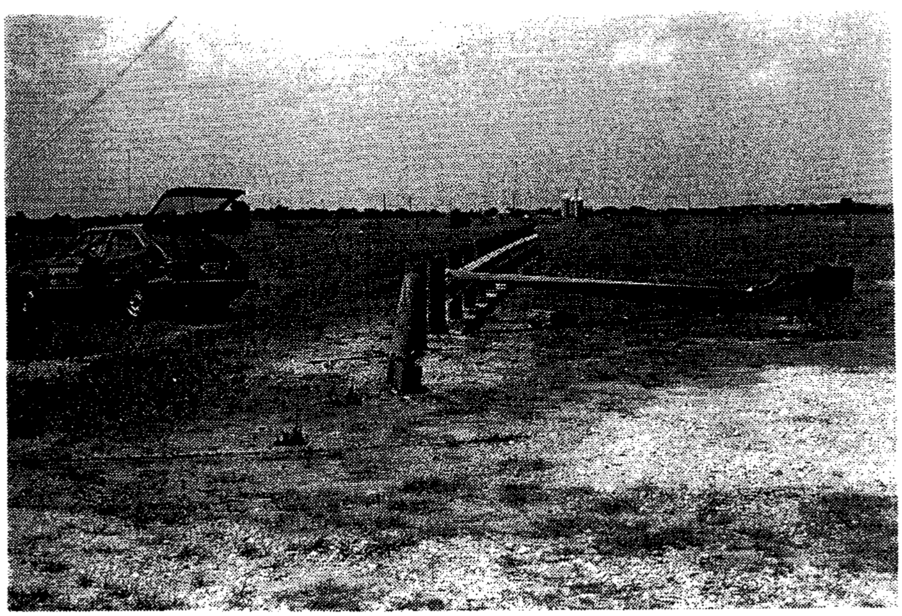

Fig. 53. Guardrail Extruder End Treatment After Test MB-3

Fig. 54. Vehicle Before And After Test MB-3

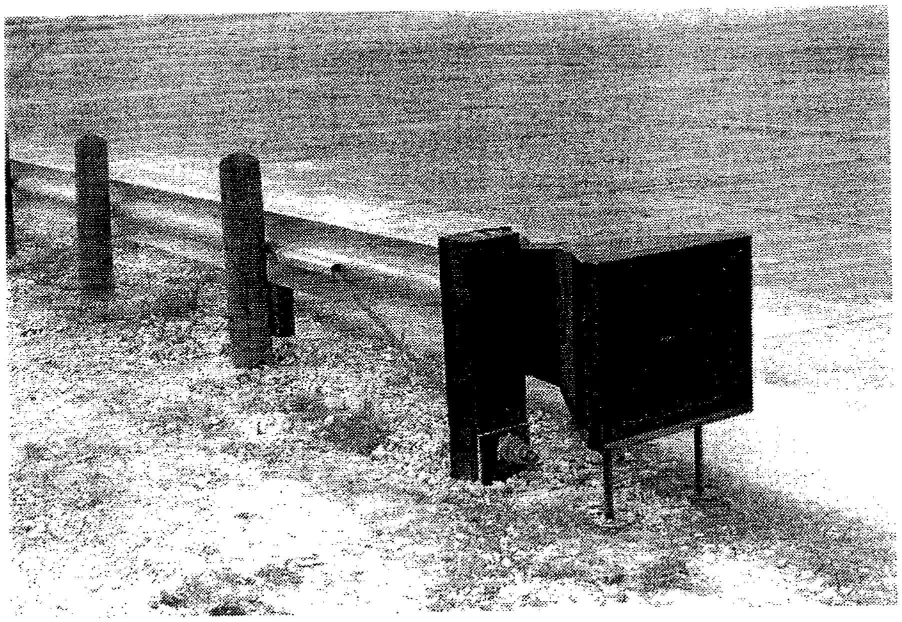

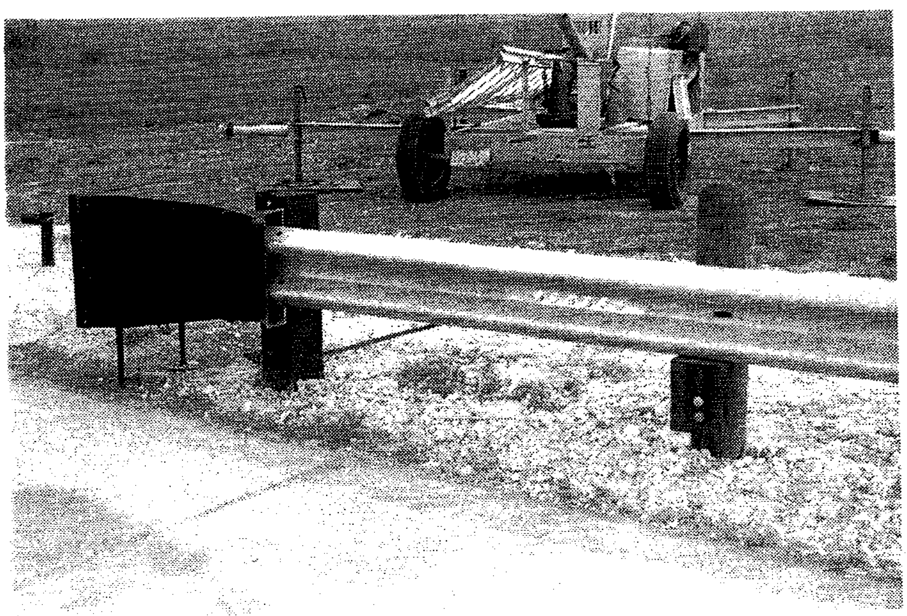

Fig. 55. Guardrail Extruder End Treatment Before Test MB-4

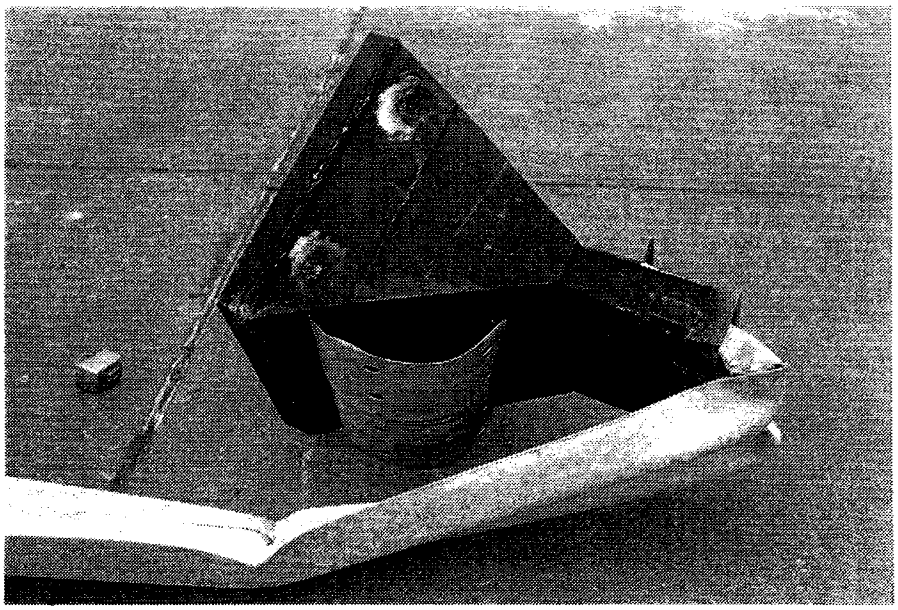

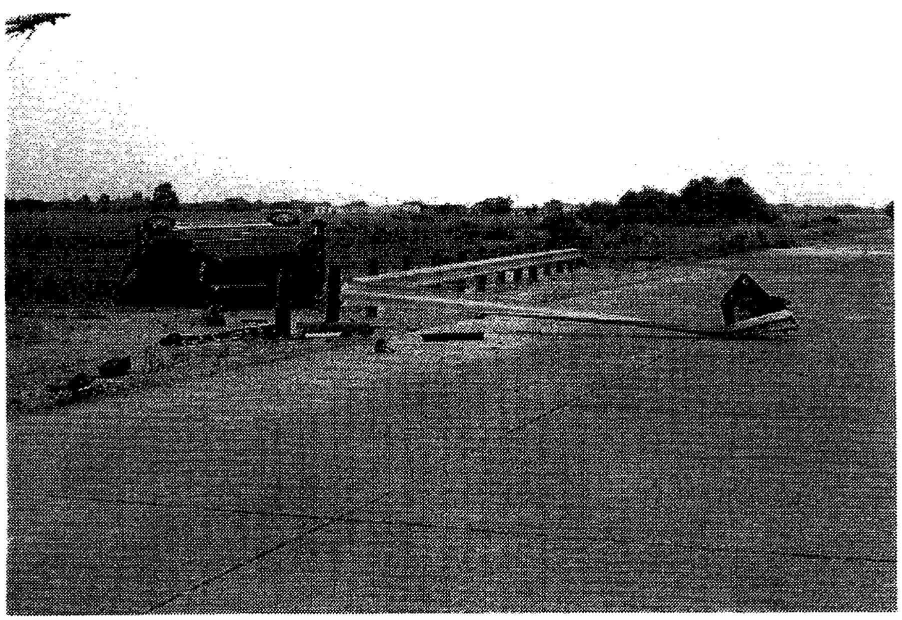

Fig. 56. Guardrail Extruder End Treatment After Test MB-4

Fig. 57. Vehicle Before And After TEst MB-4

deflector was added to the design. The def[illegible]sted of a flat bearing surface connected to the side [illegible]der, away from the roadway, and in the plane of the [illegible]e impact, the horizontal face of the deflector was a[illegible] 6 inches away from the leading post. The ground leve[illegible] was again used as in the previous test. Other insta[illegible]ails were also the same as in Test MB-4. The comple[illegible]lation is shown in Figure A-14.

A 1979 Honda weighing 1800 lbs. impac[illegible]treatment at 59.0 m.p.h and 0.0 degrees with a [illegible]set from centerline. Upon impact, the deflector cou[illegible]de enough resistance against the yaw. Further[illegible]extruder experienced pronounced pitch due to a [illegible] on this particular vehicle. Although approximate[illegible]rail did feed through the extruder, the vehicle did n[illegible]gh energy to prevent it from rolling over after [illegible]from the barrier. The occupant impact velocit[illegible]ridedown acceleration were 37.0 ft/sec and 8.4 g's re[illegible]Figure A-15 shows the installation after the test a[illegible]-16 shows the vehicle before and after the test.

TEST MB-6

For this test, a 36 inch long feeder [illegible]bricated out of standard channel sections and connec[illegible]isting 12 inch extruder. Two rubber pads were connec[illegible]e of the extruder to engage the vehicle above its b[illegible]he final extruder design is shown in Figure E1. The[illegible] details were the same as for Test MB-5 and are sho[illegible]A-17. The test vehicle was a 1979 Honda. The impact [illegible].p.h. at 0 degrees with a 15 inch offset towards the [illegible] extruder did not yaw significantly during the test.[illegible]eam rail was able to feed through it without any hi[illegible] vehicle had lost most of its energy before it sepera[illegible] extruder and was brought to a smooth controlled st[illegible]uder was undamaged. Figure A-18 shows the install[illegible]he test. The test vehicle before and after impact is [illegible]ure A-19. The occupant impact velocity and the ridec[illegible]tion were 29.0 ft/sec and 15.5 g's respectively.

TEST MB-7

This test was run to evaluate the per[illegible]he final extruder design during a head-on impact [illegible]ar. The installation was identical to that in Test [illegible] shown in Figure A-20. The vehicle was a 1978 Mercu[illegible]4600 lbs. The impact was at 61.6 m.p.h. at 0 deg[illegible]line of vehicle. After impacting the barrier, the [illegible]ed on the centerline of the rail, breaking away the [illegible]hing the extruder smoothly until all energy was d[illegible] total of 45 feet of rail was extruded during this t[illegible]uder was undamaged and the welded splice connection [illegible] intended. The occupant impact velocity and the ridec[illegible]tion were 19.8 ft/sec and 8.2 g's. Figure A-21 shows t[illegible]efore and

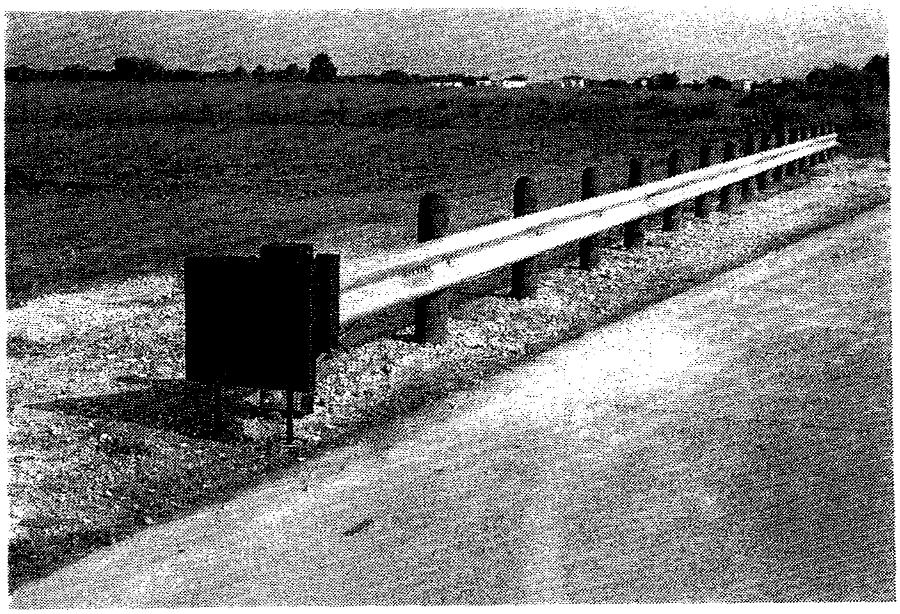

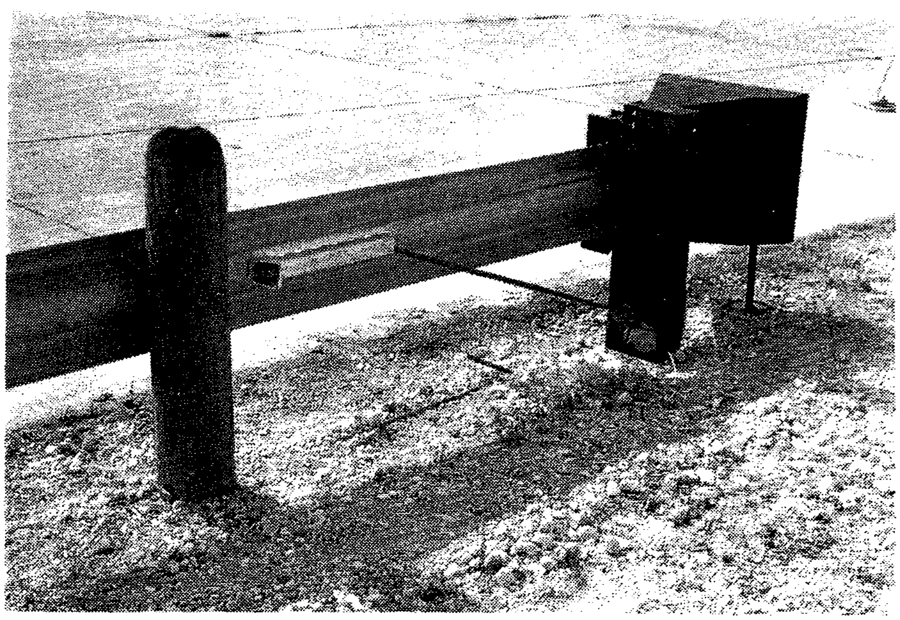

Fig. 58. Guardrail Extruder End Treatment Before Test MB-5

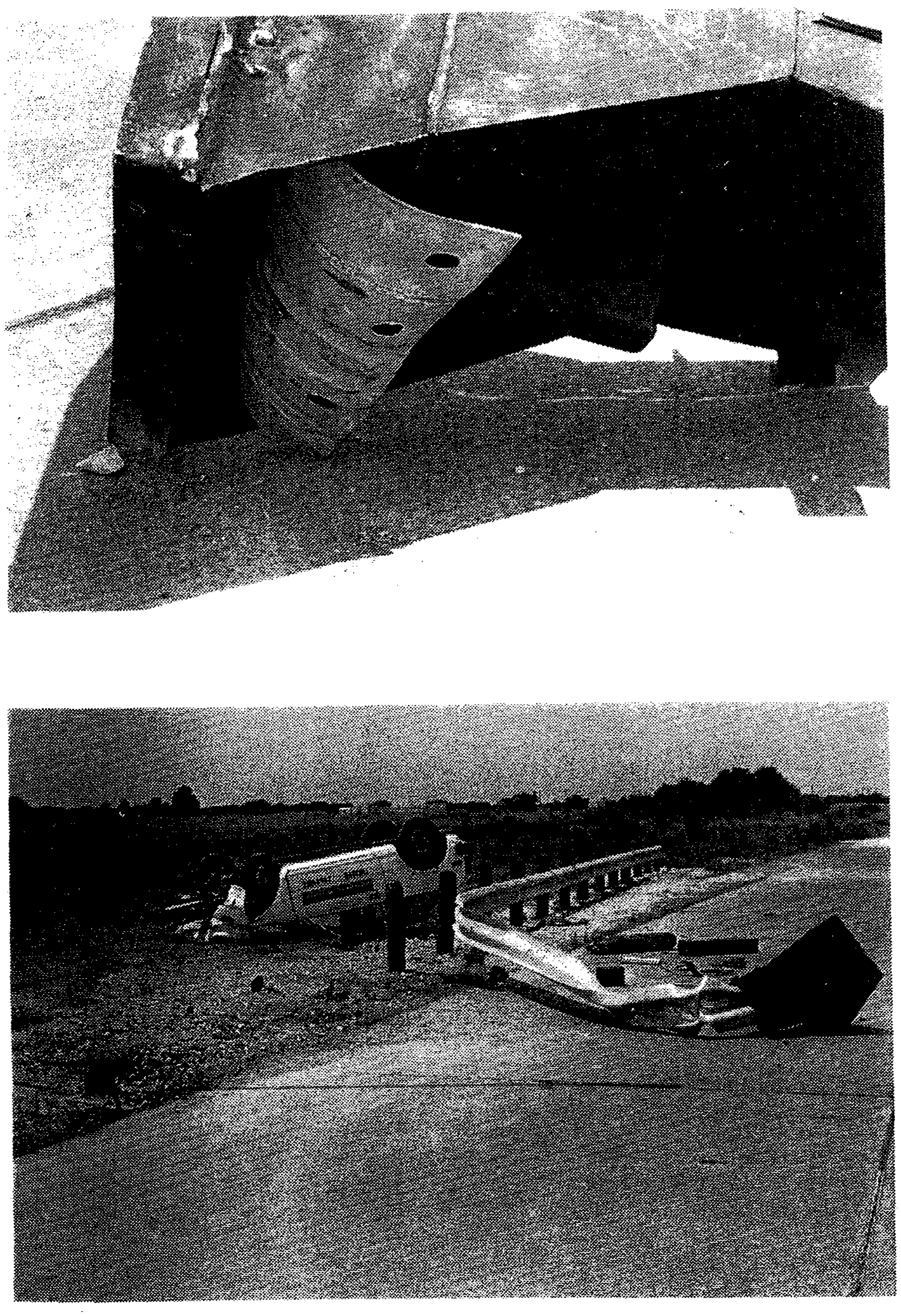

Fig. 59. Guardrail Extruder End Treatment After Test MB-5

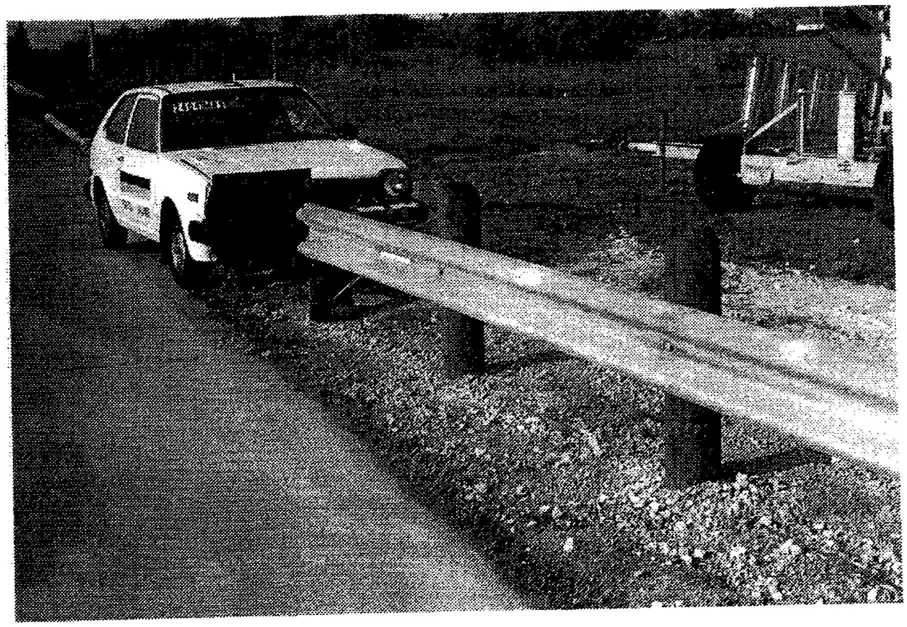

Fig. 60. Vehicle Before And After Test MB-5

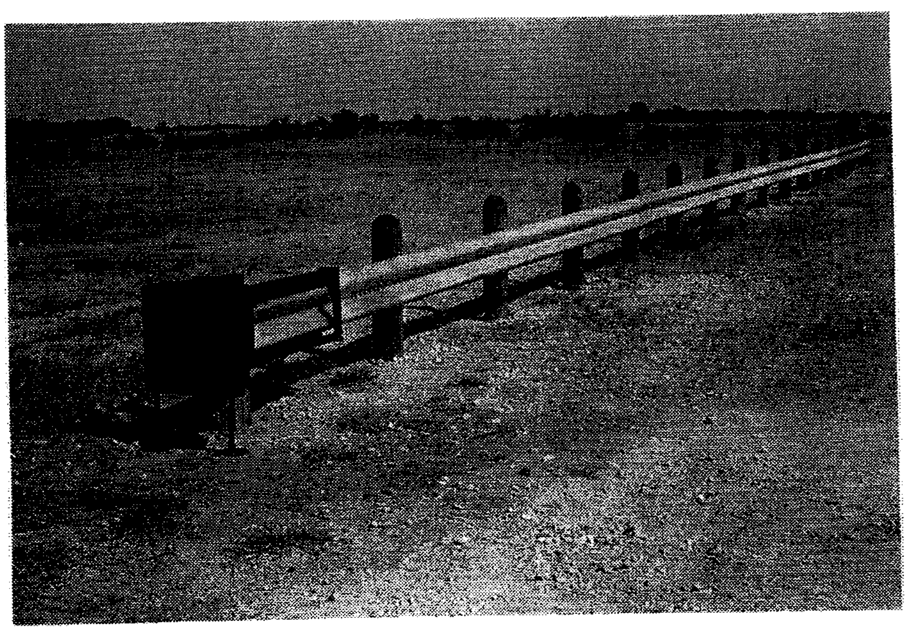

Fig. 61. Guardrail Extruder End Treatment Before Test MB-6

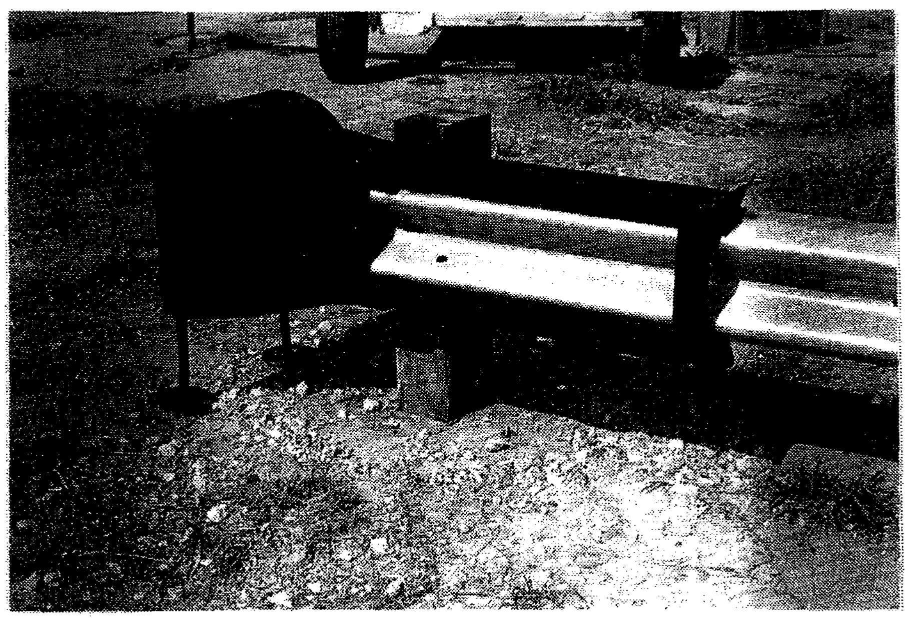

Fig. 61. Guardrail Extruder End Treatment Before Test MB-6

(Continued)

Fig. 62. Guardrail Extruder End Treatment After Test MB-6

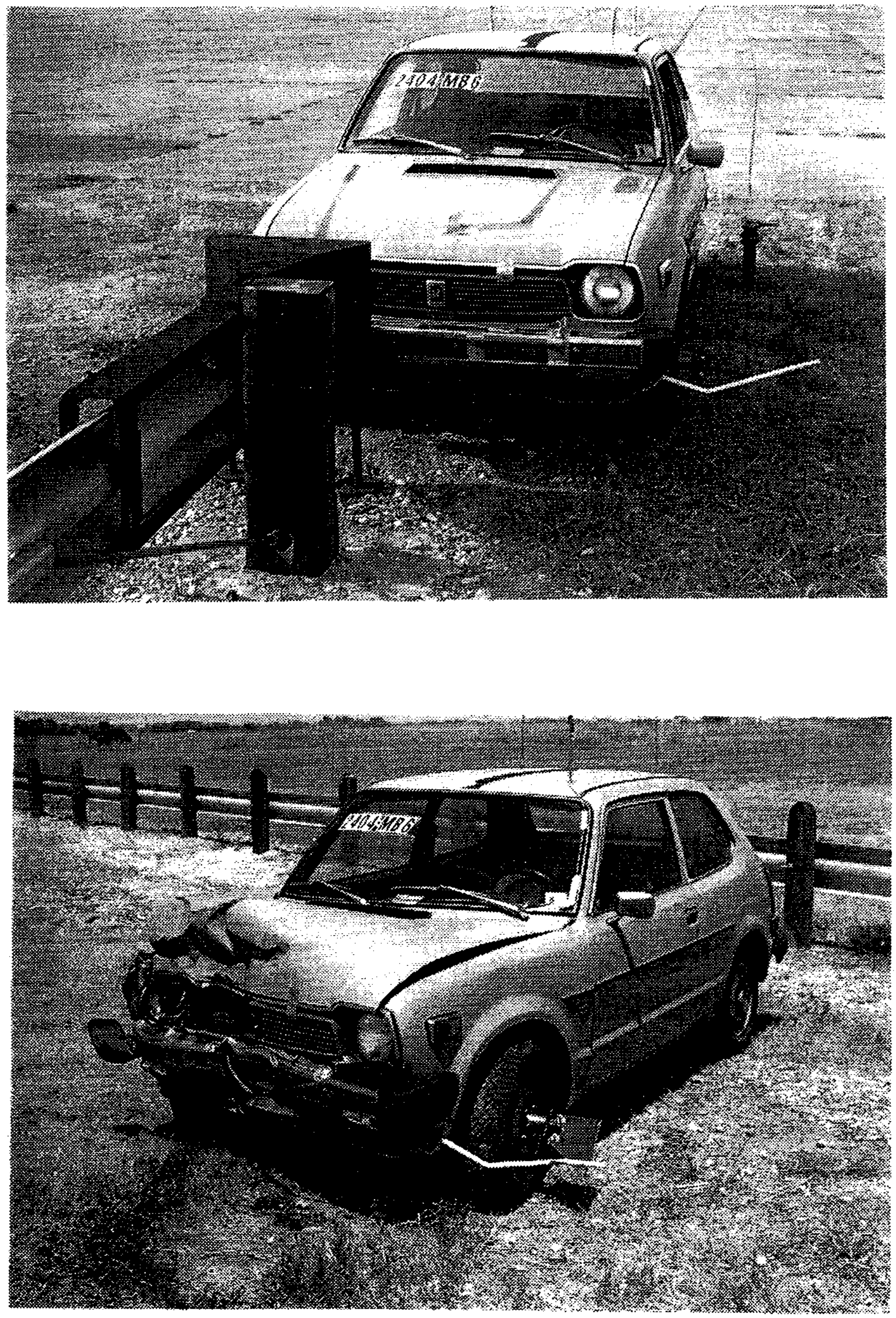

Fig. 63. Vehicle Before And After Test MB-6

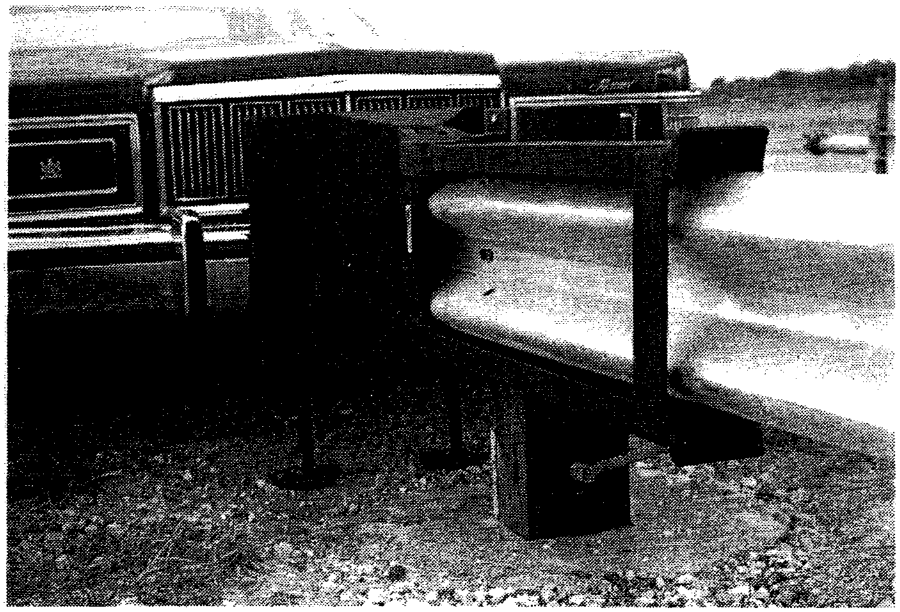

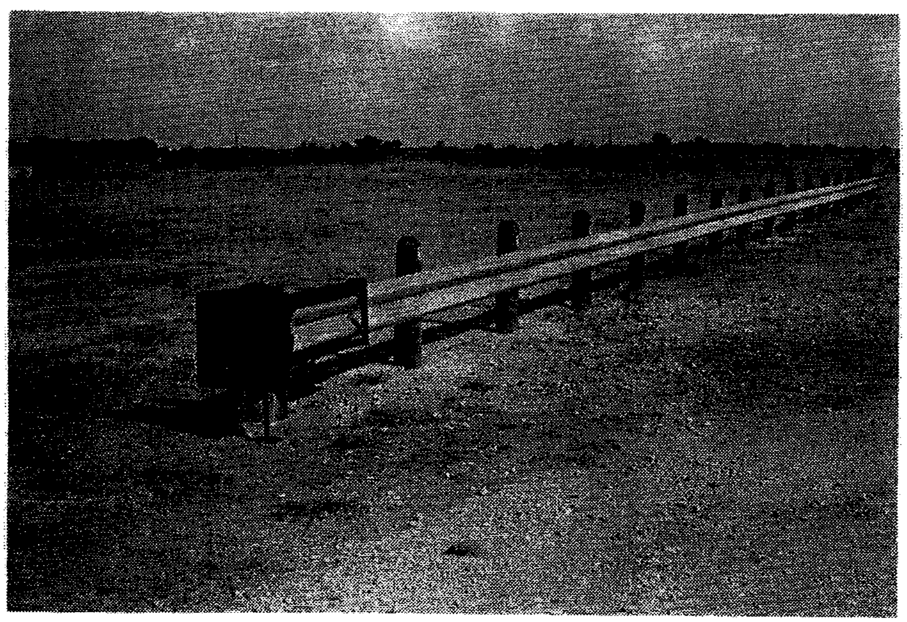

Fig. 64. Guardrail Extruder End Treatment Before Test MB-7

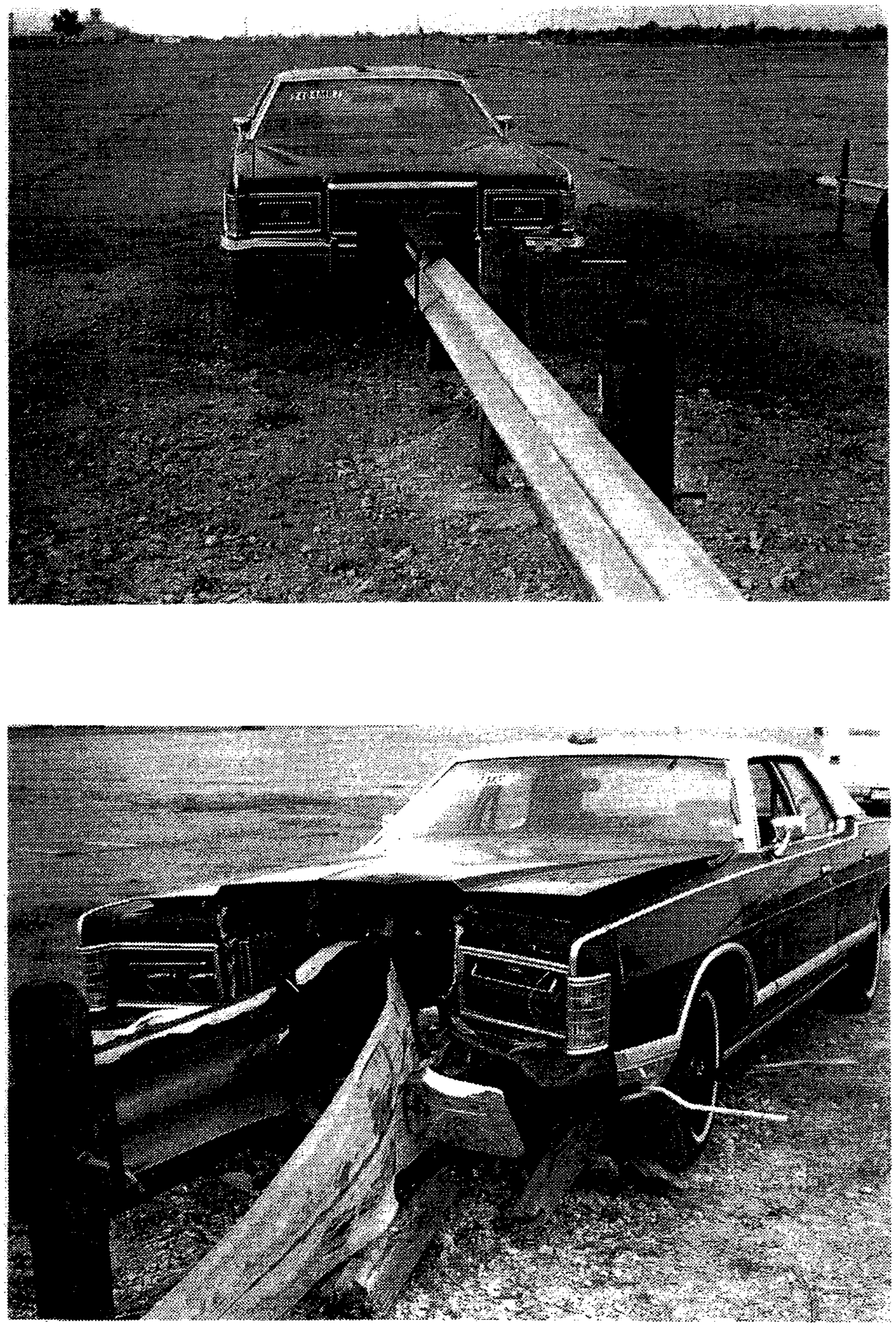

Fig. 65. Vehicle Before And After Test MB-7

after the test. Figure A-22 shows the vehicle and installation after the test. The welded splice connection after feeding is shown in Figure A-23.

TEST 9429A-1

This test was run to evaluate the redirective capabilities of the end treatment during a side hit. The installation was the same as in Tests MB6 and MB7 and is shown in Figure A-24. No blockouts were used for this test.

The vehicle was a 1979 Honda weighing 1780 lbs. Figure A-25 shows the vehicle before the test. The impact was just downstream of the second post at 59.1 m.p.h. and 15.6 degrees to the rail. The vehicle was smoothly redirected. Although some wheel snagging was evident on posts 3 and 4, damage to the vehicle was light for an impact of this severity. The installation after the test is shown in Figure A-26 and Figure A-27 shows the vehicle damage after the test. The longitudinal and lateral occupant impact velocities were 15.9 and 17.0 ft/sec respectively. The occupant ridedown accelerations were 1.4 g's longitudinal and 10.3 g's lateral. The change in vehicle velocity was 6.8 m.p.h.

TEST 9429A-2

This test was run to evaluate the redirective capabilities of the end treatment when impacted by a big car. The installation was the same as in Test 9429A-1 and is shown in Figure A-28. The vehicle was a 1979 Cadillac weighing 4410 lb. Figure A-29 shows the vehicle before the test. The impact was just downstream of the third post at 58.9 m.p.h. and 24.9 degrees to the rail. Although the vehicle deflected the barrier sufficiently to allow significant wheel snagging on the guardrail posts, the vehicle was smoothly redirected. Post 4 fractured at the groundline, and posts 5 and 6 detached from the rail. Figure A-30 shows the post damage after the test. The forces generated in the test were sufficient to cause a 3 in. displacement of the concrete footing at the first post. Figure A-31 shows the installation and the footing after the test. The vehicle damage sustained in this test was moderate for the severity of the impact. Figure A-32 shows the vehicle after the test.

The longitudinal and lateral occupant impact velocities were 23.2 ft/sec and 16.5 ft/sec respectively and the corresponding occupant ridedown accelerations were 6.2 g and 8.5 g respectively. Although no large snagging forces were generated, the exit velocity for this test was somewhat lower than safety standard recommendations (12). However, overall performance of this system was similar to the impact performance of other guardrail systems (14,15,16); and therefore, this test was considered a success. It should be noted that in both redirectional tests, the modified cable anchor performed as designed.

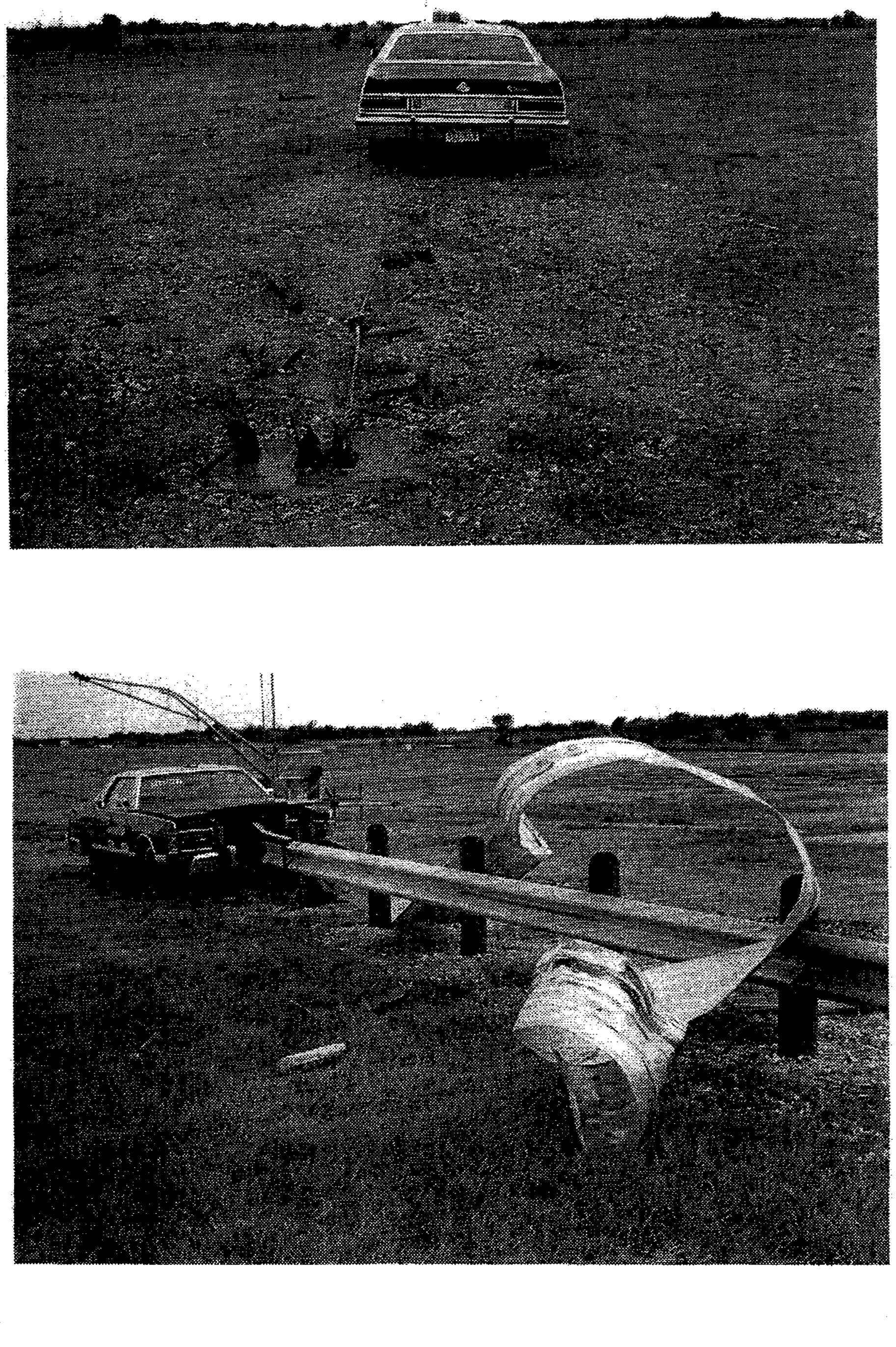

Fig. 66. Guardrail Extruder End Treatment After Test MB-7

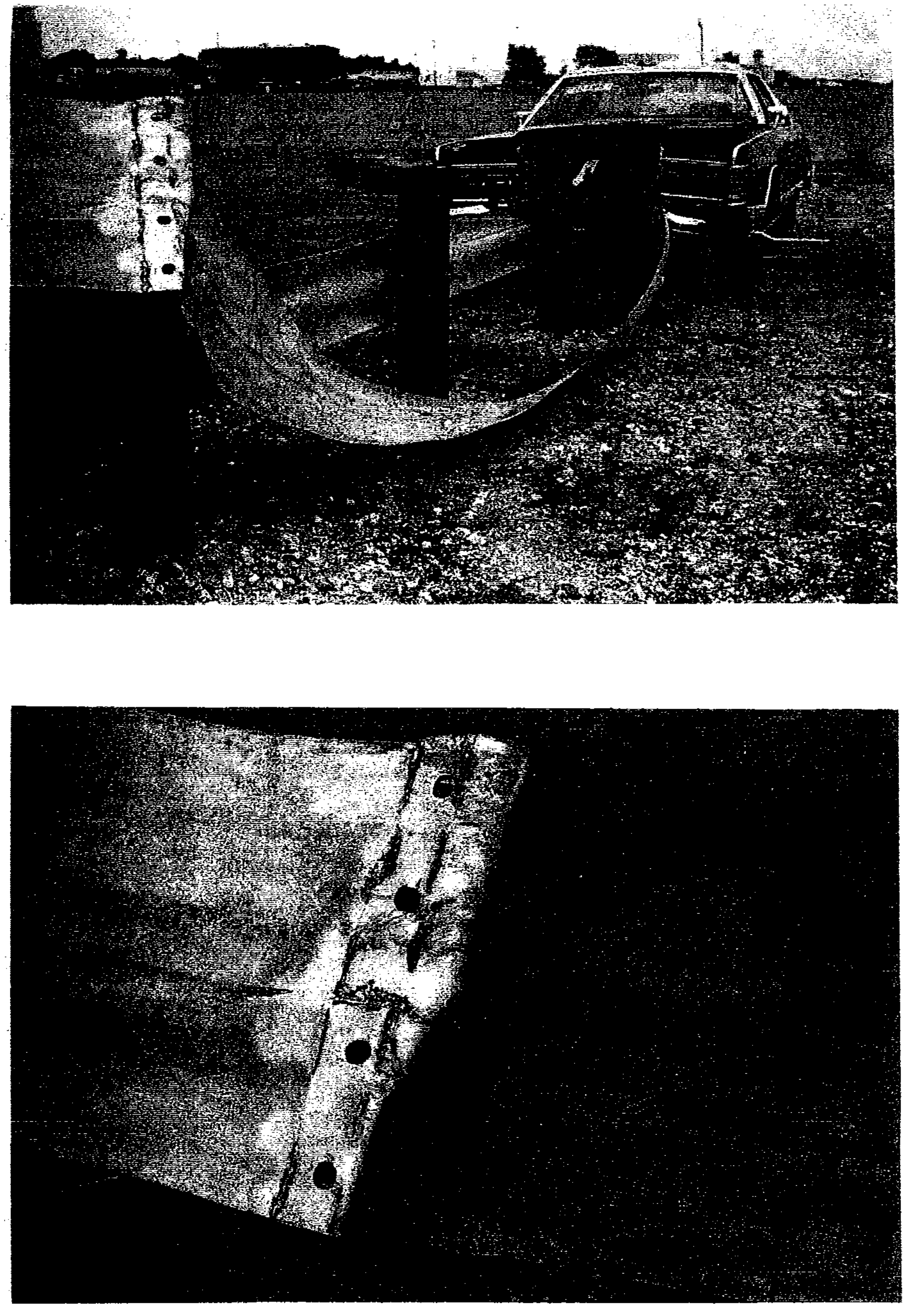

Fig. 67. Welded Splice After Test MB-7

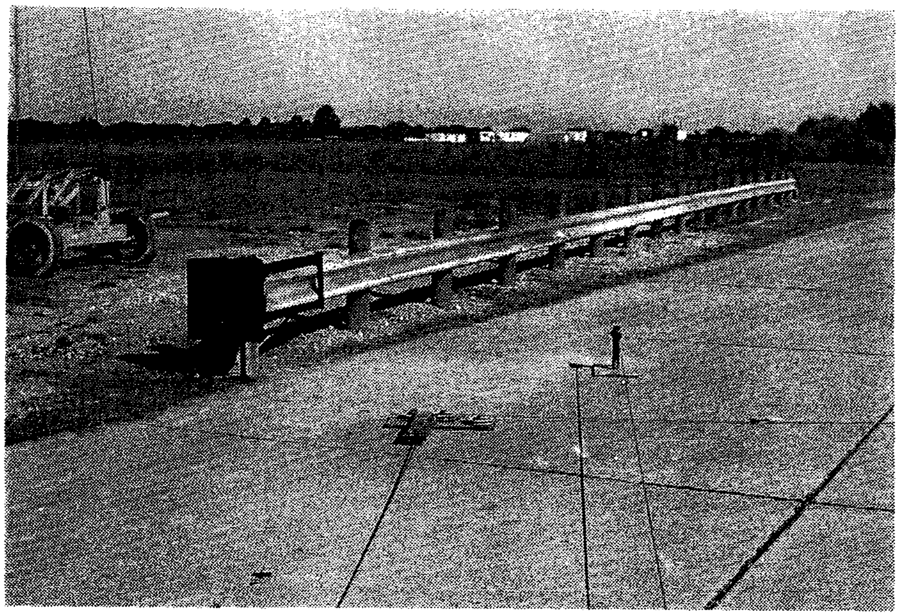

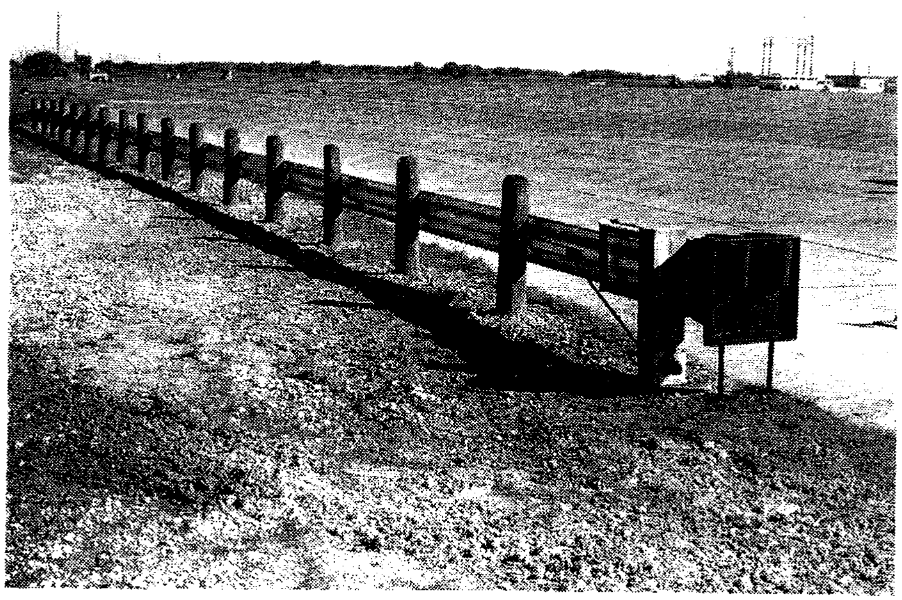

Fig. 68. Test Installation Before Test 9429A-1

Fig. 68. Test Installation Before Test 9429-1 (Continued)

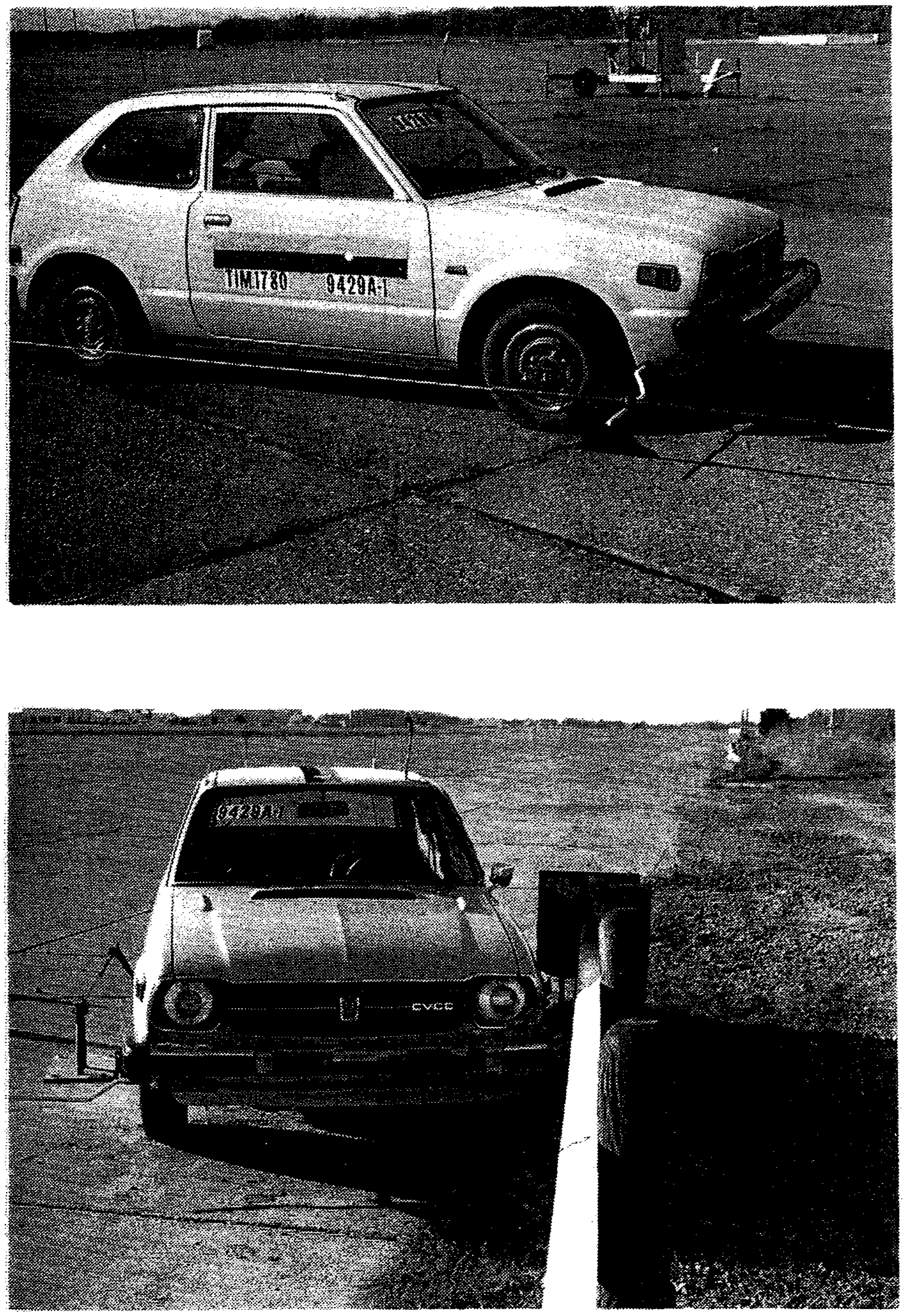

Fig. 69. Vehicle Before Test 9429A-1

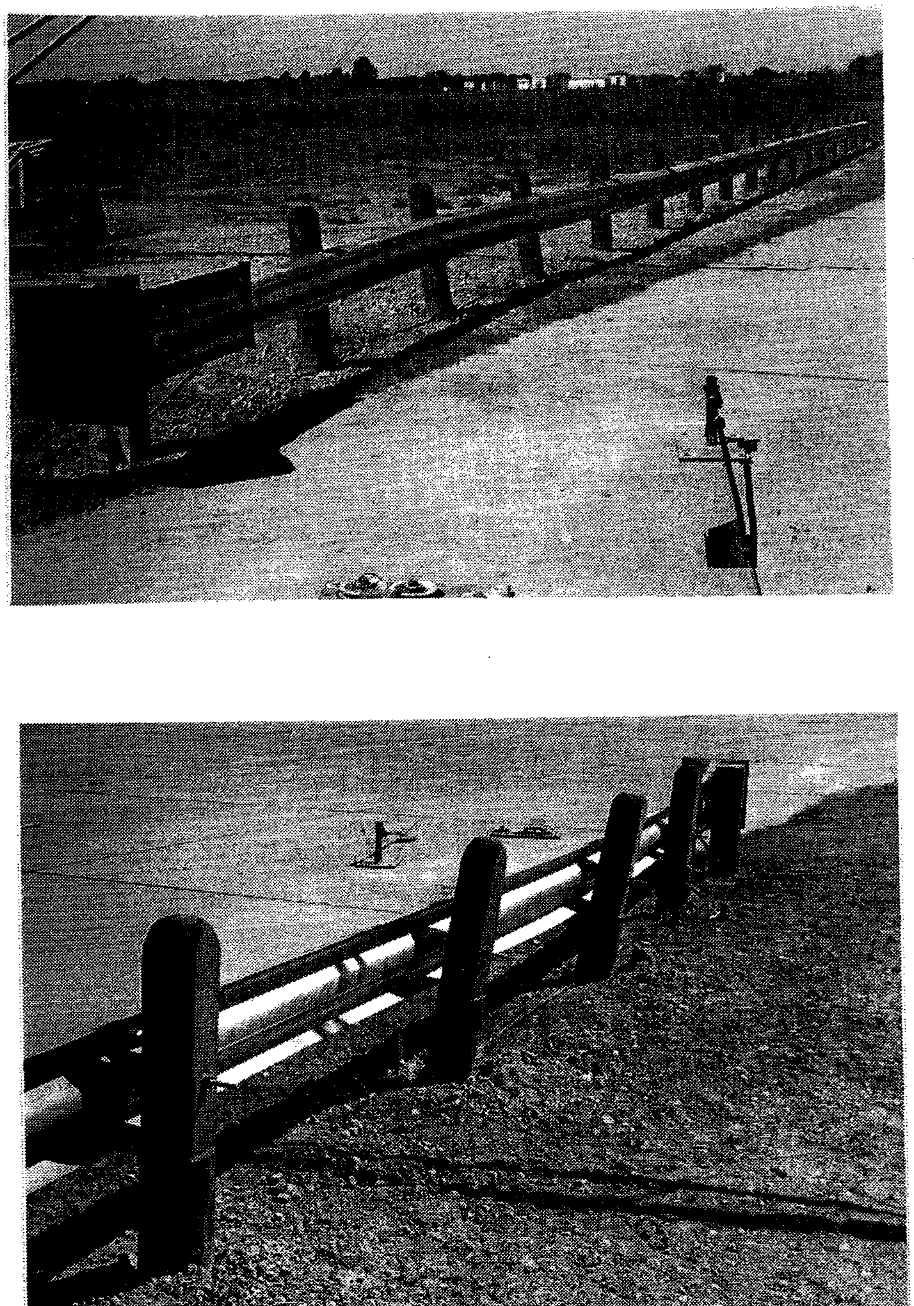

Fig. 70. Test Installation After Test 9429A-1

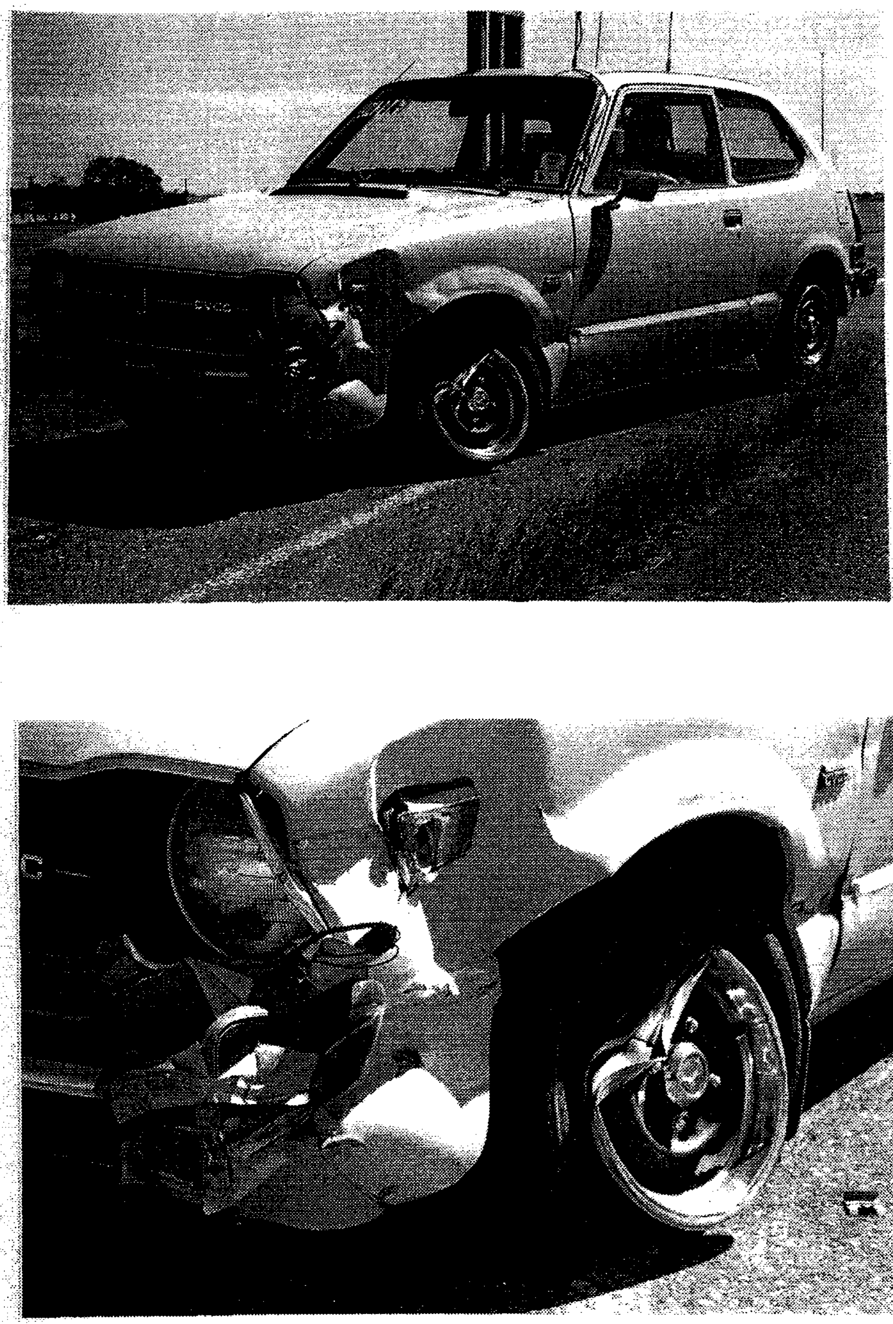

Fig. 71. Vehicle After Test 9429A-1

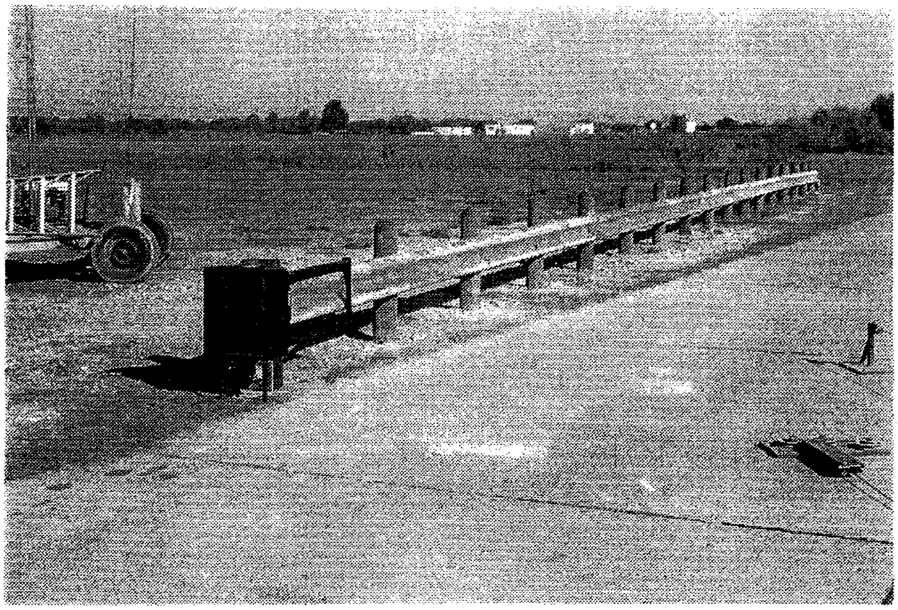

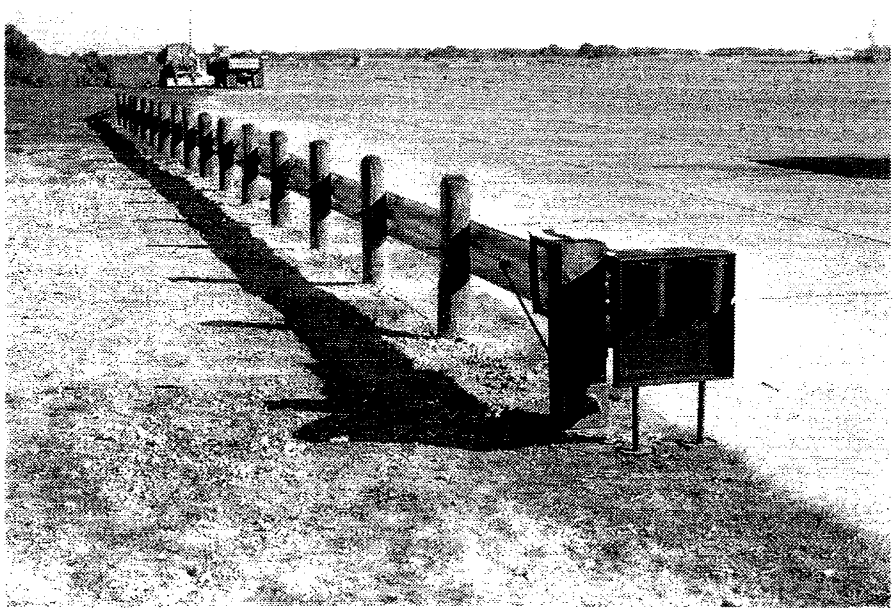

Fig. 72. Test Installation Before Test 9429A-2

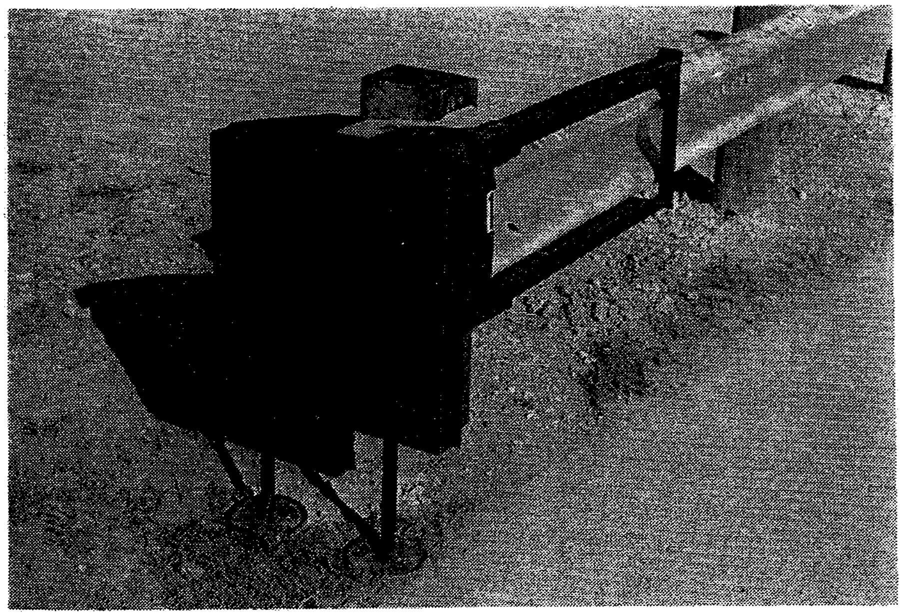

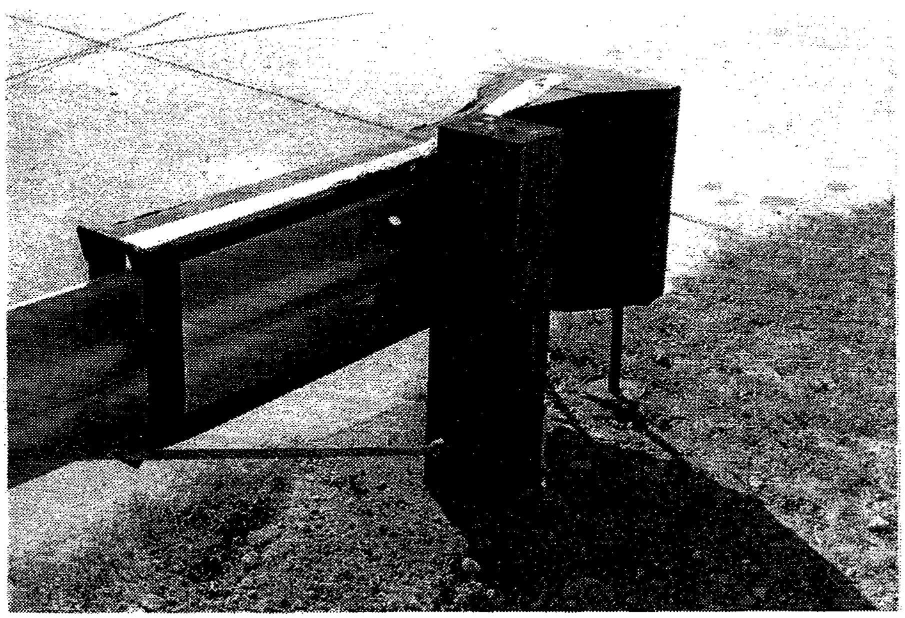

Fig. 72. Test Installation Before Test 9429A-2 (Continued)

Fig. 73. Vehicle Before Test 9429A-2

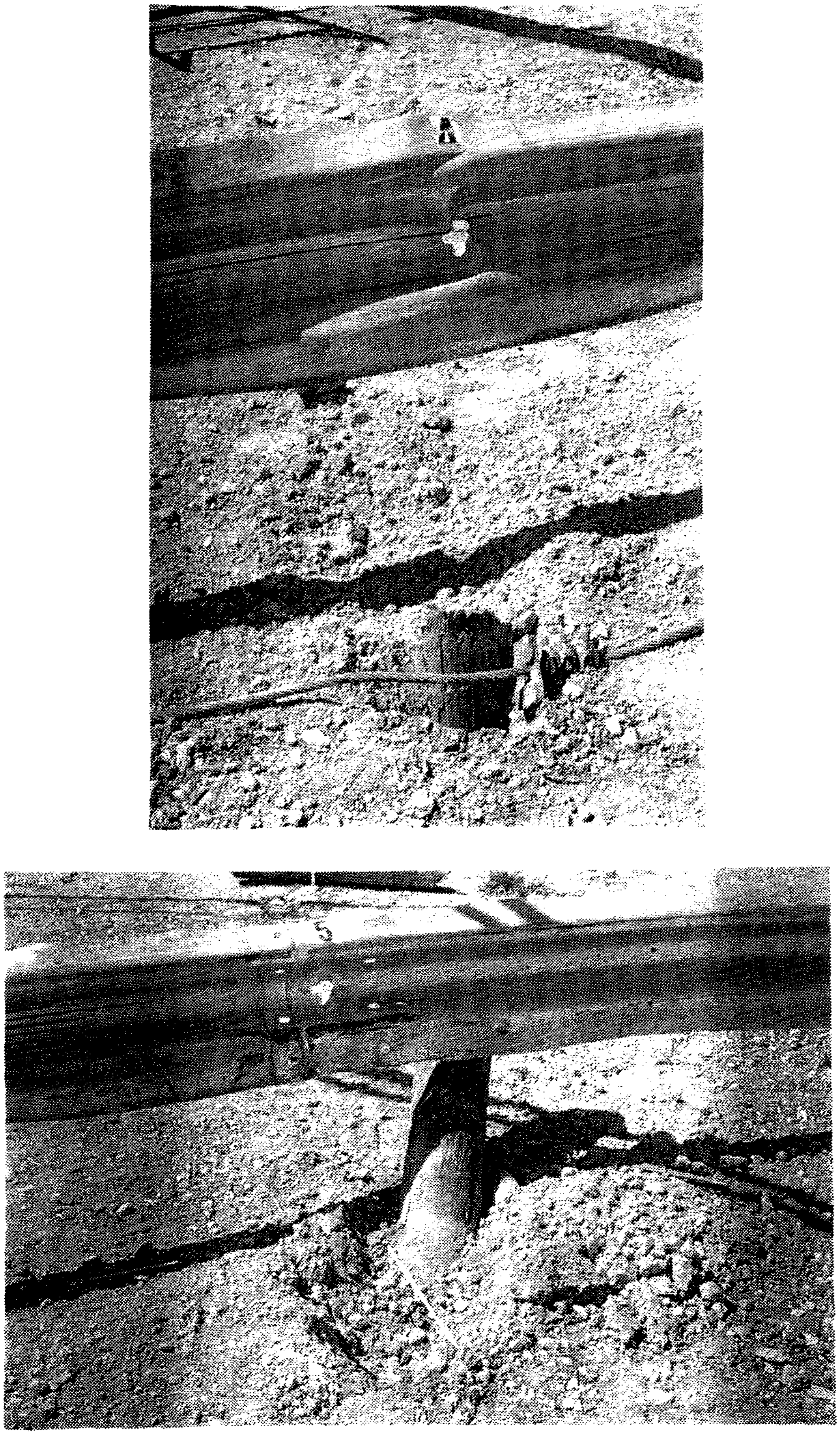

Fig. 74. Details of Damage to Post 4 And 5

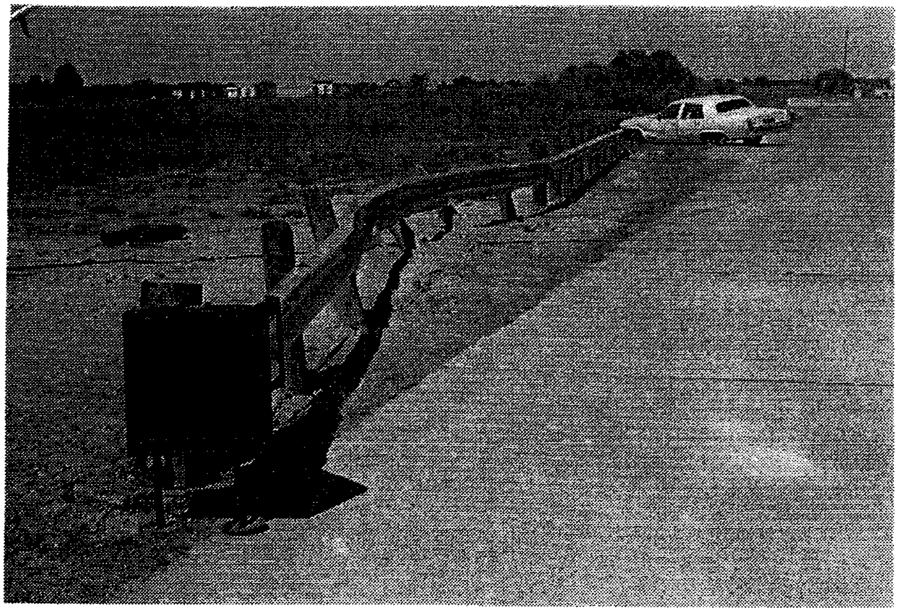

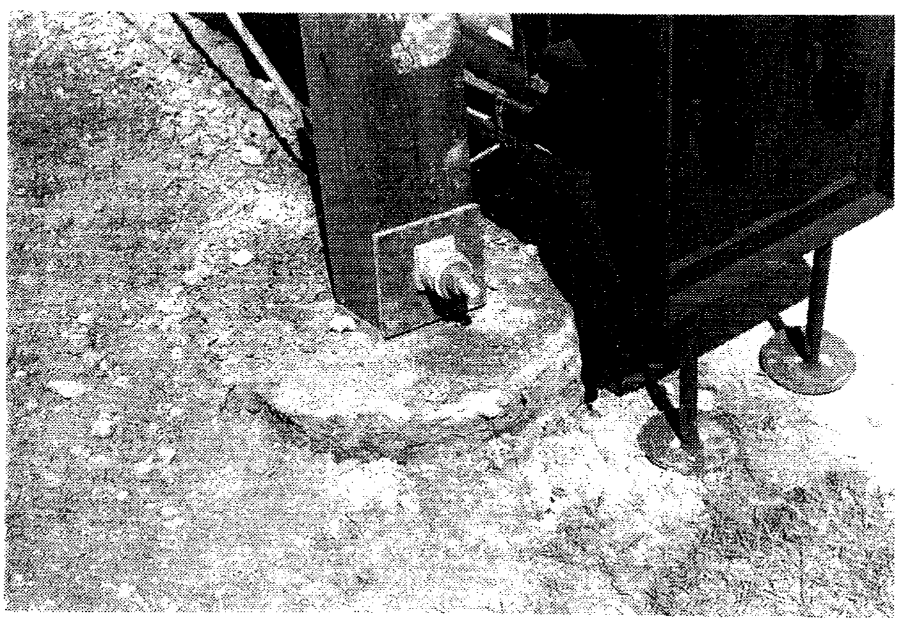

Fig. 75. Test Installation After Test 9429A-2

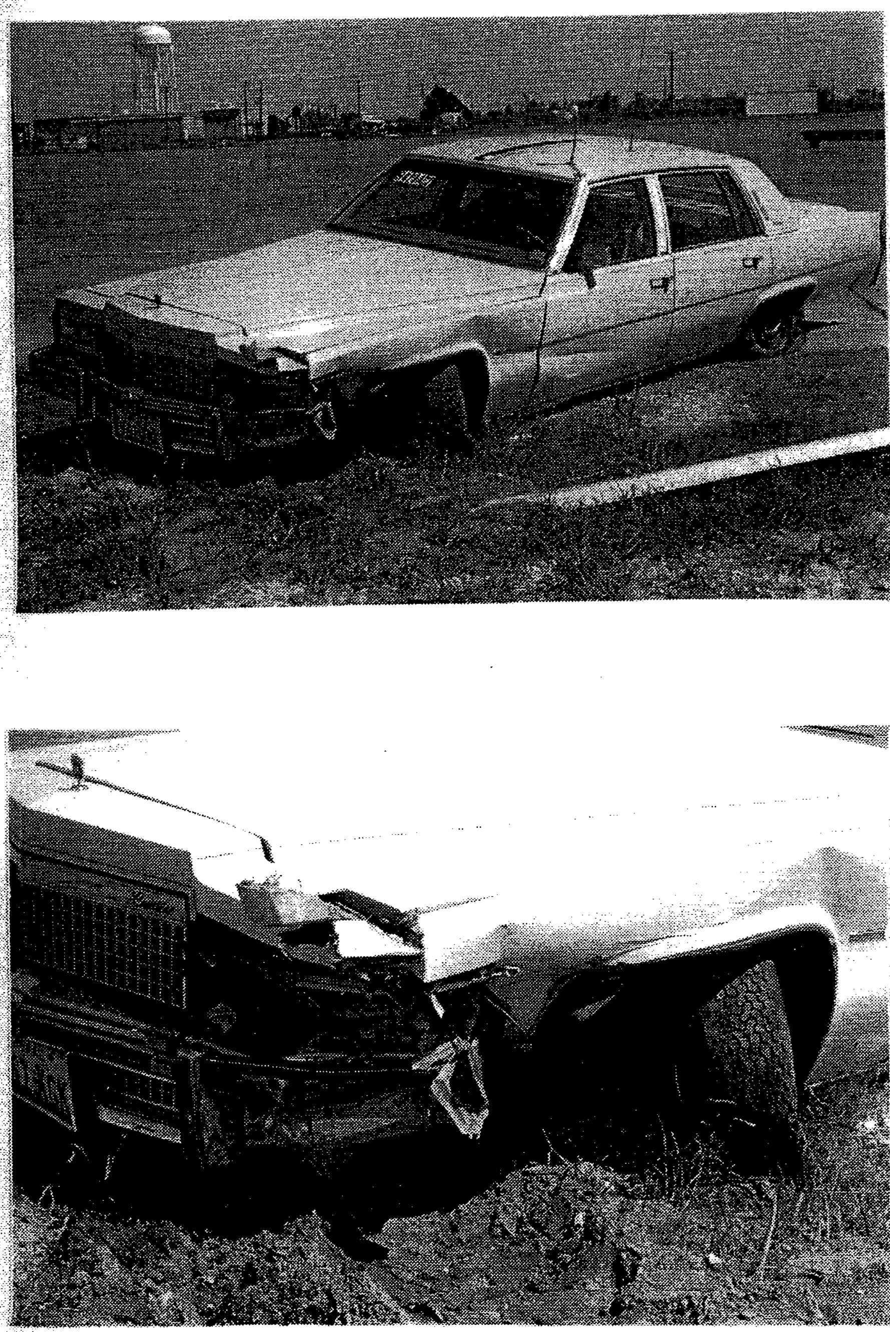

Fig. 76. Vehicle After Test 9429A-2

APPENDIX B.

SPLIT RAIL TERMINAL CRASH TESTS

SRP-1

For the first preliminary test, SRP-1, the first span of guardrail (i.e. the length of rail between the first and second posts) was slotted for 5 ft. The first post was replaced by a 2 in. x 4 in. piece of wood. The purpose of this piece of wood was to provide vertical support for the end of the rail. A 1973 Buick Century weighing 4276 lb. impacted the rail head-on at a speed of 30 m.p.h. Upon impact the slotted section collapsed and the vehicle came to an abrupt stop after coming in contact with the full strength rail. The test installation before and after impact is shown in Figure B-1. Figure B-2 shows the vehicle before and after the test.

SRP-2

For this second preliminary crash test, three spans were provided with slotted sections. The slot lengths were 5 ft. in the first span and 4 ft. in the second and third spans. A 1974 Ford Custom, weighing 4000 lb., impacted the rail head-on at a speed of 20 m.p.h. Upon impact, the first section of slotted rail collapsed completely, and the second sectioned buckled. However, the vehicle could not break the second post and was stopped. Figure B-3 shows the barrier before and after test SRP-2. The vehicle before and after impact is shown in Figure B-4.

SRP-3

For the third preliminary test, the impact speed was increased to 40 m.p.h. The vehicle was a 1974 Ford Custom, weighing 4000 lbs. The first three spans had the same slot lengths as test SRP-2. In addition, a fourth span was slotted with 3 ft. slots. The vehicle broke posts 2, 3, and 4; collapsed all of the slotted sections of rail; and came to a stop after impacting the 5th post. Figure B-5 shows the installation before and after the test. The vehicle, before and after impact, is shown in Figure B-6.

SRP-4

The purpose of this test was to investigate the performance of the slotted rail during angular hits. Eight spans of rail (i.e. two 25 ft. sections of W-beam) were fabricated with 27 in. long slots. The first post was a 6 in. x 8 in. wood post set in a concrete footing. A standard BCT cable anchor was used to provide the tensile capacity required for redirection. No block outs were used in the installation. A 1979 Buick Limited, weighing 4470 lbs, impacted the rail at the third post at 50 m.p.h. and 25 degrees. Upon impact, the bumper of the vehicle engaged the slotted section of rail. The vehicle subsequently tore through the rail and penetrated the barrier. The vehicle and barrier before and after the test are shown in Figure B-7.

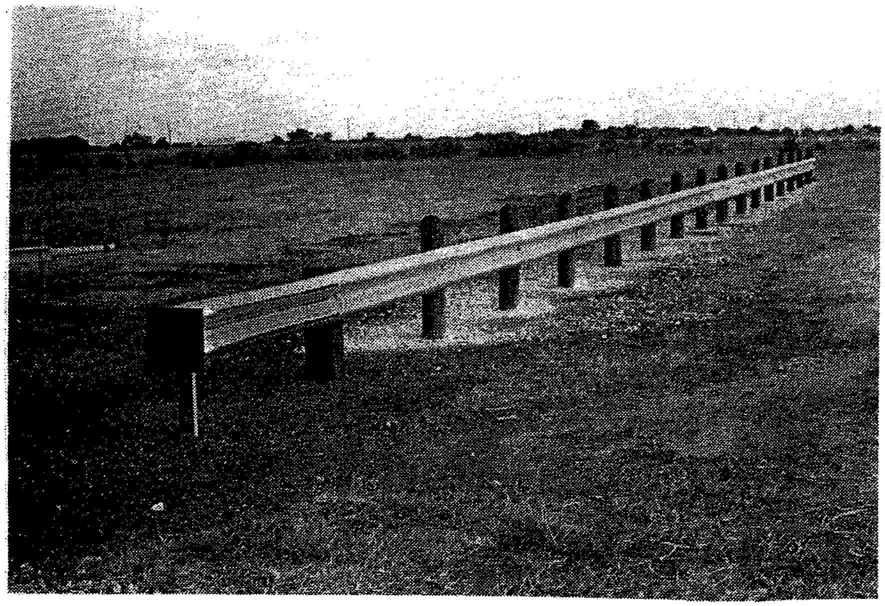

FIGURE B-1. INSTALLATION BEFORE AND AFTER TEST SRP-1.

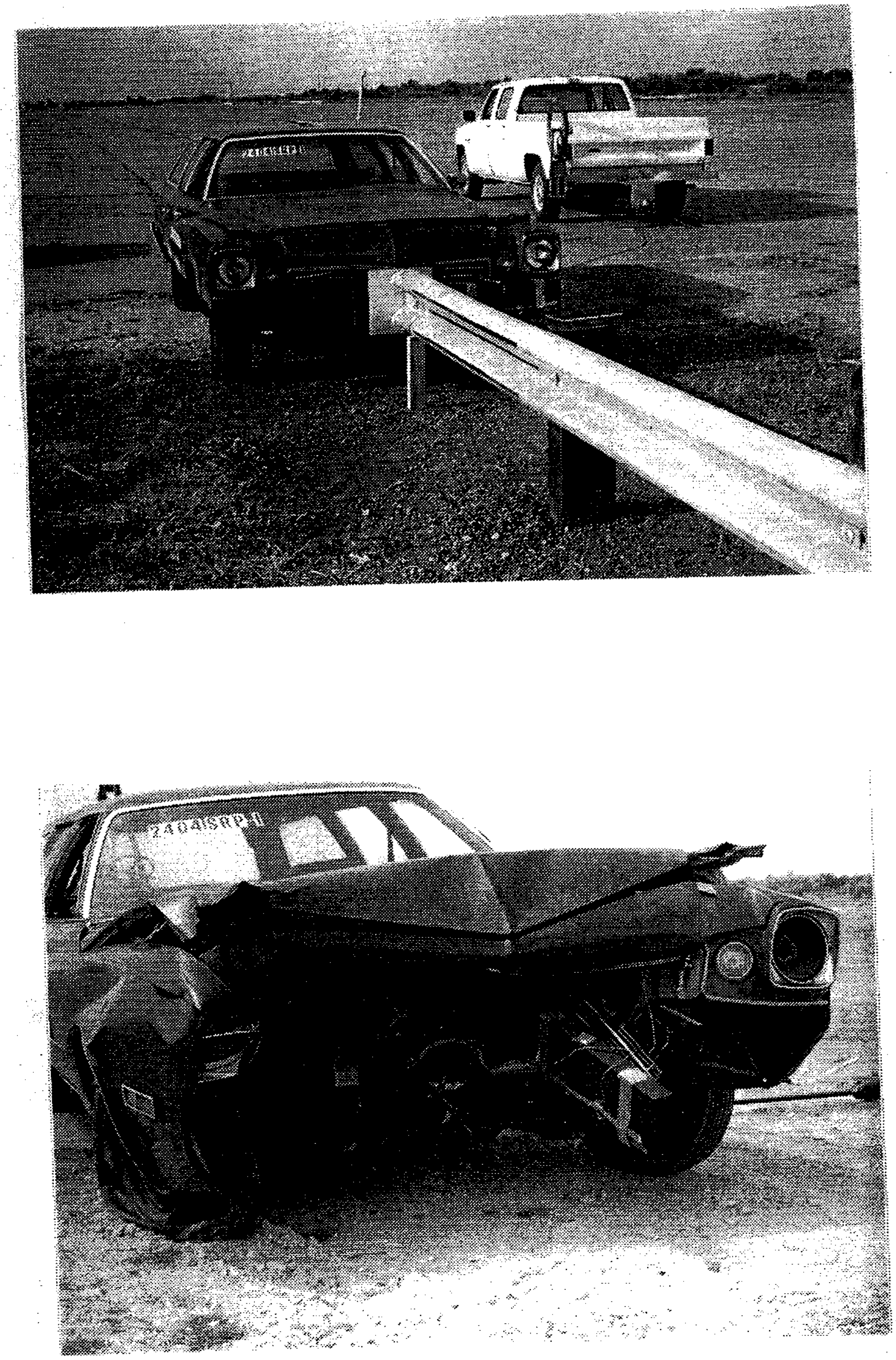

FIGURE B-2. VEHICLE BEFORE AND AFTER TEST SRP-1.

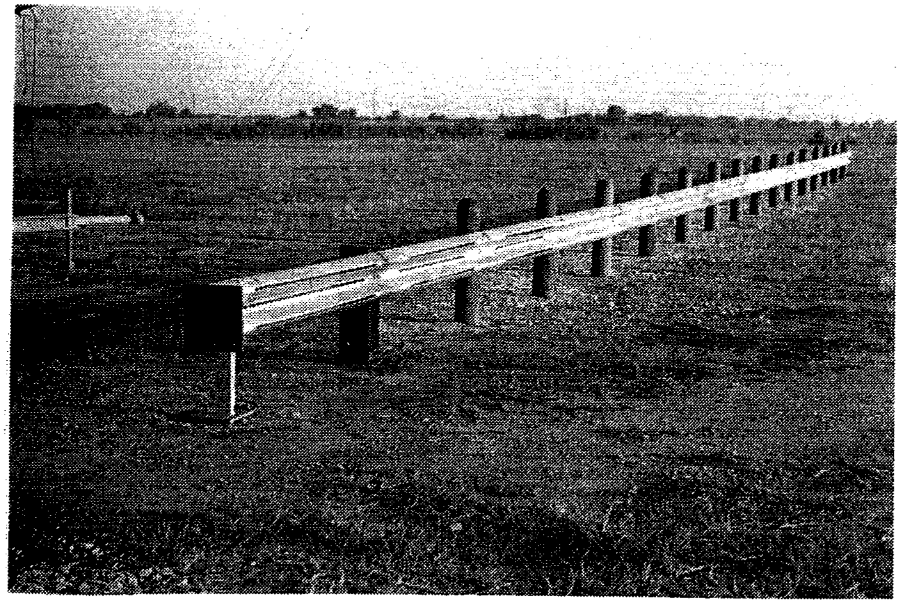

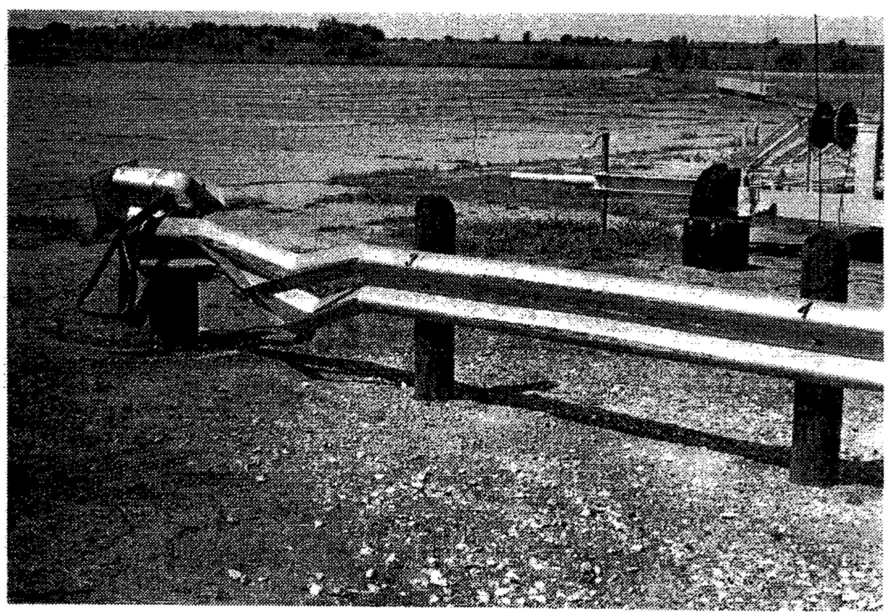

FIGURE B-3. INSTALLATION BEFORE AND AFTER TEST SRP-2.

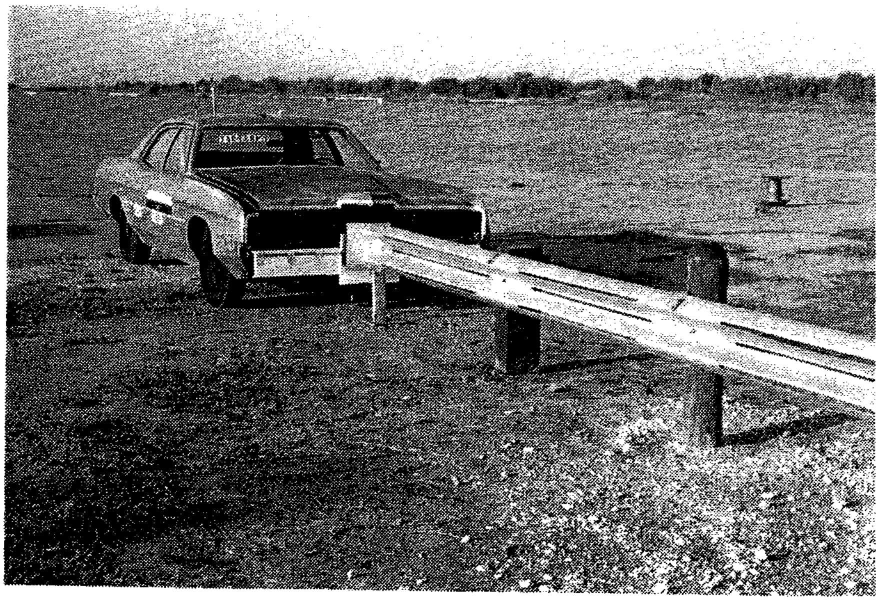

FIGURE B-4. VEHICLE BEFORE AND AFTER TEST SRP-2.

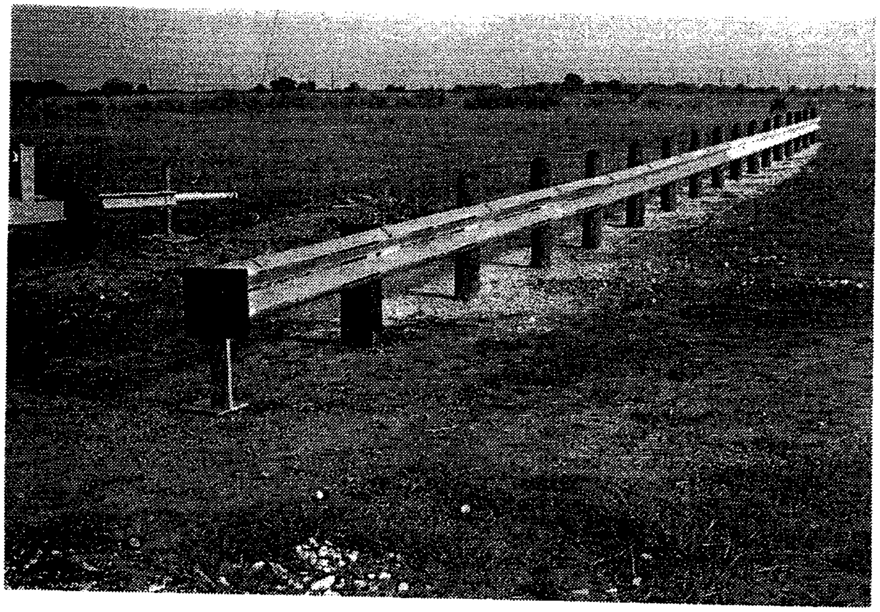

FIGURE B-5. INSTALLATION BEFORE AND AFTER TEST SRP-3.

FIGURE B-6. VEHICLE BEFORE AND AFTER TEST SRP-3.

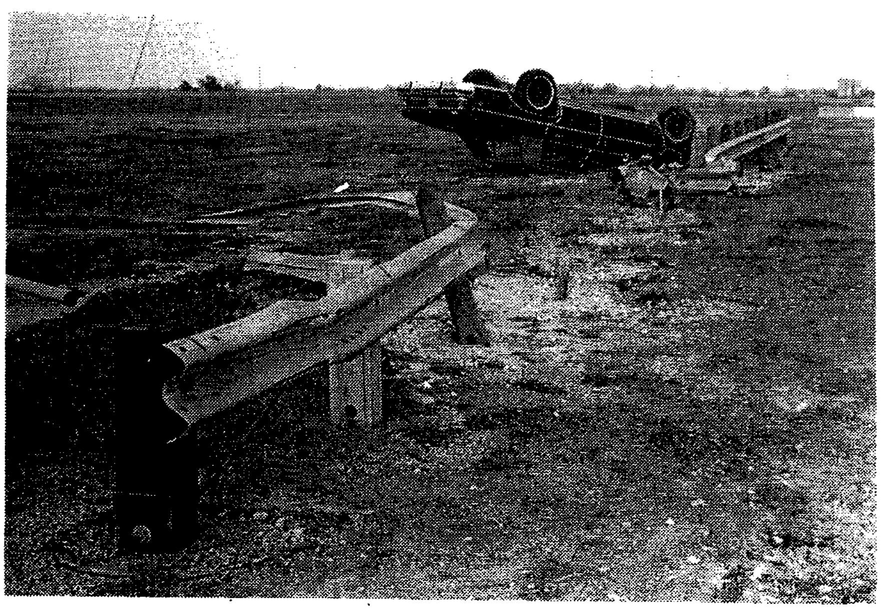

FIGURE B-7. VEHICLE AND BARRIER BEFORE AND AFTER TEST SRP-4.

SR-1

Test SR-1 was conducted to evaluate impact performance of the split rail in accordance with national safety guidelines (12). As in Test SRP-4, eight sections of rail were cut with 27 in. slots, and the posts were not blocked out. Cover plates were fitted over the slotted sections of the barrier to prevent the vehicle penetration that occured in Test SRP-4. These cover plates were fabricated from standard W-beam guardrail and were connected to the barrier with a single bolt and some clips (see Figure B-8). As in Test SRP-4, the first post was a 6 in. x 8 in. wood post set in a concrete footing. The second, third, and fourth posts of the installation were weakened to facilitate fracture during head-on impacts and, thereby, prevent the posts from laying over and forming a potential ramp for an impacting vehicle. A 3/4 in. galvanized steel rope was looped around the concrete footing and threaded through 2 3/8 in. diameter holes that were drilled through the posts at groundline. A steel bearing plate was fixed against the post with cable clamps. This cable system prevented the posts from rotating in the soil and promoted fracture of the posts at ground level. The completed test installation is shown in Figure B-9. Figure B-10 shows the vehicle before Test SR-1.

A 4600 lb, 1978 Mercury impacted the end treatment at 0.0 degrees and 60 m.p.h. Upon impact, the rail was pushed under the vehicle, forming a ramp. The vehicle was launched over posts 4, 5, and 6, and then rode over the remaining length of the installation. Figure B-11 shows the damage to the barrier after Test SR-1. Vehicle damage is shown in Figure B-12.

SR-2

The purpose of this test was to evaluate the performance of the split rail end treatment for a head on impact with a small car. In order to reduce the potential for vehicle ramping, the installation was flared away from the roadside with a maximum offset of 4 ft. Only four sections of slotted rail with 27 in. slots were used in conjunction with the flared installation. Furthermore, the cover plates were connected to the rail with three bolts (instead of a single bolt) in order to increase the bending strength in the vertical plane. The modified cover plate is shown in Figure B-13. Block outs were used throughout the length of the flared section. The complete test installation is shown in Figure B-14.

A 1979 Honda weighing 1750 lb. impacted the end treatment at 0.0 degrees and 58.2 m.p.h. The vehicle centerline was offset 15 in. towards the roadside. The first and second posts fractured upon impact, and the vehicle came to a stop behind the rail. The slotted sections of rail performed as intended. Barrier damage after the test is shown in Figure B-15, and the vehicle, before and after impact, is shown in Figure B-16. Occupant impact velocity and ridedown acceleration were 35.1 ft/sec and 10.7 g's

FIGURE B-8. COVER PLATE BOLTED TO
SPLIT RAIL (TEST SR-1).

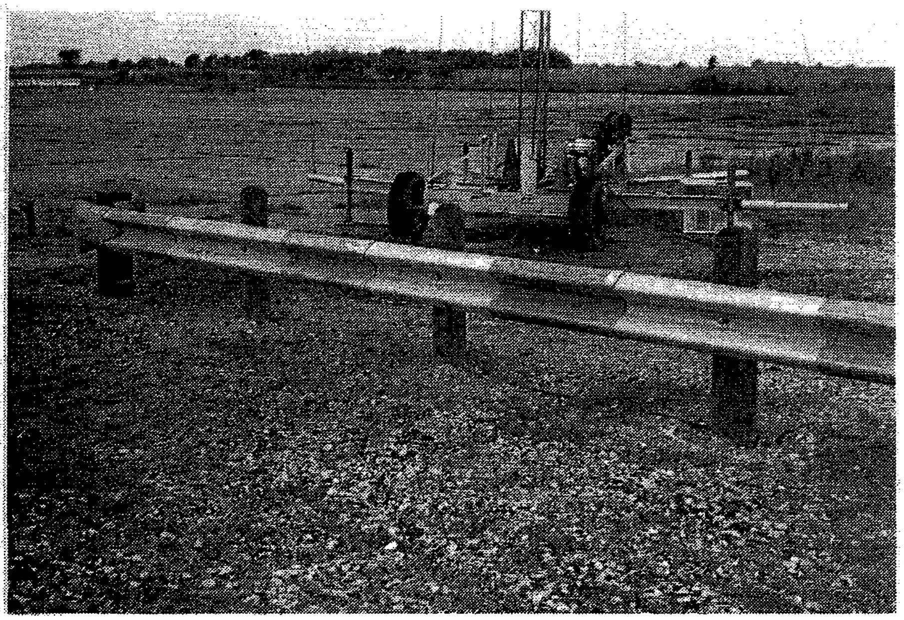

FIGURE B-9. SPLIT RAIL END TREATMENT
BEFORE TEST SR-1.

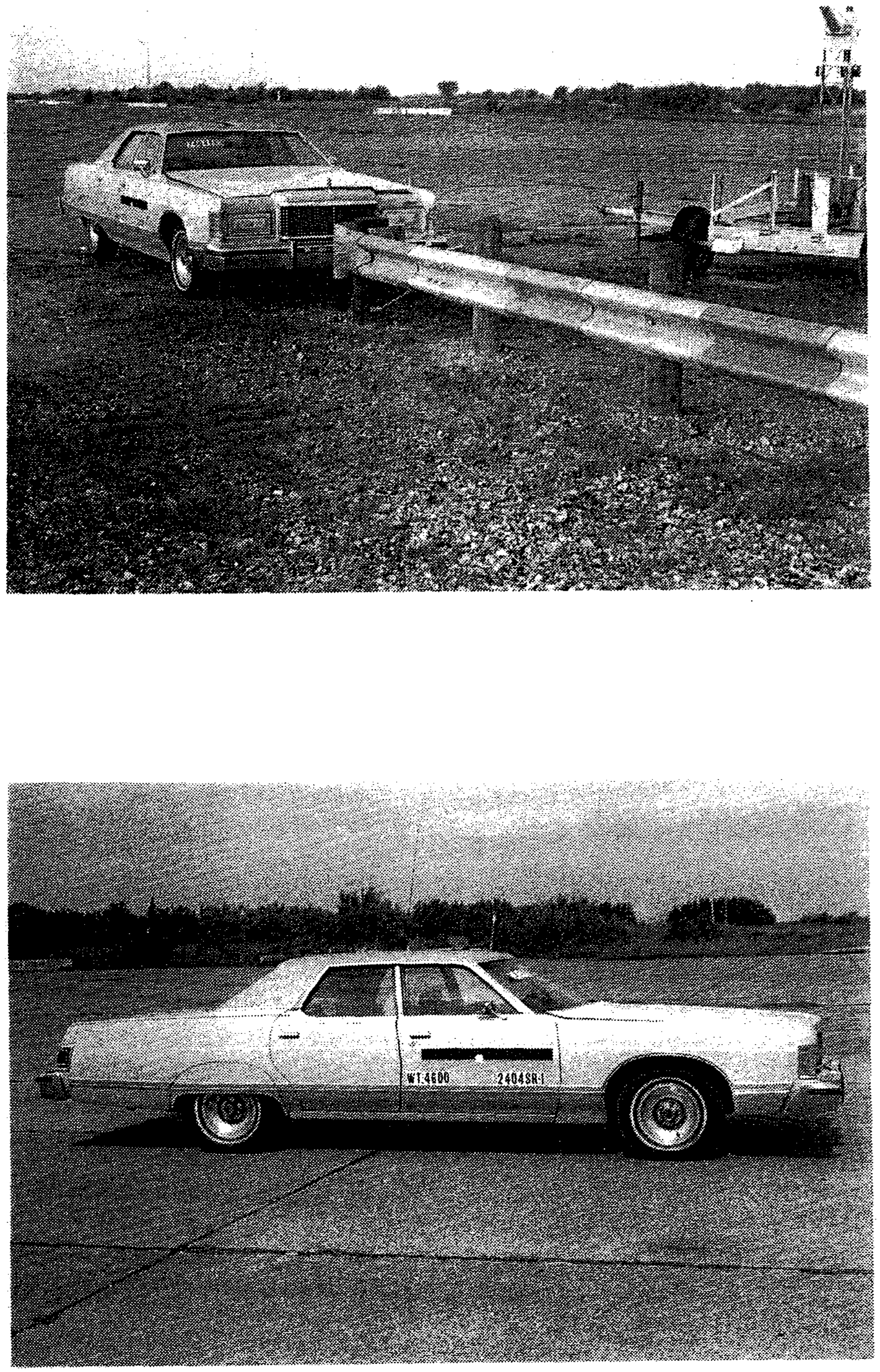

FIGURE B-10. VEHICLE BEFORE TEST SR-1.

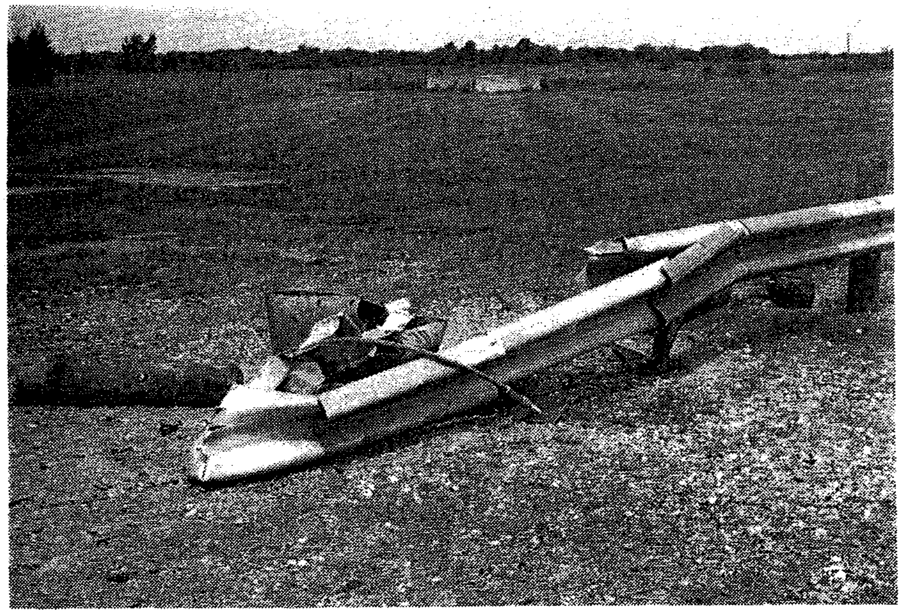

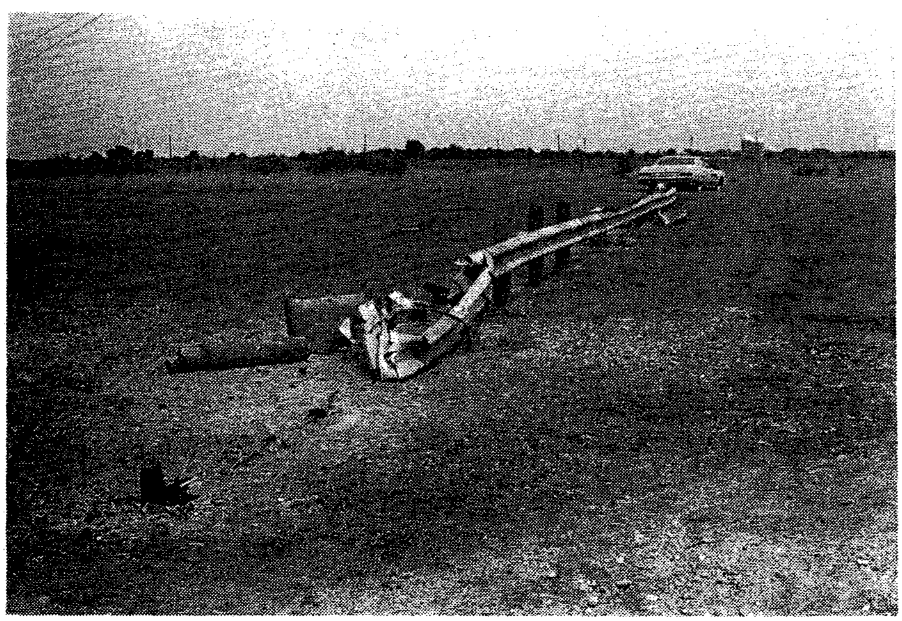

FIGURE B-11. SPLIT RAIL END TREATMENT
AFTER TEST SR-1.

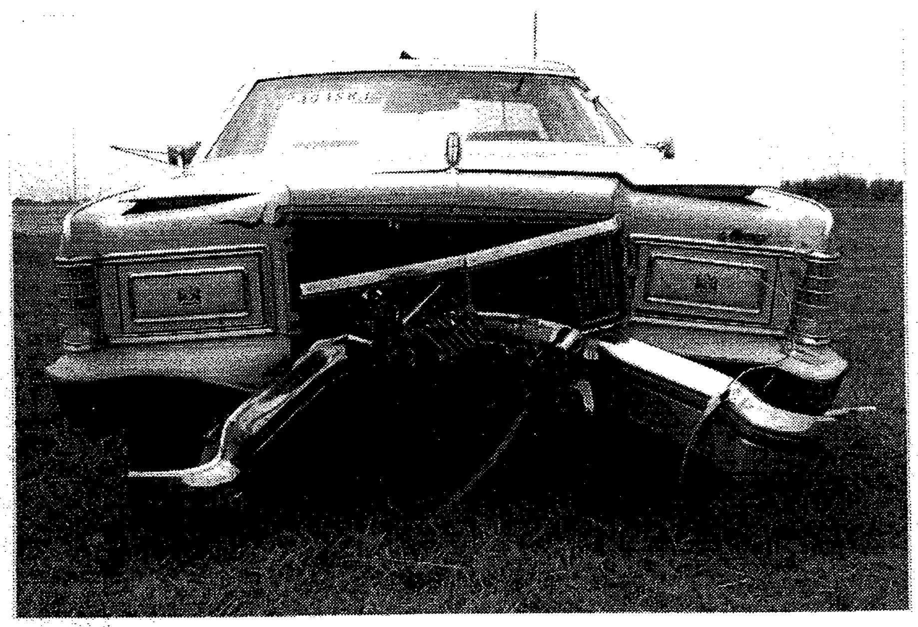

FIGURE B-12. VEHICLE AFTER TEST SR-1.

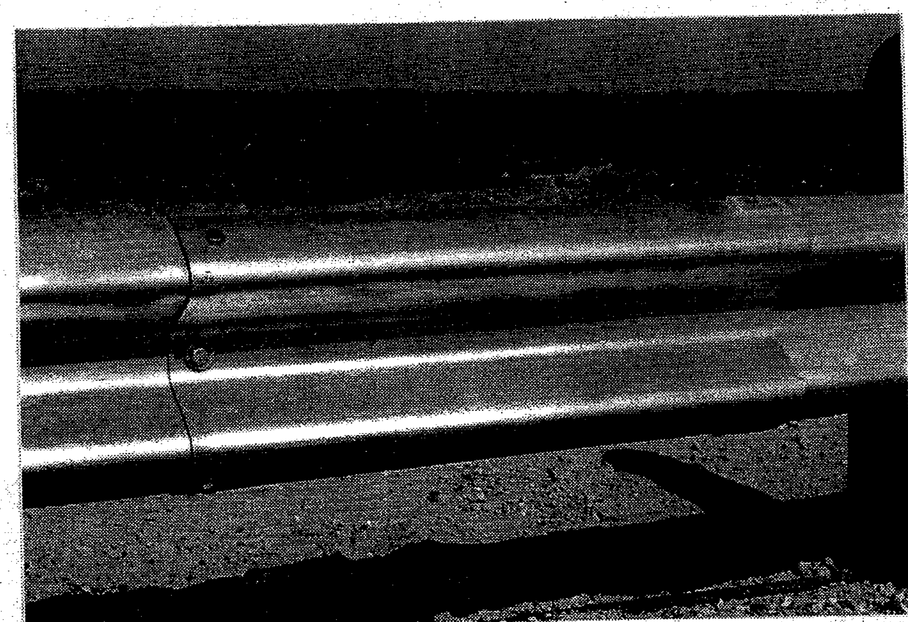

FIGURE B-13. COVER PLATE BOLTED TO SPLIT RAIL (TEST SR-2).

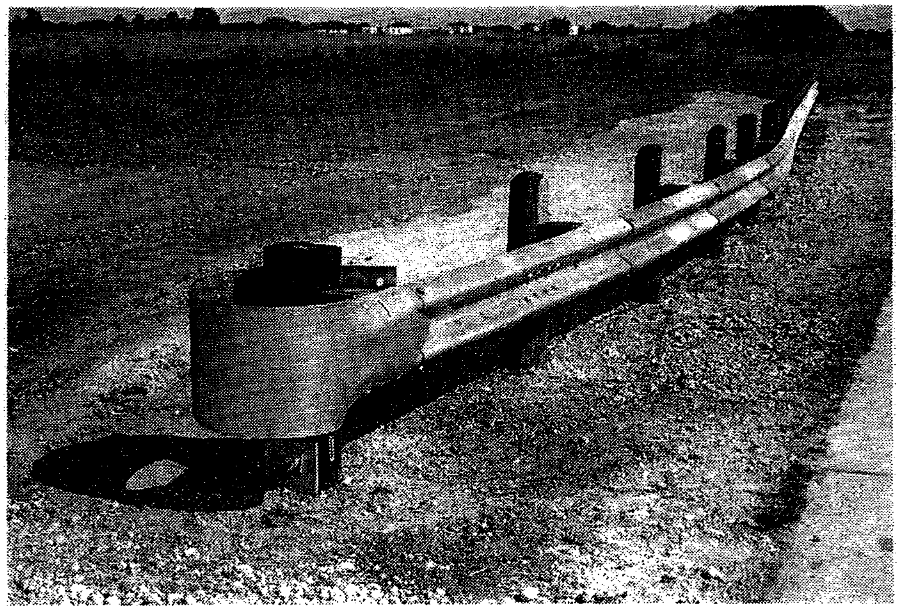

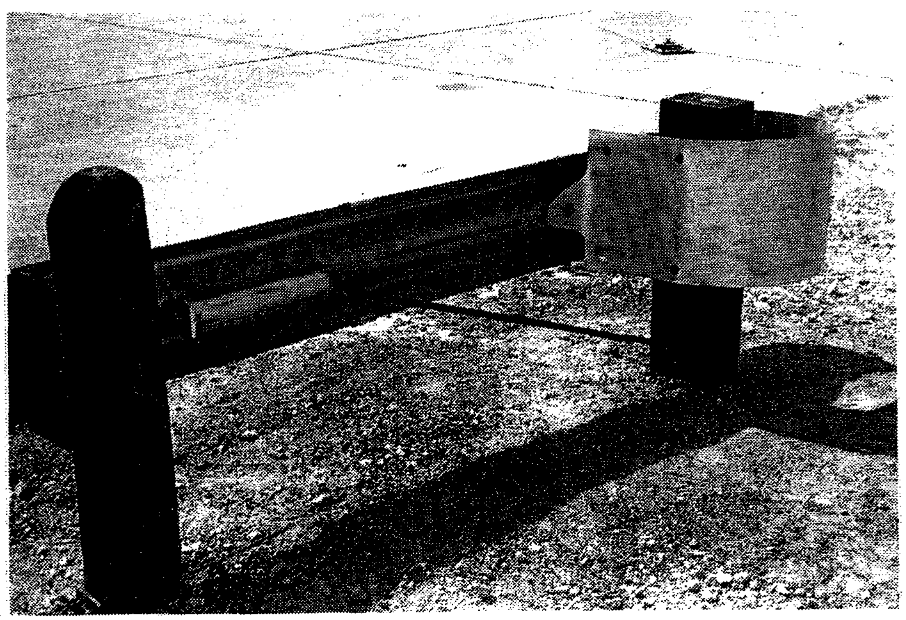

FIGURE B-14. SPLIT RAIL END TREATMENT
BEFORE TEST SR-2.

FIGURE B-15. SPLIT RAIL END TREATMENT
AFTER TEST SR-2.

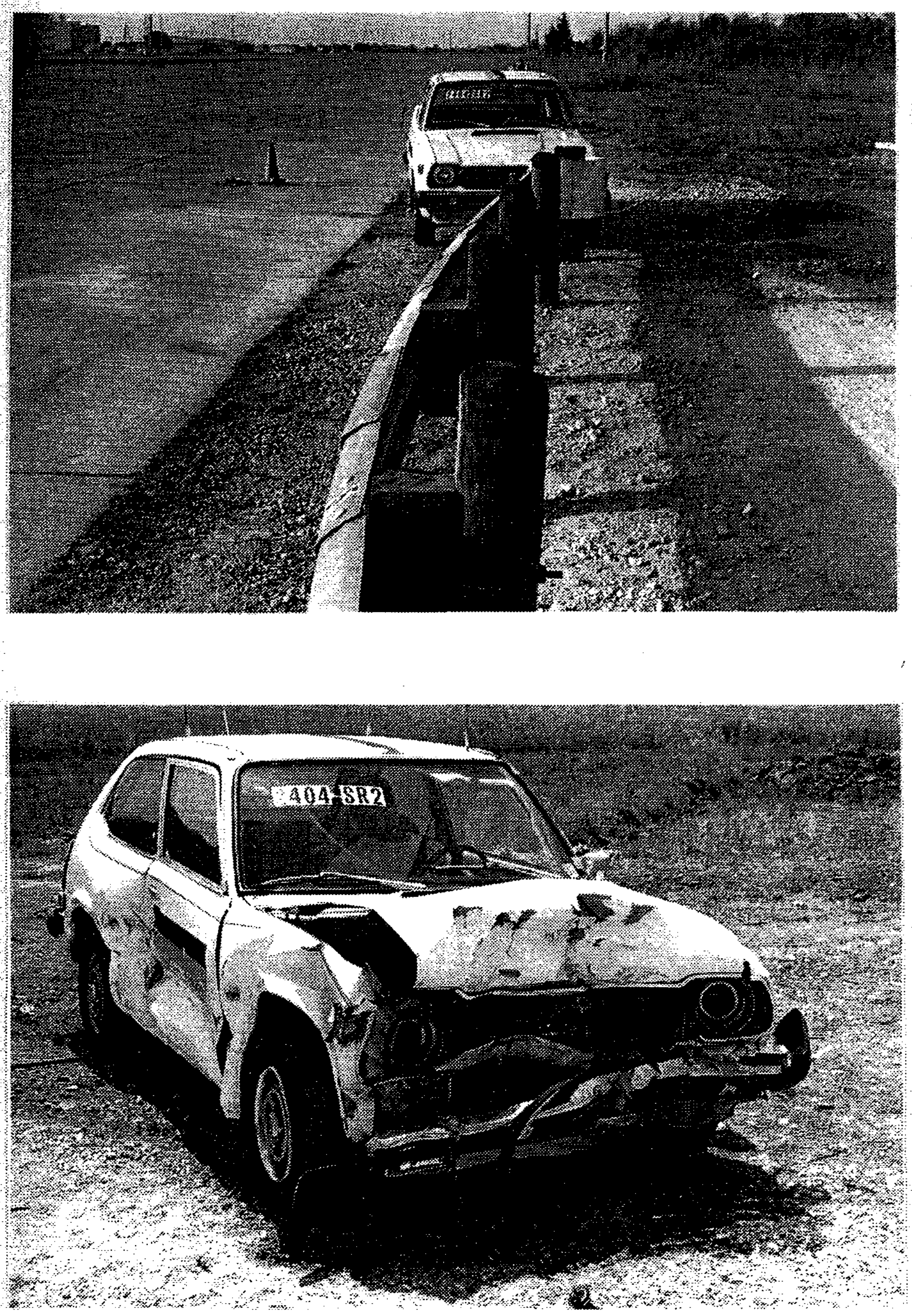

FIGURE B-16. VEHICLE BEFORE AND AFTER TEST SR-2.

respectively. Although the occupant impact velocity was above the recommended value (12), it was below the maximum acceptable value (12) and the test was considered a success.

Note that although posts 5 through 9 were weakened by holes drilled at the groundline, none of these posts fractured during this test, or subsequent tests, and thus this modification was not considered important to the design.

SR-3

This test evaluated the ability of the split rail end treatment to redirect a large car. The test installation was identical to that in Test SR-2 and is shown in Figure B-17. A 1977 Cadillac weighing 4508 lb. impacted the split rail at 61.3 m.p.h. and 25 degrees at a point just downstream of the third post. The vehicle had begun to redirect when a tear occured at a full strength bolt splice between the first two sections of W-beam. Upon the ensuing tensile failure of the guardrail, the vehicle yawed and was brought to a stop after impacting the exposed section of rail. Barrier damage after Test SR-3 is shown in Figure B-18. Figure B-19 shows the test vehicle before and after impact.

SR-4

This test was run with the same intent as Test SR-3. The test installation was the same as for Test SR-3 with the addition of two extra posts. These posts were centered in the third and fourth sections of slotted rail, reducing the effective post spacing in these sections from 6ft.- 3 in. to 3 ft.- 1.5 in. The additional posts were blocked out and were not attached to the barrier. The post placed in the third section of slotted rail was attached to the cable system through a 1 in. diameter hole drilled at groundline. The additional post placed in the fourth section of rail was a standard 7 in. diam. full strength post. This modified installation is shown in Figure B-20.

A 1977 Caprice weighing 4463 lb. impacted the split rail at 60.3 m.p.h. and 25 degrees. The impact occurred at the third post downstream from the end of the barrier. The vehicle was smoothly redirected. Figure B-21 shows the split rail installation after Test SR-4. The test vehicle before and after impact is shown in Figure B-22. The longitudinal and lateral occupant impact velocities were 20.9 ft/sec and 17.2 ft/sec respectively. The ridedown accelerations were 6.3 g's longitudinally and 9.1 g's laterally. Although no large snagging forces were generated, the exit velocity for this test was somewhat lower than safety standard recommendations (12). However, overall performance of this system was similar to the impact performance of other guardrail systems (14,15,16); and therefore, this test was considered to be a success.

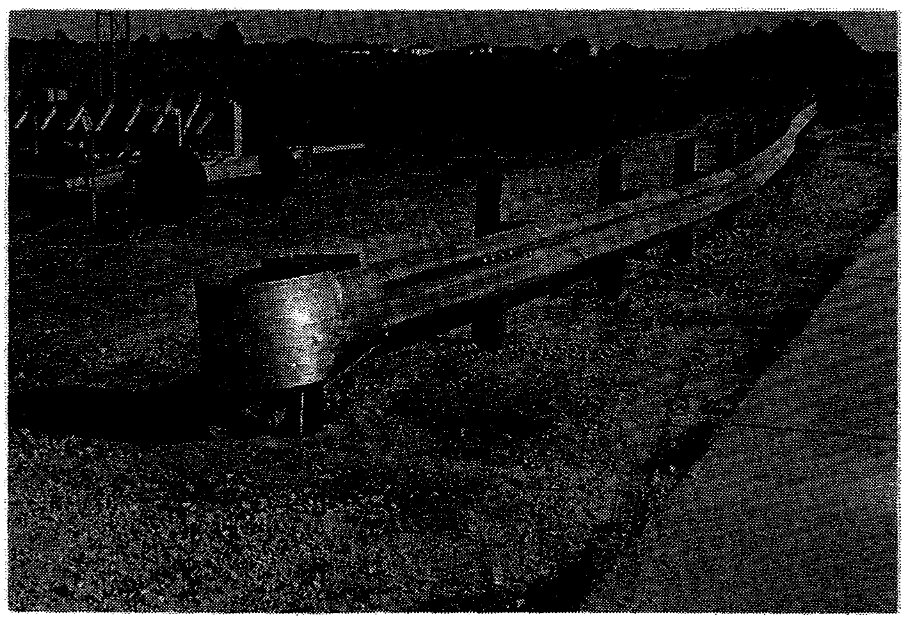

FIGURE B-17. SPLIT RAIL END TREATMENT
BEFORE TEST SR-3.

FIGURE B-18. SPLIT RAIL END TREATMENT
AFTER TEST SR-3.

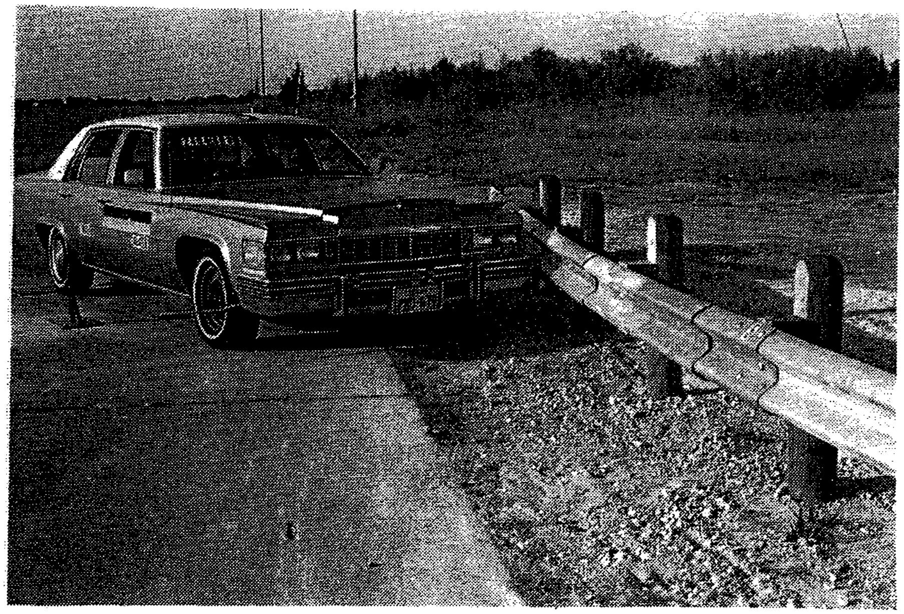

FIGURE B-19. VEHICLE BEFORE AND AFTER TEST SR-3.

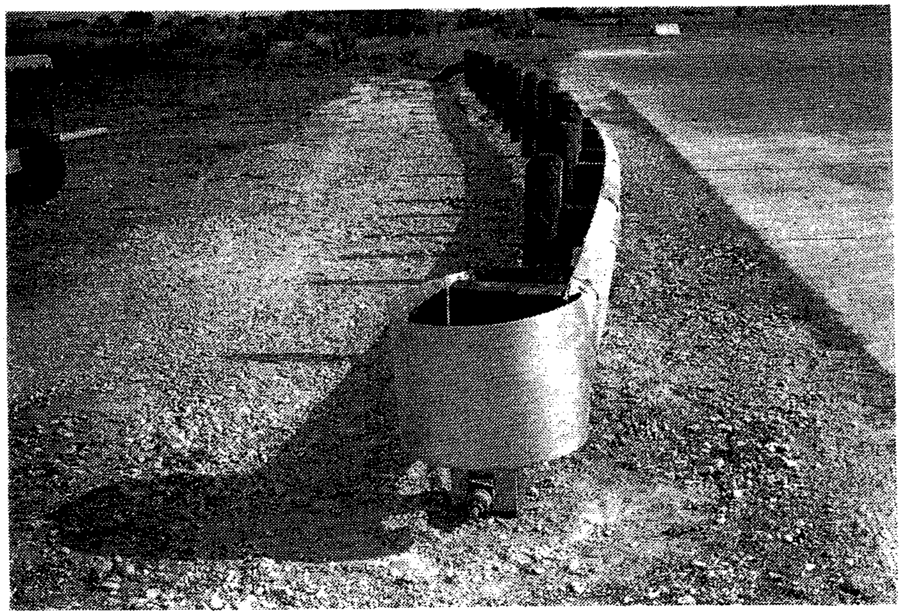

FIGURE B-20. SPLIT RAIL END TREATMENT
BEFORE TEST SR-4.

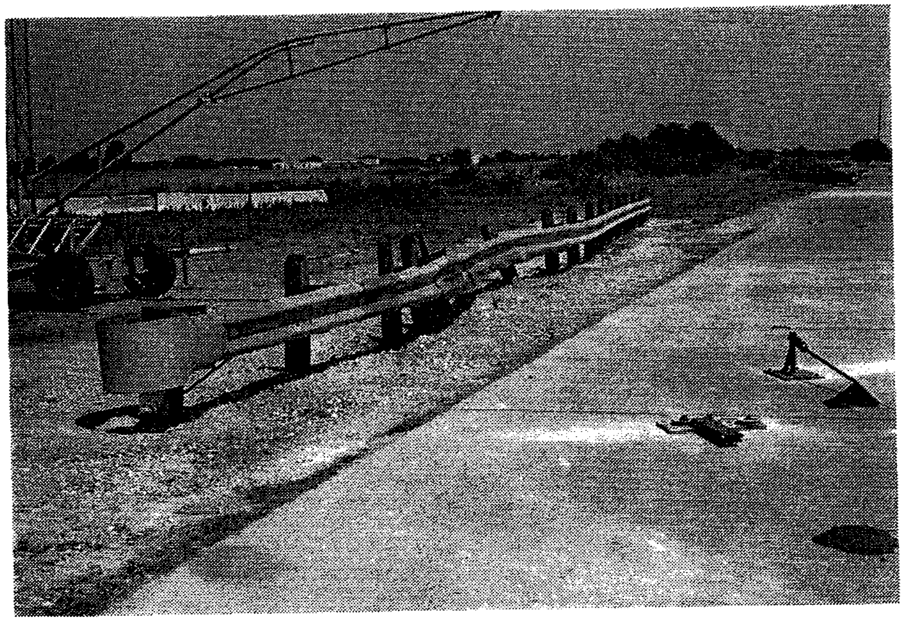

FIGURE B-21. SPLIT RAIL END TREATMENT
AFTER TEST SR-4.

FIGURE B-22. VEHICLE BEFORE AND AFTER TEST SR-4.

SR-5

This test was run to evaluate the ability of the split rail to redirect a small car during a side impact. The test installation was identical to Test SR-4 and is shown in Figure B-23. A 1979 Honda weighing 1810 lb. impacted the barrier just downstream of the second post at an angle of 15 degrees. The impact speed was 63.3 m.p.h. The vehicle was smoothly redirected. The barrier damage after Test SR-5 is shown in Figure B-24. Figure B-25 shows the test vehicle before and after the test.

The occupant impact velocities were 19.2 ft/sec longitudinally and 23.7 ft/sec laterally. The longitudinal and lateral ridedown accelerations were 1.8 g's and 13.8 g's respectively. The change in vehicle was 10.2 m.p.h. Although the lateral occupant impact velocity was slightly above recommended values (12), it was well within maximum acceptable limits and the test was considered to be a success.

SR-6

This test evaluated the performance of the split rail end treatment for a head-on impact with a large car. The test installation was identical to Tests SR-4 and SR-5 and is shown in Figure B-26. A 1979 Cadillac weighing 4470 lb. impacted the test installation at 0.0 degrees and 60.0 m.p.h. The vehicle fractured the first three posts and penetrated behind the barrier in a controlled manner. The vehicle traveled parallel to the barrier and came to rest approximately 100 ft. past the point of impact. Figure B-27 shows the barrier after Test SR-6. The vehicle before and after impact is shown in Figure B-28.

The flared end and slotted sections of rail performed as intended, and the test was considered a success. The occupant impact velocity and ridedown acceleration were 17.4 ft/sec and 5.8 g's respectively.

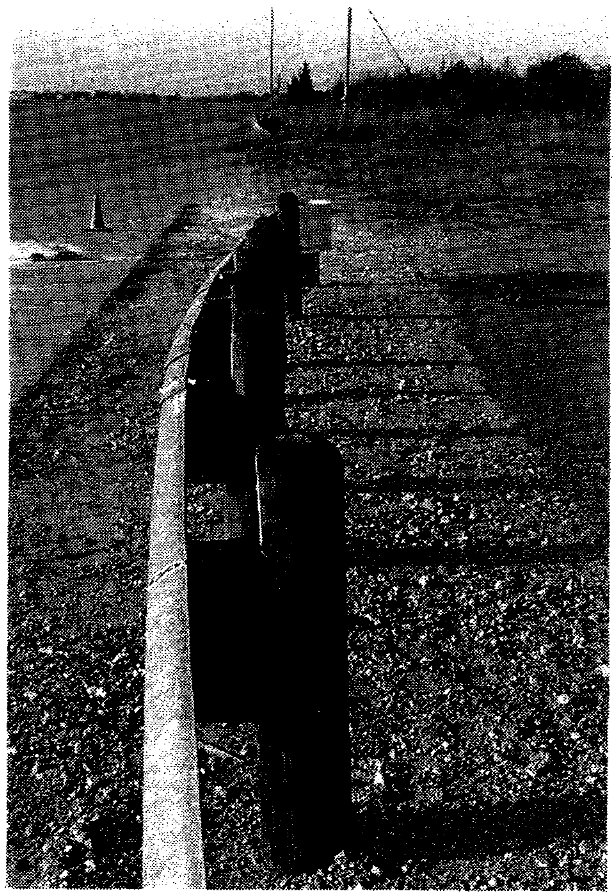

FIGURE B-23. SPLIT RAIL END TREATMENT BEFORE TEST SR-5.

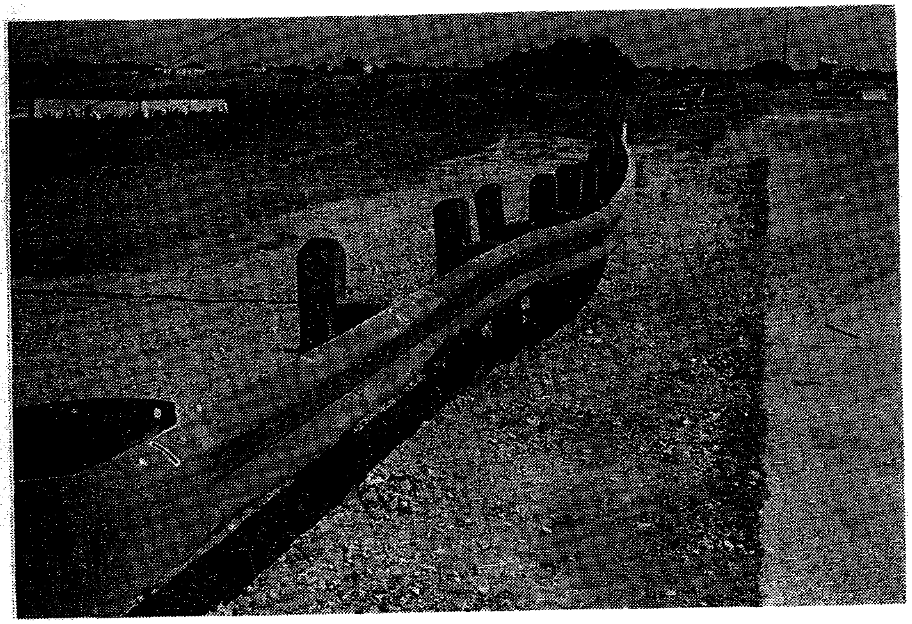

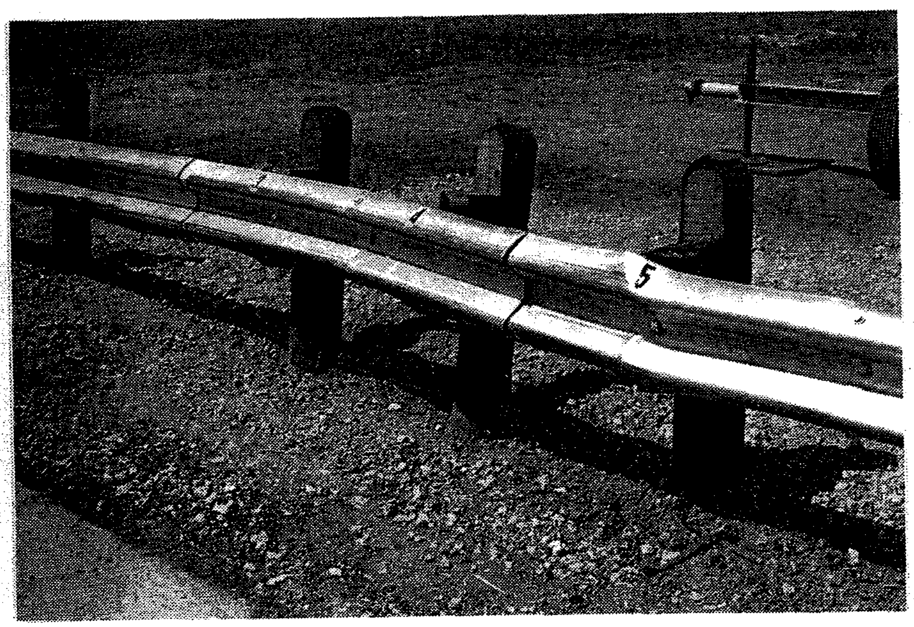

FIGURE B-24. SPLIT RAIL END TREATMENT AFTER TEST SR-5.

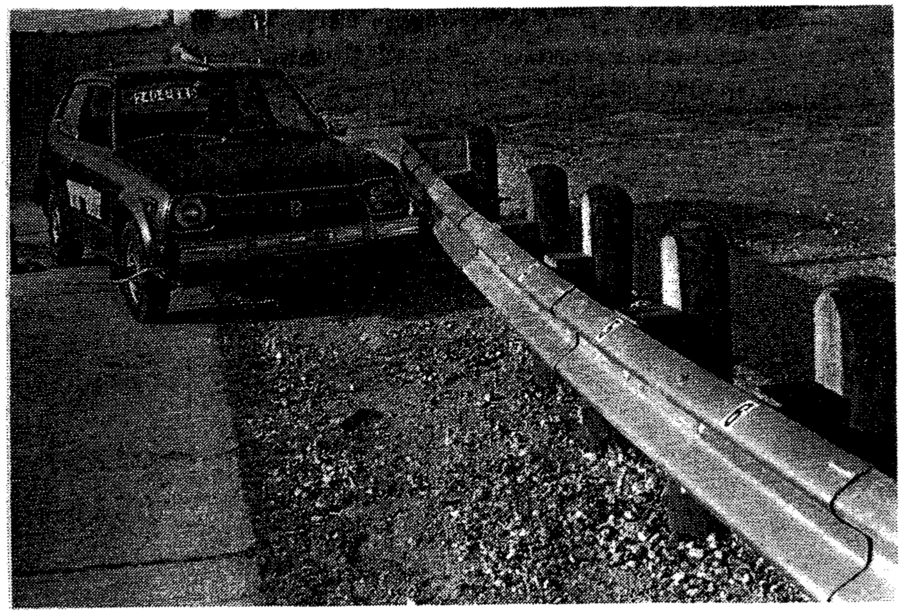

FIGURE B-25. VEHICLE BEFORE AND AFTER
TEST SR-5.

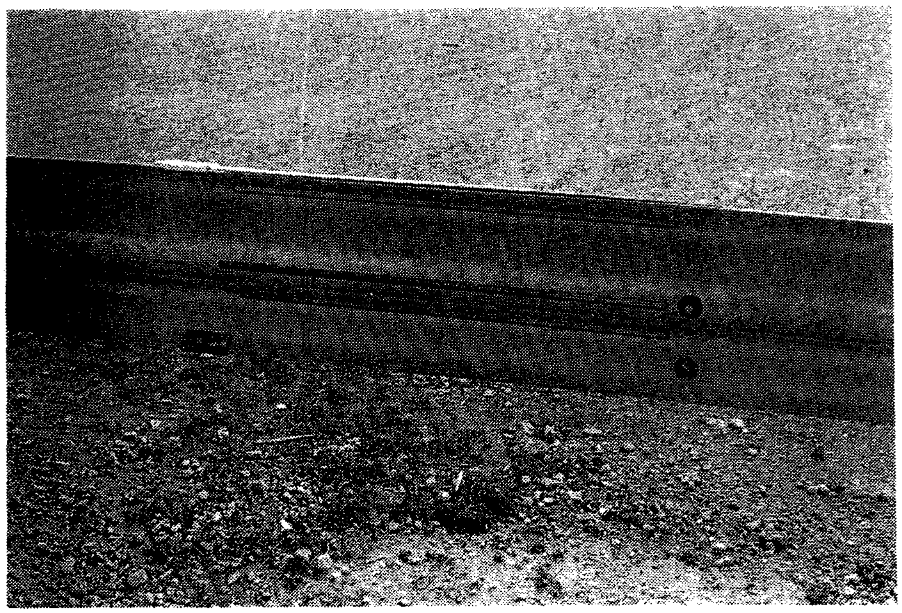

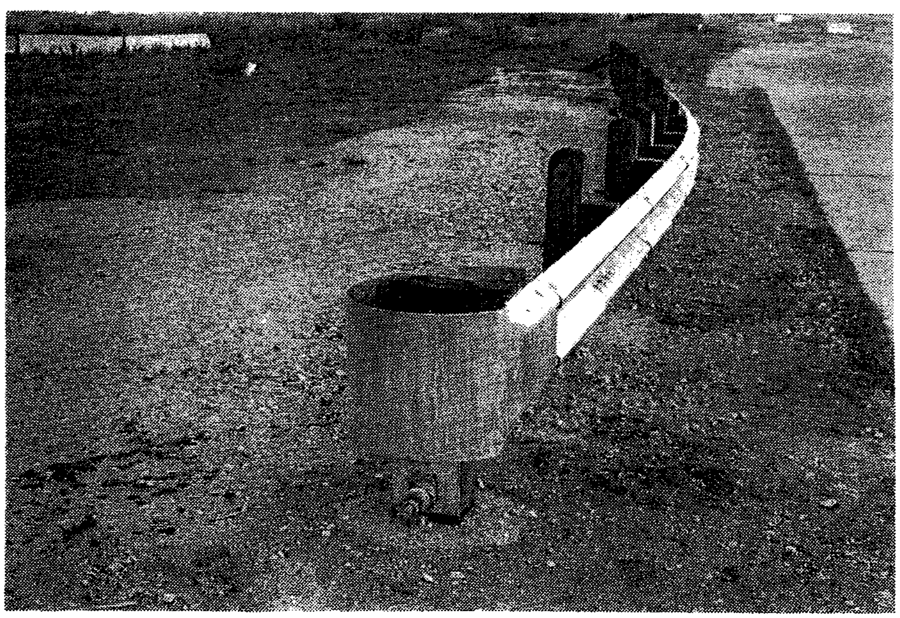

FIGURE B-26. SPLIT RAIL END TREATMENT
BEFORE TEST SR-6.

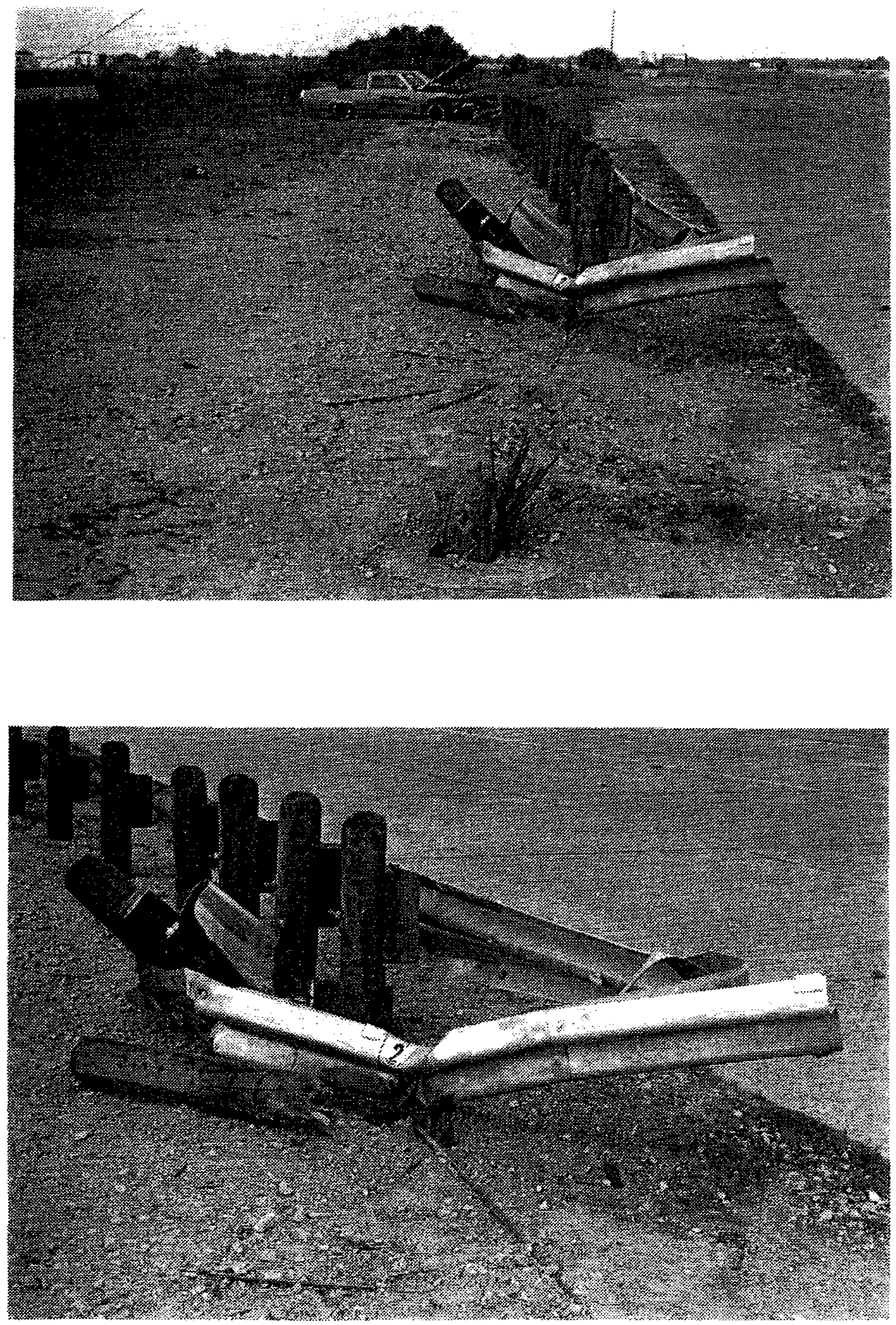

FIGURE B-27. SPLIT RAIL END TREATMENT
AFTER TEST SR-6.

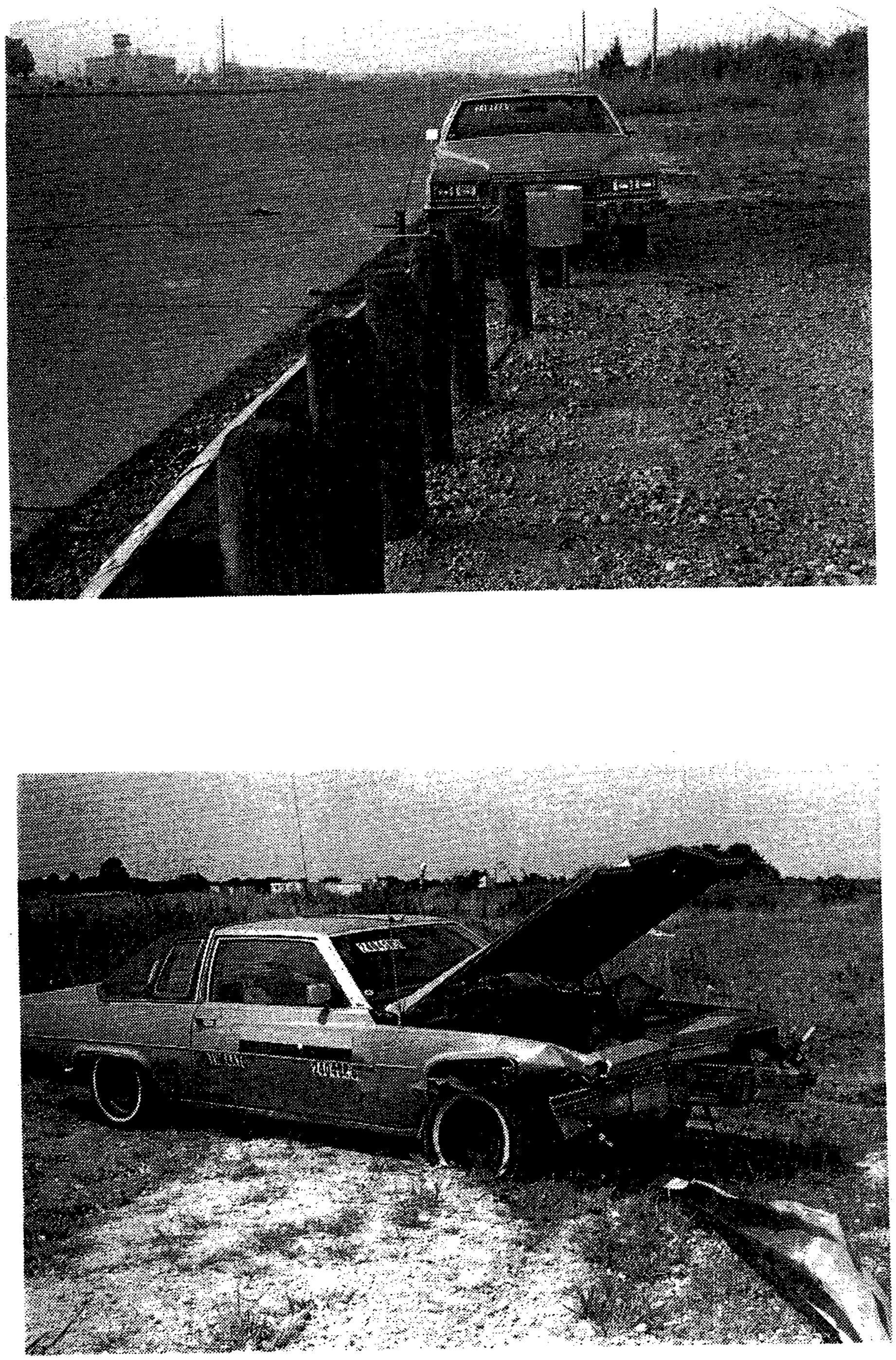

FIGURE B-28. VEHICLE BEFORE AND AFTER TEST SR-6.

APPENDIX C.

ROTATIONAL DISPLACEMENT PLOTS

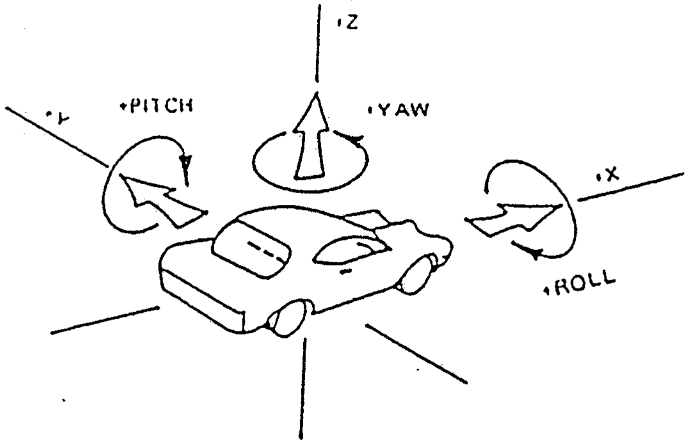

Axes are vehicle fixed.
Sequence for determining orientation is:

1. Yaw
2. Pitch
3. Roll

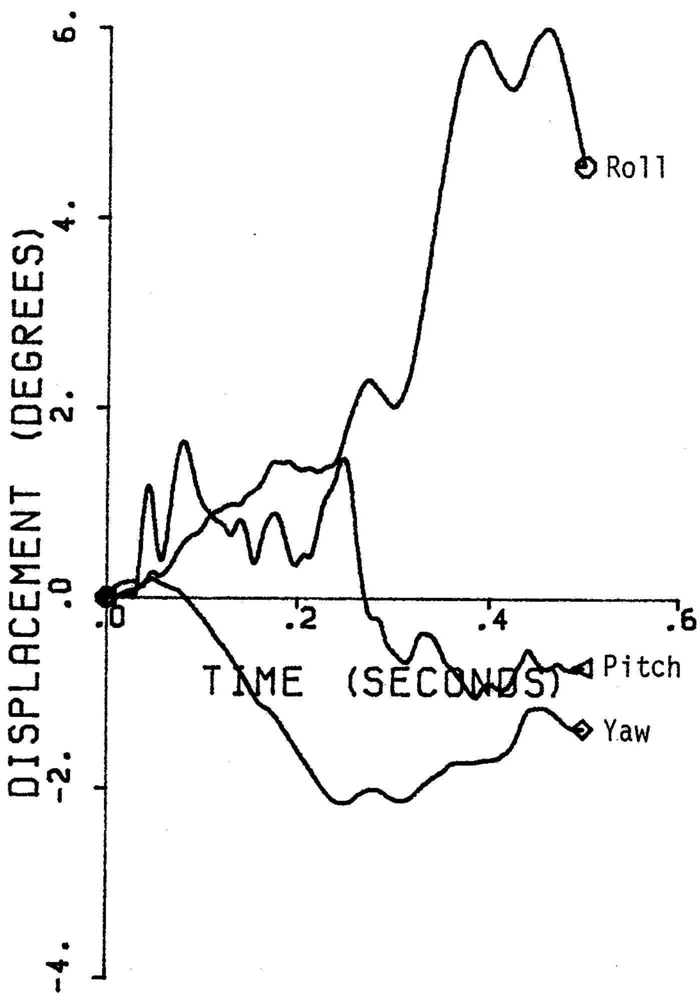

FIGURE C-1. VEHICLE ANGULAR DISPLACEMENTS FOR TEST MB-1.

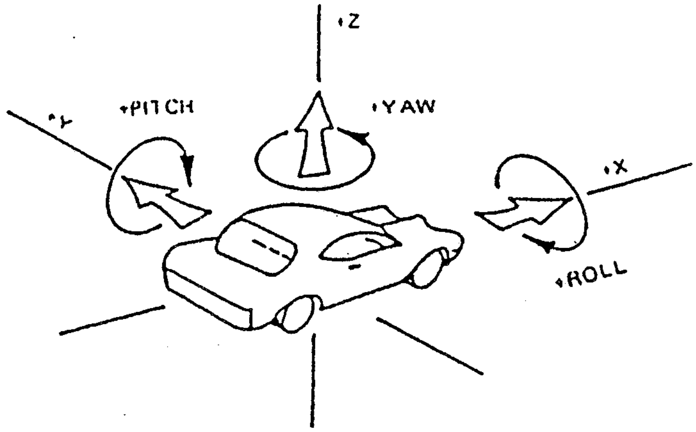

Axes are vehicle fixed.
Sequence for determining orientation is:

1. Yaw
2. Pitch
3. Roll

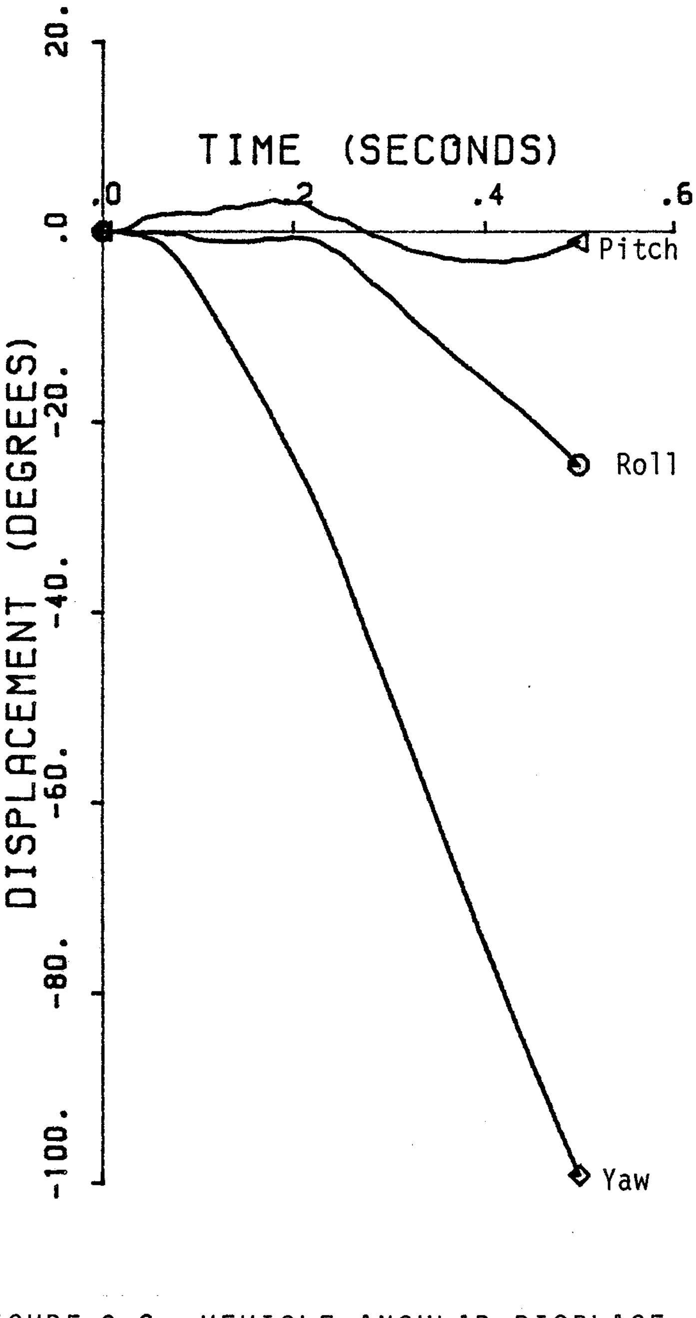

FIGURE C-2. VEHICLE ANGULAR DISPLACEMENTS FOR TEST MB-2.

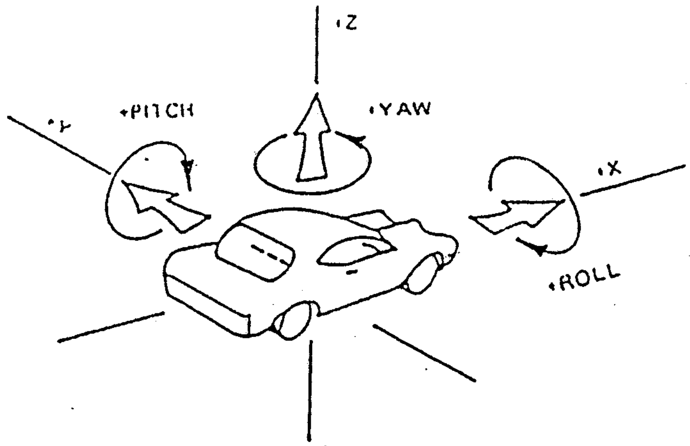

Axes are vehicle fixed.
Sequence for determining orientation is:

1. Yaw
2. Pitch
3. Roll

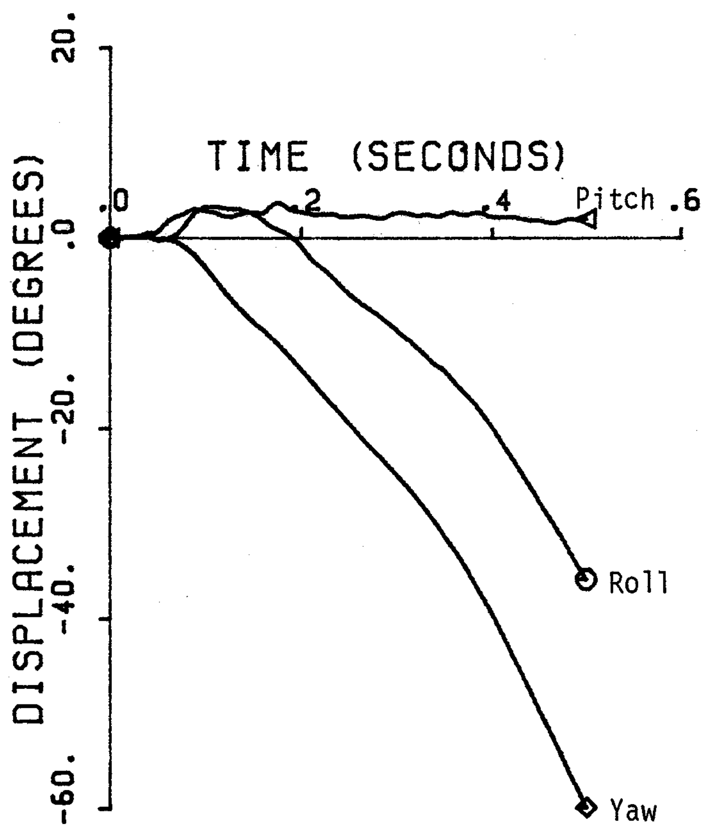

FIGURE C-3. VEHICLE ANGULAR DISPLACEMENTS FOR TEST MB-3.

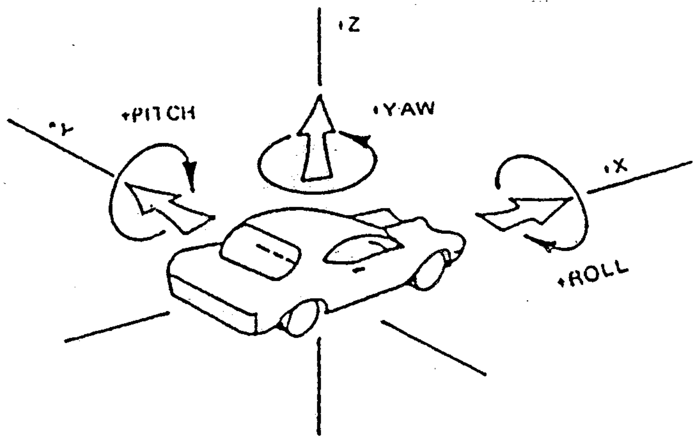

Axes are vehicle fixed.
Sequence for determining orientation is:

1. Yaw
2. Pitch
3. Roll

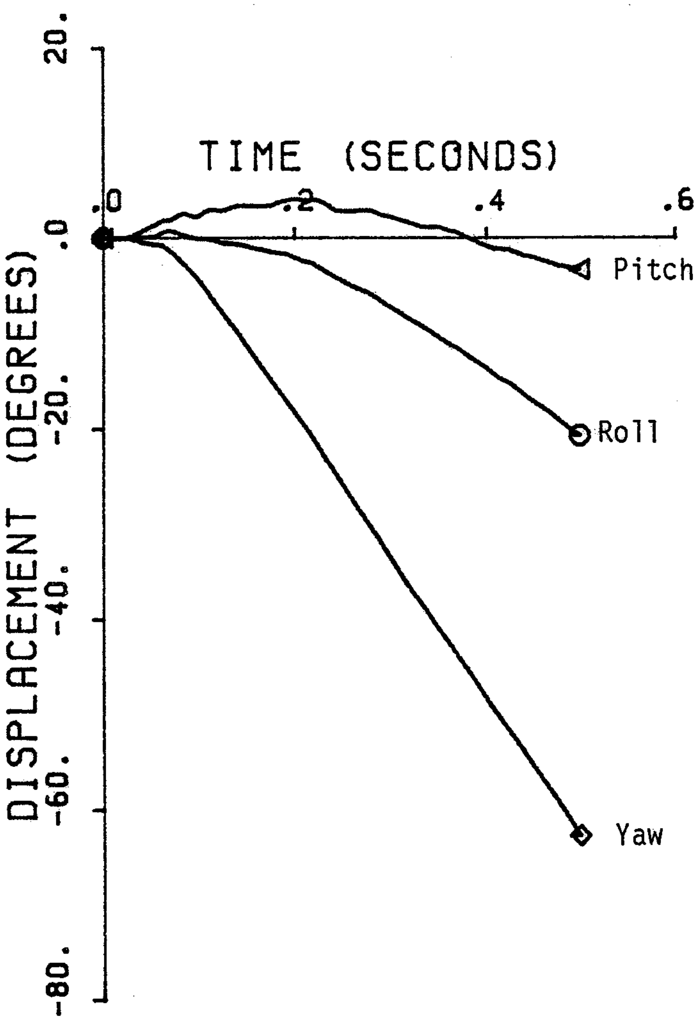

FIGURE C-4. VEHICLE ANGULAR DISPLACEMENTS FOR TEST MB-4.

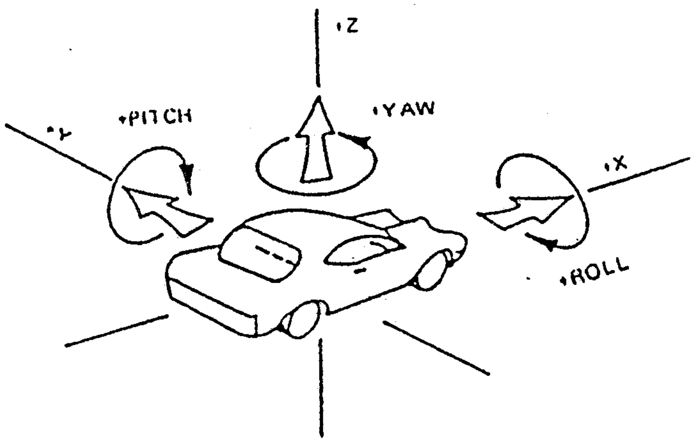

Axes are vehicle fixed.
Sequence for determining orientation is:
1. Yaw
2. Pitch
3. Roll

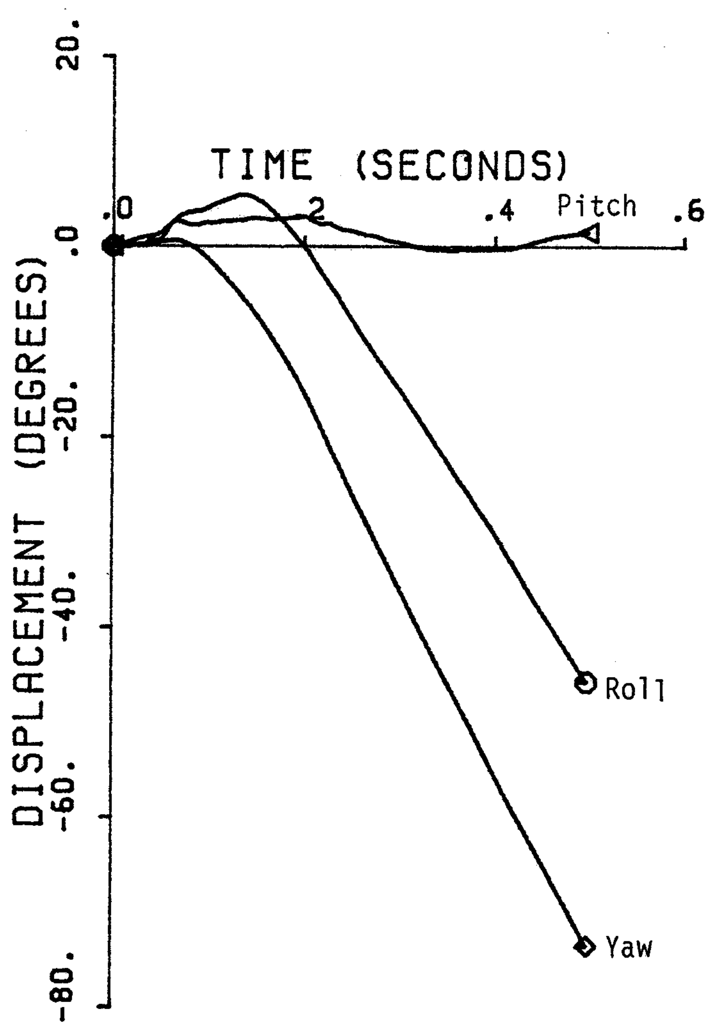

FIGURE C-5. VEHICLE ANGULAR DISPLACEMENTS FOR TEST MB-5.

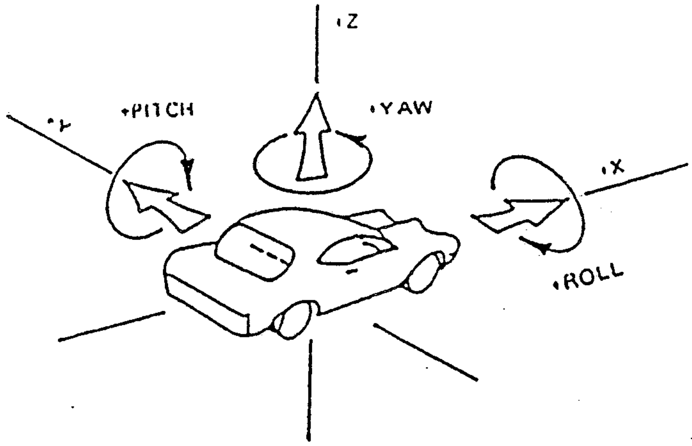

Axes are vehicle fixed.
Sequence for determining orientation is:

1. Yaw
2. Pitch
3. Roll

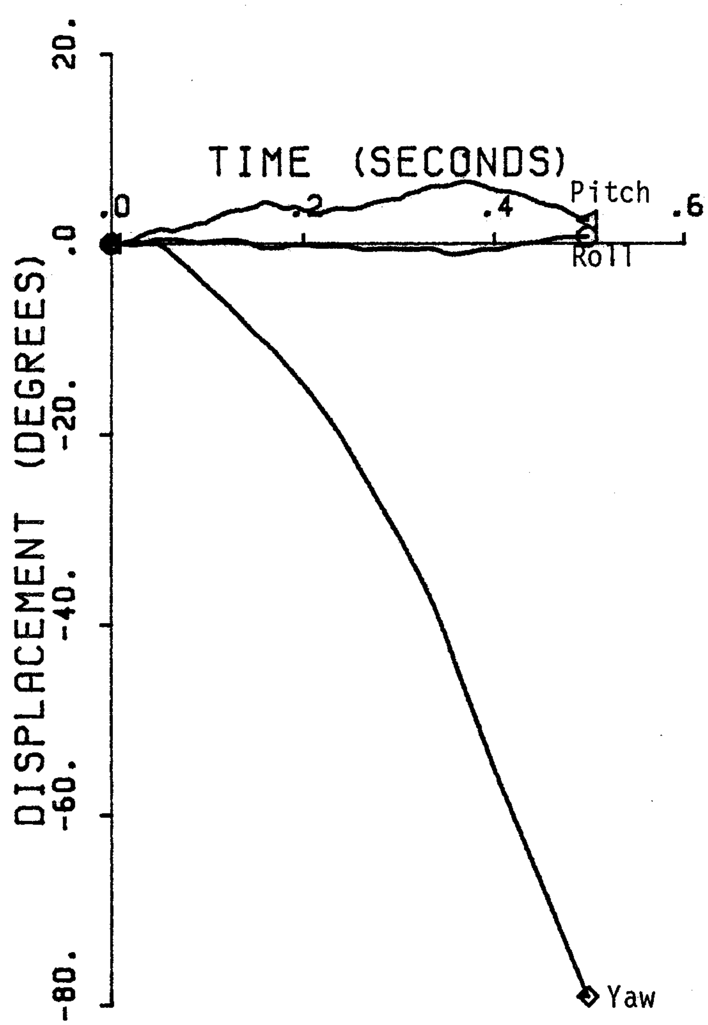

FIGURE C-6. VEHICLE ANGULAR DISPLACEMENTS FOR TEST MB-6.

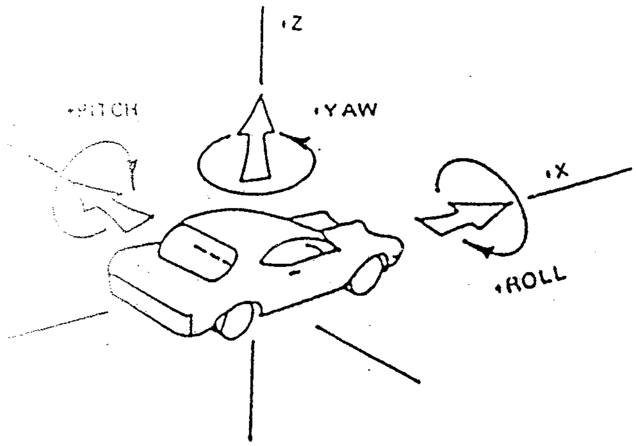

Axes are vehicle fixed.
Sequence for determining orientation is:

1. Yaw
2. Pitch
3. Roll

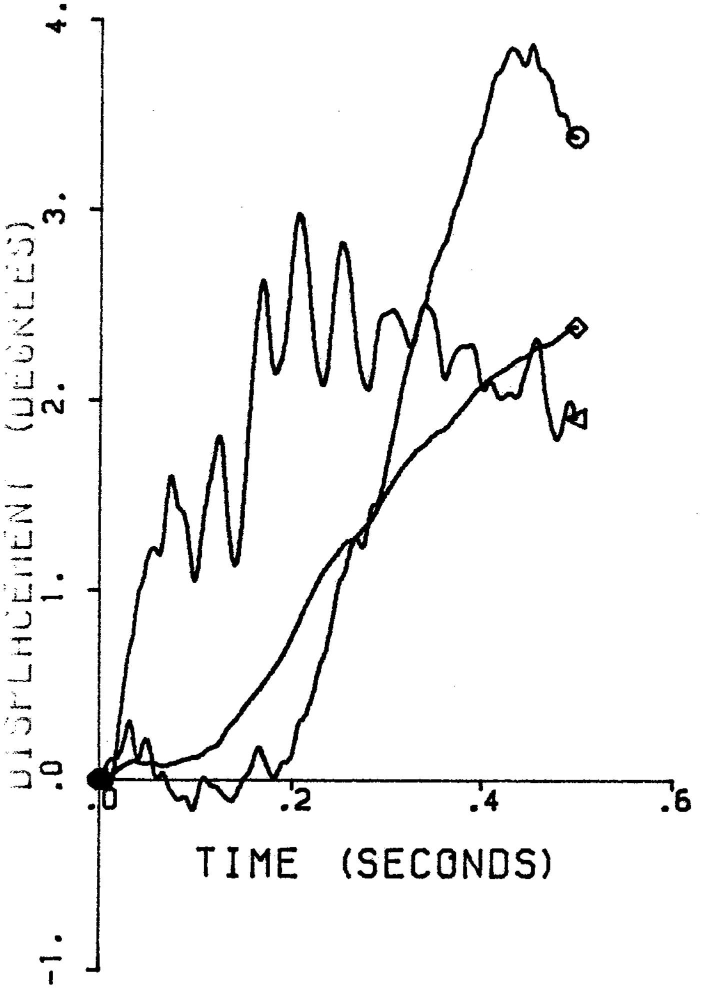

FIGURE C-7. VEHICLE ANGULAR DISPLACEMENTS FOR TEST MB-7.

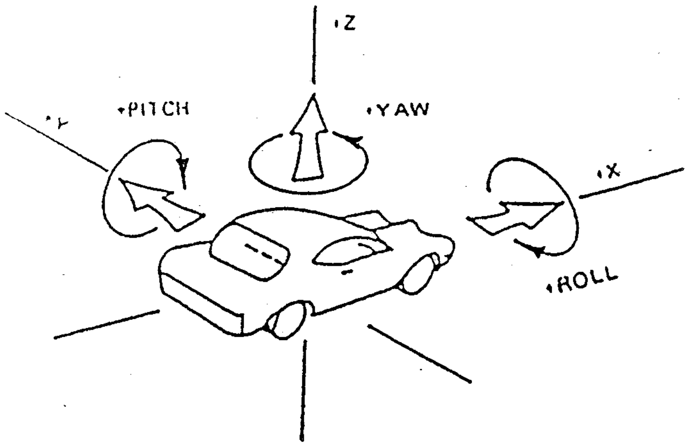

Axes are vehicle fixed.
Sequence for determining orientation is:
1. Yaw
2. Pitch
3. Roll

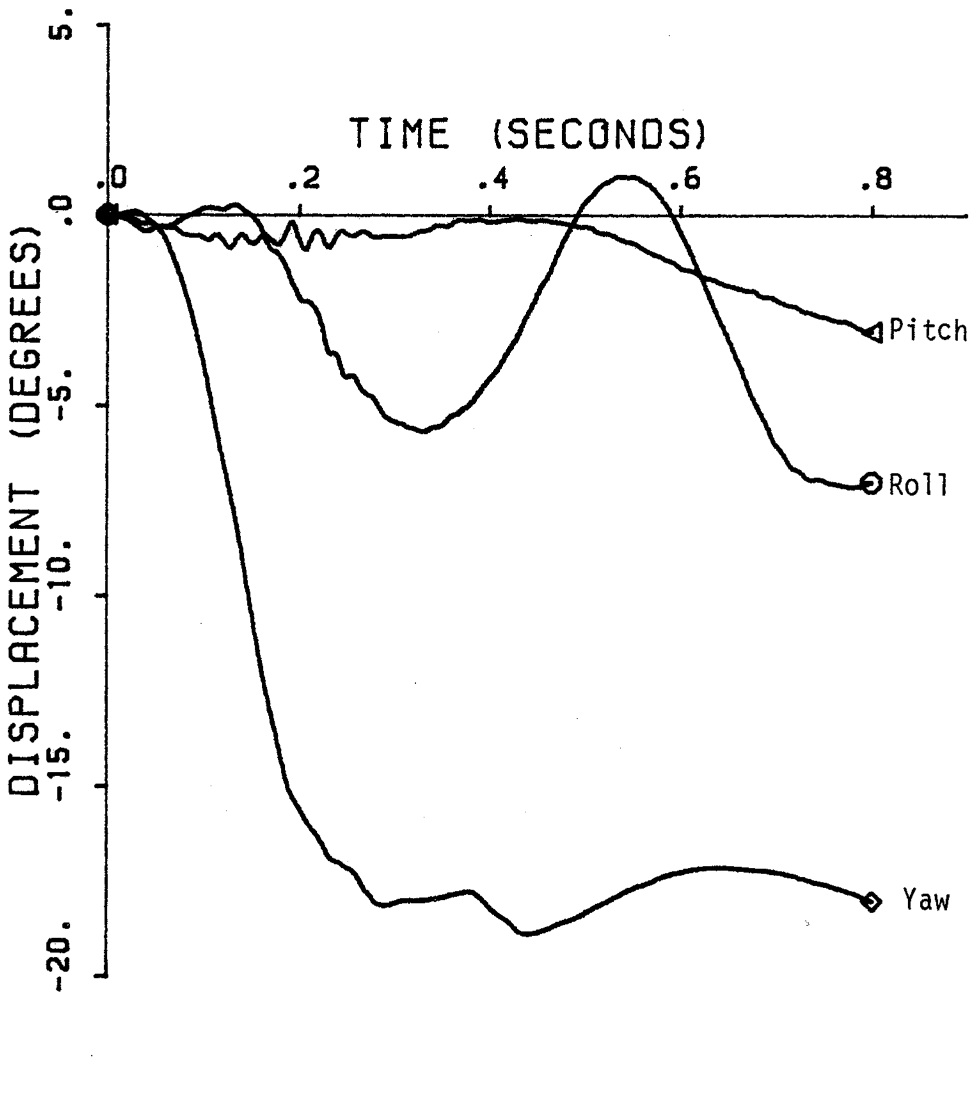

FIGURE C-8. VEHICLE ANGULAR DISPLACEMENTS FOR TEST 9429A-1.

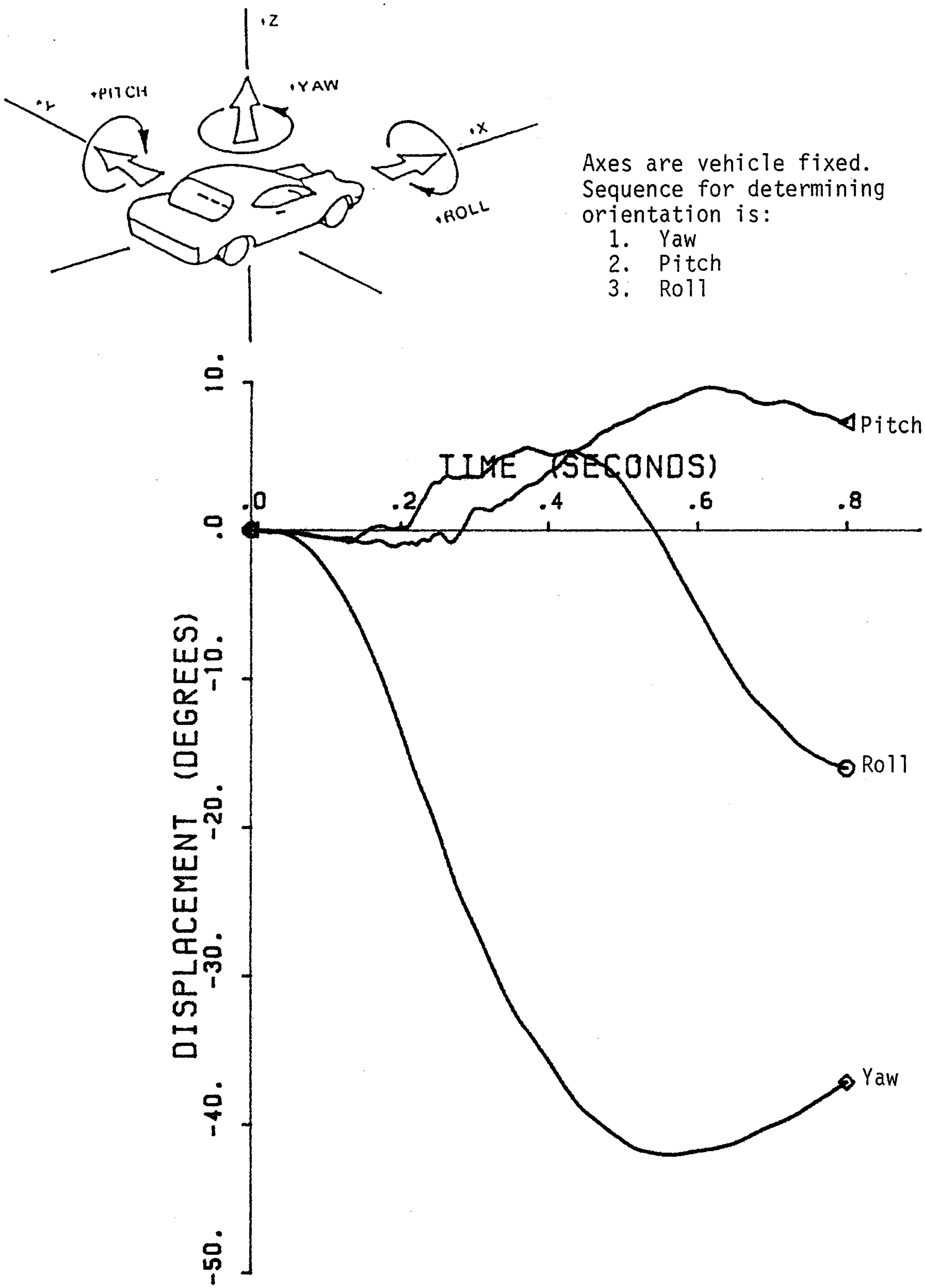

FIGURE C-9. VEHICLE ANGULAR DISPLACEMENTS FOR TEST 9429A-2.

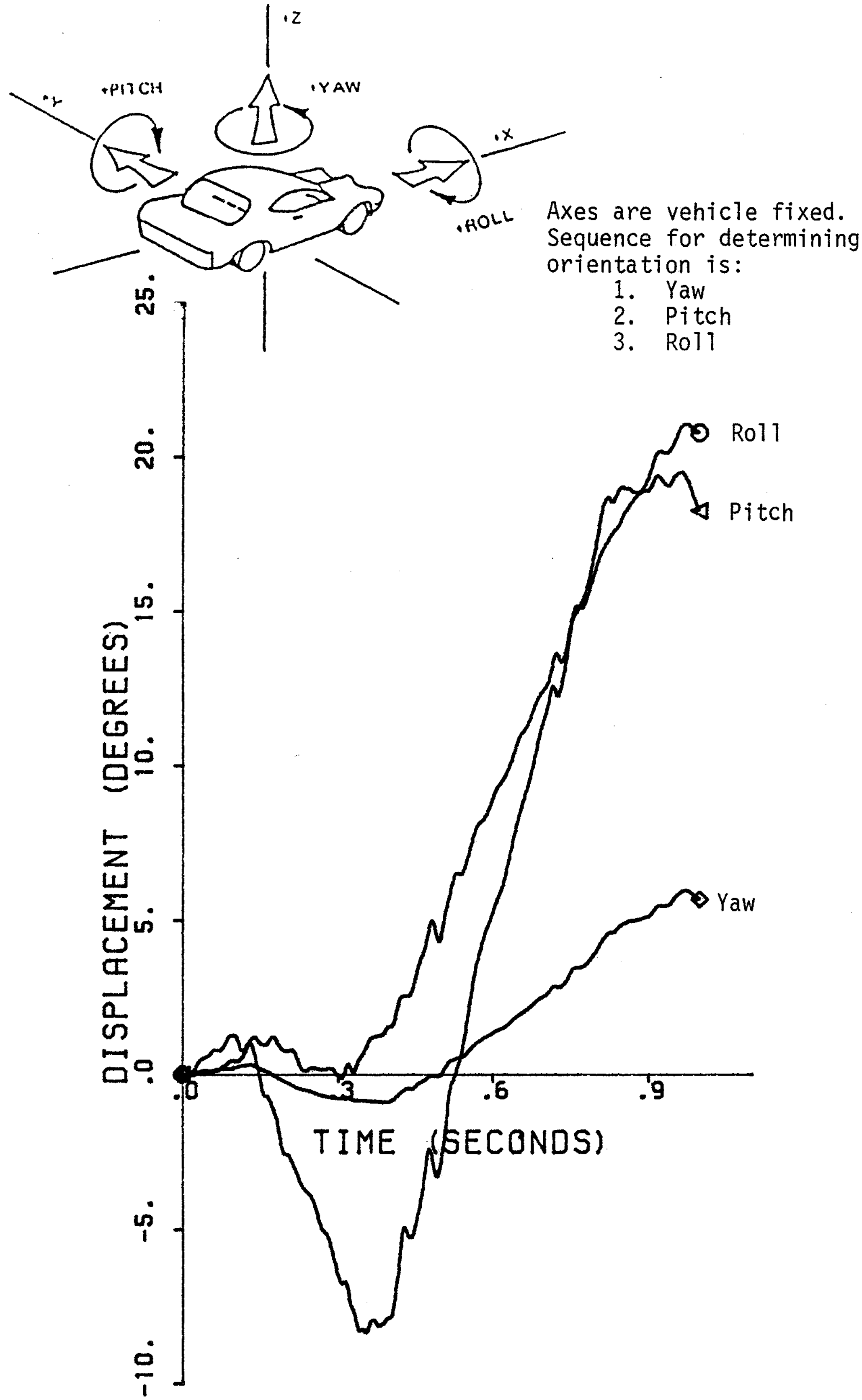

FIGURE C-10. VEHICLE ANGULAR DISPLACEMENTS FOR TEST SR-1.

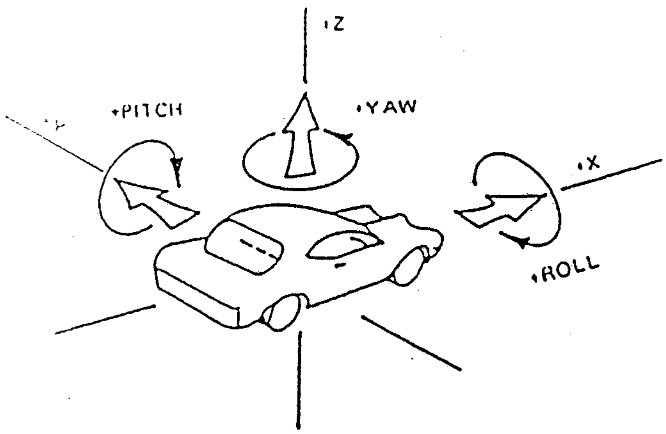

Axes are vehicle fixed.
Sequence for determining orientation is:

1. Yaw
2. Pitch
3. Roll

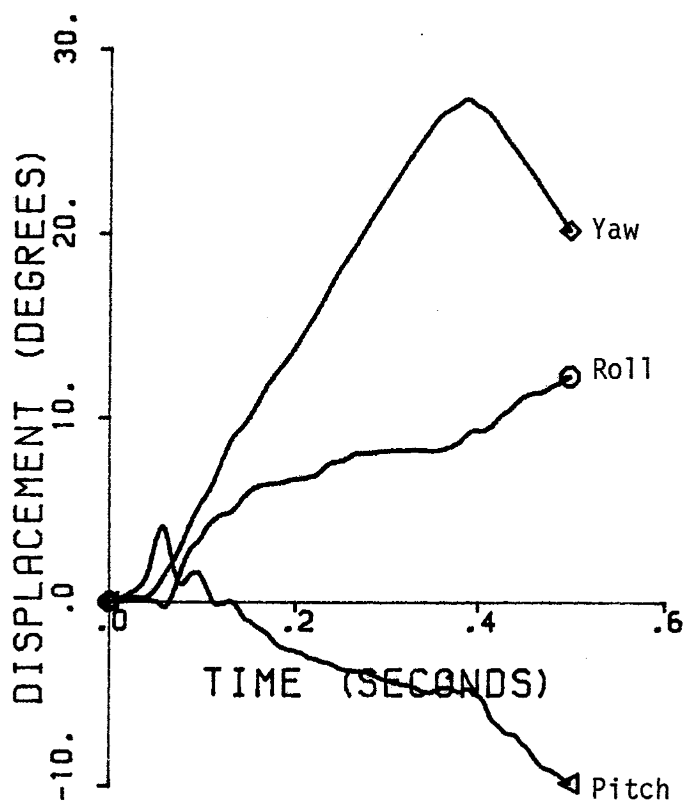

FIGURE C-11. VEHICLE ANGULAR DISPLACEMENTS FOR TEST SR-2.

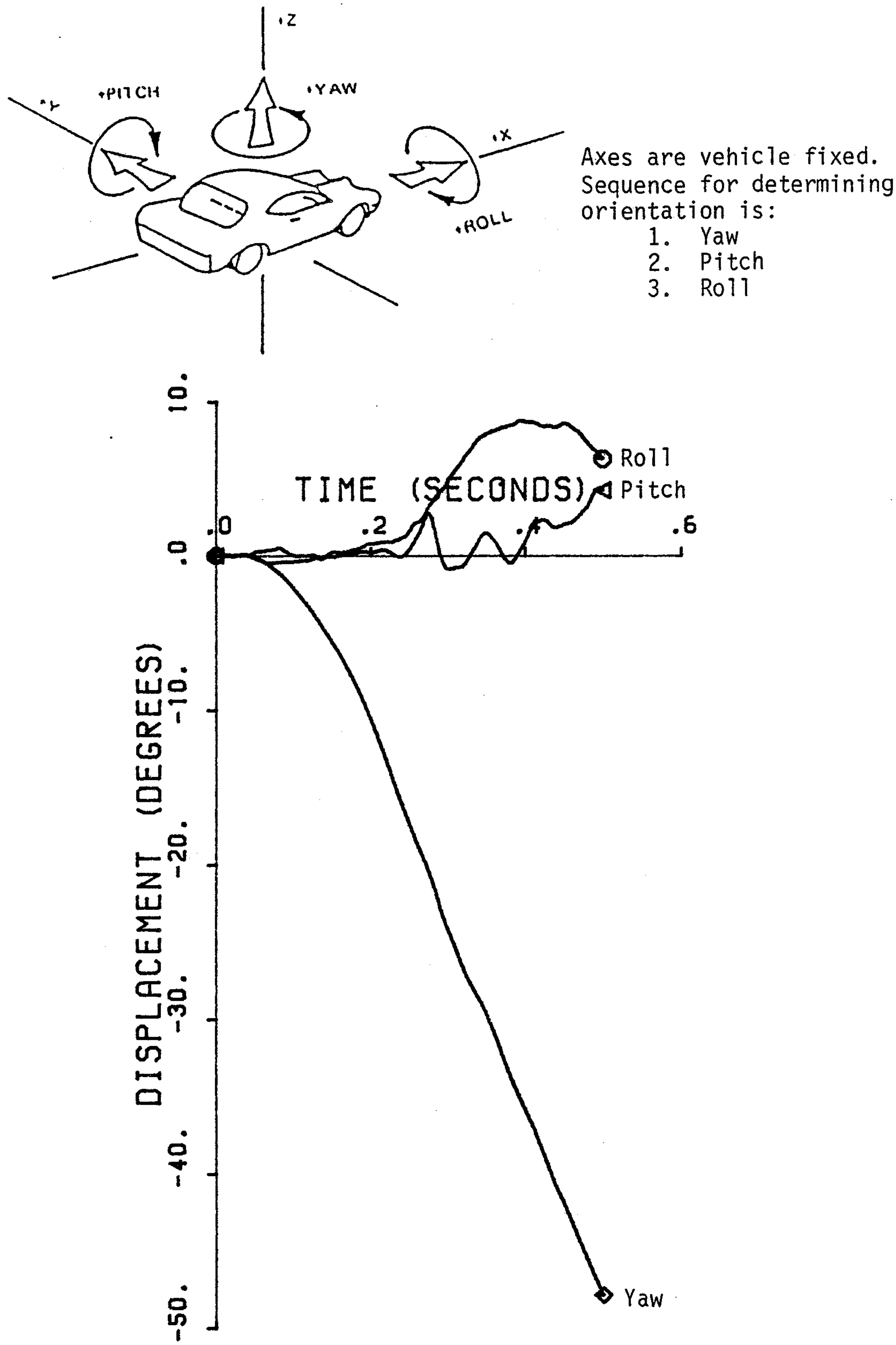

FIGURE C-12. VEHICLE ANGULAR DISPLACEMENTS FOR TEST SR-3.

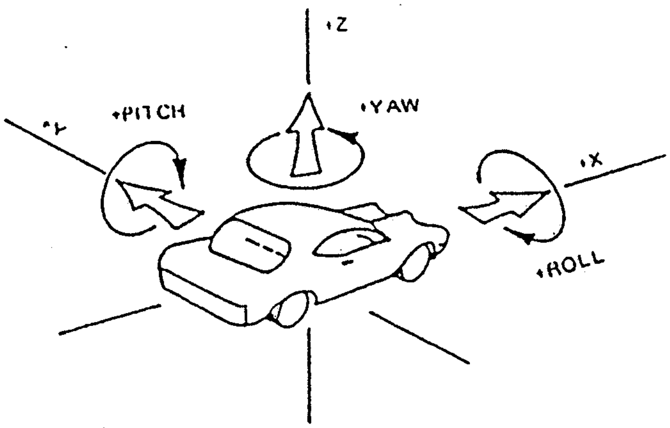

Axes are vehicle fixed.
Sequence for determining orientation is:
1. Yaw
2. Pitch
3. Roll

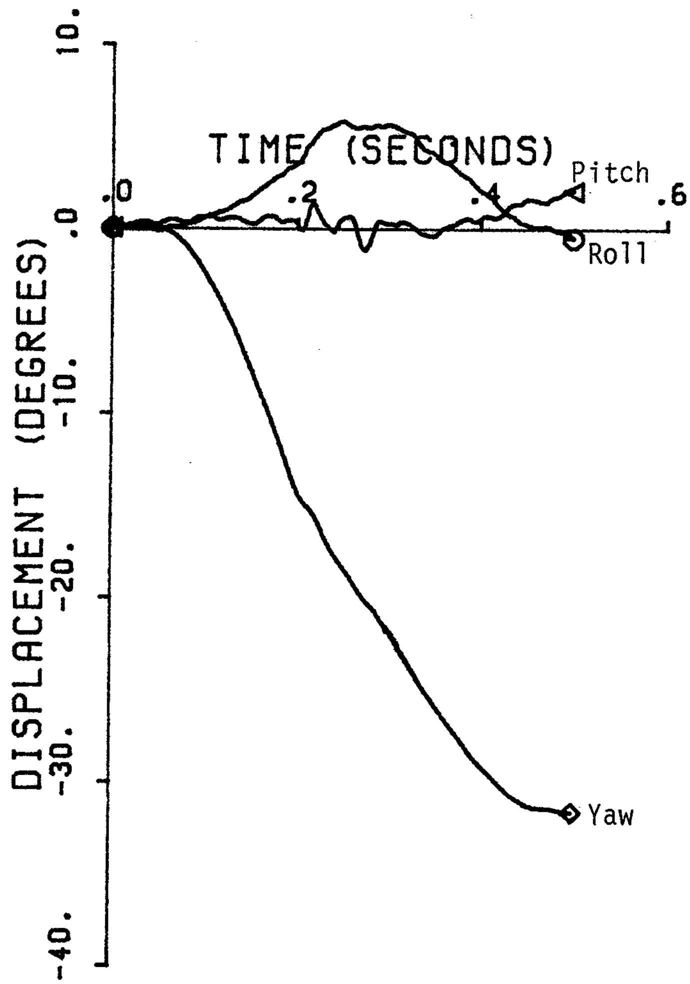

FIGURE C-13. VEHICLE ANGULAR DISPLACEMENTS FOR TEST SR-4.

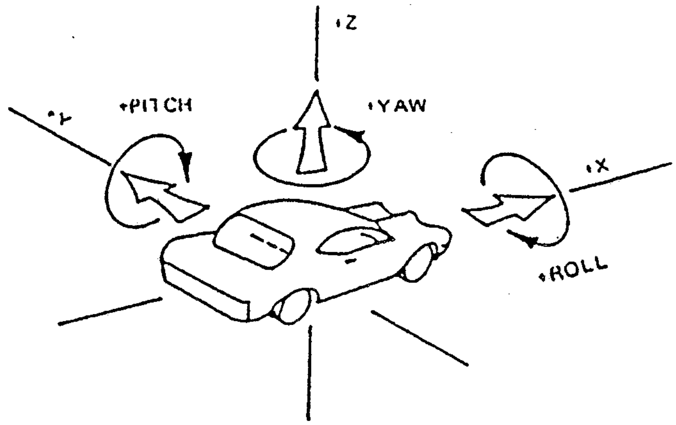

Axes are vehicle fixed.
Sequence for determining
orientation is:

1. Yaw
2. Pitch
3. Roll

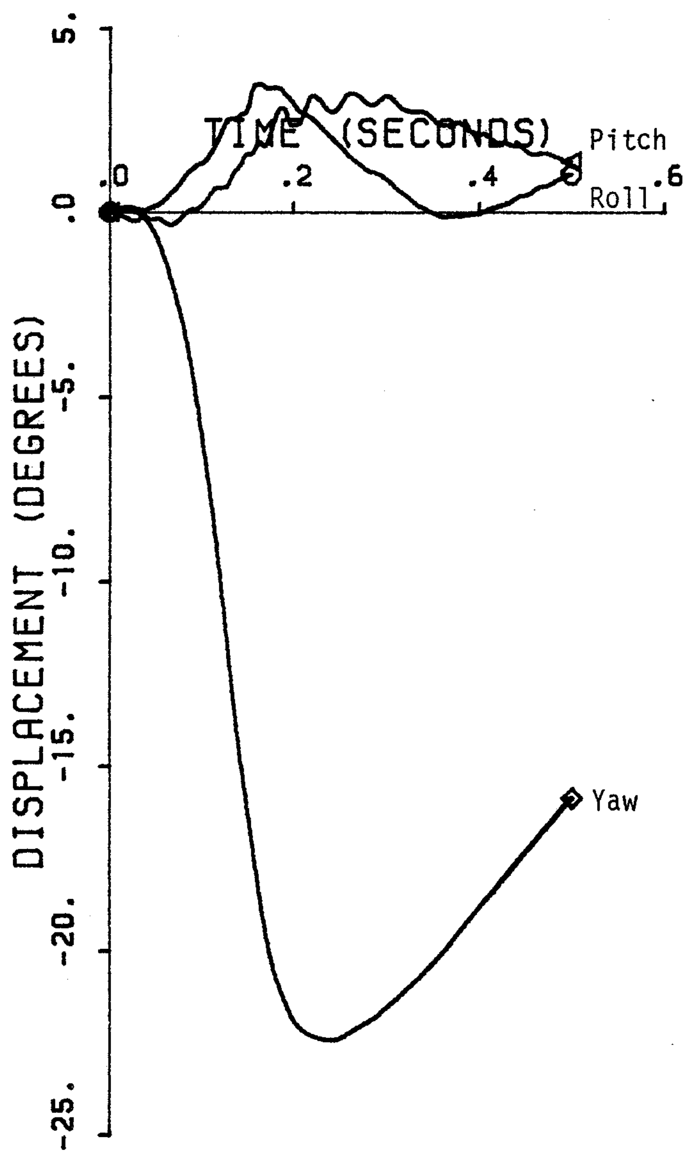

FIGURE C-14. VEHICLE ANGULAR DISPLACEMENTS FOR TEST SR-5.

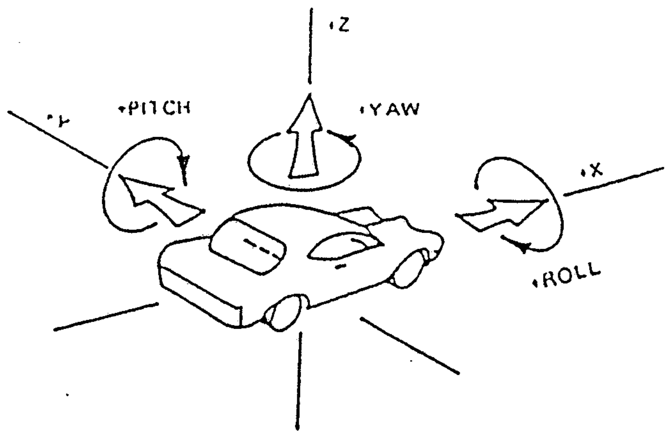

Axes are vehicle fixed.
Sequence for determining orientation is:

1. Yaw
2. Pitch
3. Roll

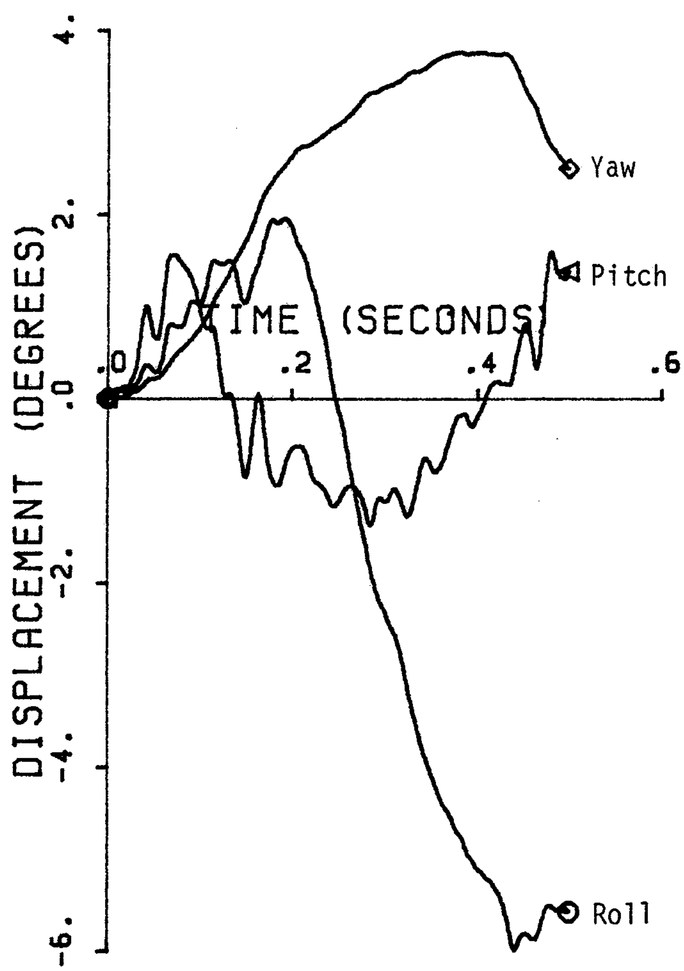

FIGURE C-15. VEHICLE ANGULAR DISPLACEMENTS FOR TEST SR-6.

APPENDIX D.

SEQUENTIAL PHOTOGRAPHS

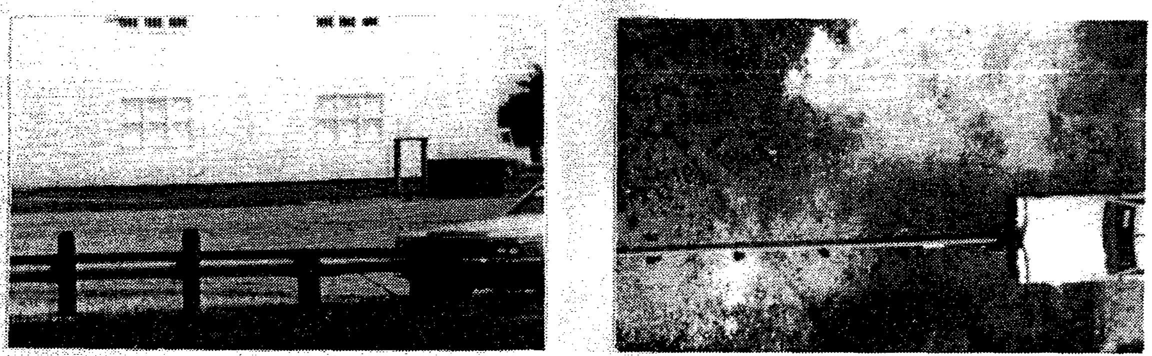

0.000 s

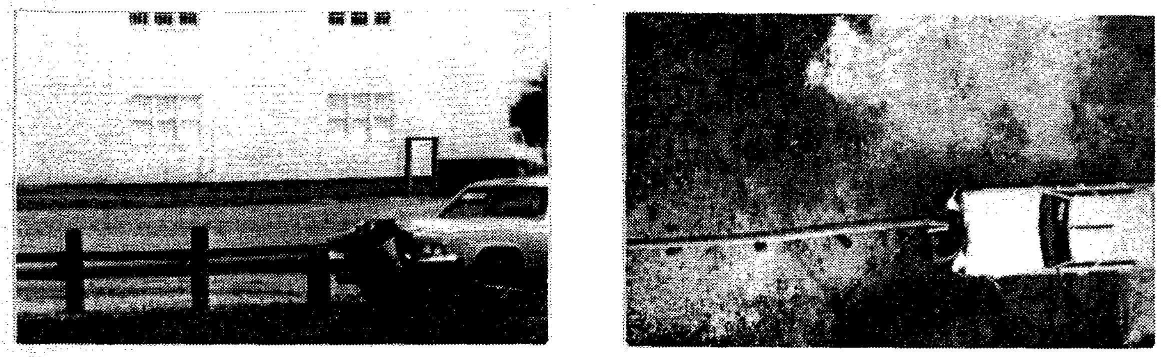

0.077 s

0.154 s

0.232 s

Fig. 86. Sequential Photographs For Test MB-1

0.309 s

0.386 s

0.463 s

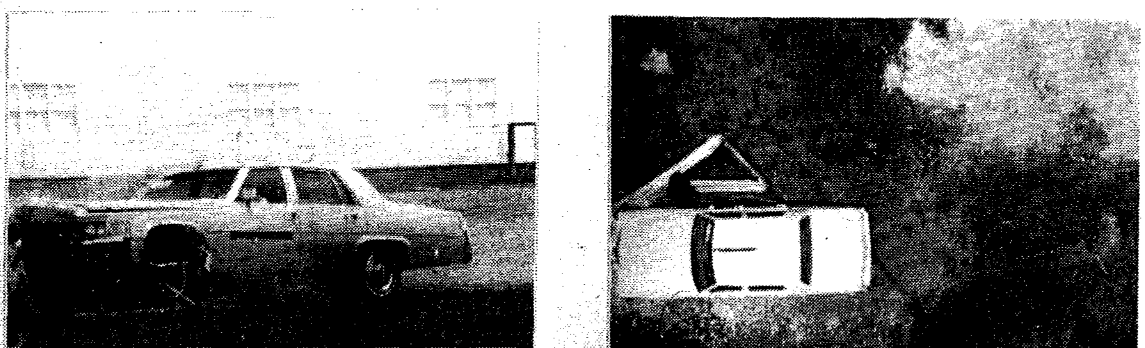

0.543 s

Fig. 86. Sequential Photographs For Test MB-1 (Continued)

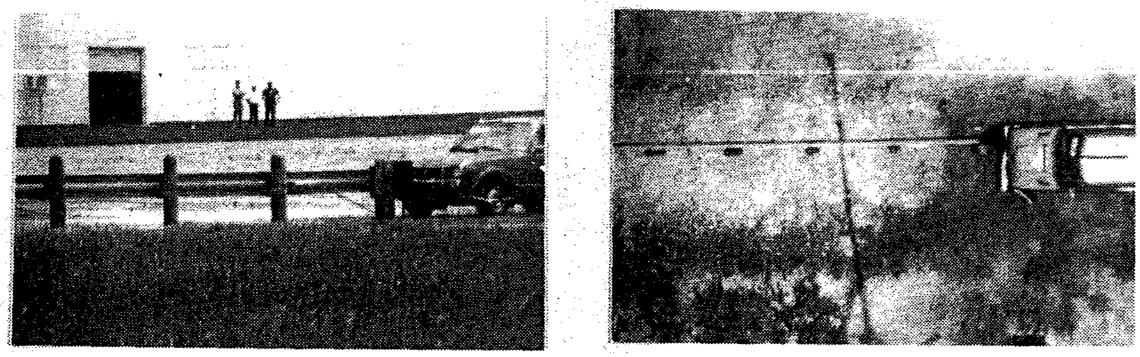

0.000 s

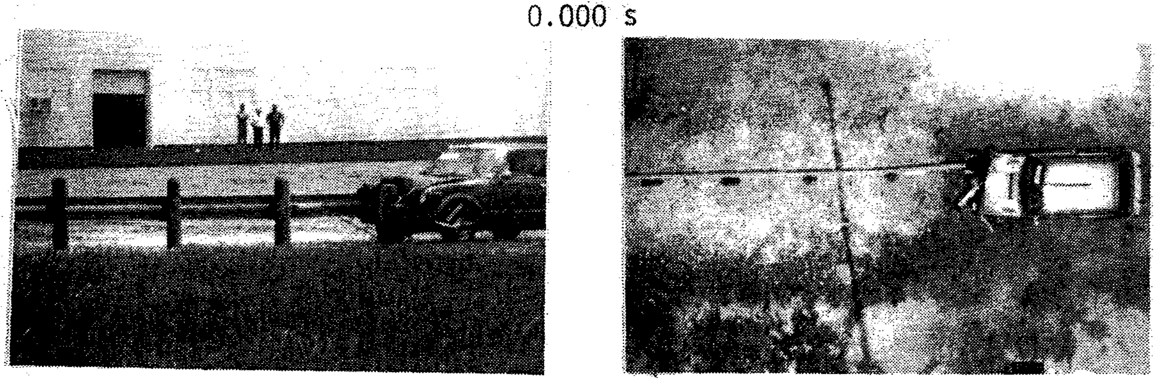

0.025 s

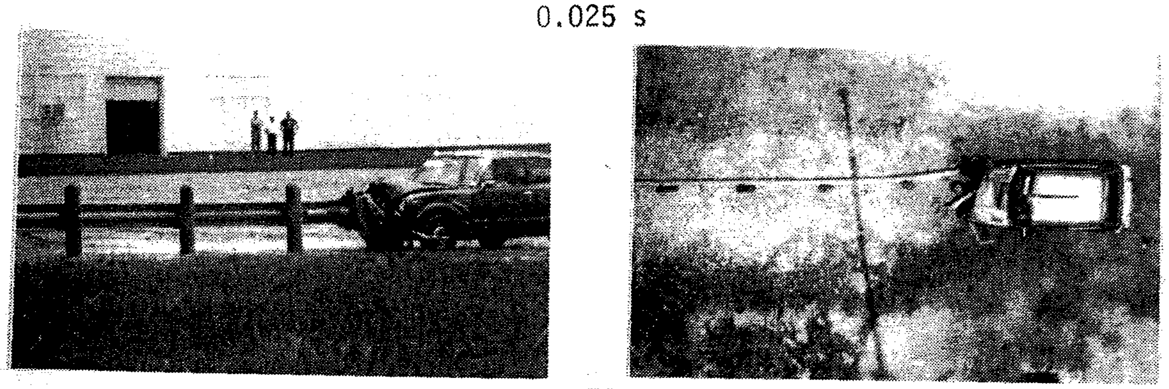

0.050 s

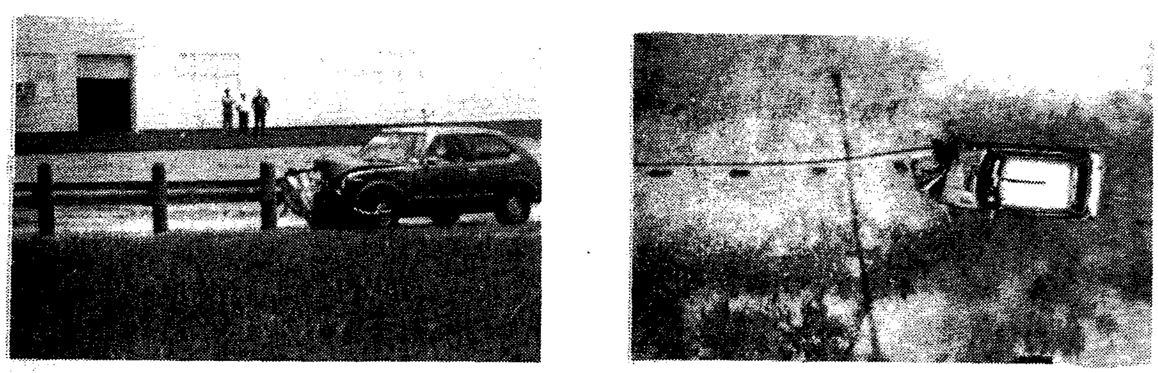

0.075 s

Fig. 87. Sequential Photographs For Test MB-2

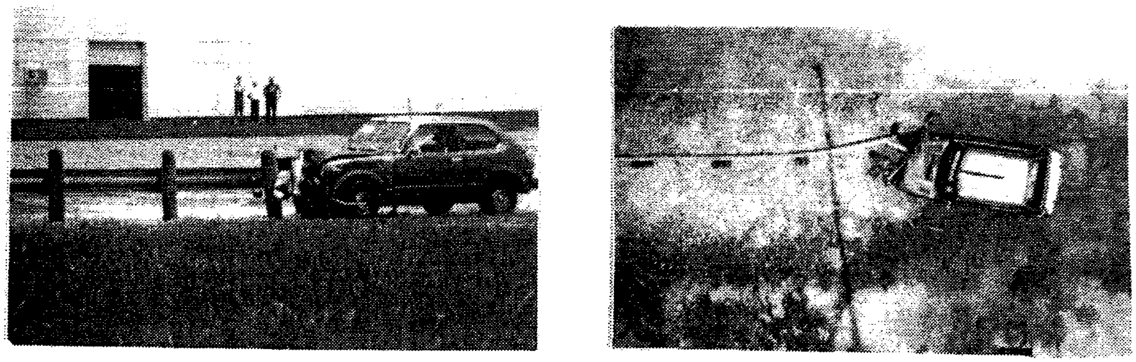

0.100 s

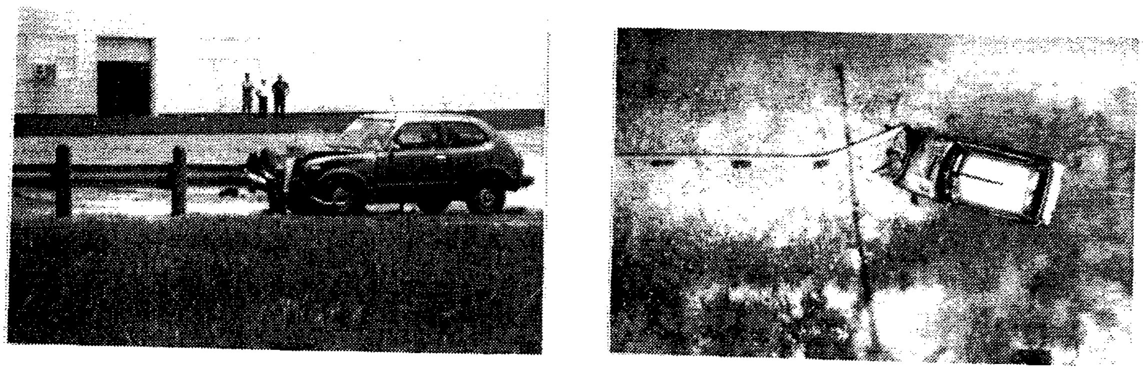

0.125 s

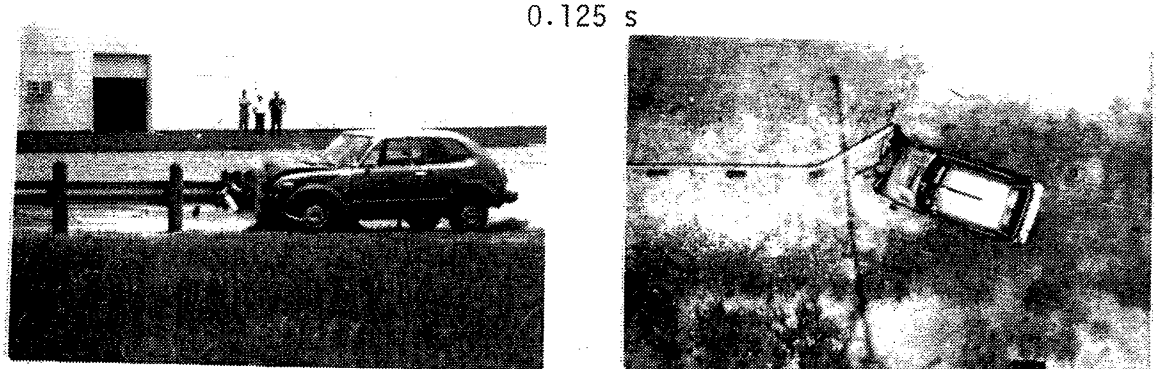

0.150 s

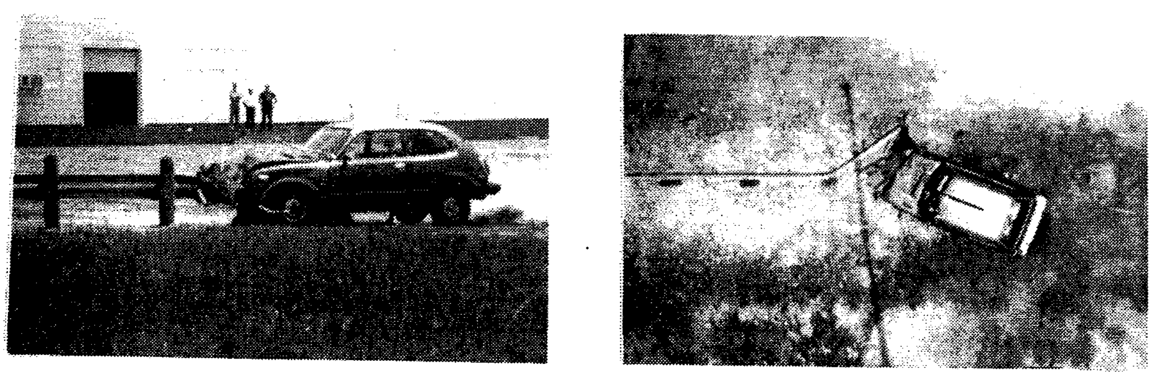

0.167 s

Fig. 87. Sequential Photographs For Test MB-2 (Continued)

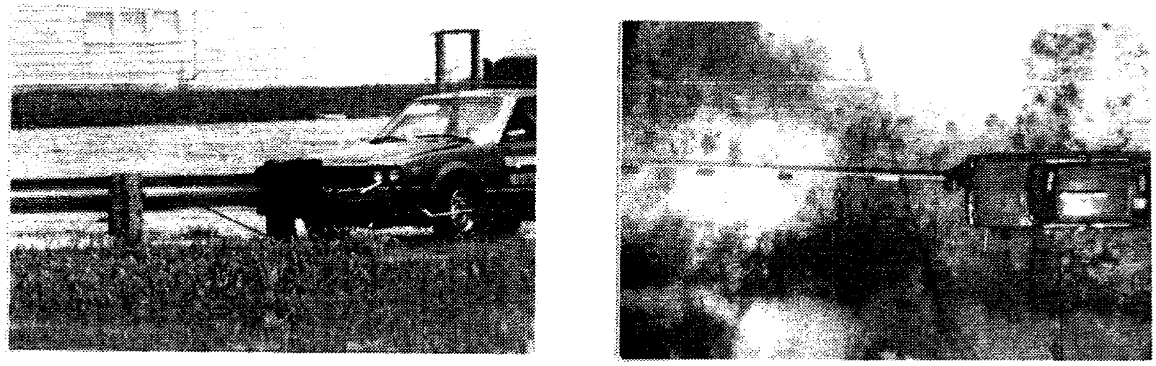

0.000 s

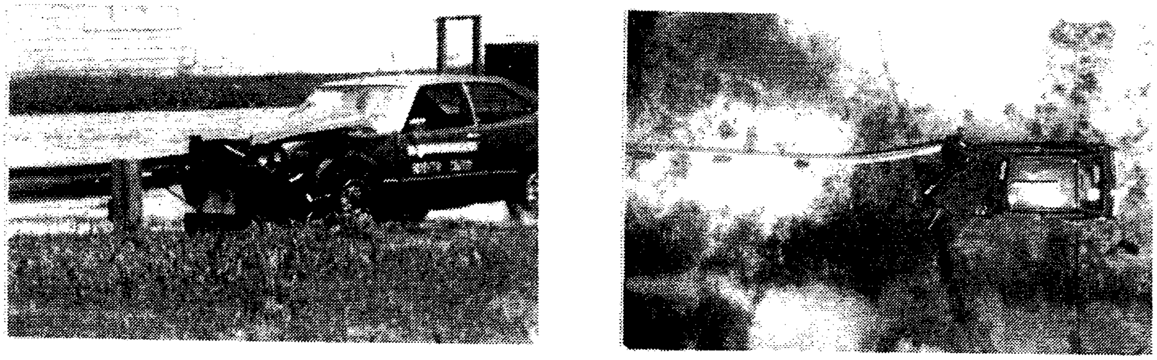

0.055 s

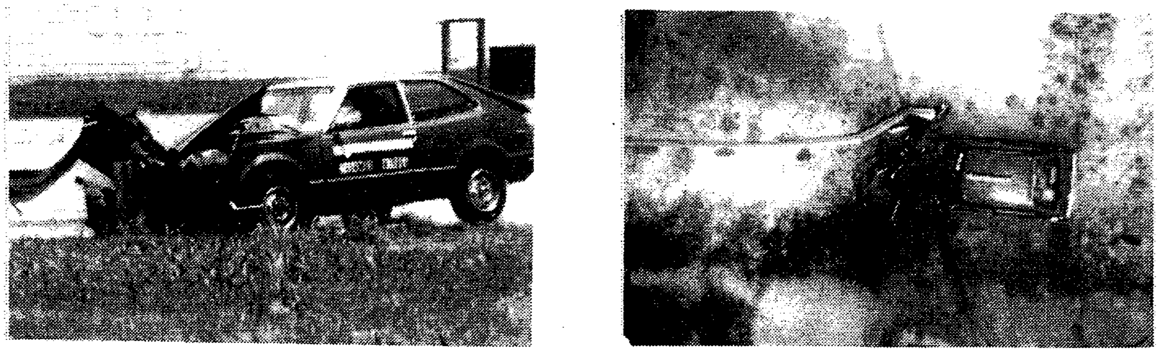

0.110 s

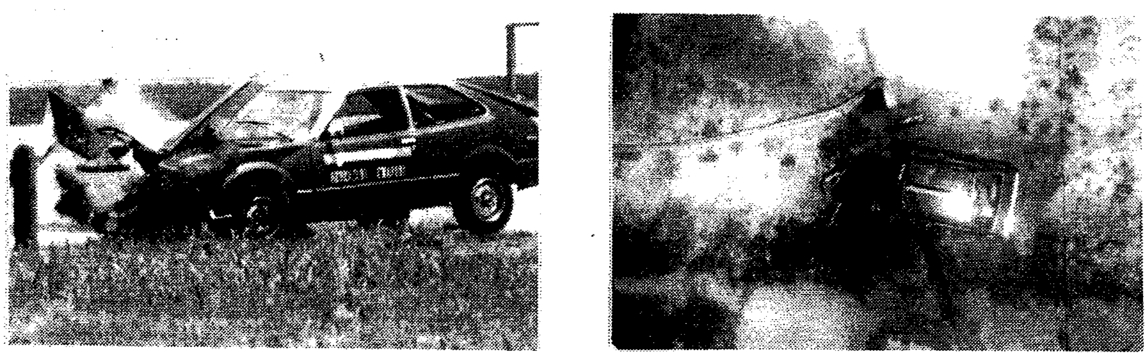

0.166 s

Fig. 88. Sequential Photographs For Test MB-3

0.221 s

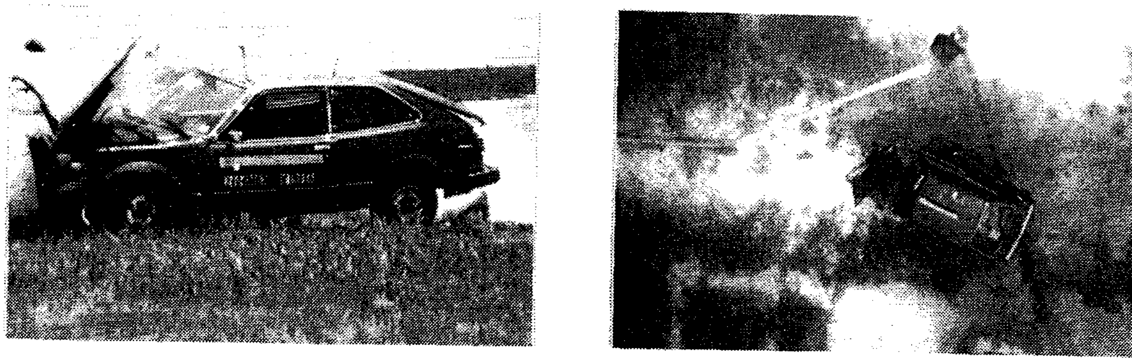

0.276 s

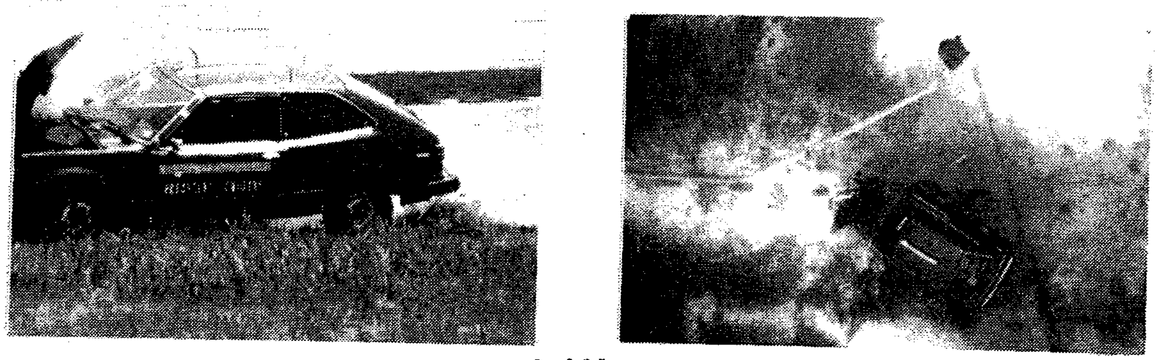

0.331 s

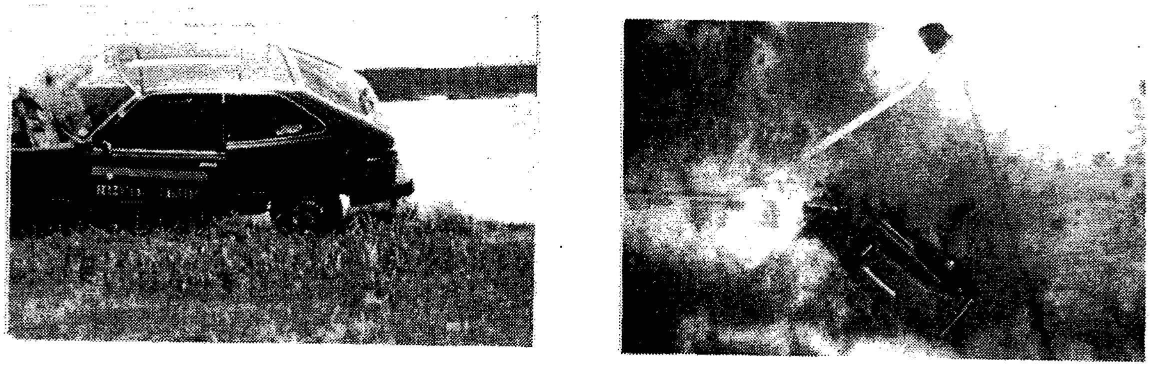

0.389 s

Fig. 88. Sequential Photographs For Test MB-3 (Continued)

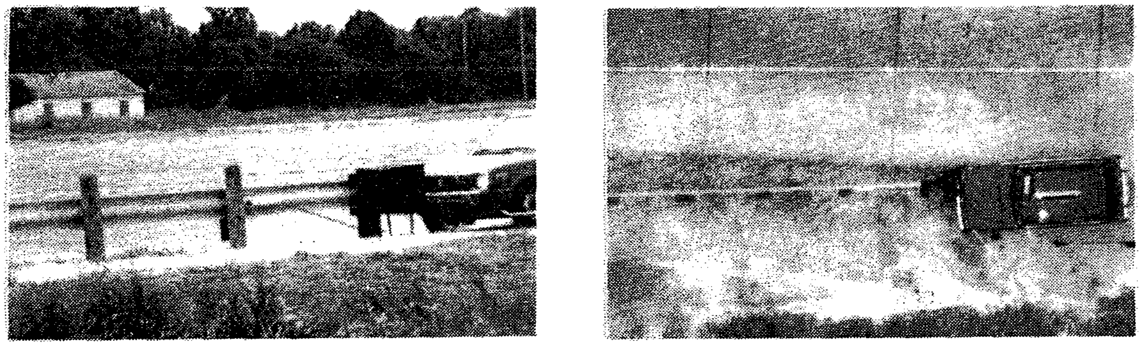

0.000 s

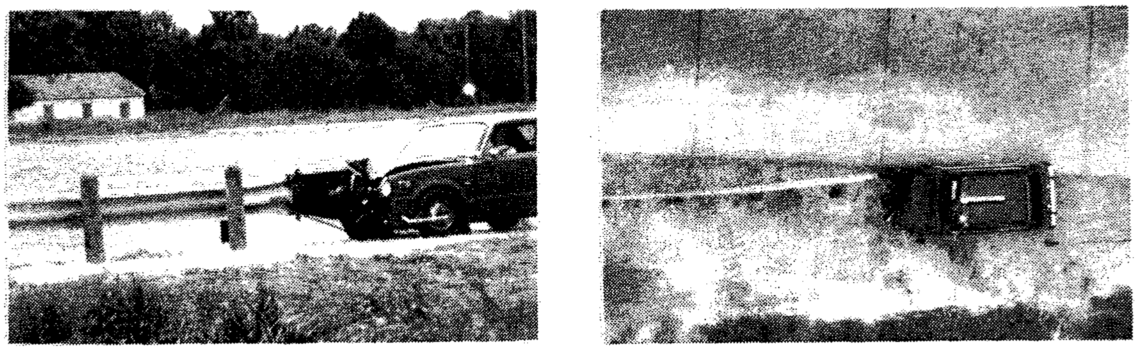

0.061 s

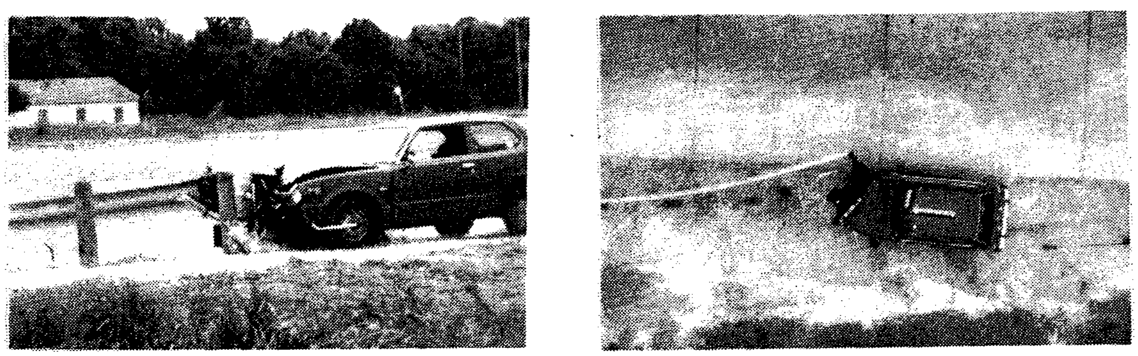

0.123 s

0.185 s

Fig. 89. Sequential Photographs For Test MB-4

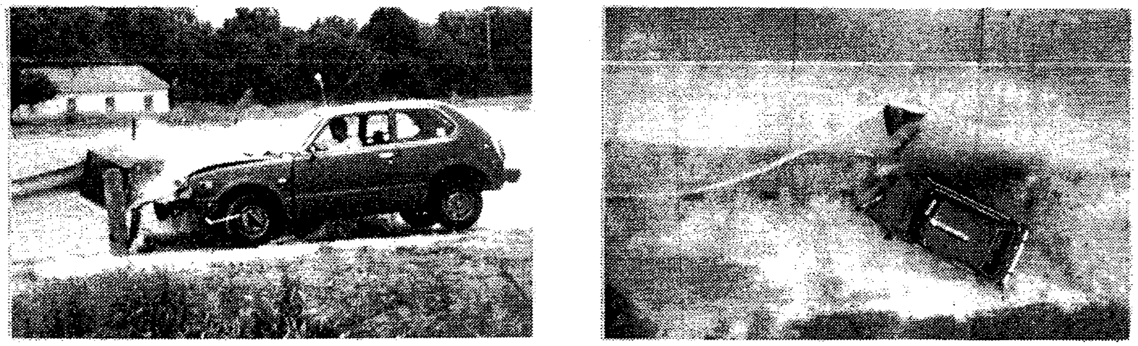

0.247 s

0.309 s

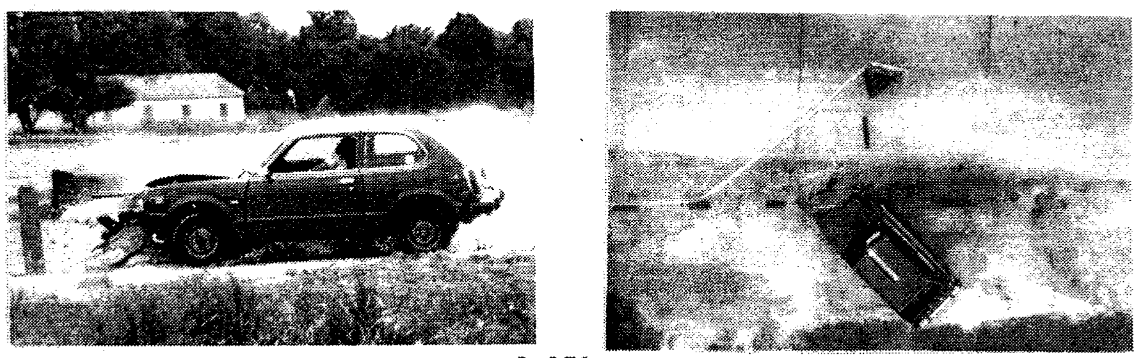

0.371 s

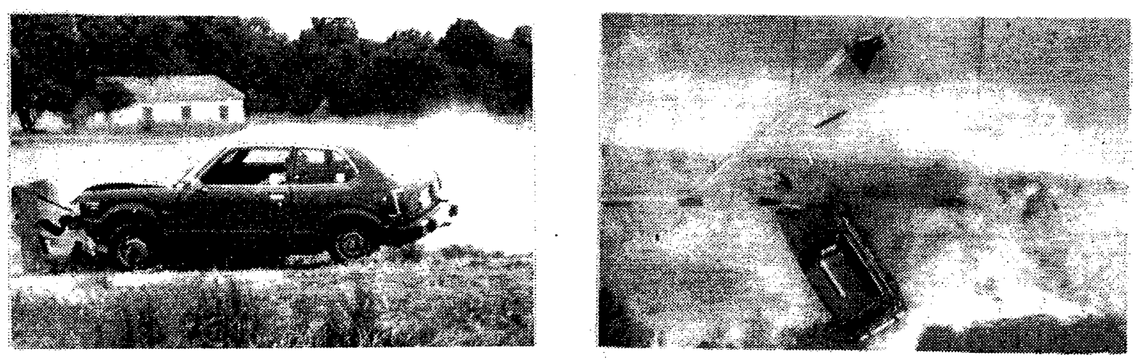

0.445 s

Fig. 89. Sequential Photographs For Test MB-4 (Continued)

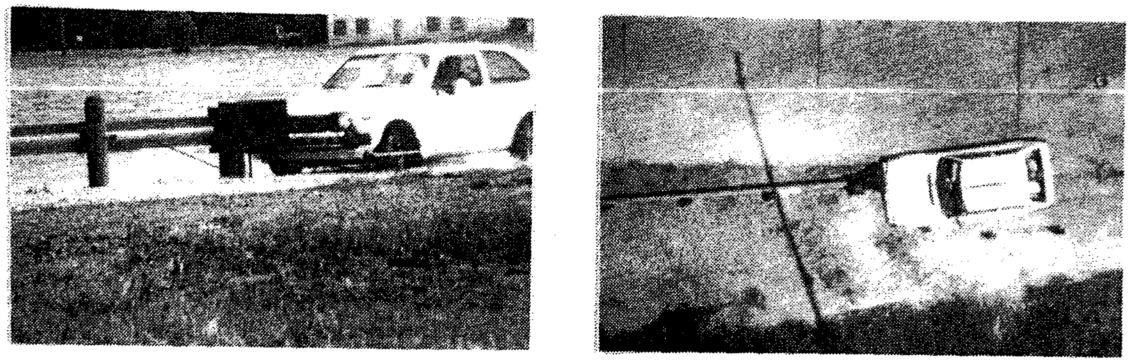

0.000 s

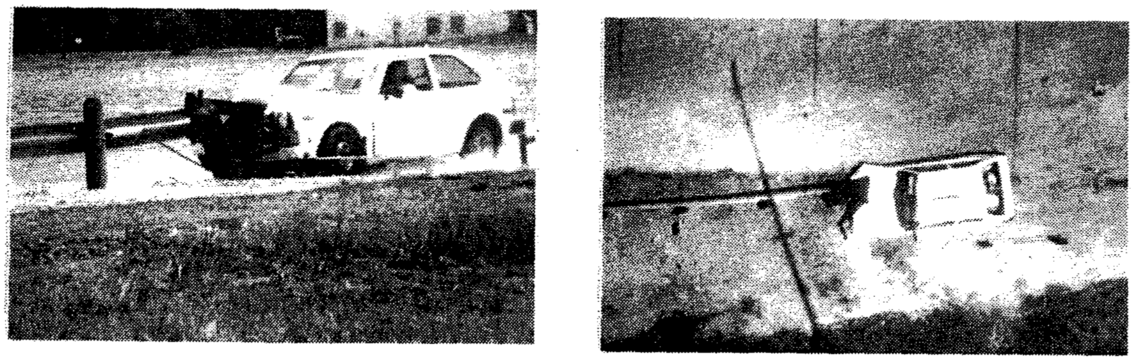

0.034 s

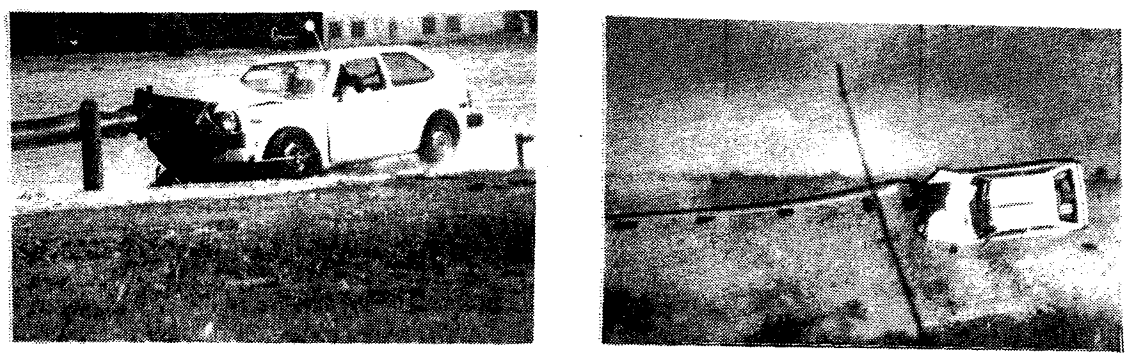

0.069 s

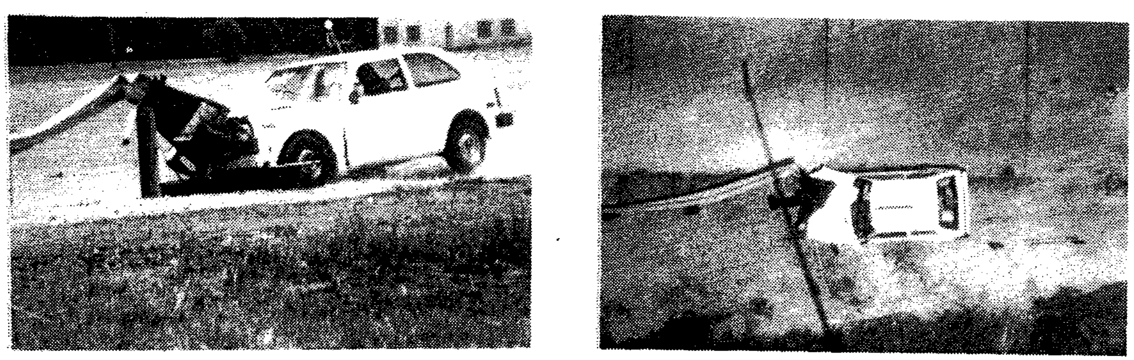

0.104 s

Fig. 90. Sequential Photographs For Test MB-5

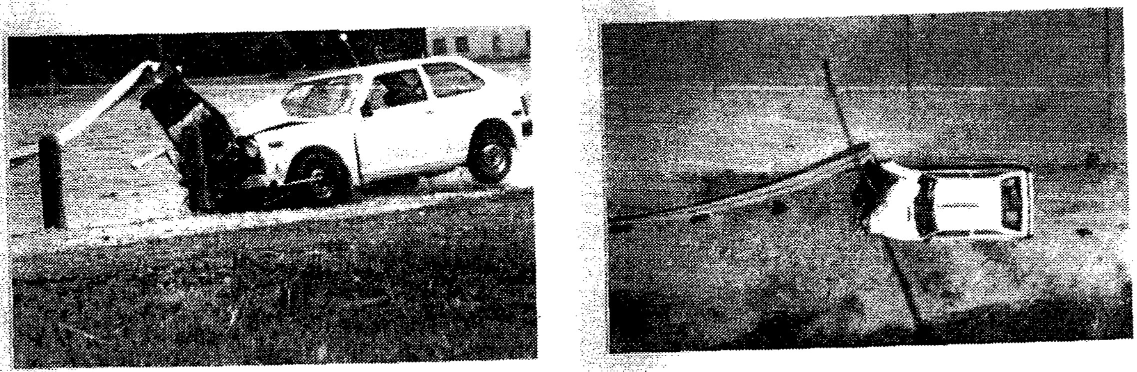

0.139 s

0.174 s

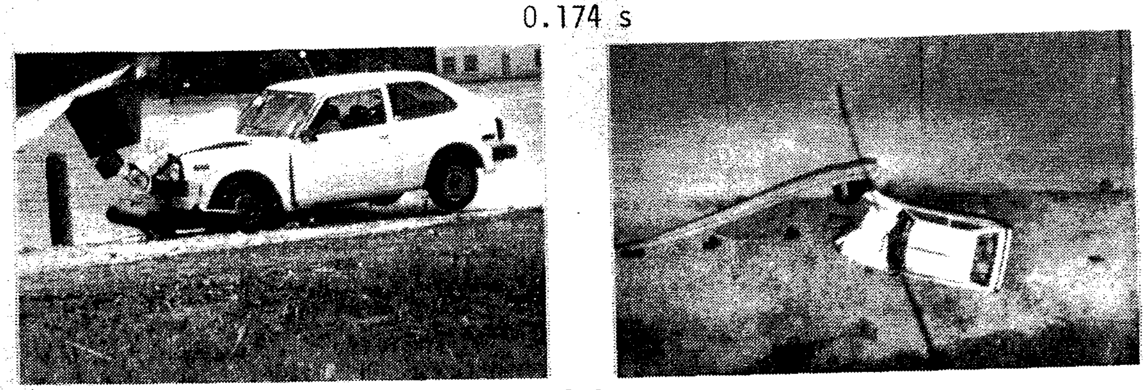

0.209 s

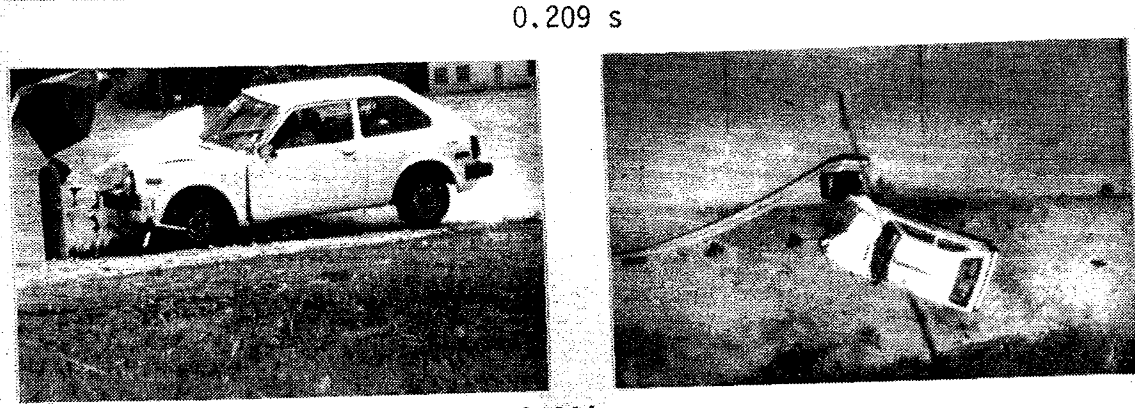

0.244 s

Fig. 90. Sequential Photographs For Test MB-5 (Continued)

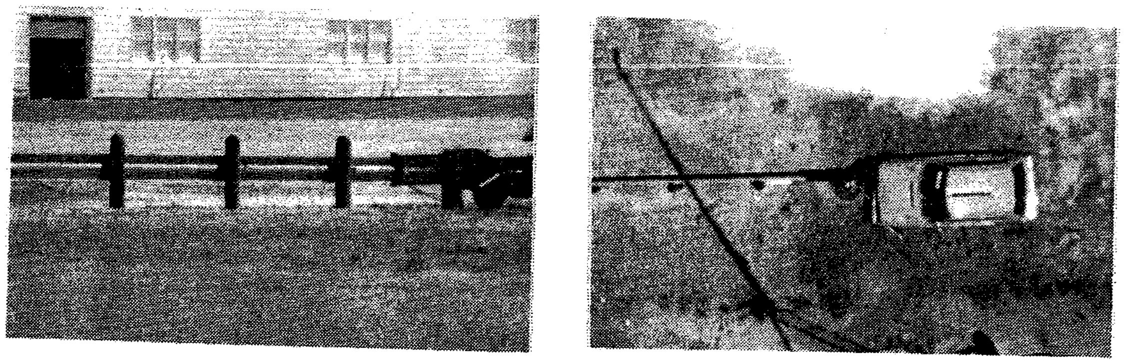

0.000 s

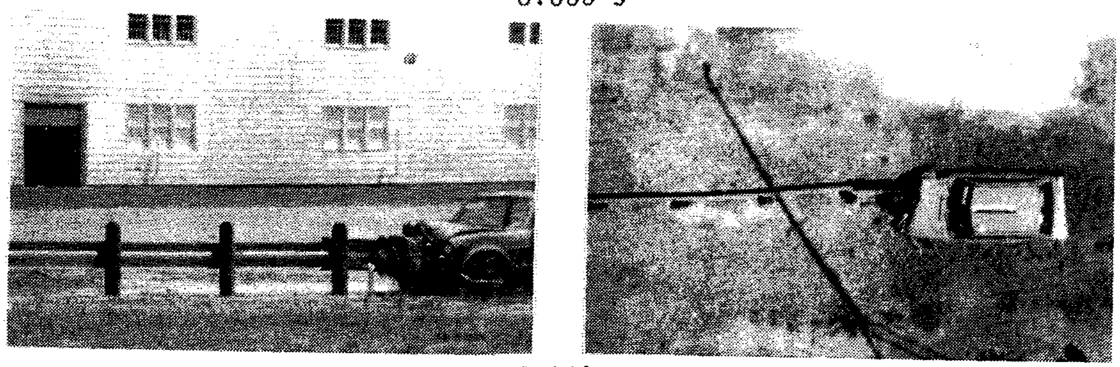

0.063 s

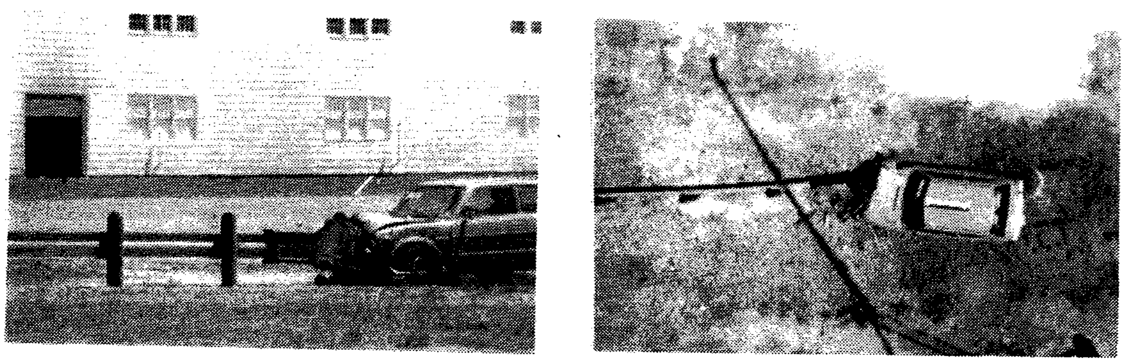

0.125 s

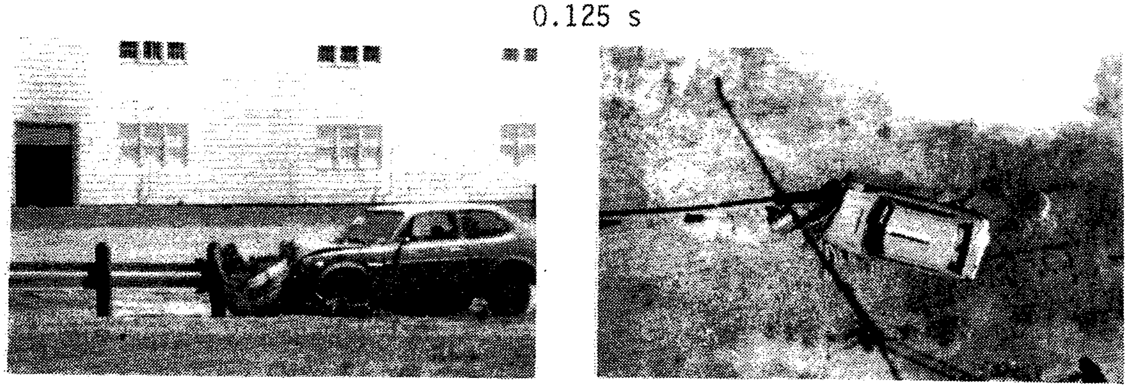

0.190 s

Fig. 91. Sequential Photographs For Test MB-6

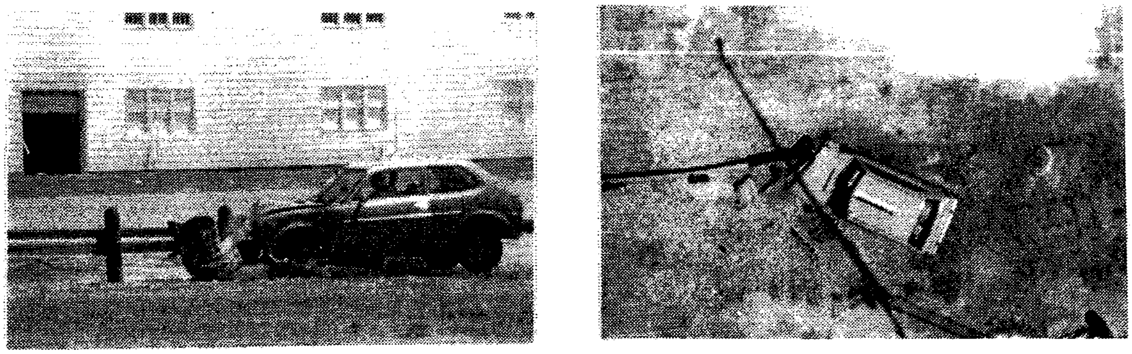

0.255 s

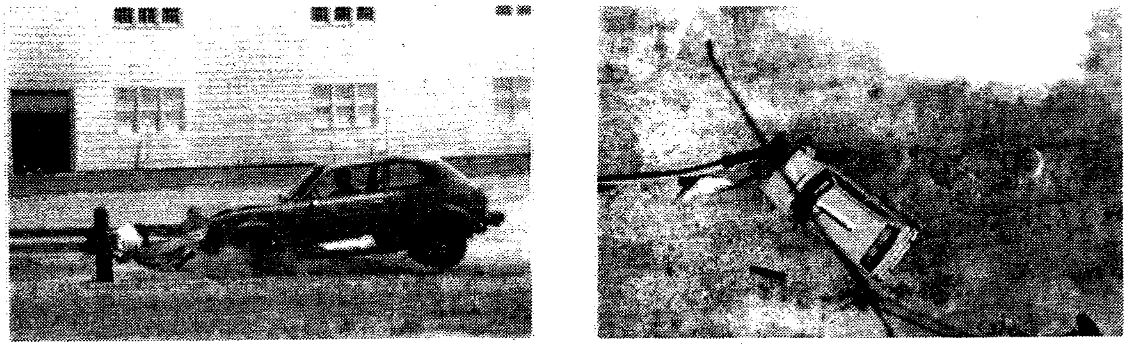

0.320 s

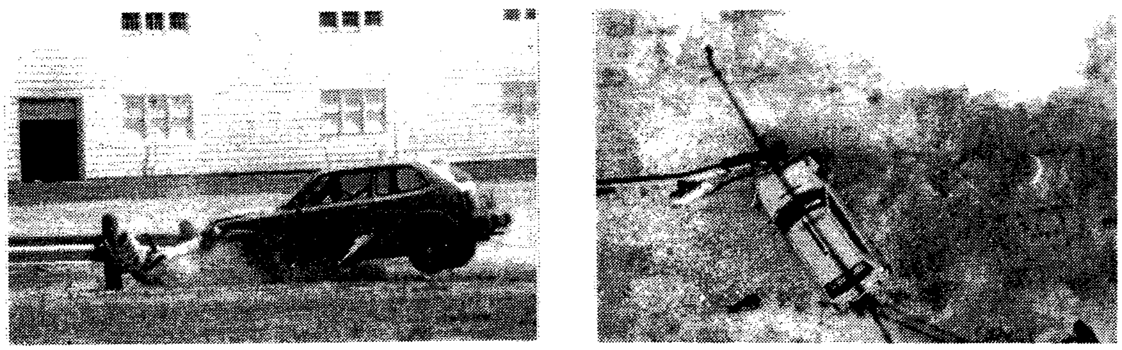

0.385 s

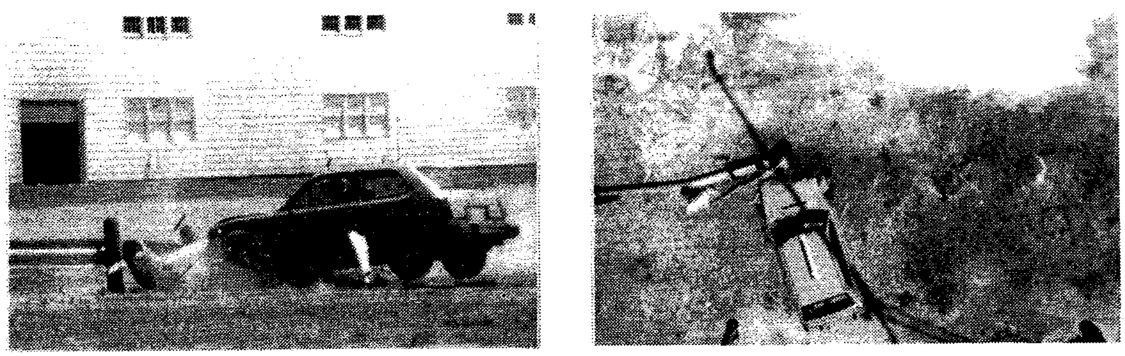

0.450 s

Fig. 91. Sequential Photographs For Test MB-6 (Continued)

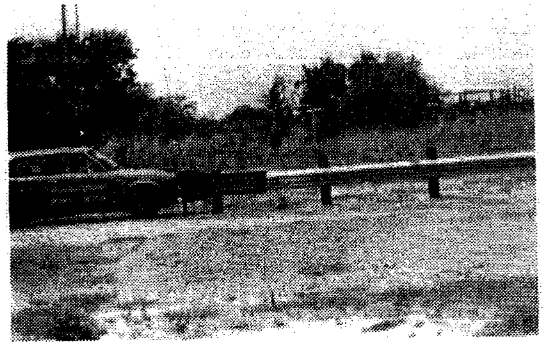

0.000 s

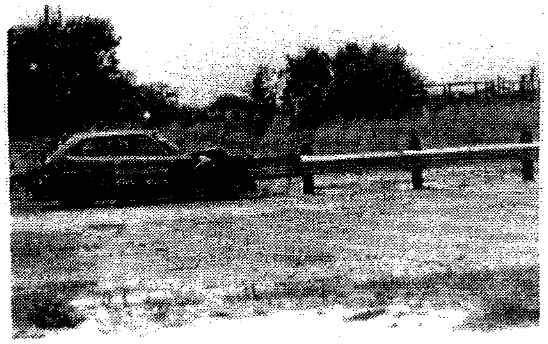

0.063 s

0.125 s

0.190 s

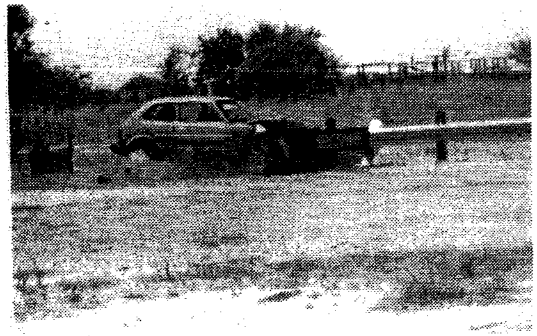

0.255 s

0.320 s

0.385 s

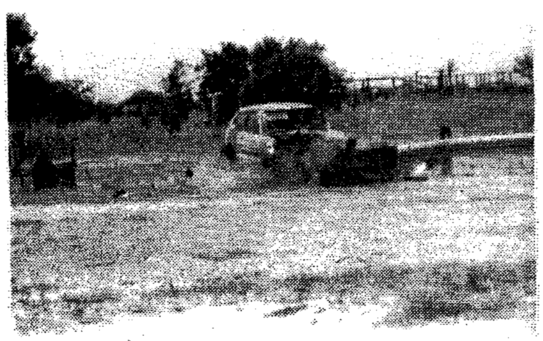

0.450 s

Fig. 91. Sequential Photographs For Test MB-6 (Continued)

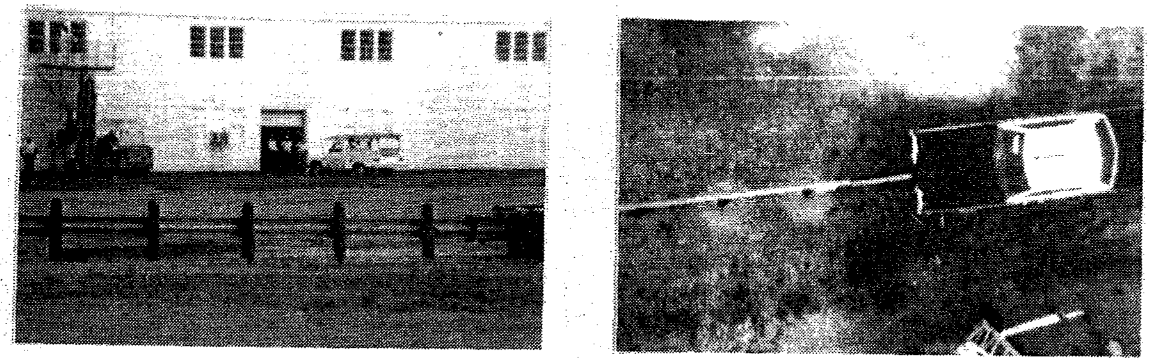

0.000 s

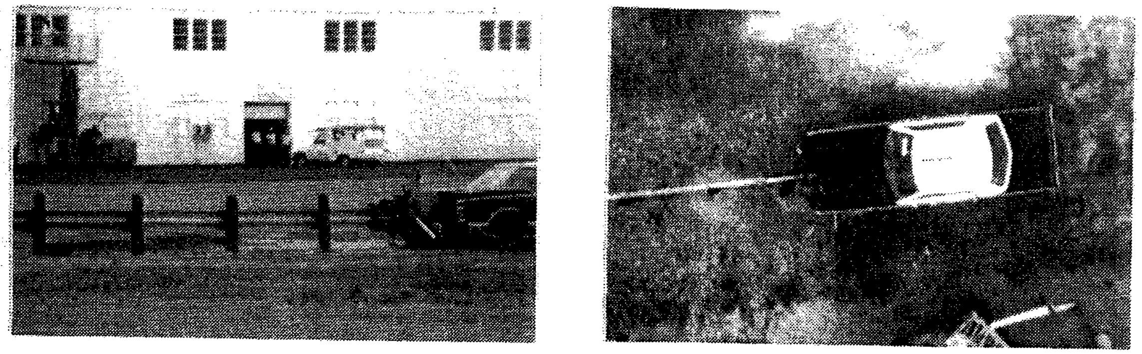

0.088 s

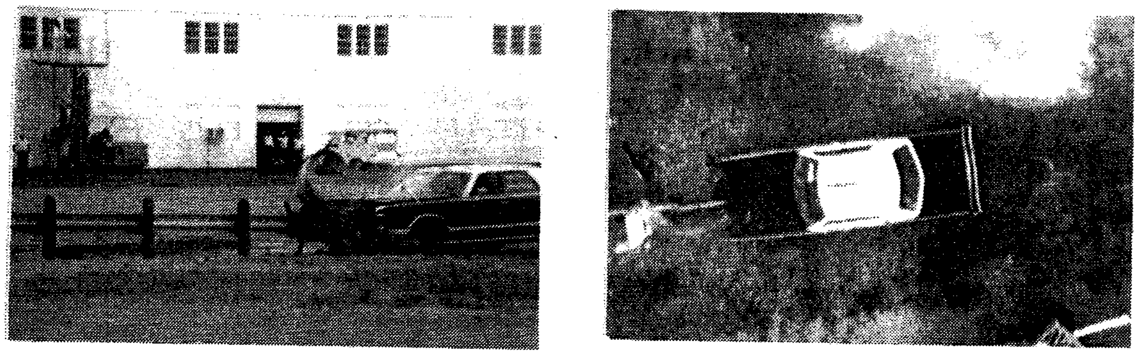

0.175 s

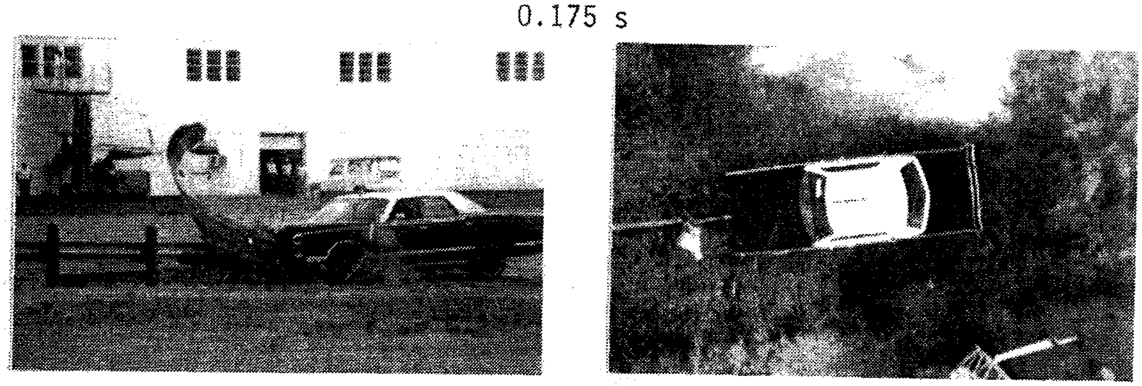

0.265 s

Fig. 92. Sequential Photographs For Test MB-7

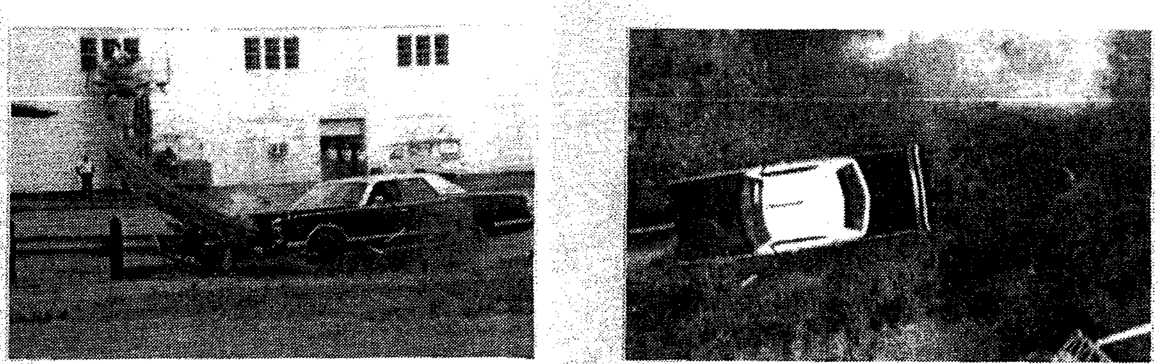

0.355 s

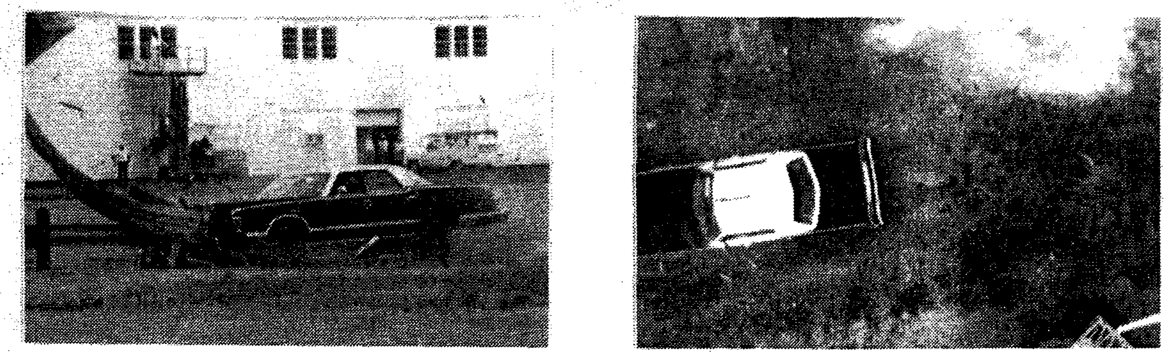

0.446 s

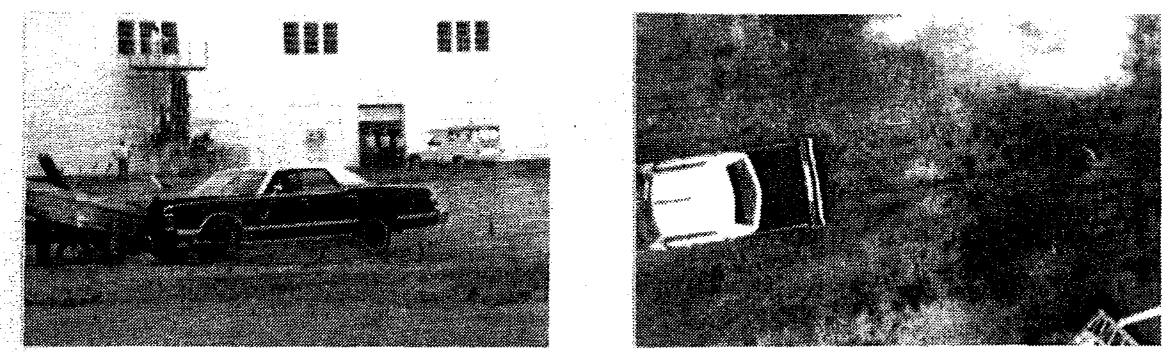

0.536 s

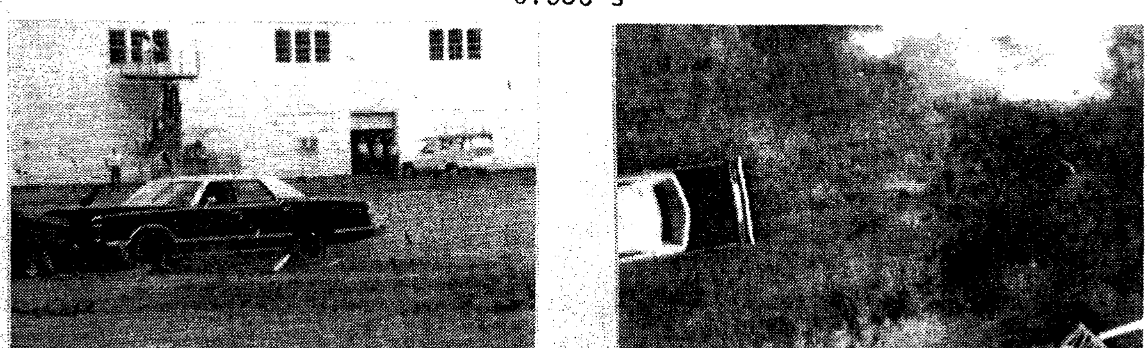

0.626 s

Fig. 92. Sequential Photographs For Test MB-7 (Continued)

0.000 s

0.088 s

0.175 s

0.265 s

0.355 s

0.446 s

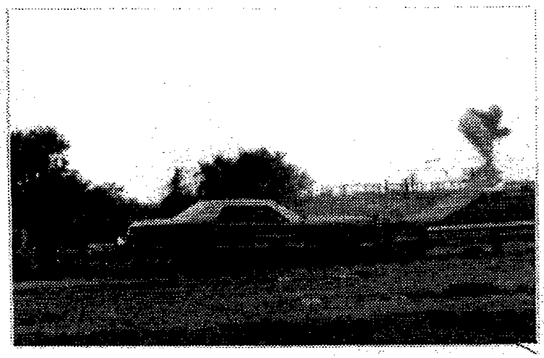

0.536 s

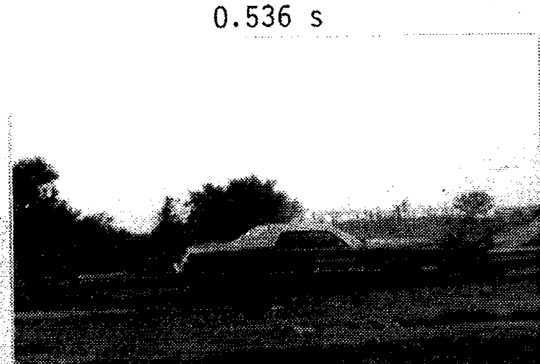

0.626 s

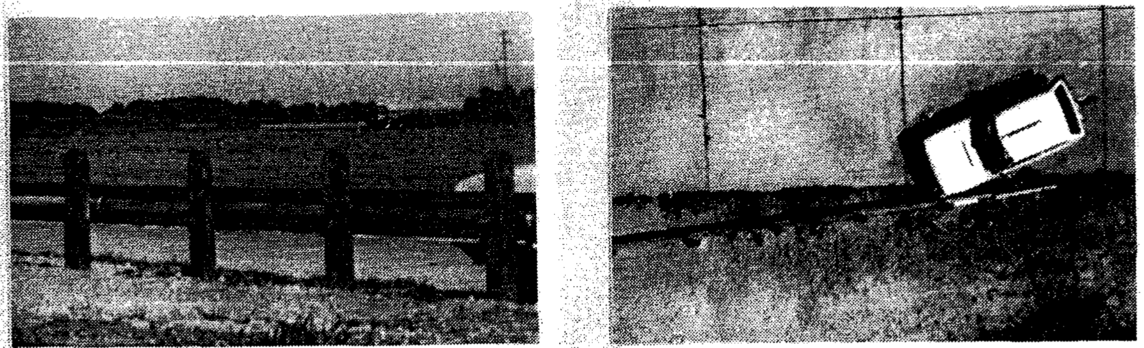

0.000 s

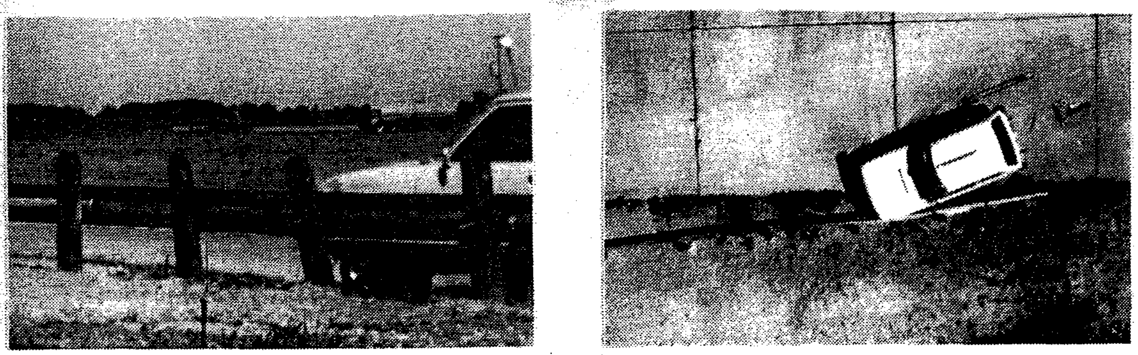

0.049 s

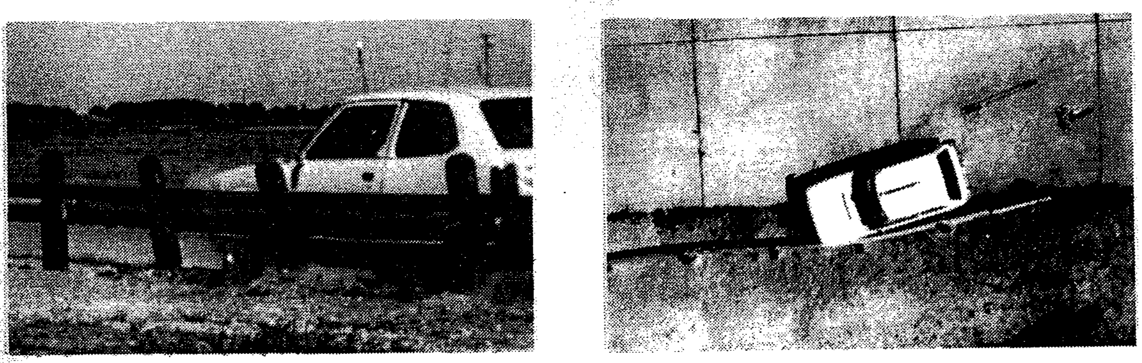

0.101 s

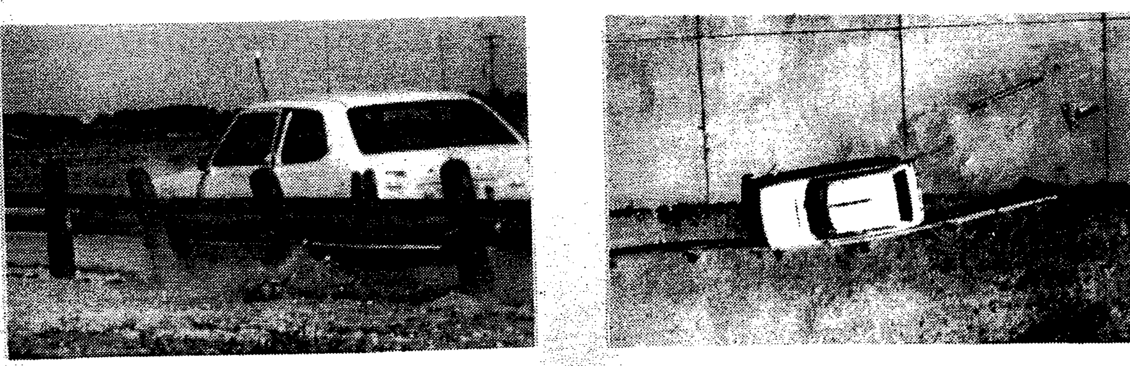

0.150 s

Fig. 93. Sequential Photographs For Test 9429A-1

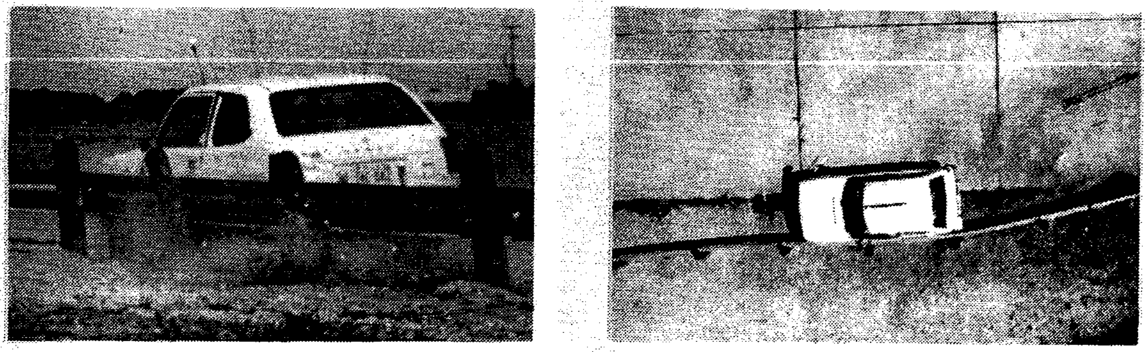

0.202 s

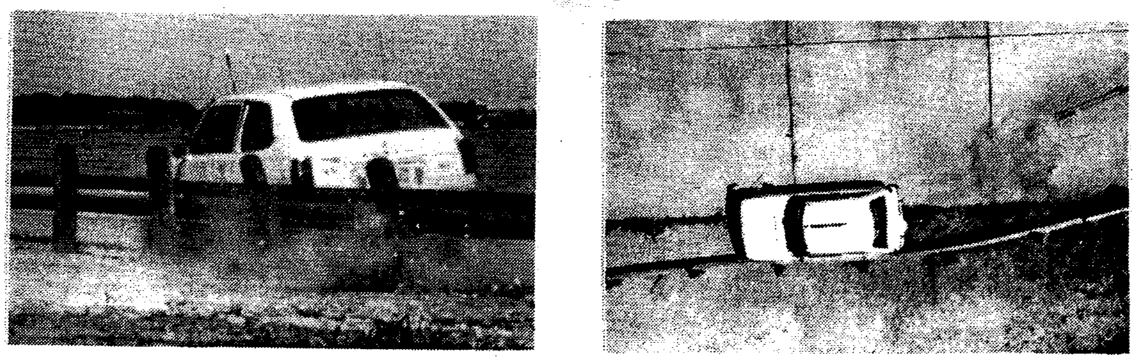

0.252 s

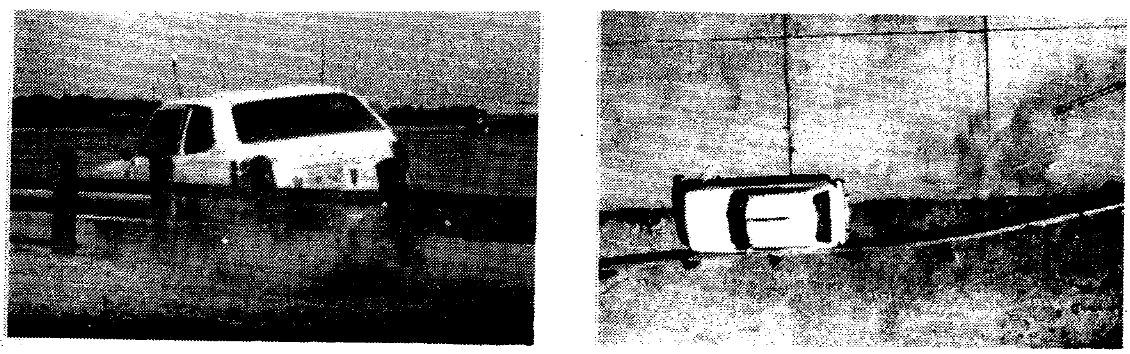

0.303 s

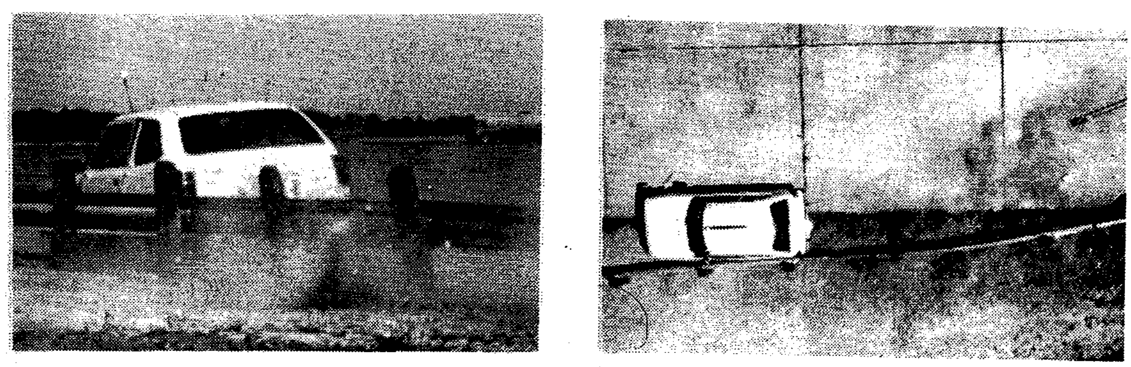

0.355 s

Fig. 93. (Continued)

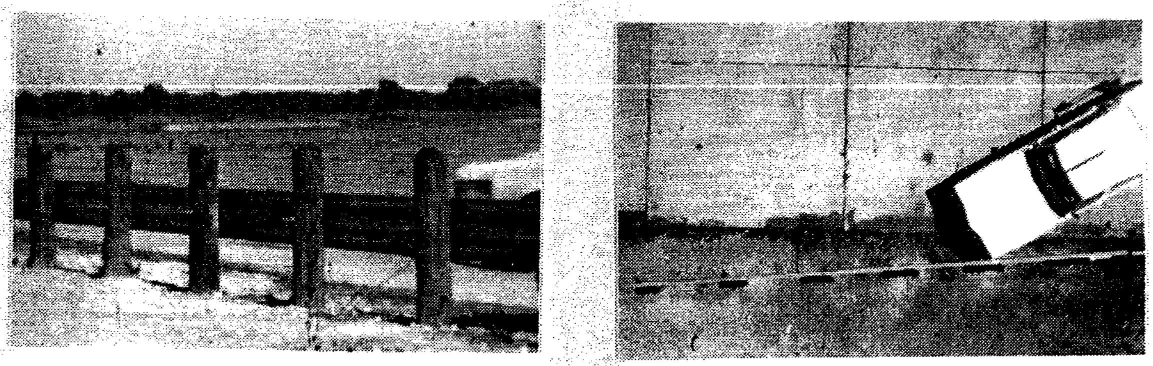

0.000 s

0.099 s

0.199 s

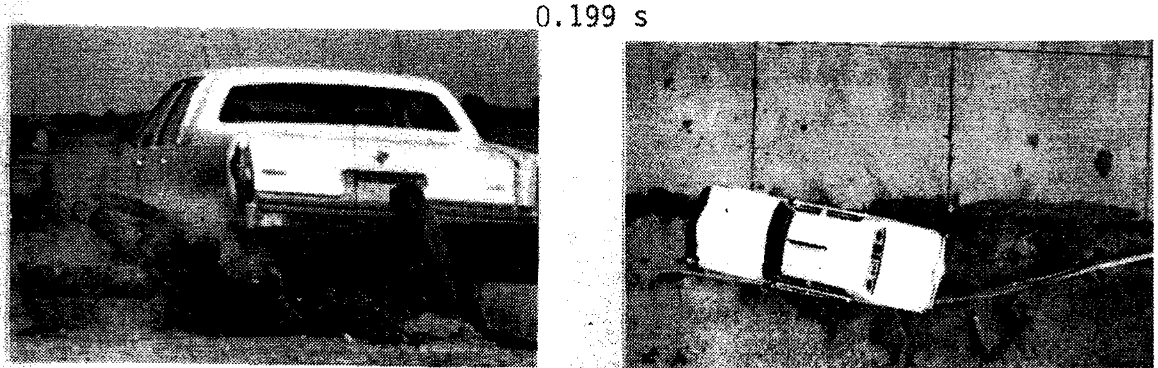

0.298 s

Fig. 94. Sequential Photographs For Test 9429A-2

0.397 s

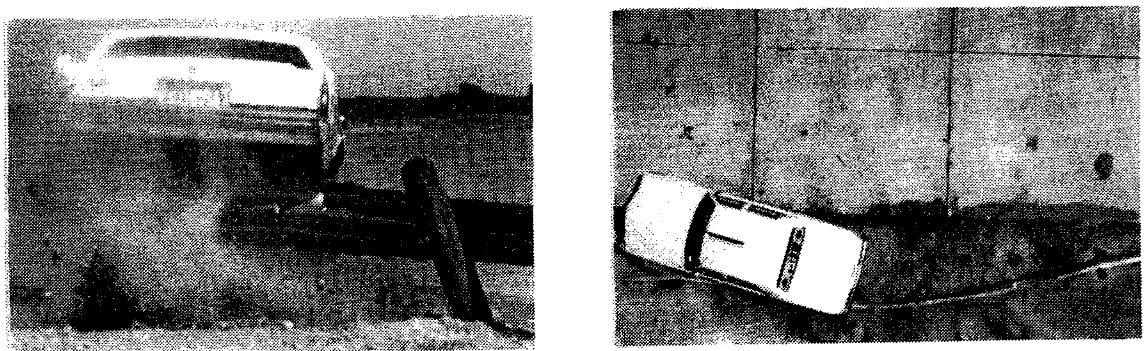

0.497 s

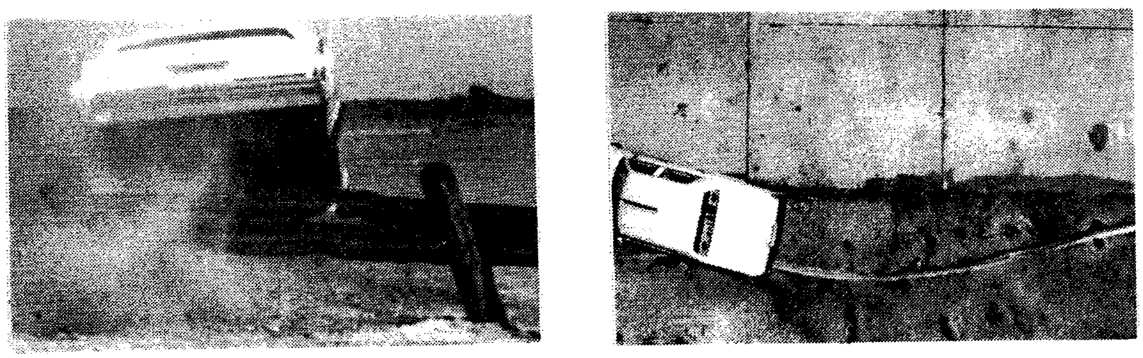

0.596 s

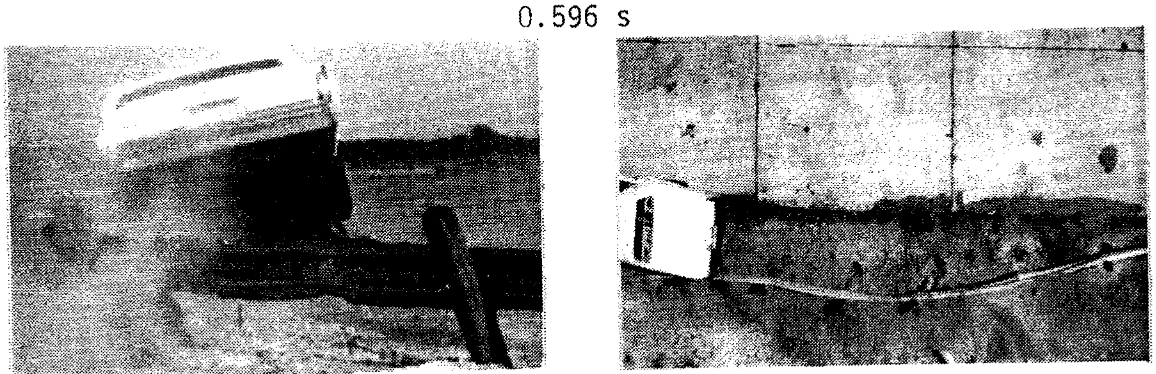

0.695 s

Fig. 94. (Continued)

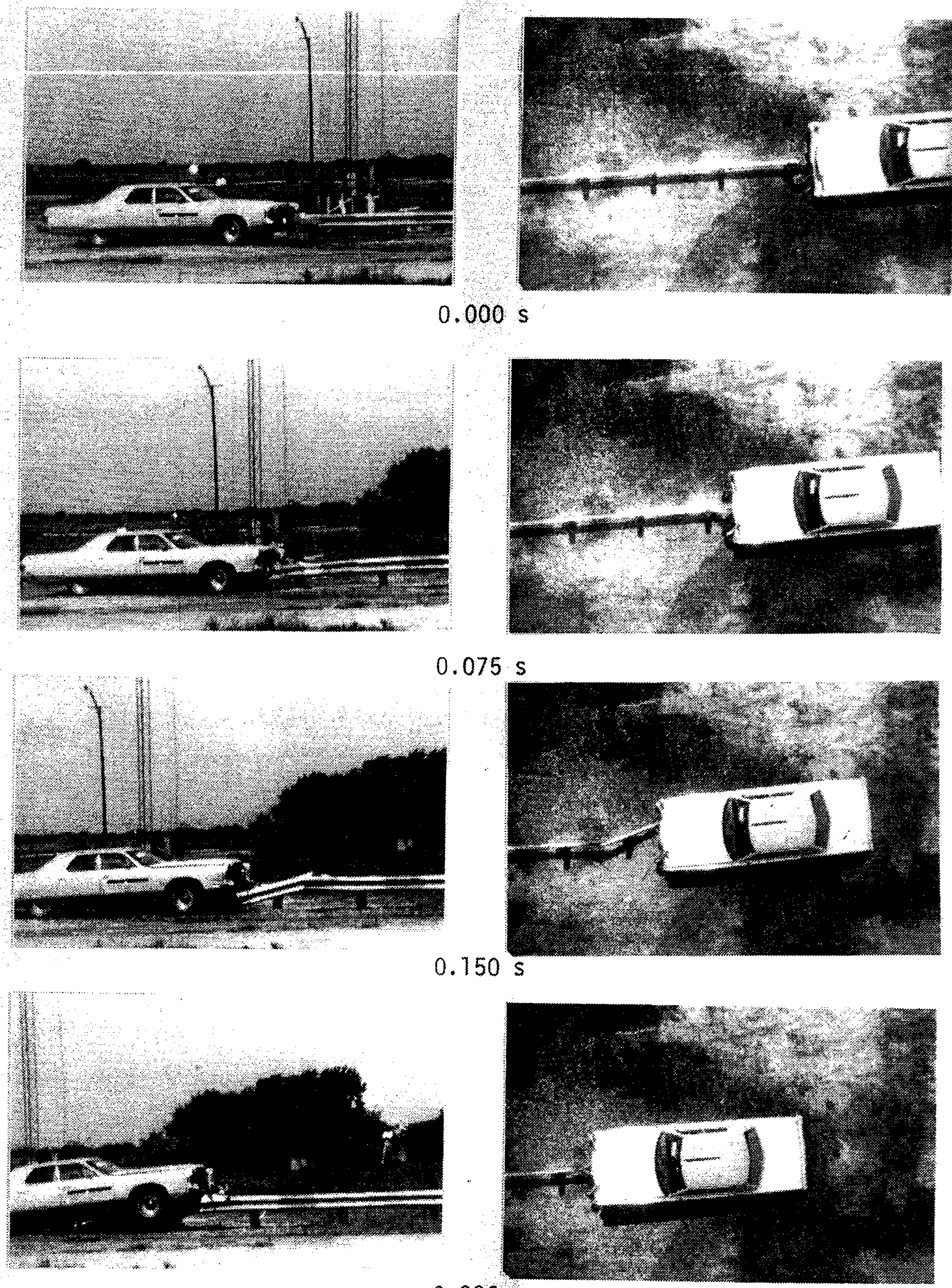

FIGURE D-10. SEQUENTIAL PHOTOGRAPHS FOR TEST SR-1.

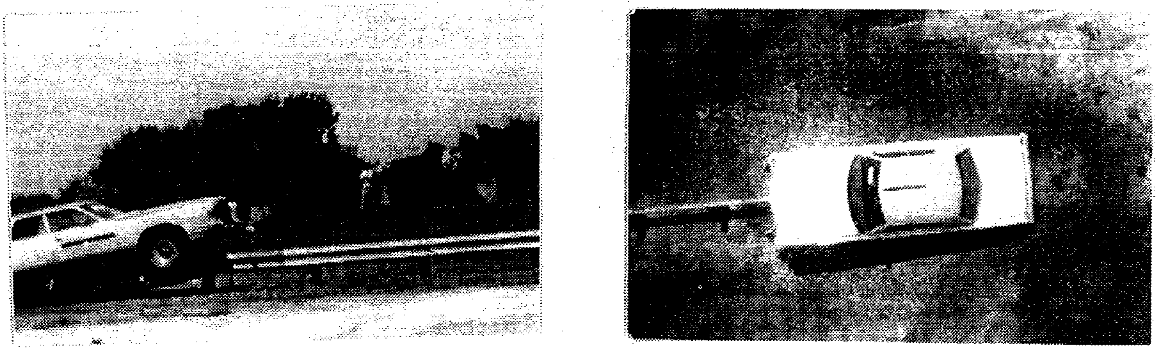

0.301 s

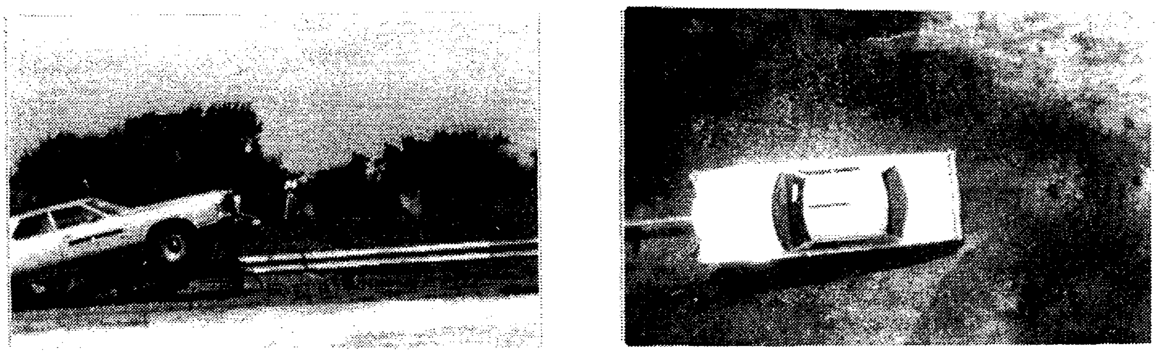

0.376 s

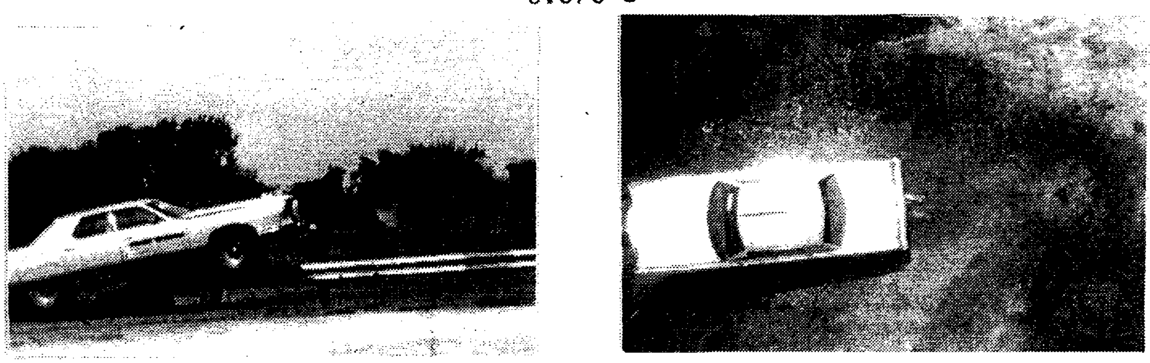

0.451 s

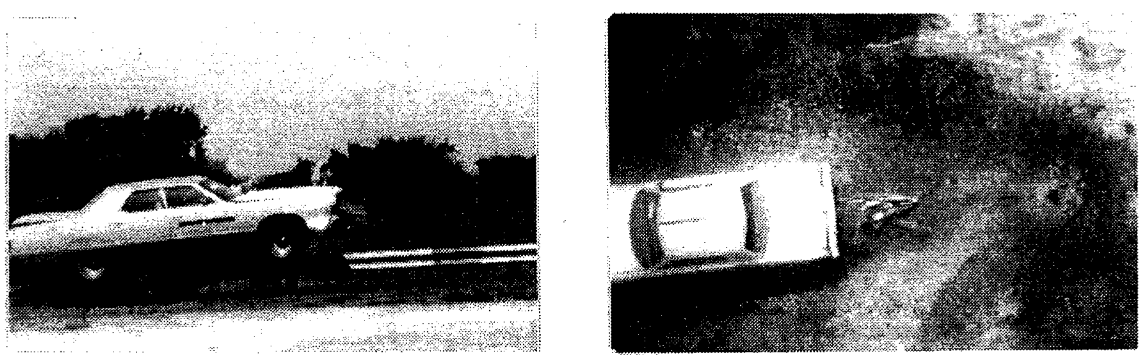

0.526 s

FIGURE D-10. SEQUENTIAL PHOTOGRAPHS FOR
TEST SR-1. (CONTINUED)

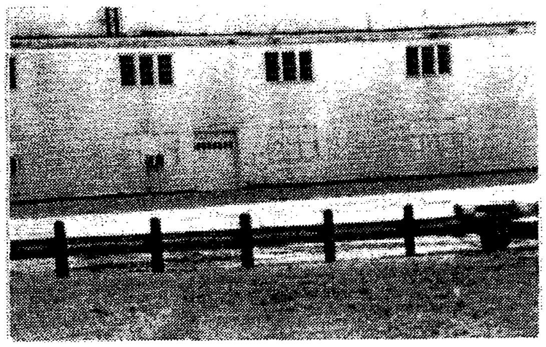

0.000 s

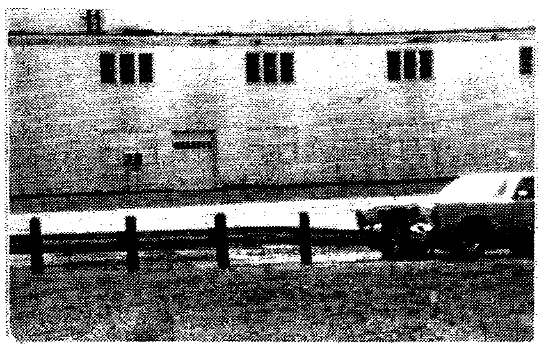

0.074 s

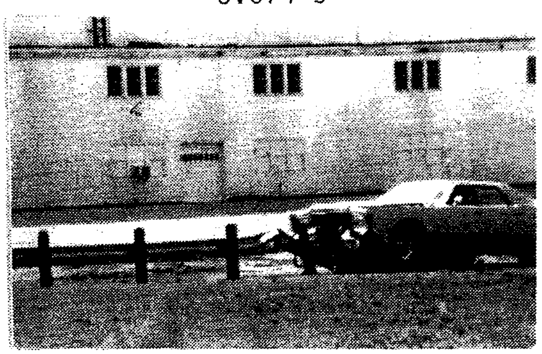

0.149 s

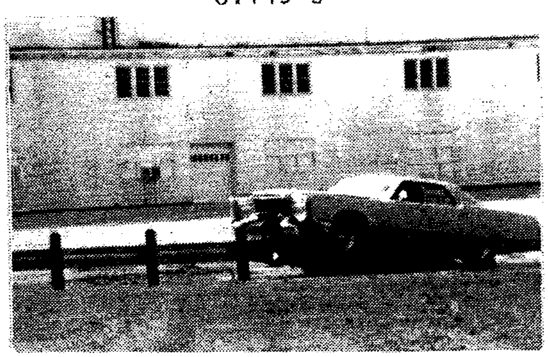

0.226 s

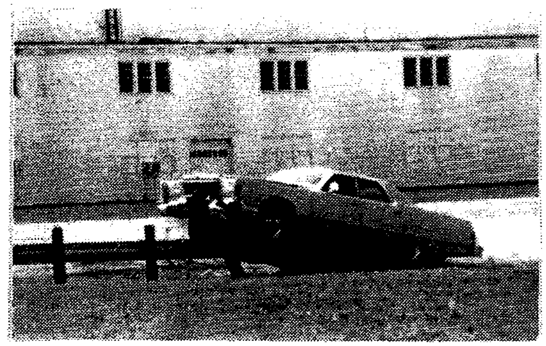

0.300 s

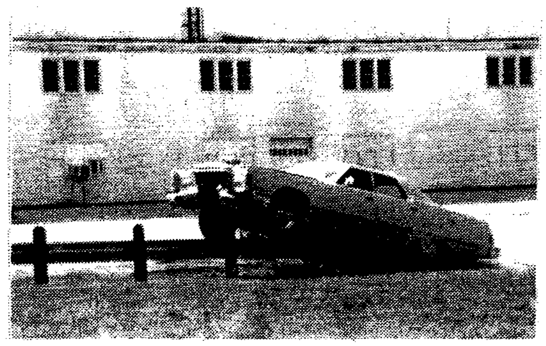

0.375 s

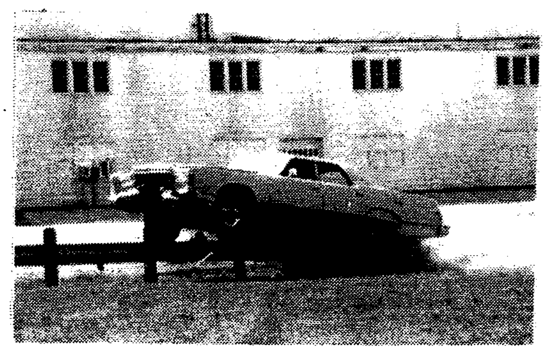

0.452 s

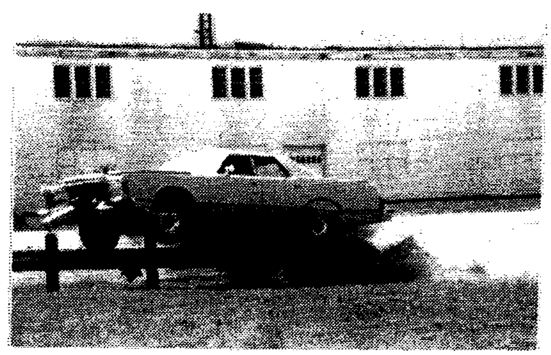

0.526 s

FIGURE D-10. SEQUENTIAL PHOTOGRAPHS FOR TEST SR-1. (CONTINUED)

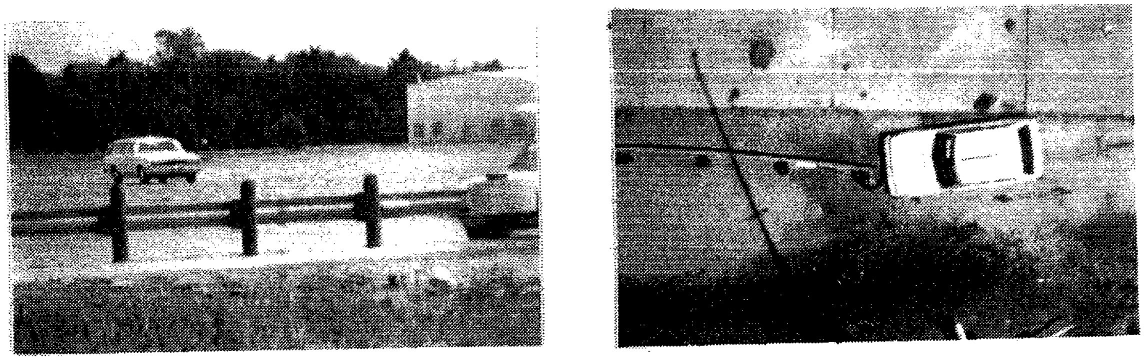

0.000 s

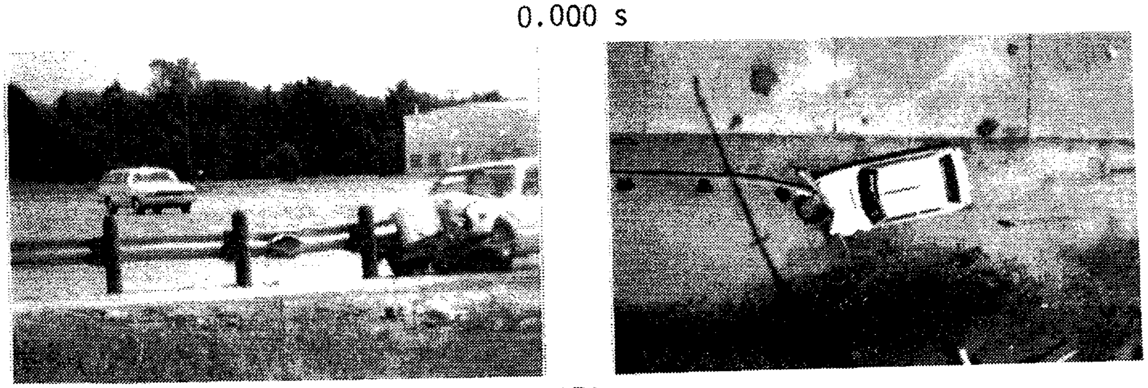

0.079 s

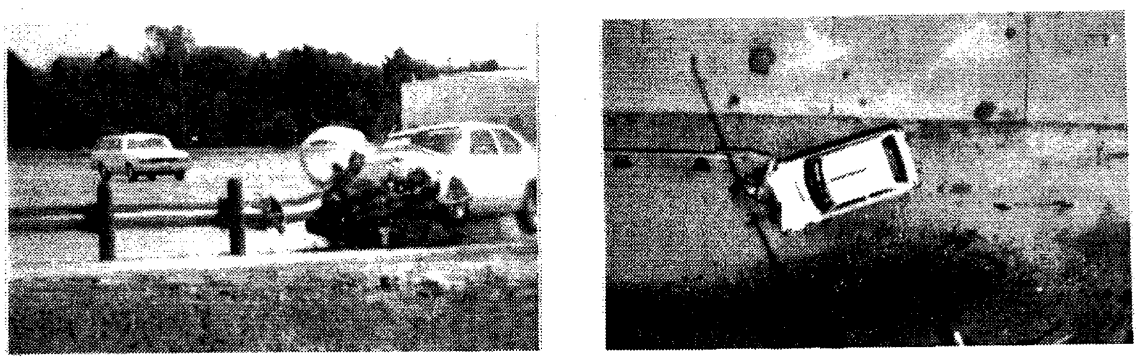

0.158 s

0.237 s

FIGURE D-11. SEQUENTIAL PHOTOGRAPHS FOR TEST SR-2.

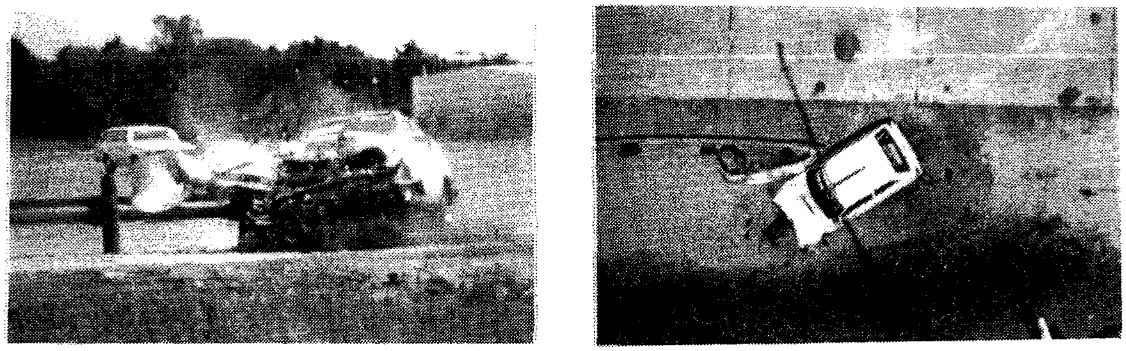

0.316 s

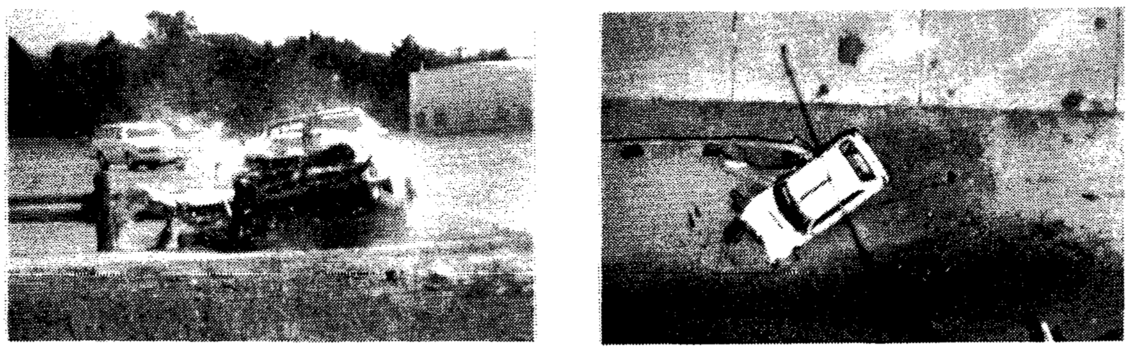

0.395 s

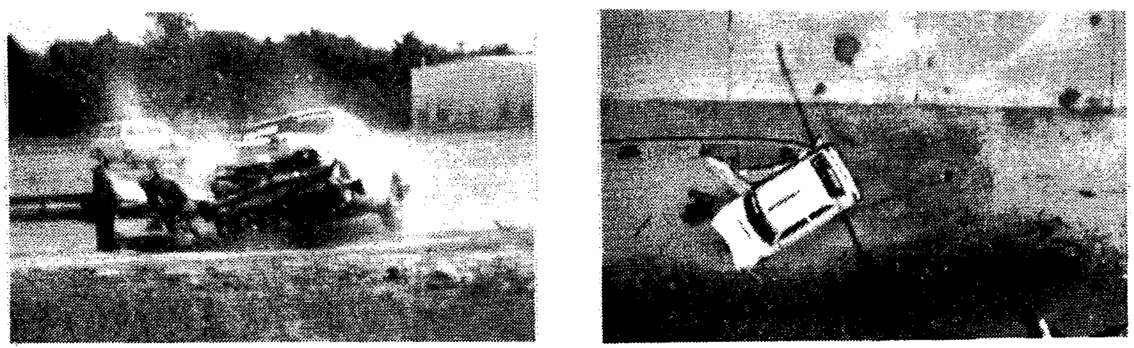

0.474 s

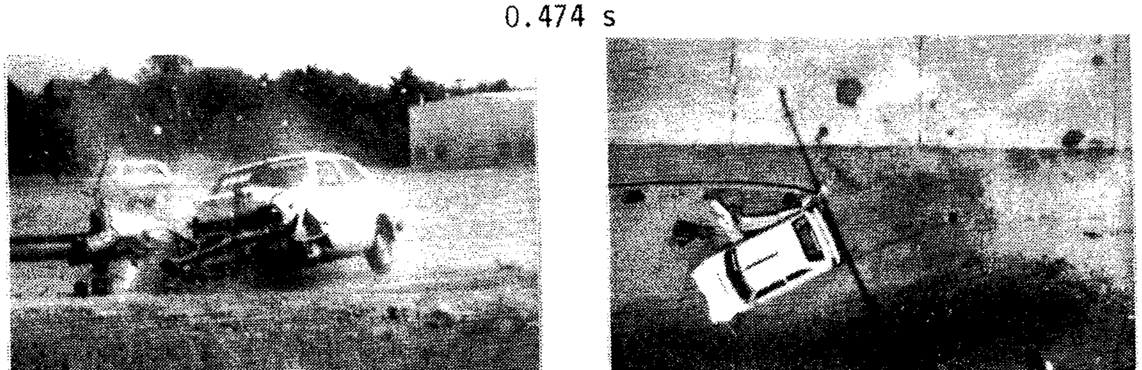

0.553 s

FIGURE D-11. SEQUENTIAL PHOTOGRAPHS FOR TEST SR-2. (CONTINUED)

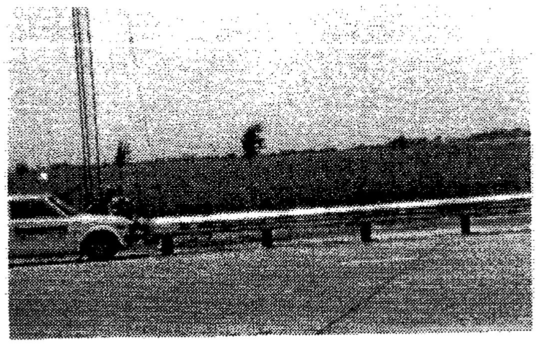

0.000 s

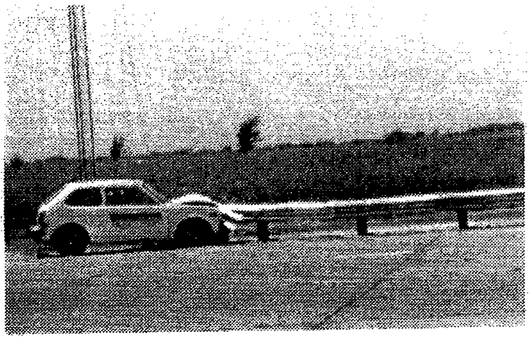

0.079 s

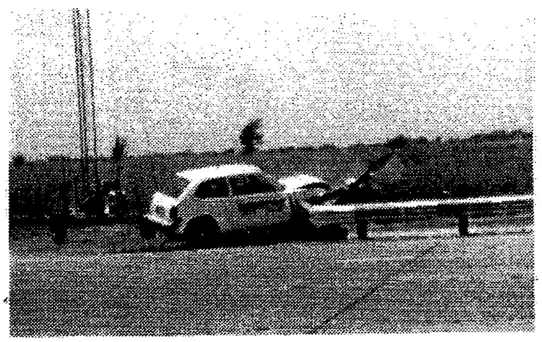

0.158 s

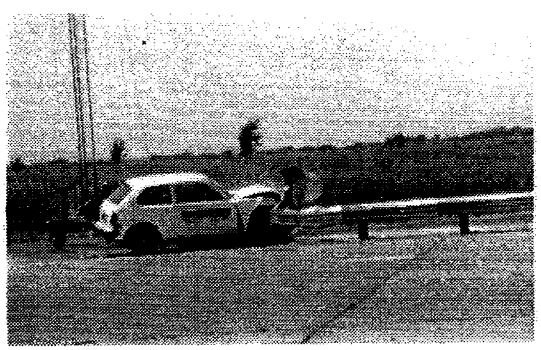

0.237 s

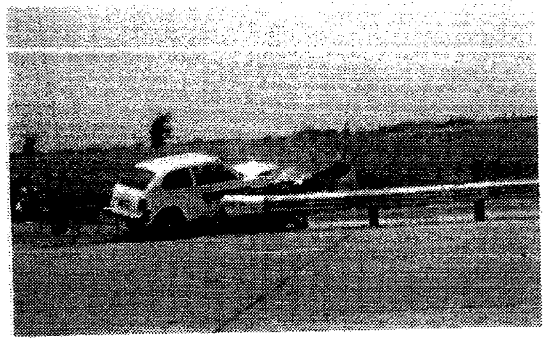

0.316 s

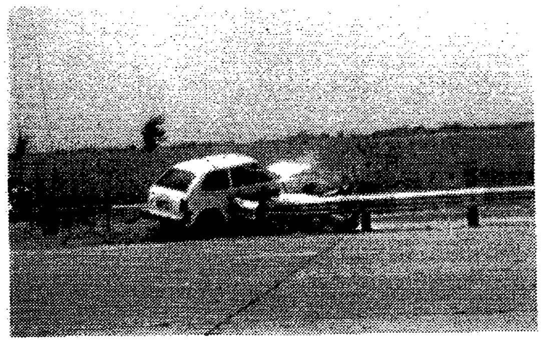

0.395 s

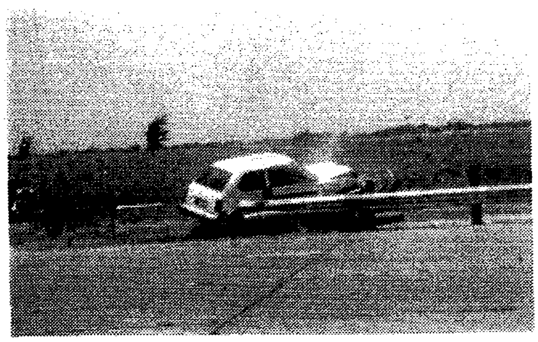

0.474 s

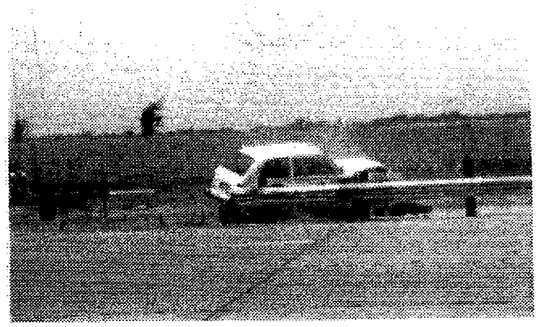

0.553 s

FIGURE D-11 SEQUENTIAL PHOTOGRAPHS FOR TEST SR-2. (CONTINUED)

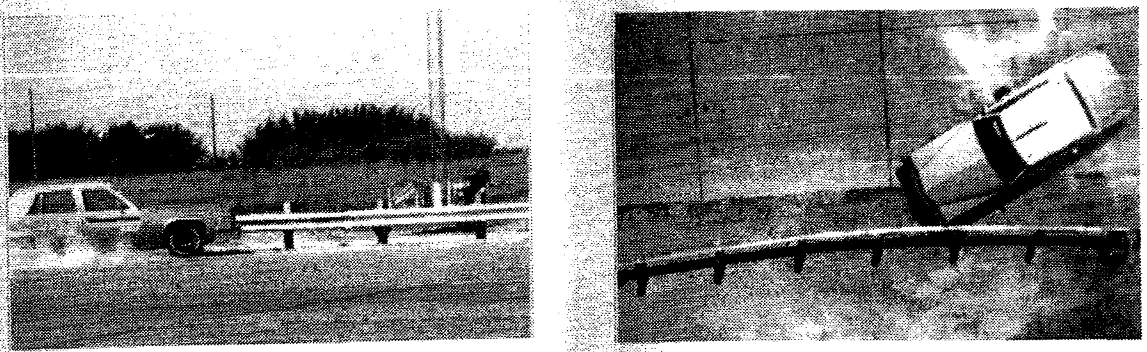

0.000 s

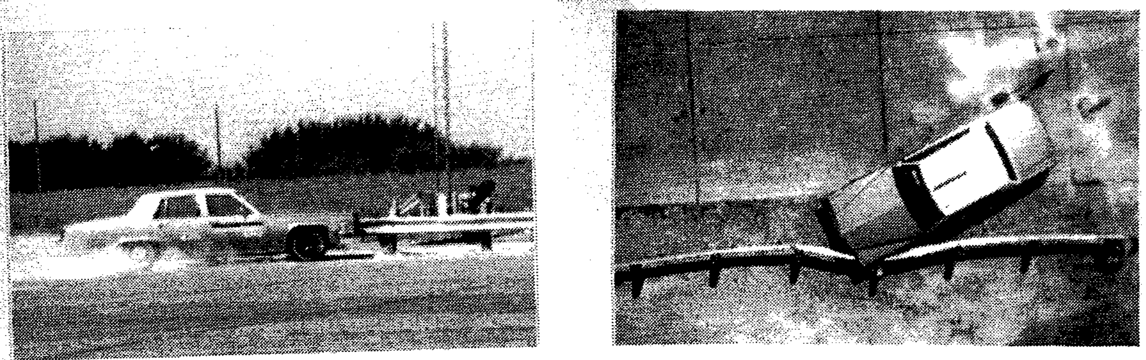

0.083 s

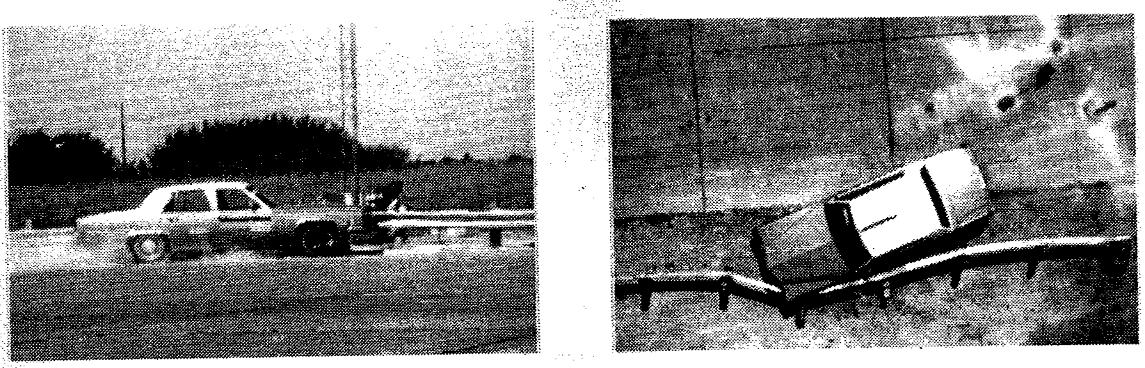

0.167 s

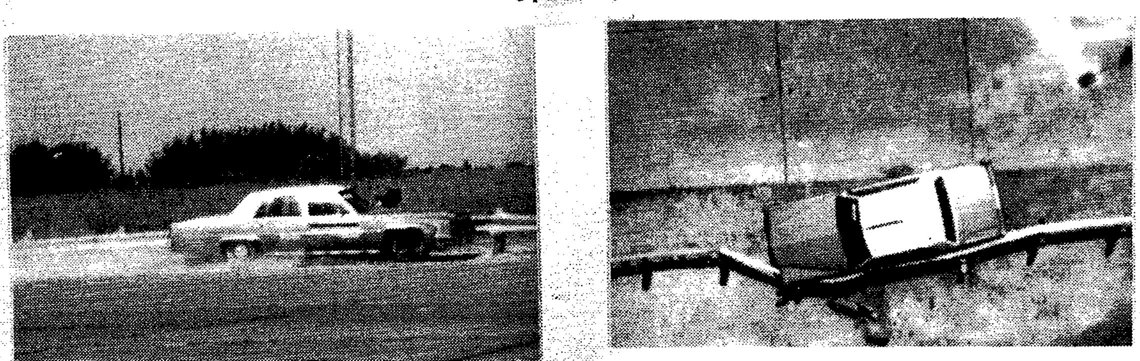

0.250 s

FIGURE D-12. SEQUENTIAL PHOTOGRAPHS FOR TEST SR-3.

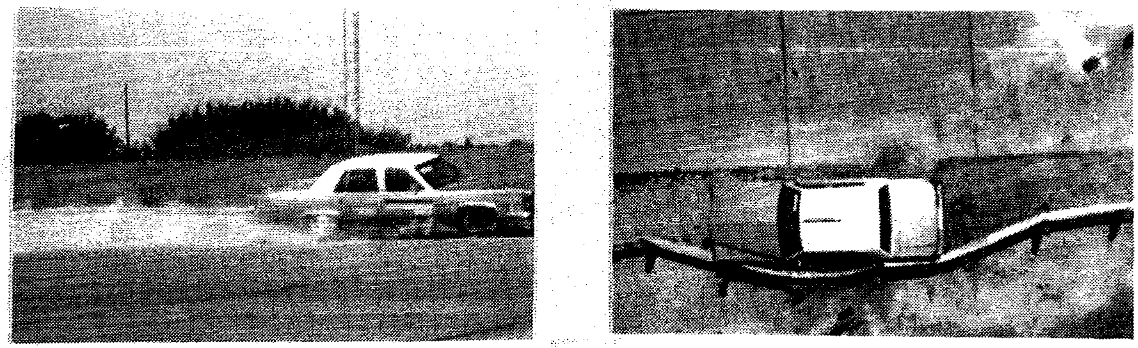

0.333 s

0.416 s

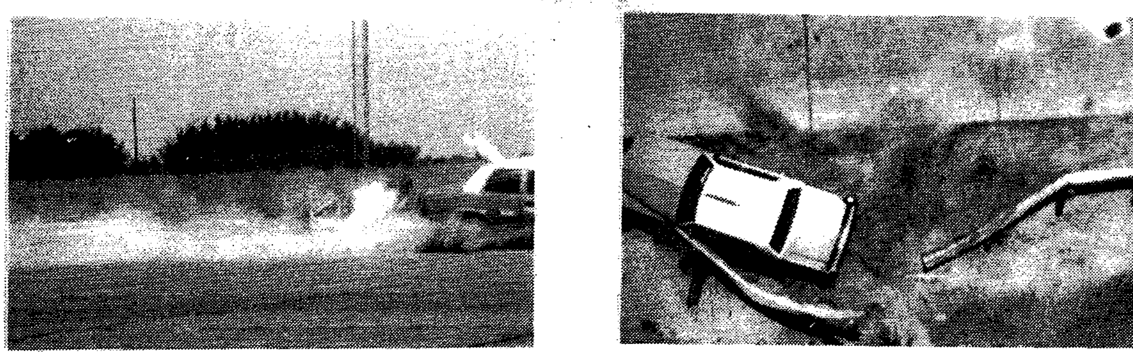

0.500 s

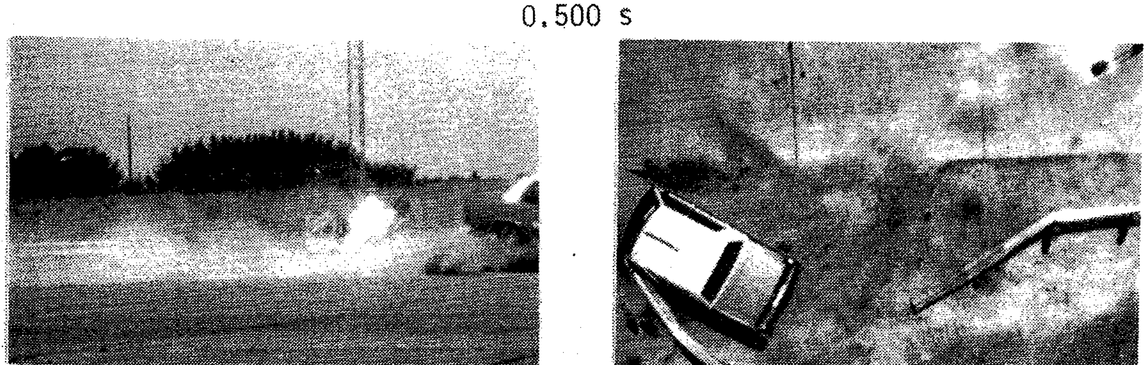

0.583 s

FIGURE D-12. SEQUENTIAL PHOTOGRAPHS FOR TEST SR-3. (CONTINUED)

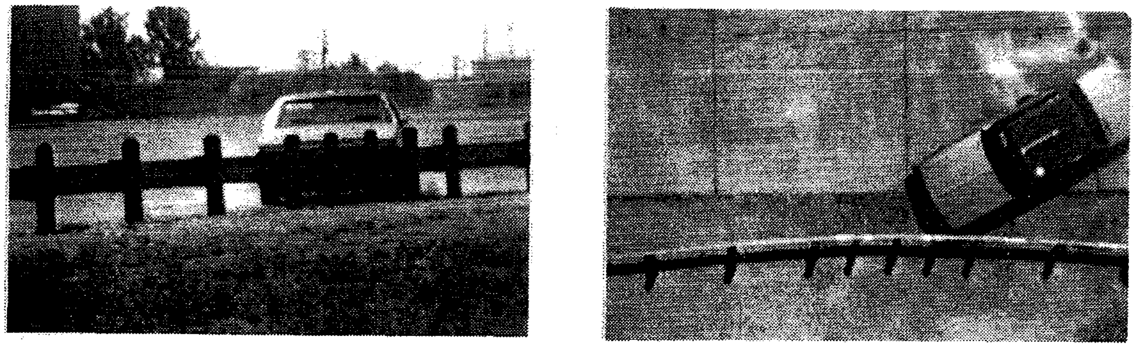

0.000 s

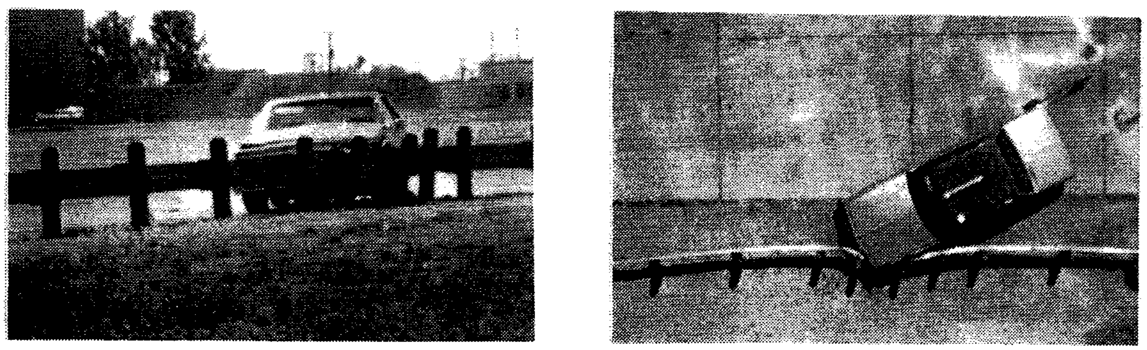

0.076 s

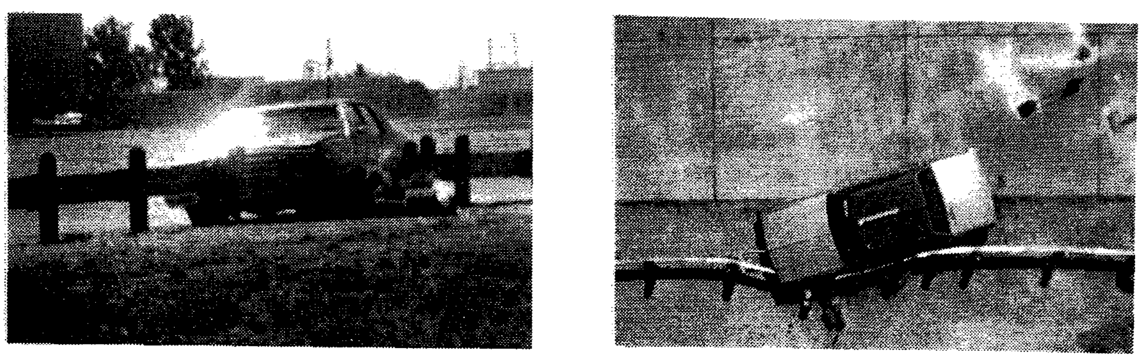

0.153 s

0.229 s

FIGURE D-13. SEQUENTIAL PHOTOGRAPHS FOR TEST SR-4.

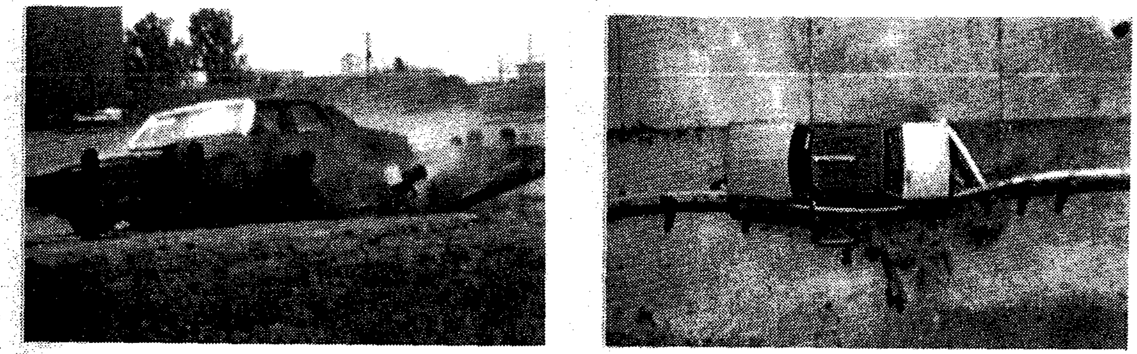

0.306 s

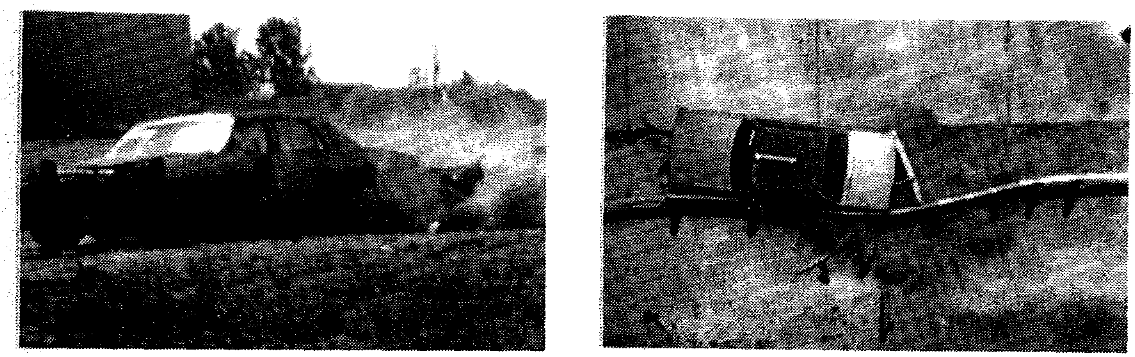

0.382 s

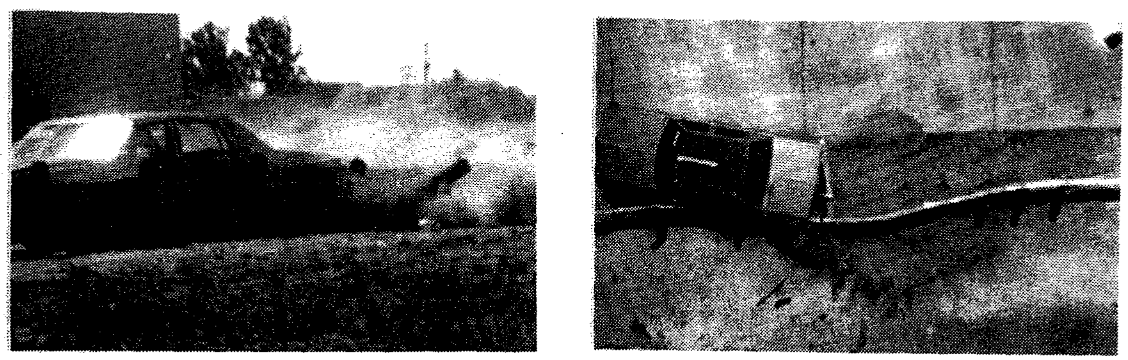

0.459 s

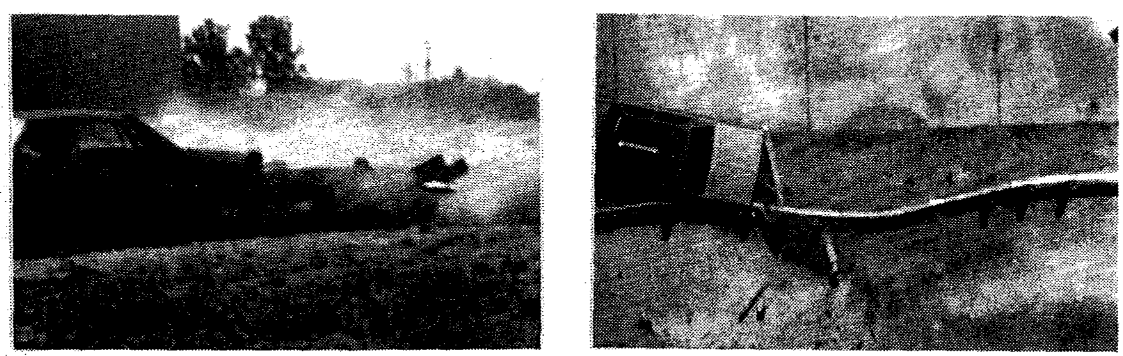

0.535 s

FIGURE D-13. SEQUENTIAL PHOTOGRAPHS FOR TEST SR-4. (CONTINUED)

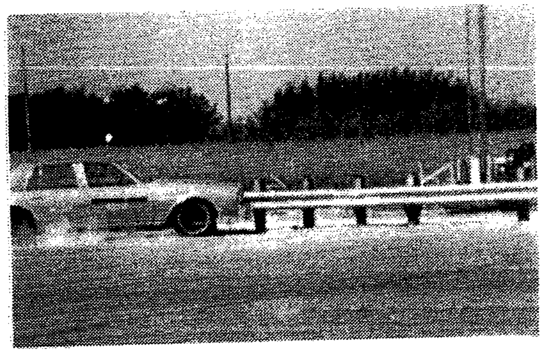

0.000 s

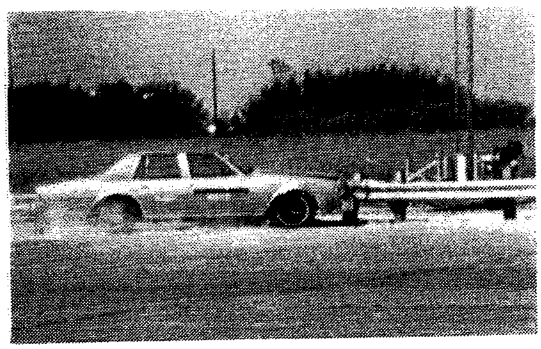

0.076 s

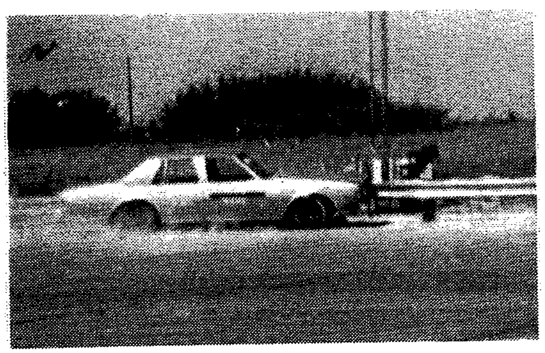

0.153 s

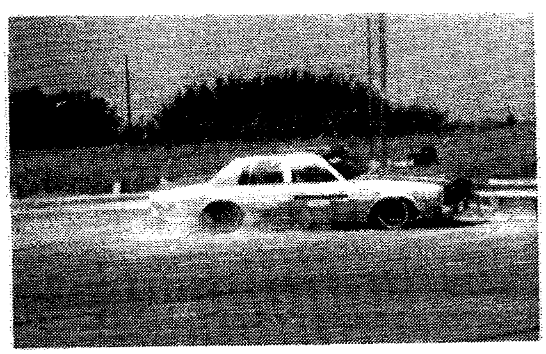

0.229 s

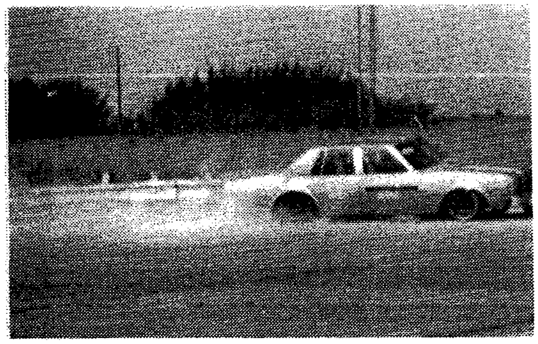

0.306 s

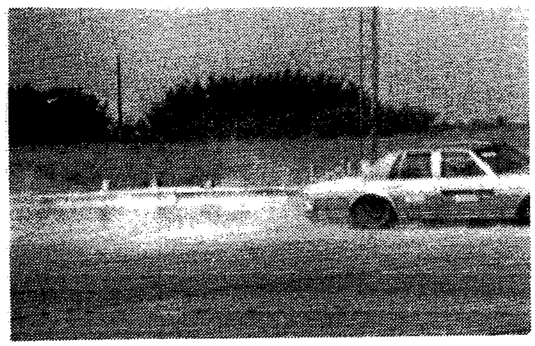

0.382 s

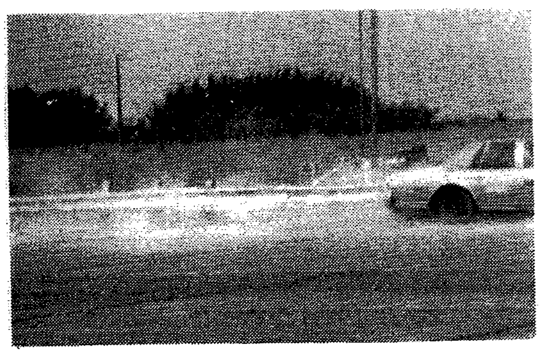

0.459 s

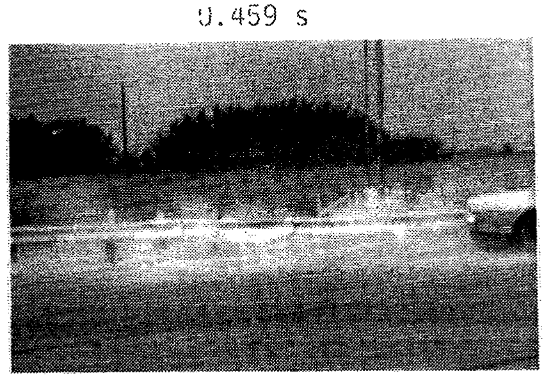

0.535 s

FIGURE D-13. SEQUENTIAL PHOTOGRAPHS FOR
TEST SR-4. (CONTINUED)

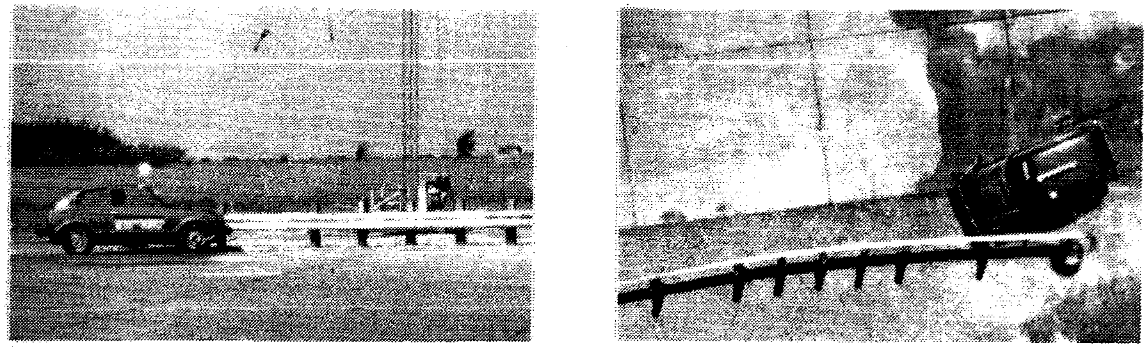

0.000 s

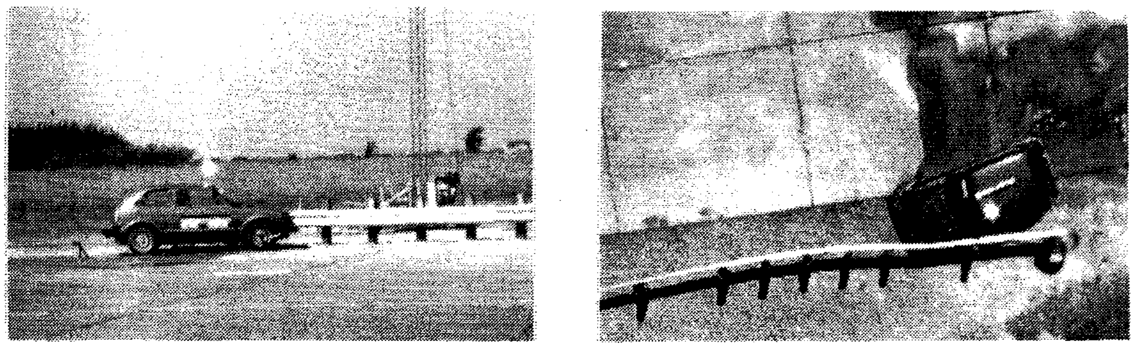

0.037 s

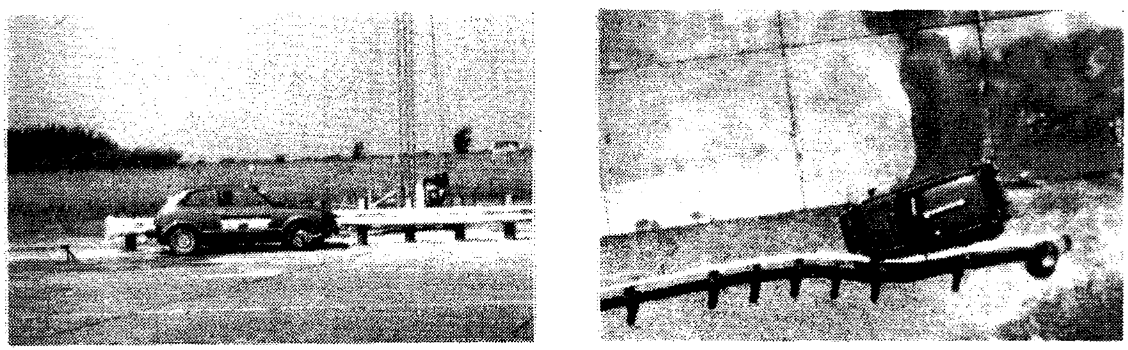

0.075 s

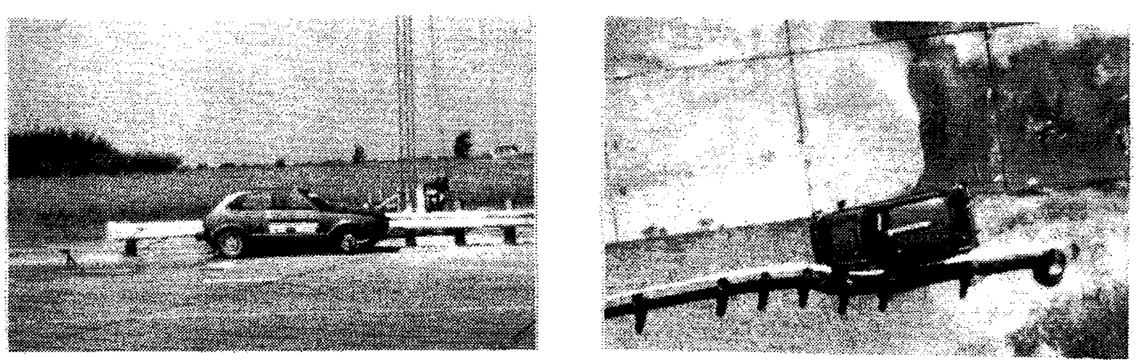

0.112 s

FIGURE D-14. SEQUENTIAL PHOTOGRAPHS FOR TEST SR-5.

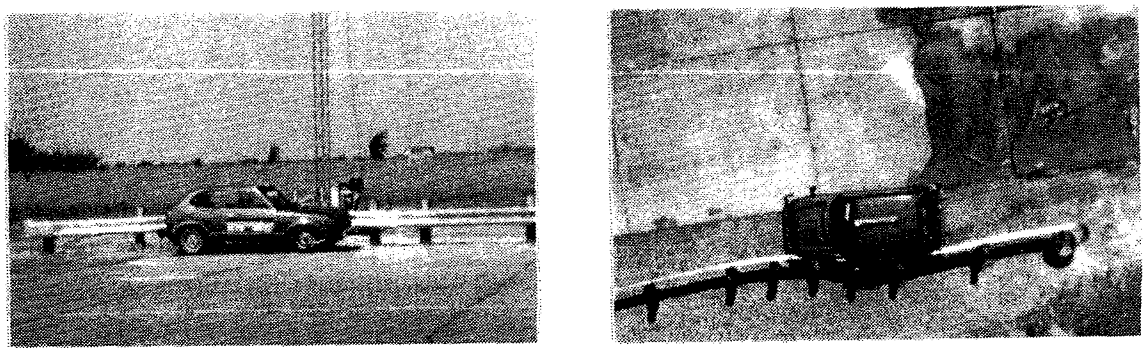

0.149 s

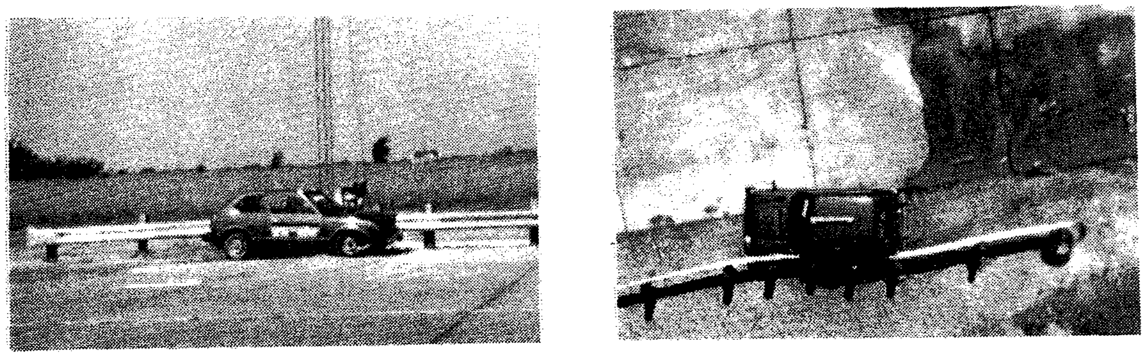

0.187 s

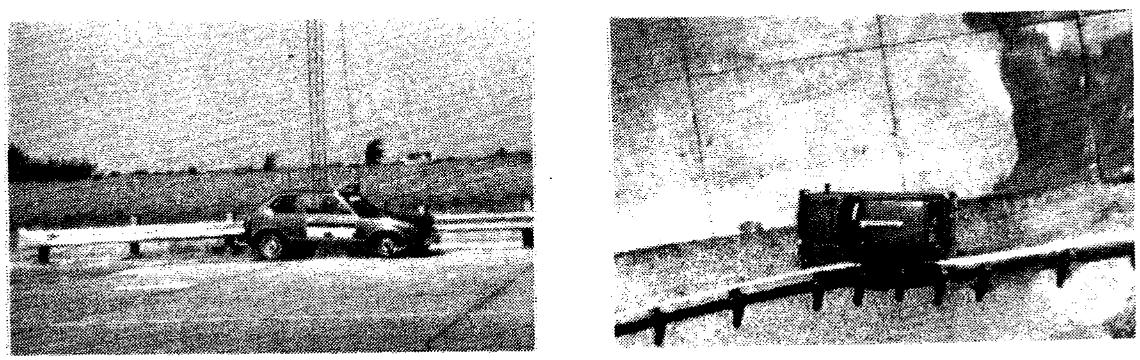

0.224 s

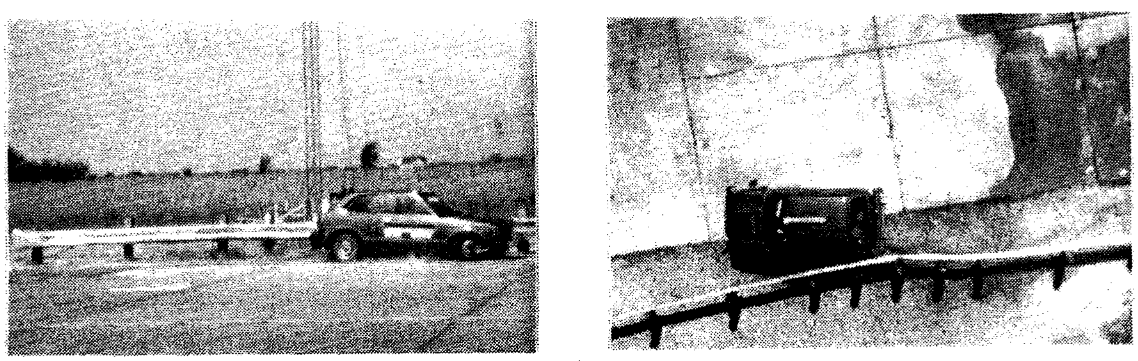

0.294 s

FIGURE D-14. SEQUENTIAL PHOTOGRAPHS FOR TEST SR-5. (CONTINUED)

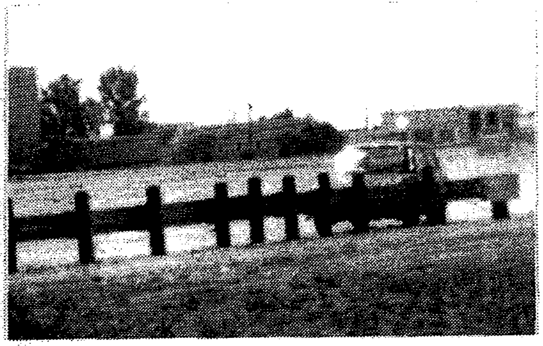

0.000 s

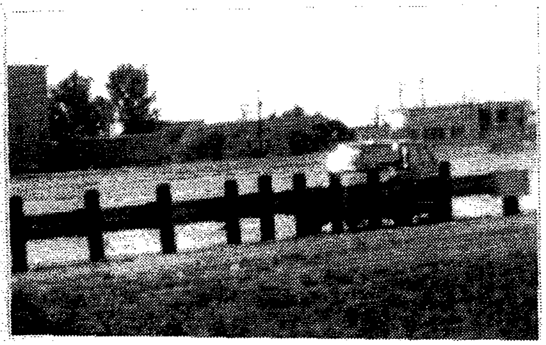

0.037 s

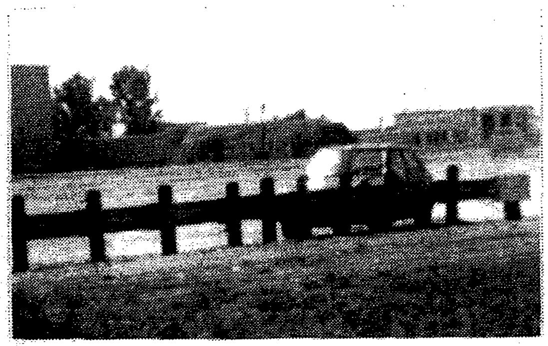

0.075 s

0.112 s

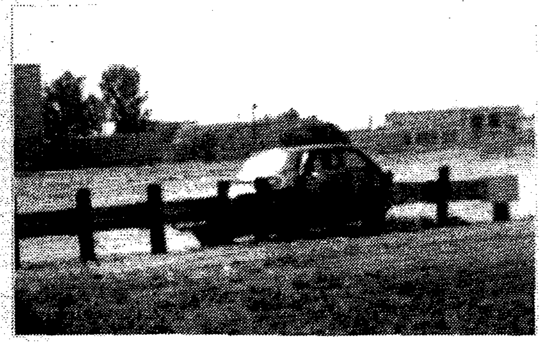

0.149 s

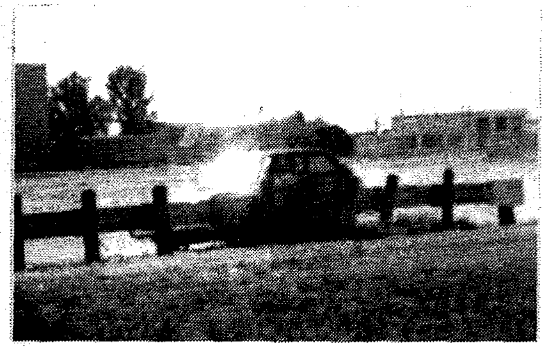

0.187 s

0.224 s

0.294 s

FIGURE D-14. SEQUENTIAL PHOTOGRAPHS FOR TEST SR-5. (CONTINUED)

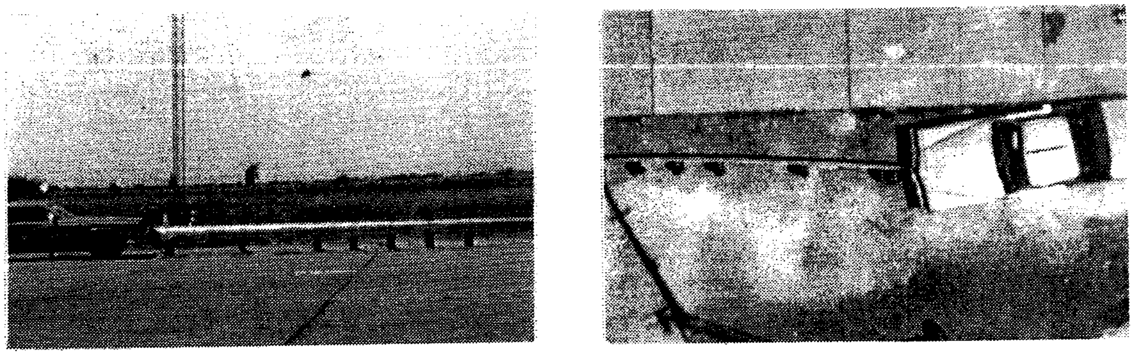

0.000 s

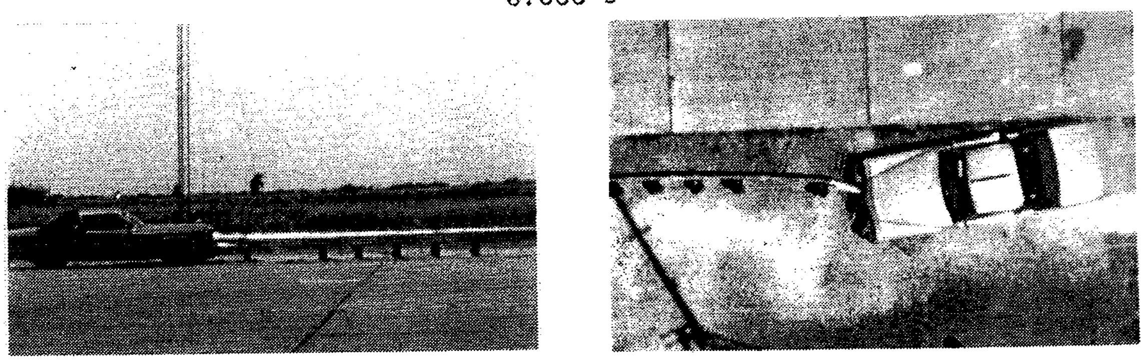

0.062 s

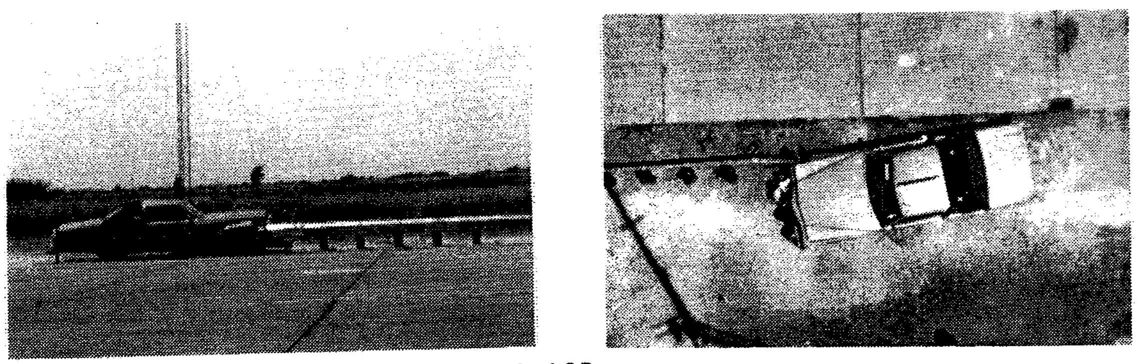

0.125 s

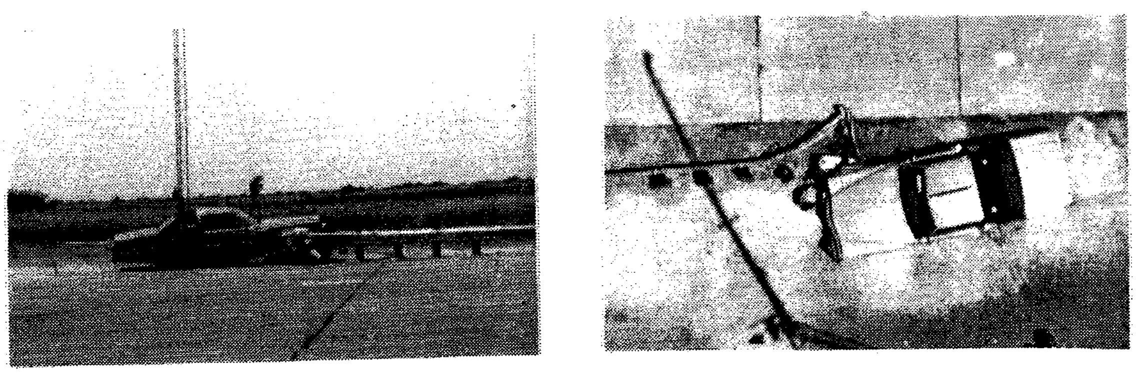

0.190 s

FIGURE D-15. SEQUENTIAL PHOTOGRAPHS FOR TEST SR-6.

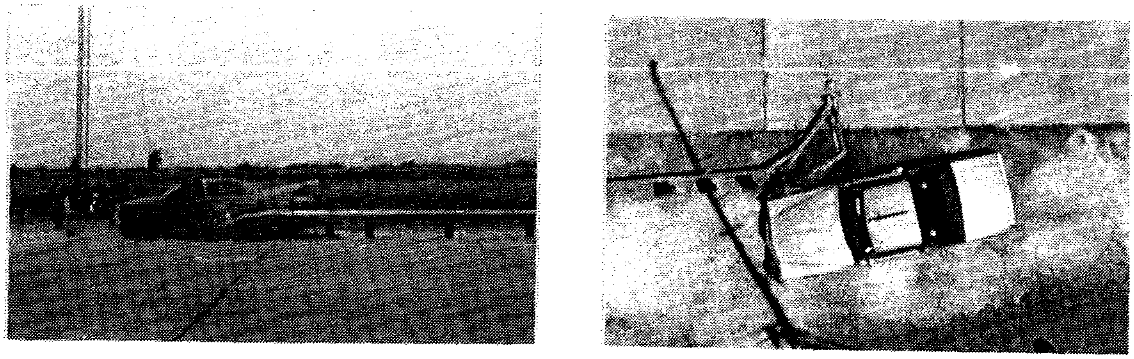

0.255 s

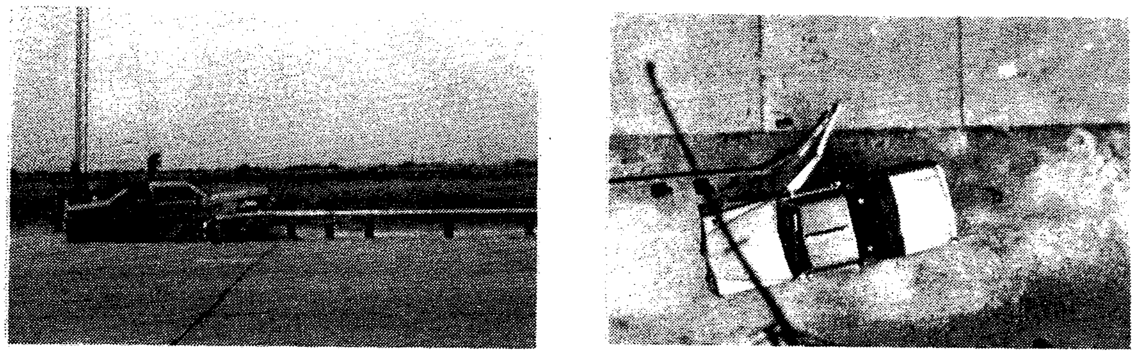

0.320 s

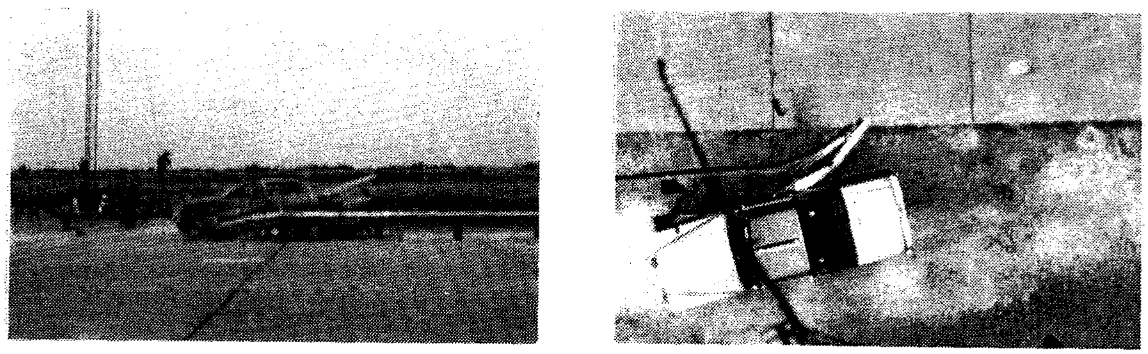

0.385 s

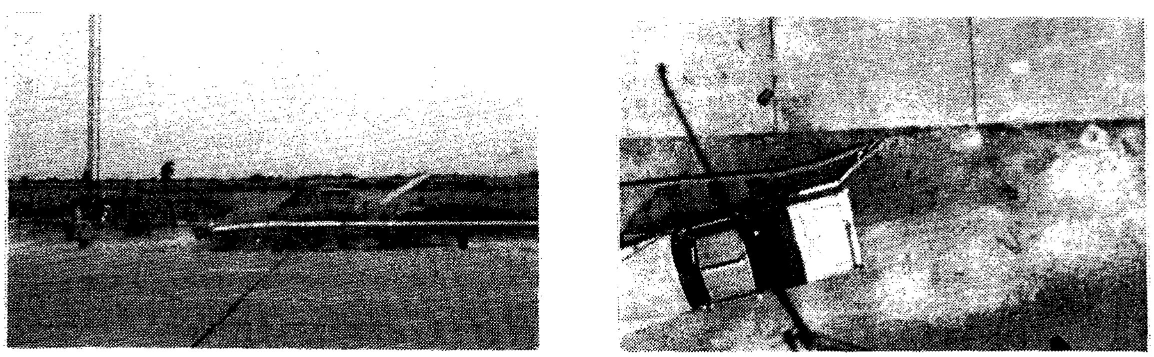

0.450 s

FIGURE D-15. SEQUENTIAL PHOTOGRAPHS FOR TEST SR-6. (CONTINUED)

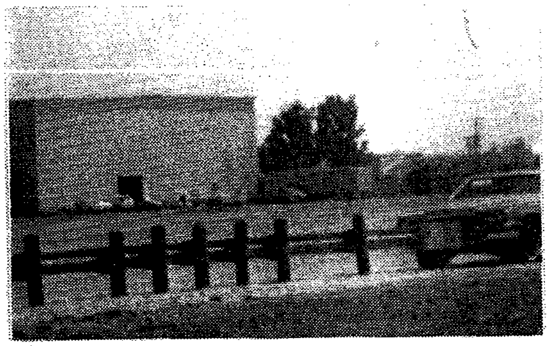

0.000 s

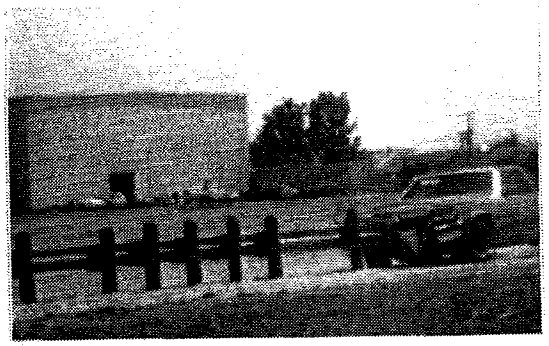

0.062 s

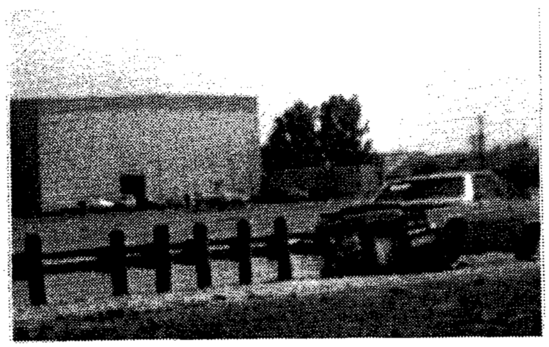

0.125 s

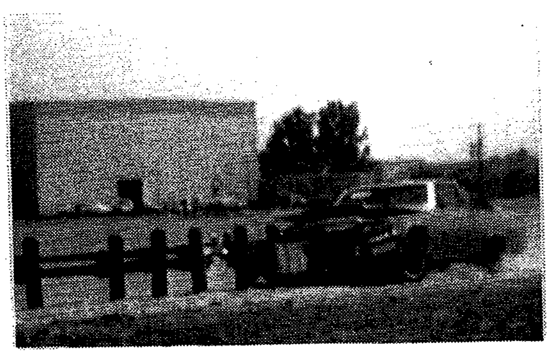

0.190 s

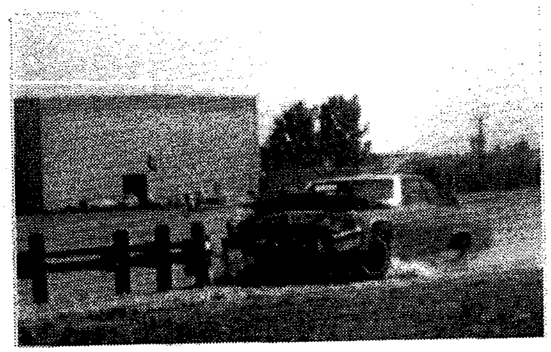

0.255 s

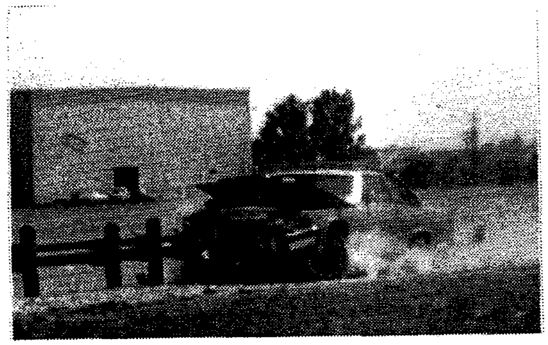

0.320 s

0.385 s

0.450 s

FIGURE D-15. SEQUENTIAL PHOTOGRAPHS FOR TEST SR-6. (CONTINUED)

APPENDIX E.

CONSTRUCTION DRAWINGS

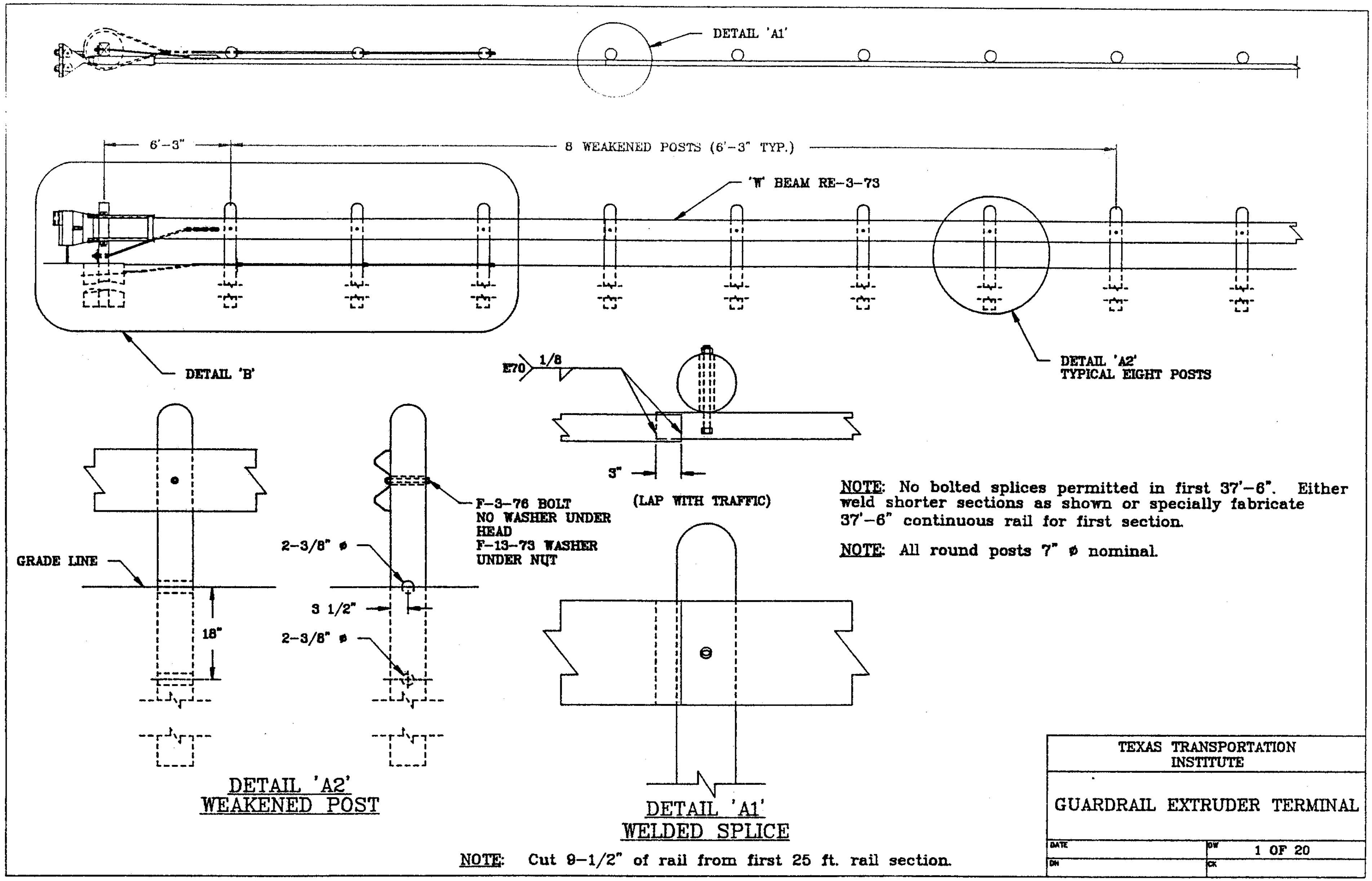

FIGURE E-1. GUARDRAIL EXTRUDER TERMINAL CONSTRUCTION DRAWINGS

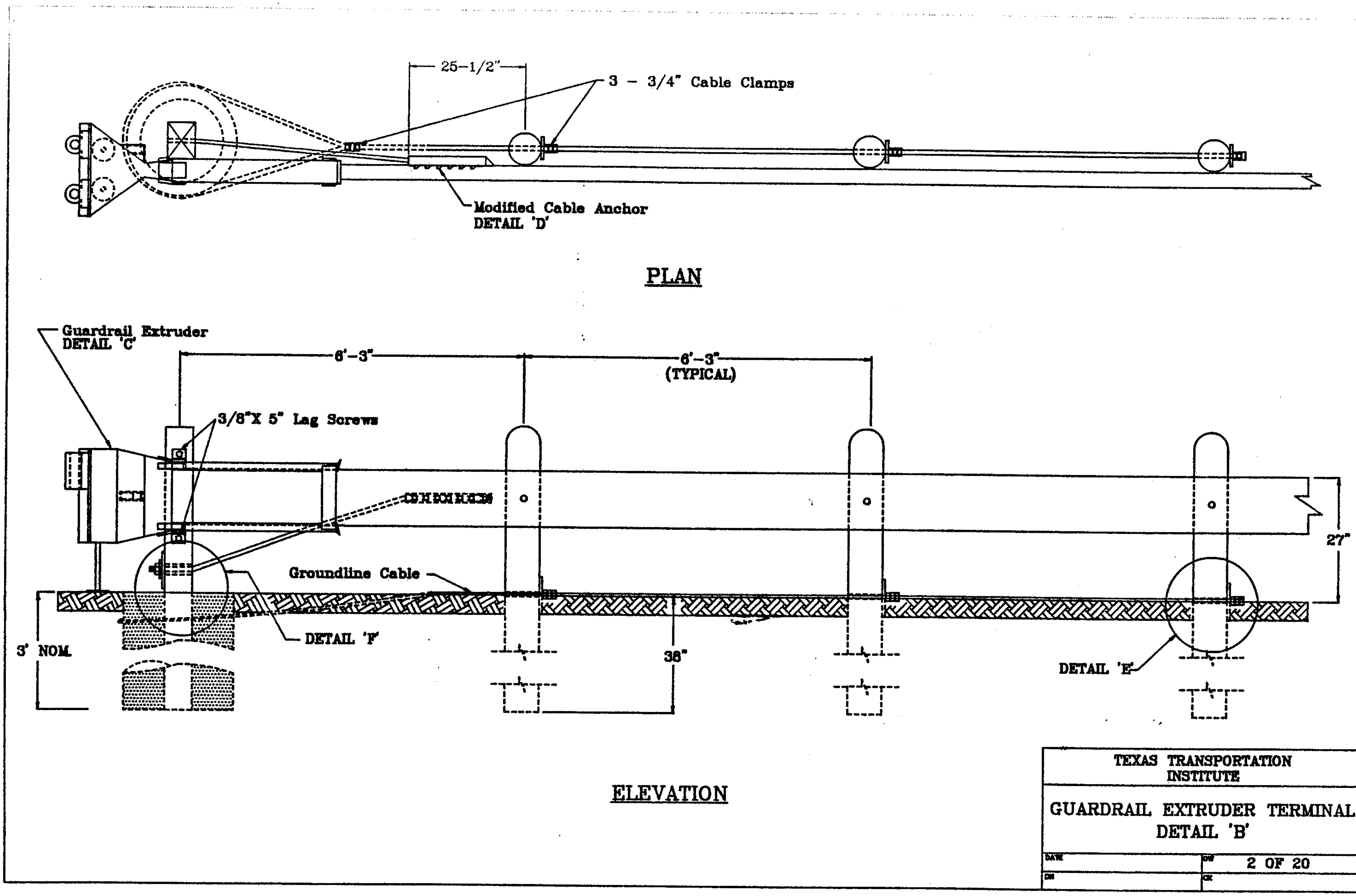

FIGUER E-1. GUARDRAIL EXTRUDER TERMINAL CONSTRUCTION DRAWINGS. (CONTINUED)

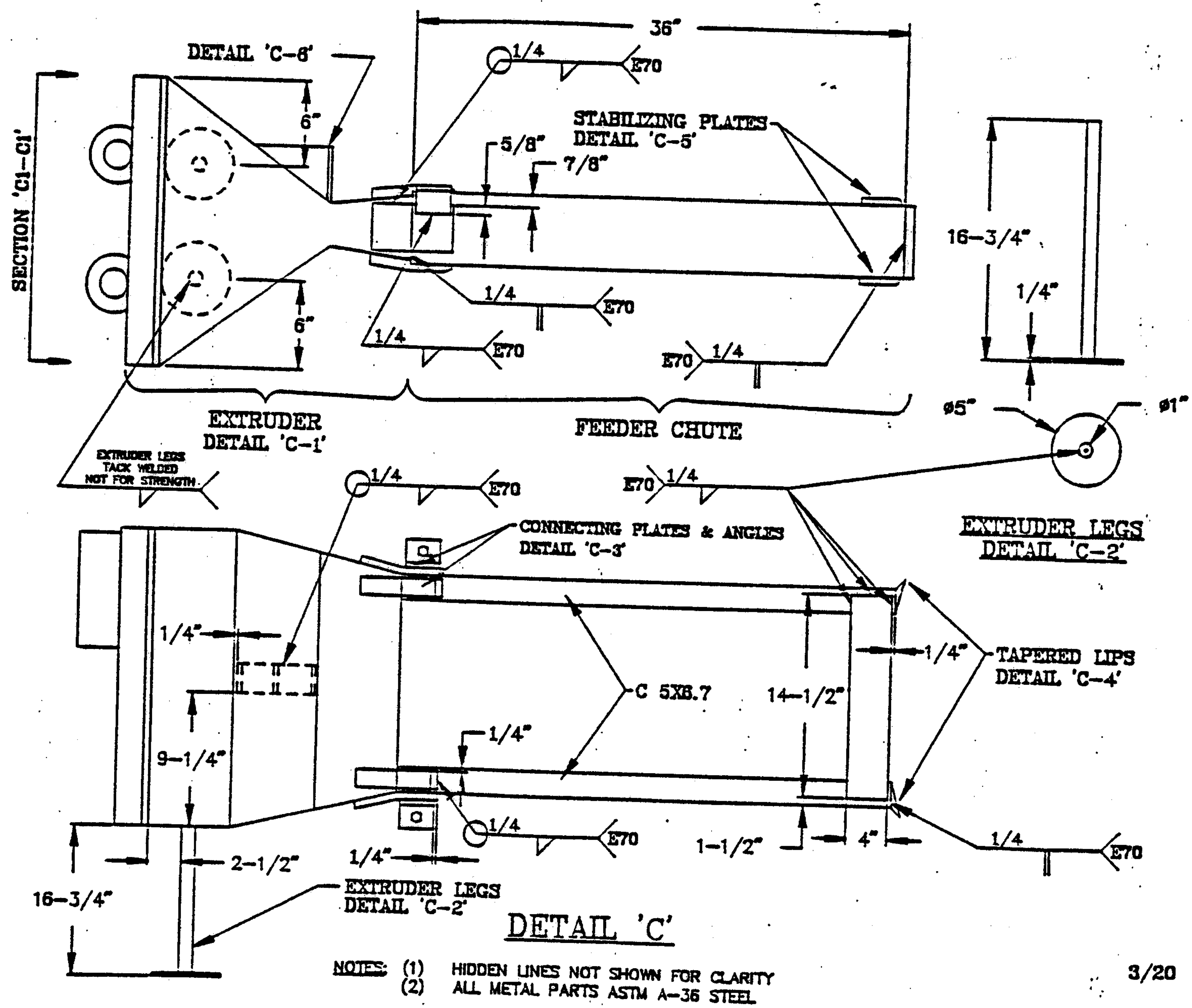

FIGURE E-1. GUARDRAIL EXTRUDER TERMINAL CONSTRUCTION DRAWINGS. (CONTINUED)

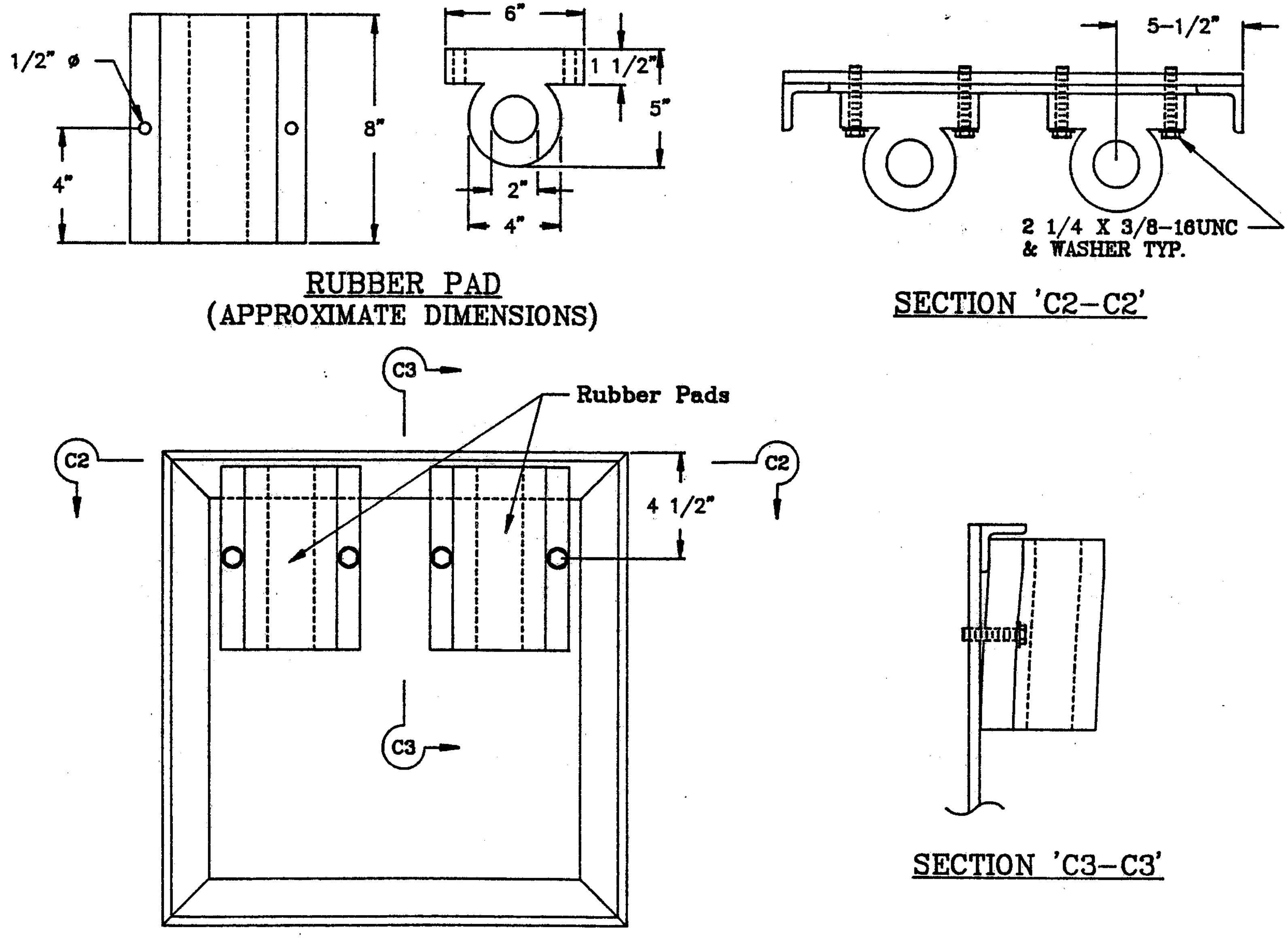

NOTE: Rubber pads may be bonded to the extruder.

4/20

FIGURE E-1. GUARDRAIL EXTRUDER TERMINAL CONSTRUCTION

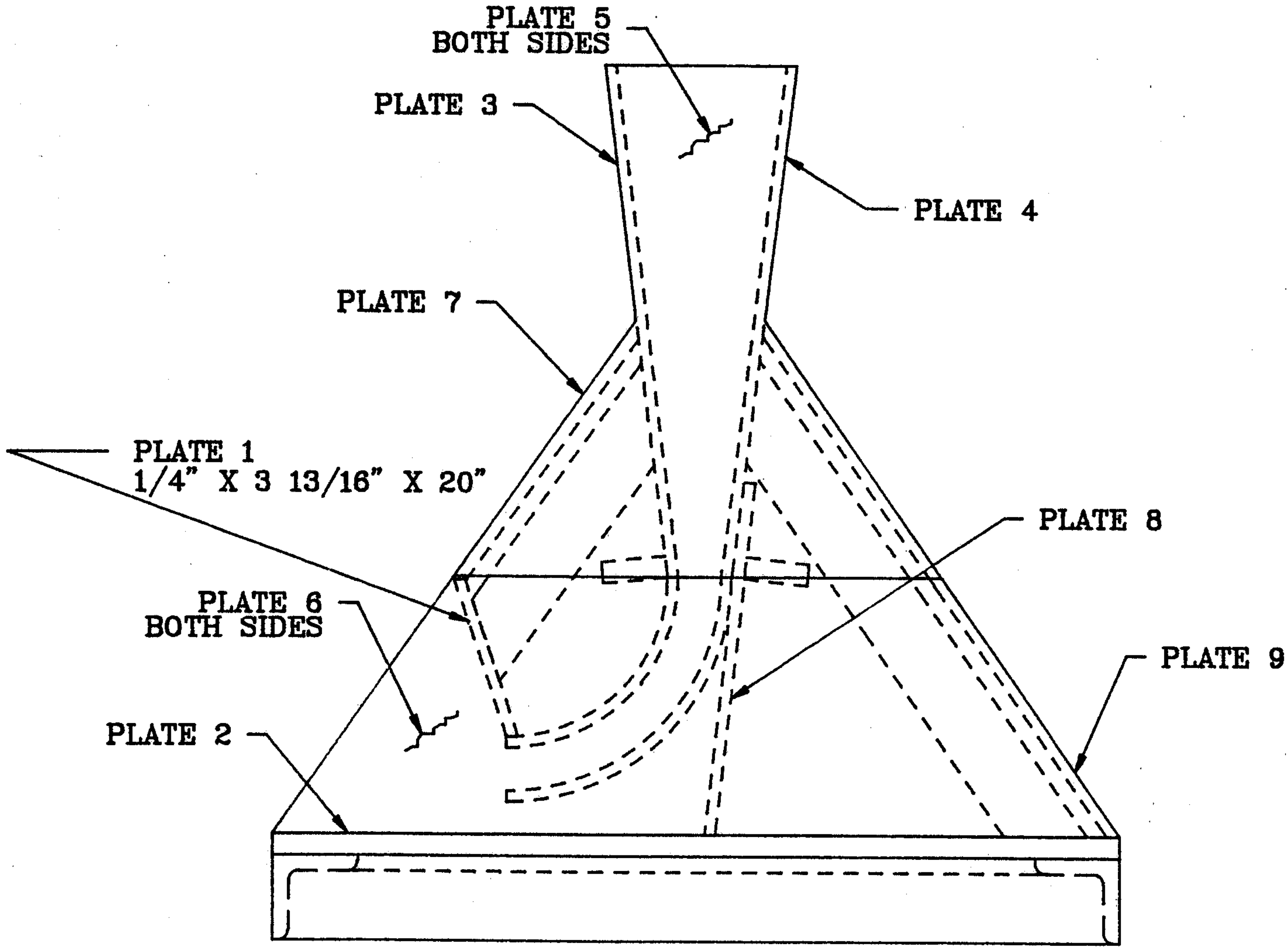

EXTRUDER
DETAIL 'C-1'

5/20

FIGURE E-1. GUARDRAIL EXTRUDER

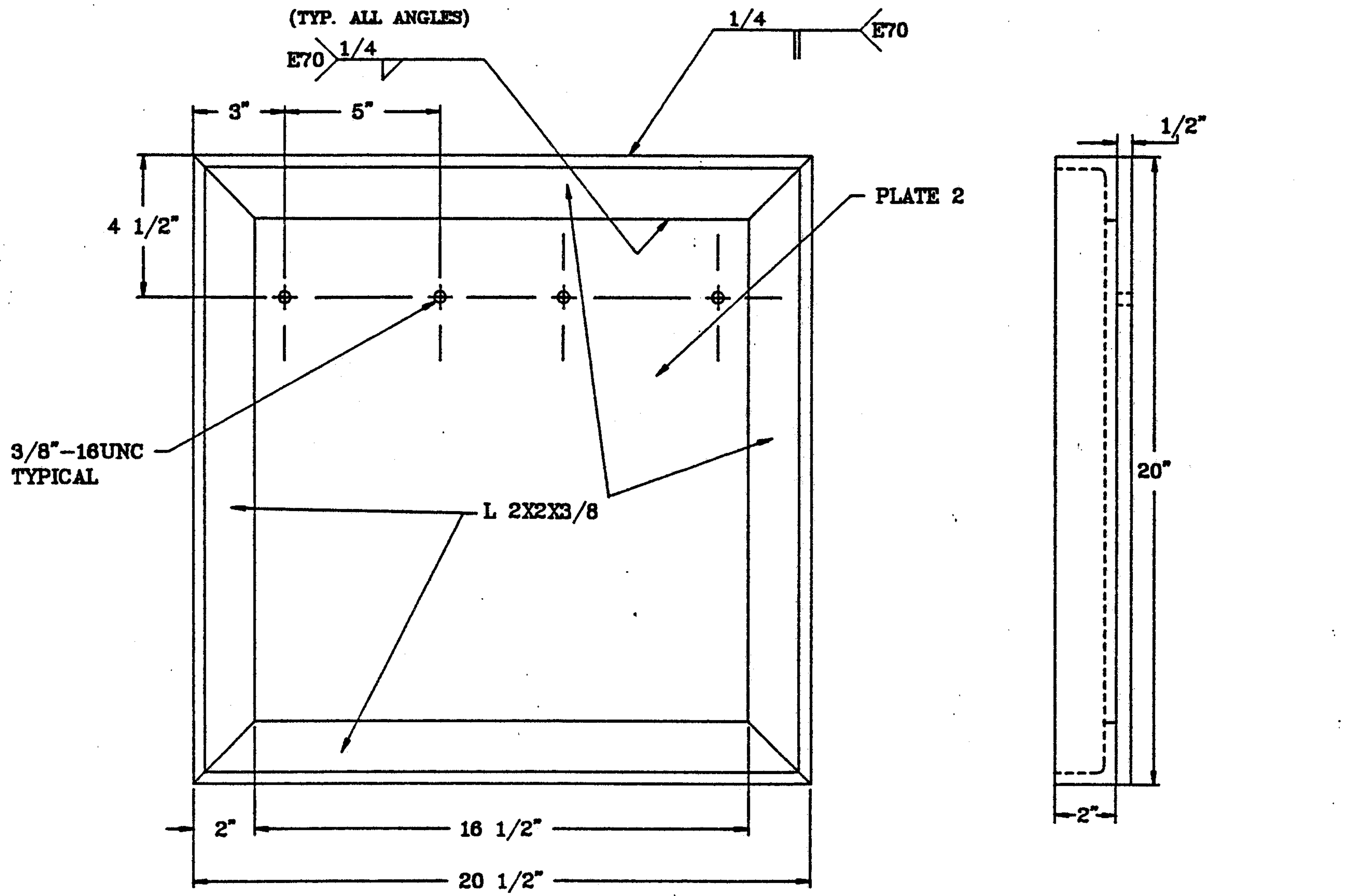

PLATE 2

6/20

FIGURE E-1. GUARDRAIL EXTRUDER TERMINAL CONSTRUCTION DRAWINGS. (CONTINUED)

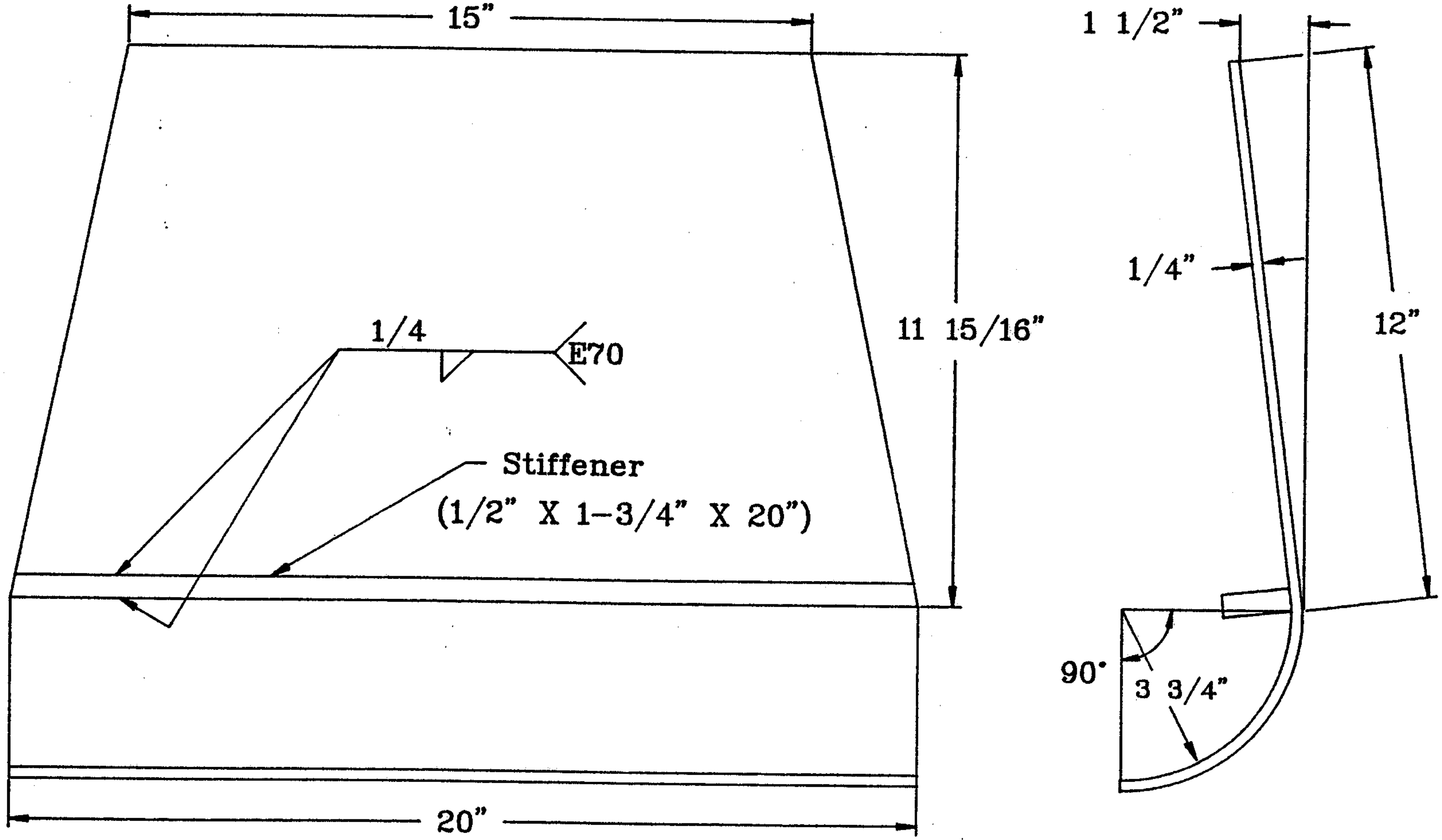

7/20

PLATE 3

FIGURE E-1. GUARDRAIL EXTRUDER TERMINAL CONSTRUCTION DRAWINGS (CONTINUED)

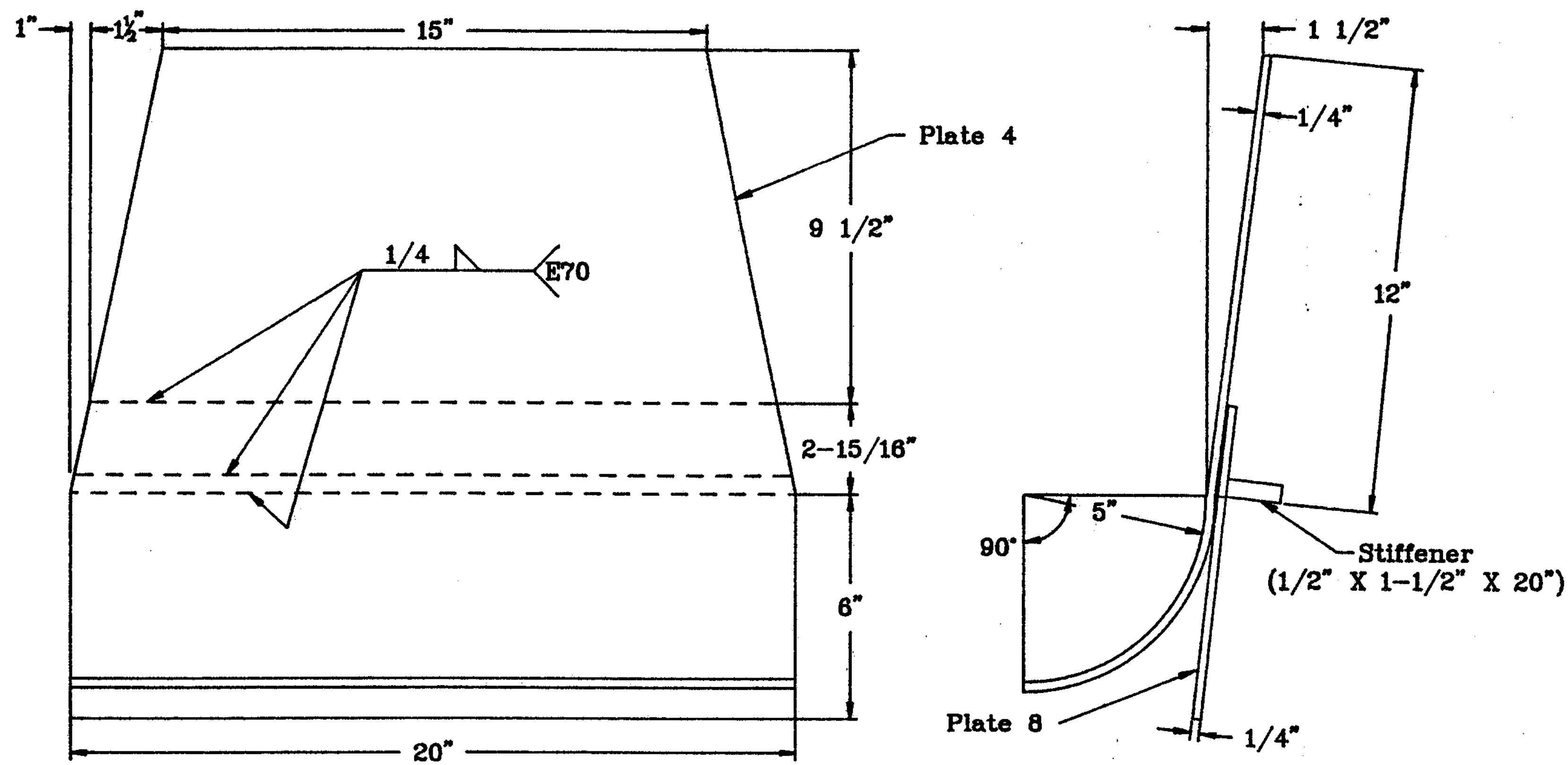

PLATES 4 AND 8

8/20

FIGURE E-1. GUARDRAIL EXTRUDER TERMINAL CONSTRUCTION DRAWINGS. (CONTINUED)

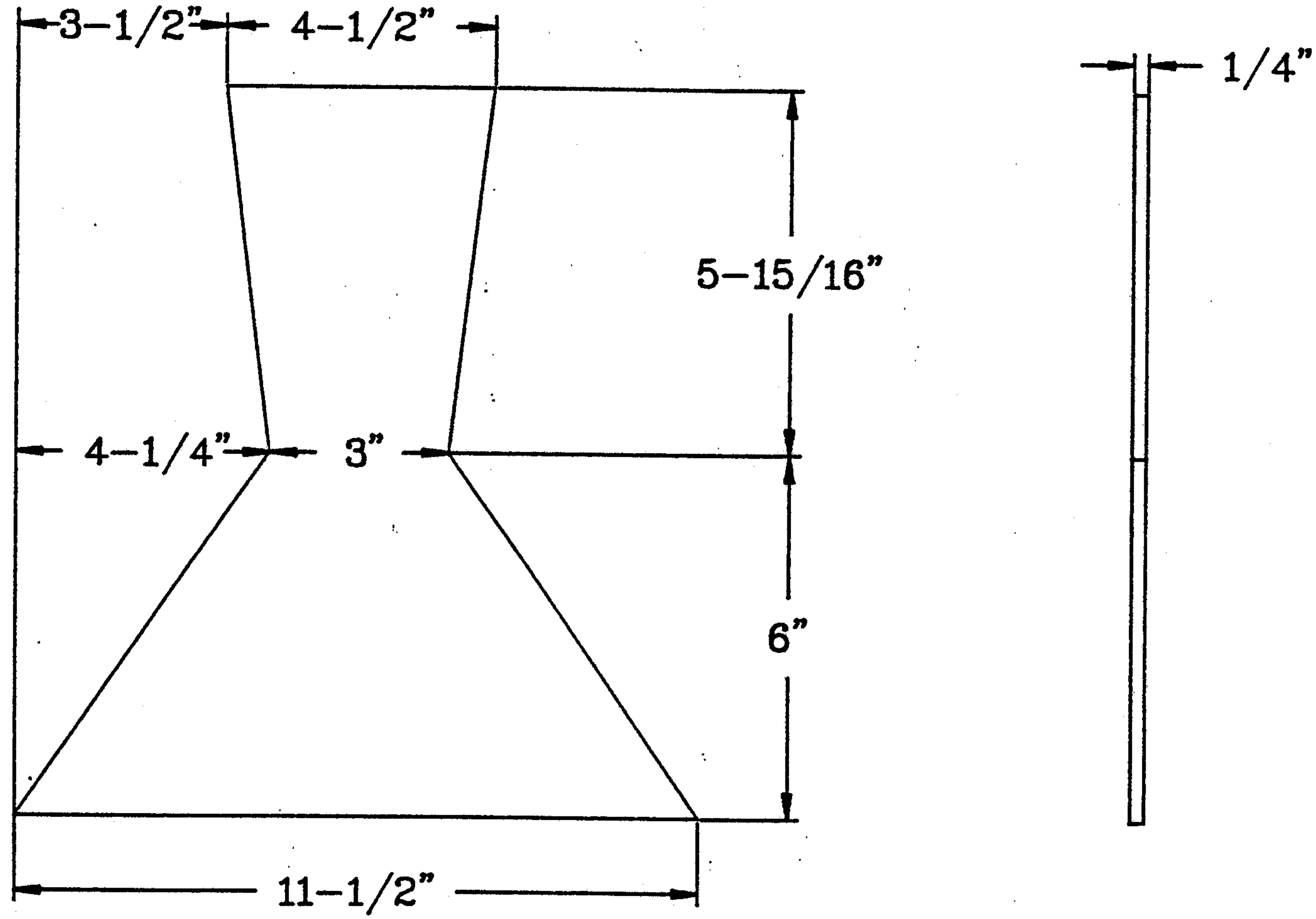

PLATE 5

9/20

FIGURE E-1. GUARDRAIL EXTRUDER TERMINAL CONSTRUCTION DRAWINGS. (CONTINUED)

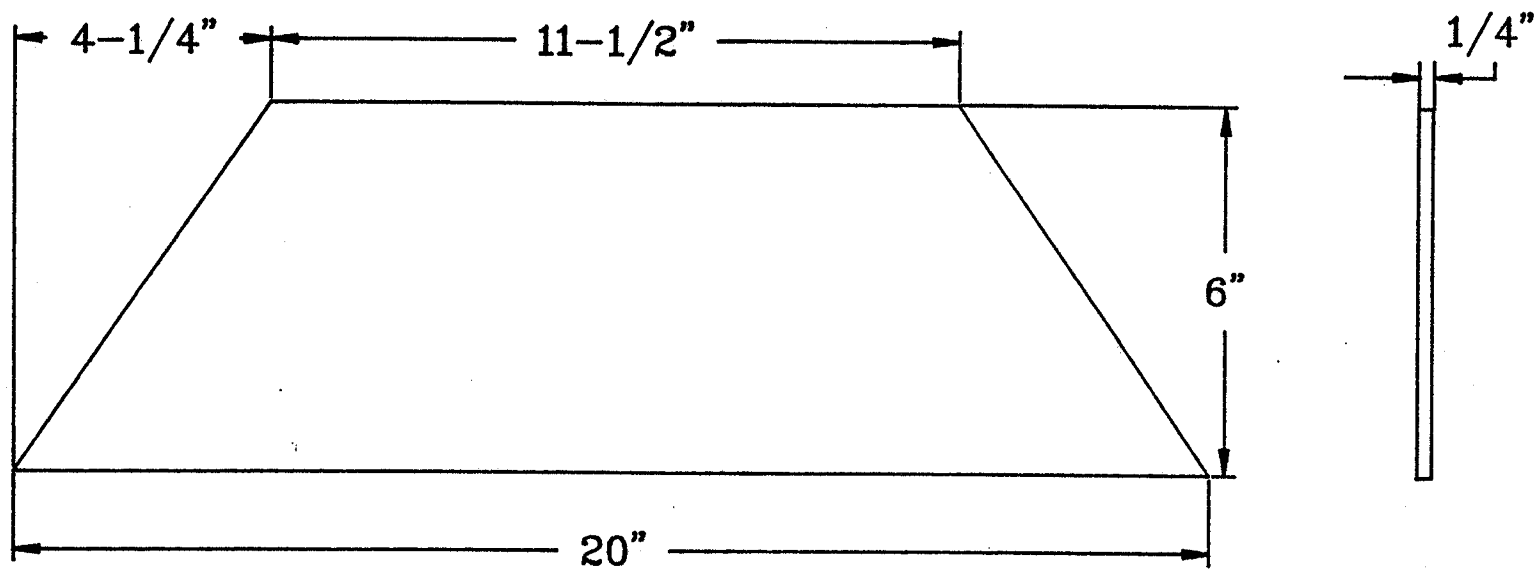

PLATE 6

FIGURE E-1. GUARDRAIL EXTRUDER TERMINAL CONSTRUCTION DRAWINGS. (CONTINUED)

10/20

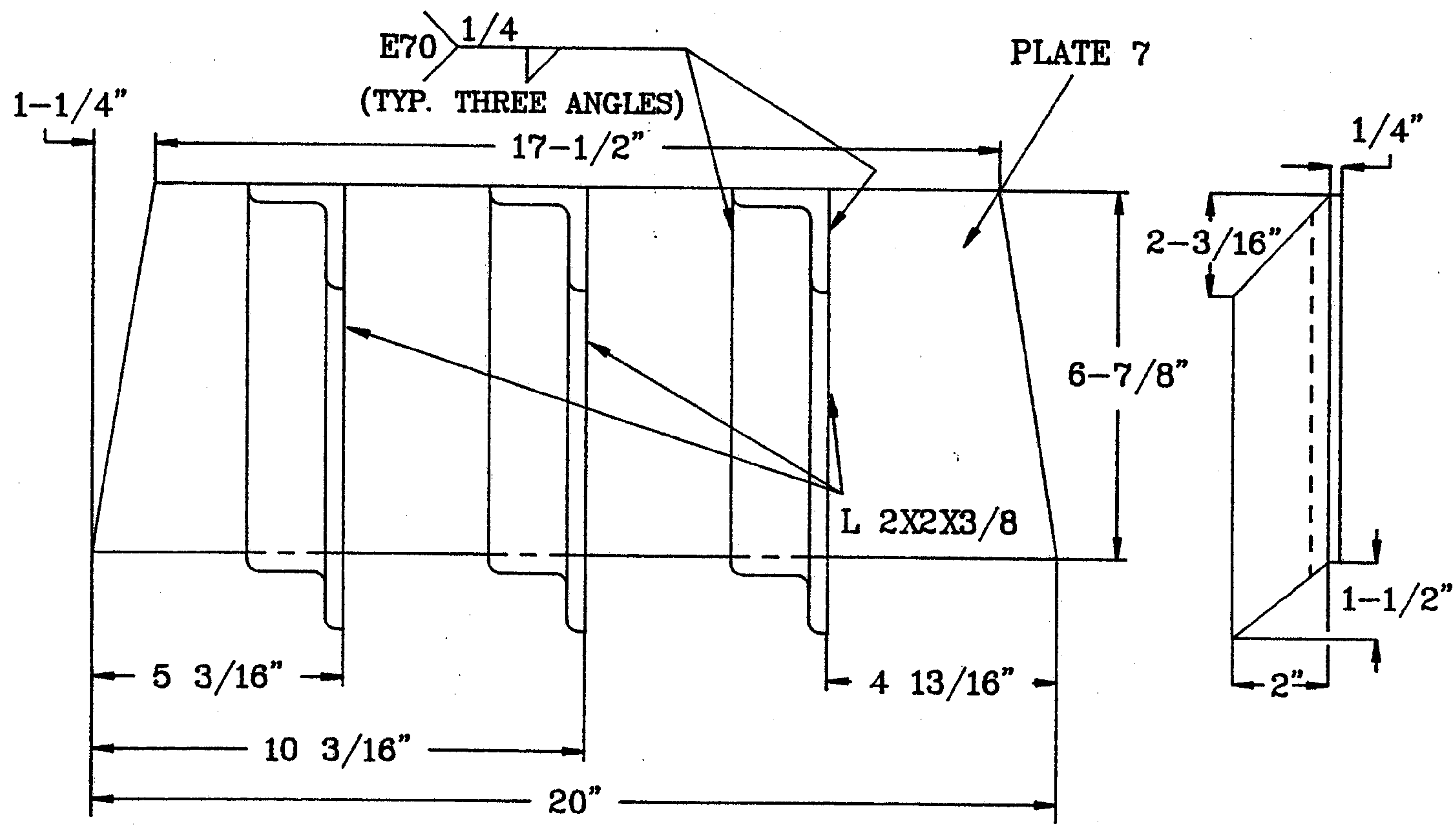

PLATE 7

11/20

FIGURE E-1. GUARDRAIL EXTRUDER TERMINAL CONSTRUCTION DRAWINGS. (CONTINUED)

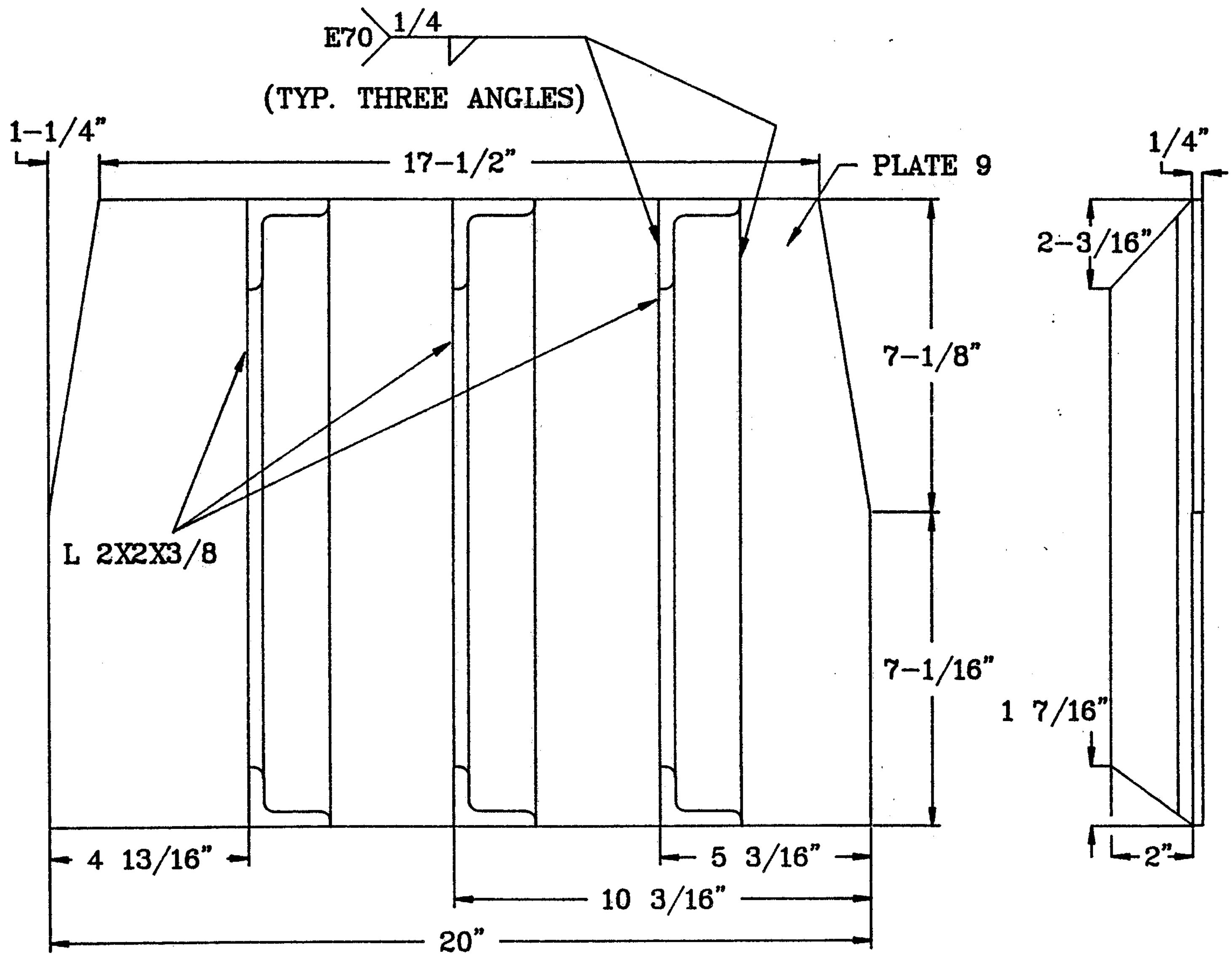

12/20

PLATE 9

FIGURE E-1. GUARDRAIL EXTRUDER TERMINAL CONSTRUCTION DRAWINGS. (CONTINUED)

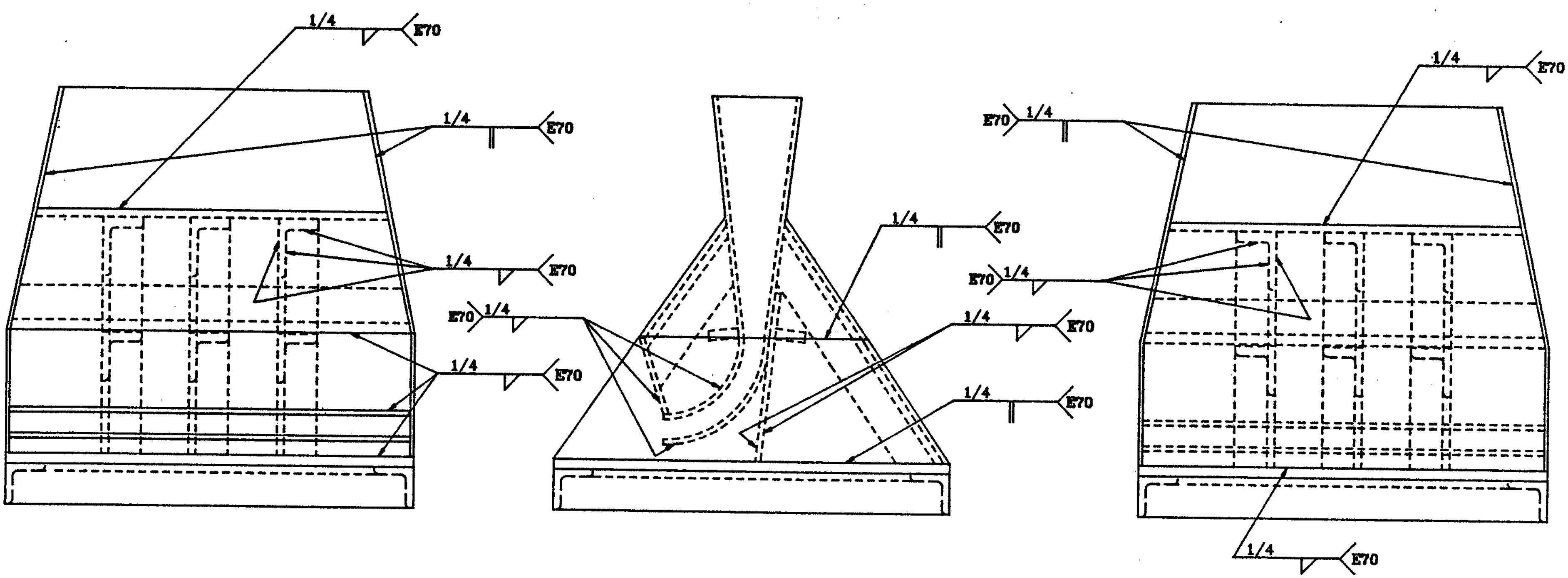

EXTRUDER
WELD DETAILS

13/20

FIGURE E-1. GUARDRAIL EXTRUDER TERMINAL CONSTRUCTION DRAWINGS. (CONTINUED)

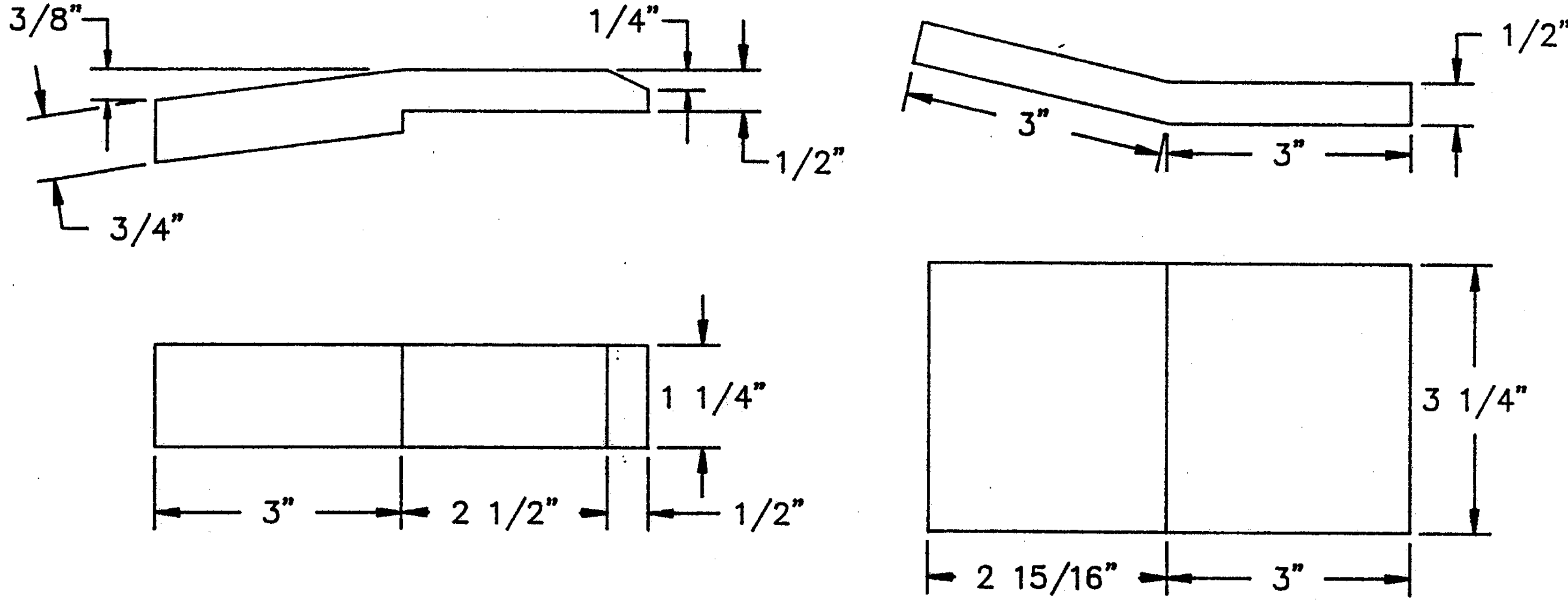

CONNECTING CLIPS

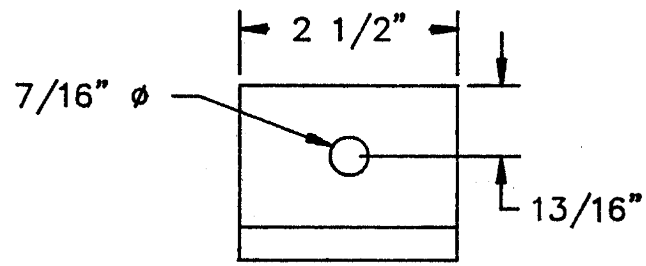

CONNECTING ANGLE
L 2X2X3/8

DETAIL 'C-3'

14/20

FIGURE E-1. GUARDRAIL EXTRUDER TERMINAL CONSTRUCTION DRAWINGS. (CONTINUED)

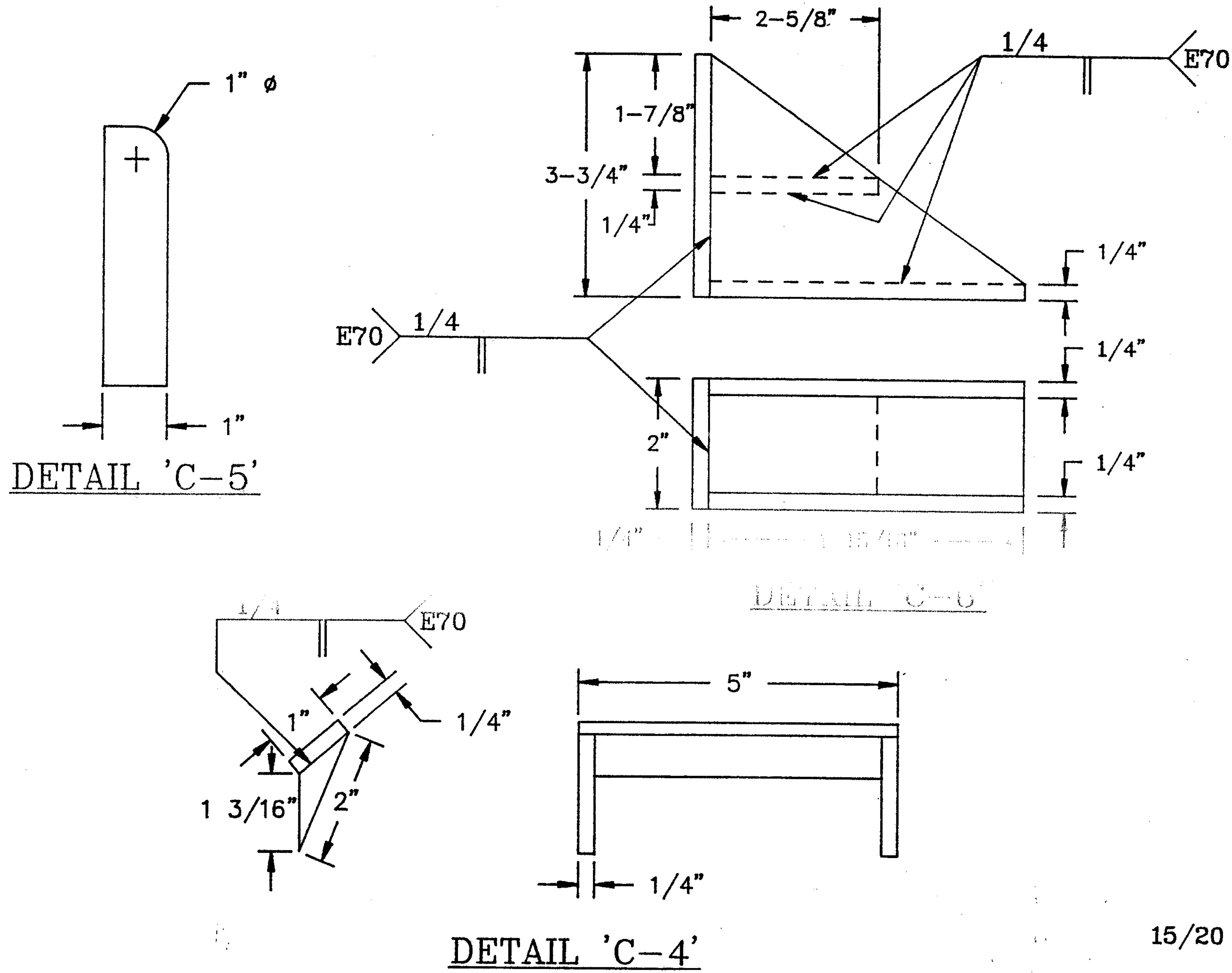

FIGURE E-1. GUARDRAIL EXTRUDER TERMINAL CONSTRUCTION

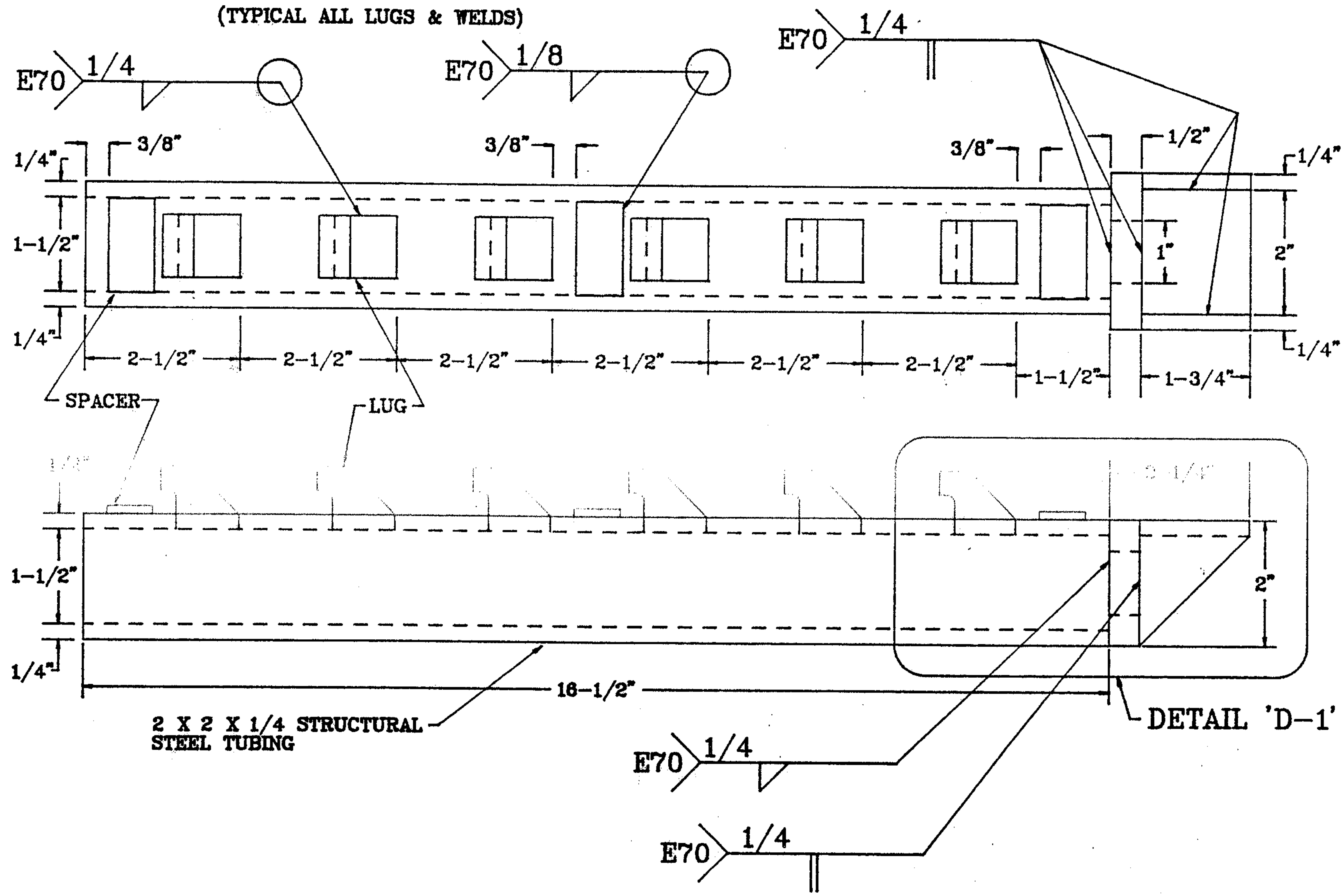

MODIFIED CABLE ANCHOR DETAIL 'D'

16/20

FIGURE E-1. GUARDRAIL EXTRUDER TERMINAL CONSTRUCTION

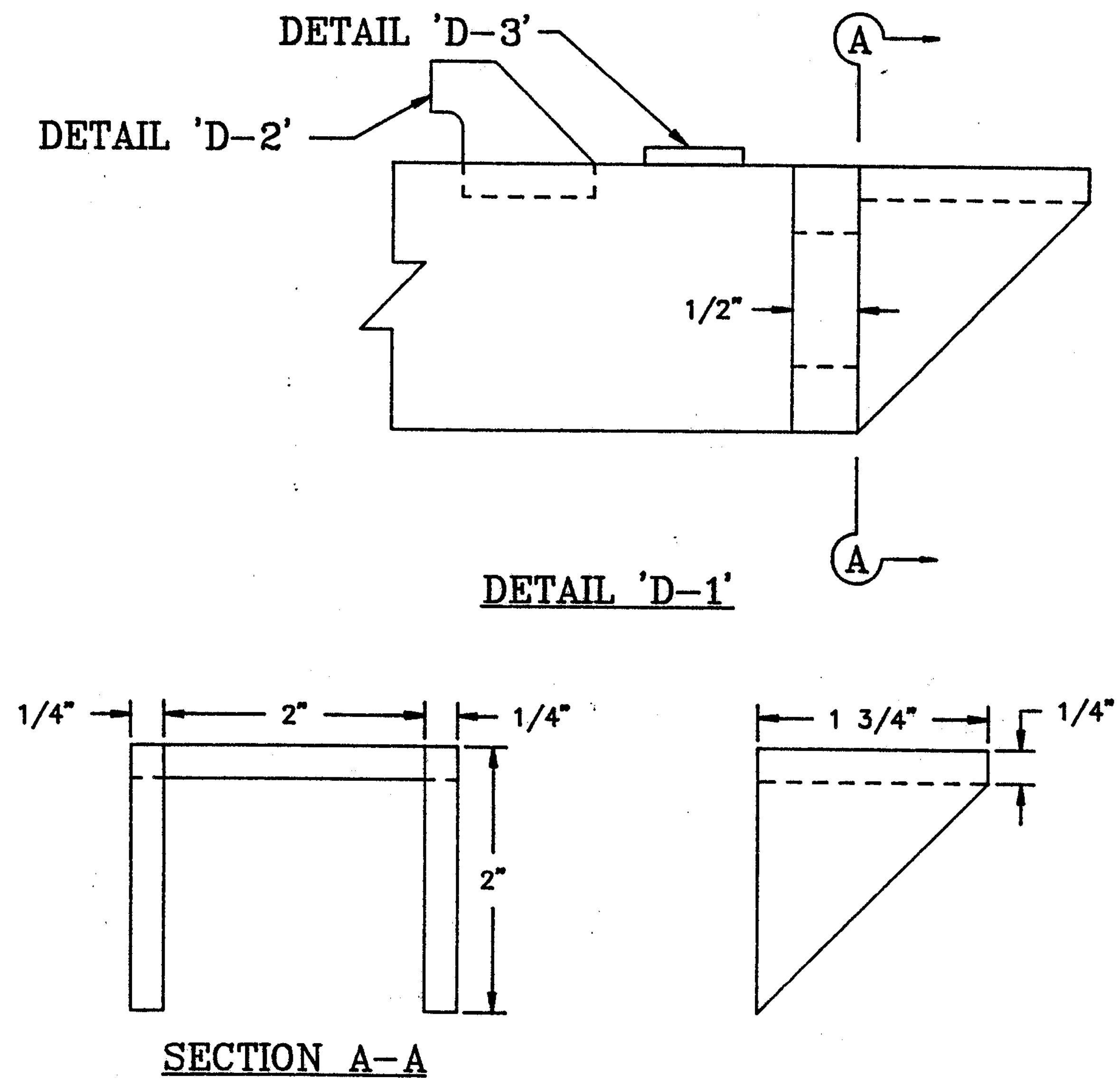

MODIFIED CABLE ANCHOR

17/20

FIGURE E-1. GUARDRAIL EXTRUDER TERMINAL CONSTRUCTION DRAWINGS. (CONTINUED)

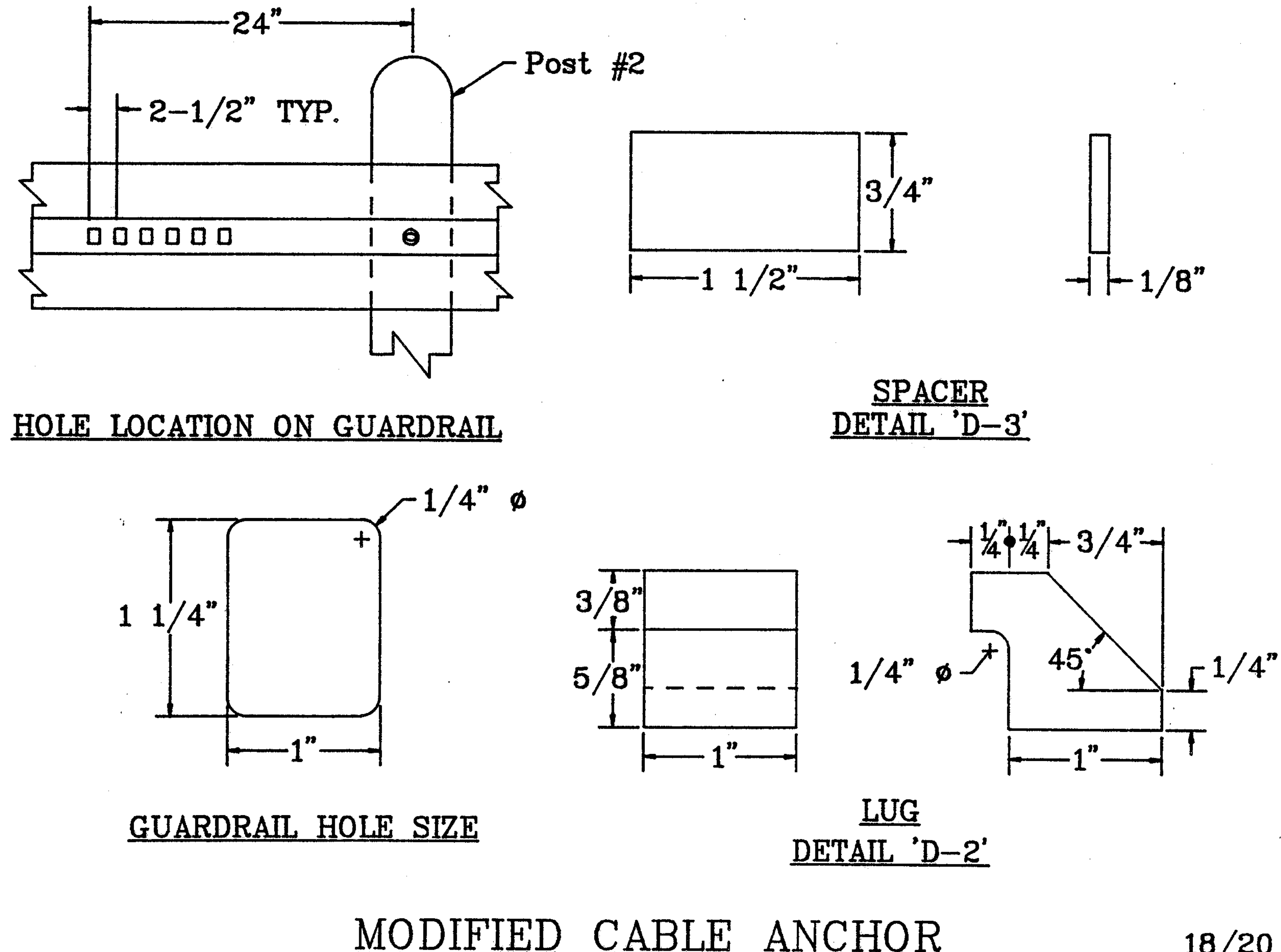

FIGURE E-1. GUARDRAIL EXTRUDER TERMINAL CONSTRUCTION DRAWINGS. (CONTINUED)

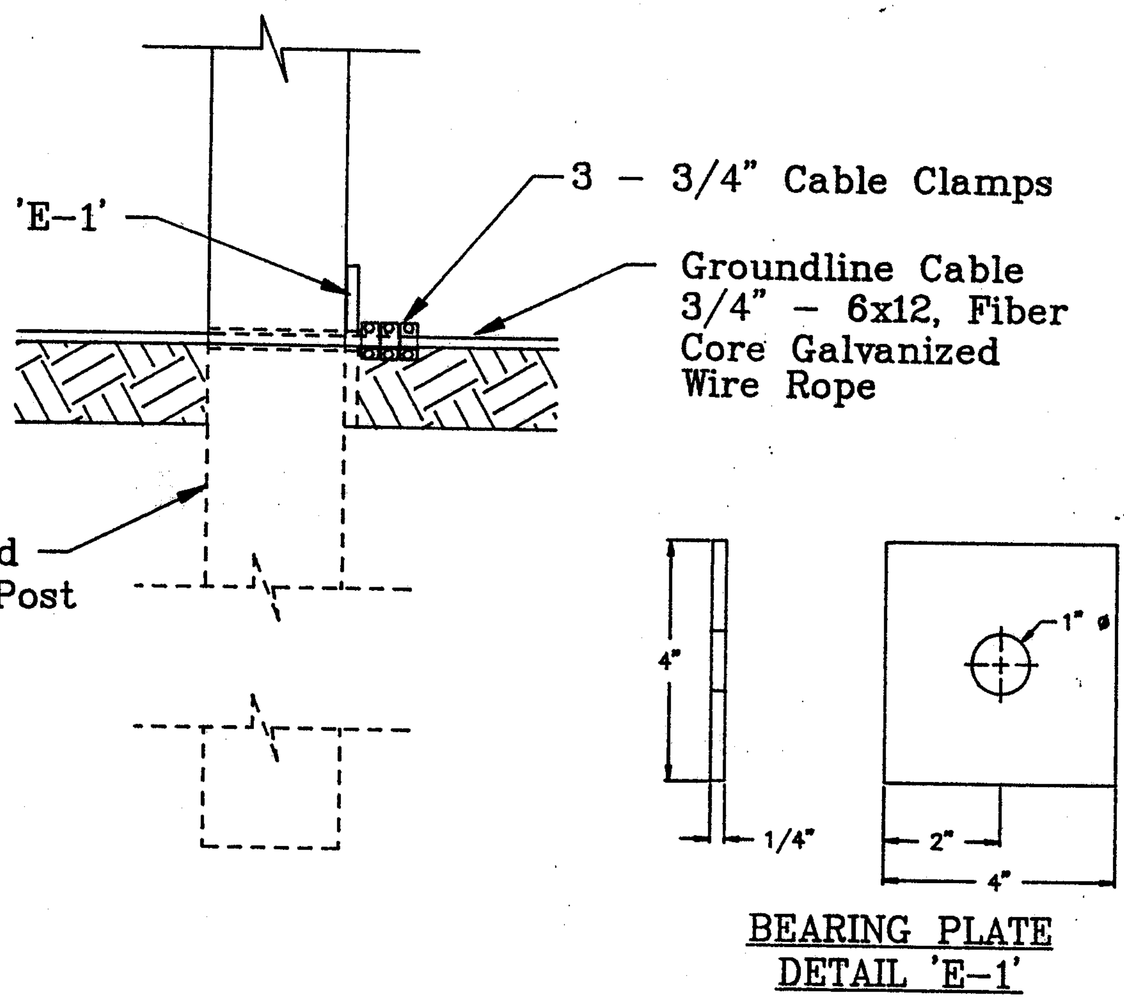

DETAIL 'E'

FIGURE E-1. GUARDRAIL EXTRUDER TERMINAL CONSTRUCTION DRAWINGS. (CONTINUED)

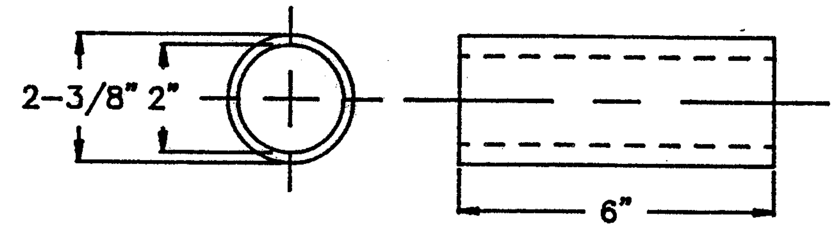

DETAIL 'F-1'

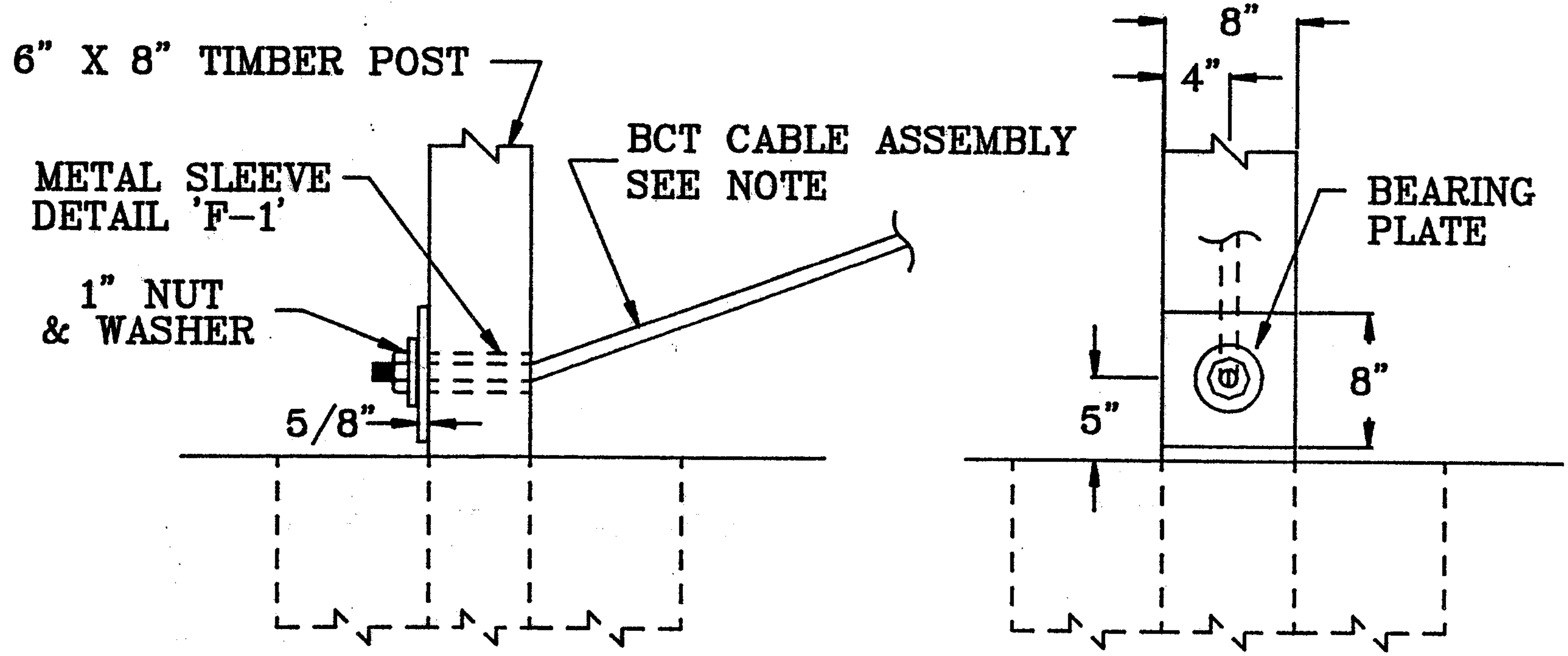

DETAIL 'F'

NOTE: Cable assembly F-37-76 as shown in ARTBA Technical Bulletin No. 268-B

20/20

FIGURE E-1. GUARDRAIL EXTRUDER TERMINAL CONSTRUCTION DRAWINGS (CONTINUED)

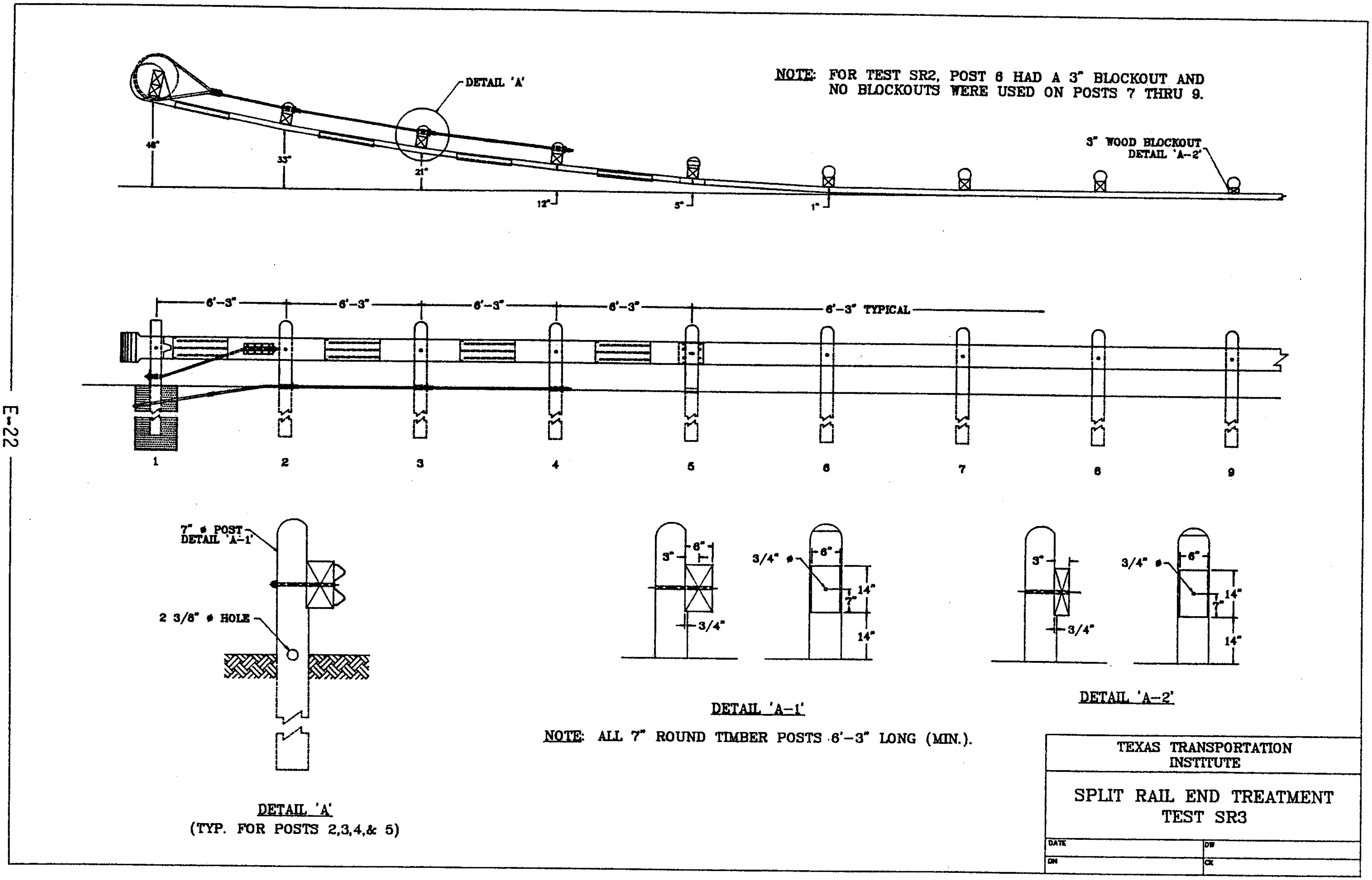

FIGURE E-2. INITIAL SPLIT RAIL END TREATMENT DESIGN

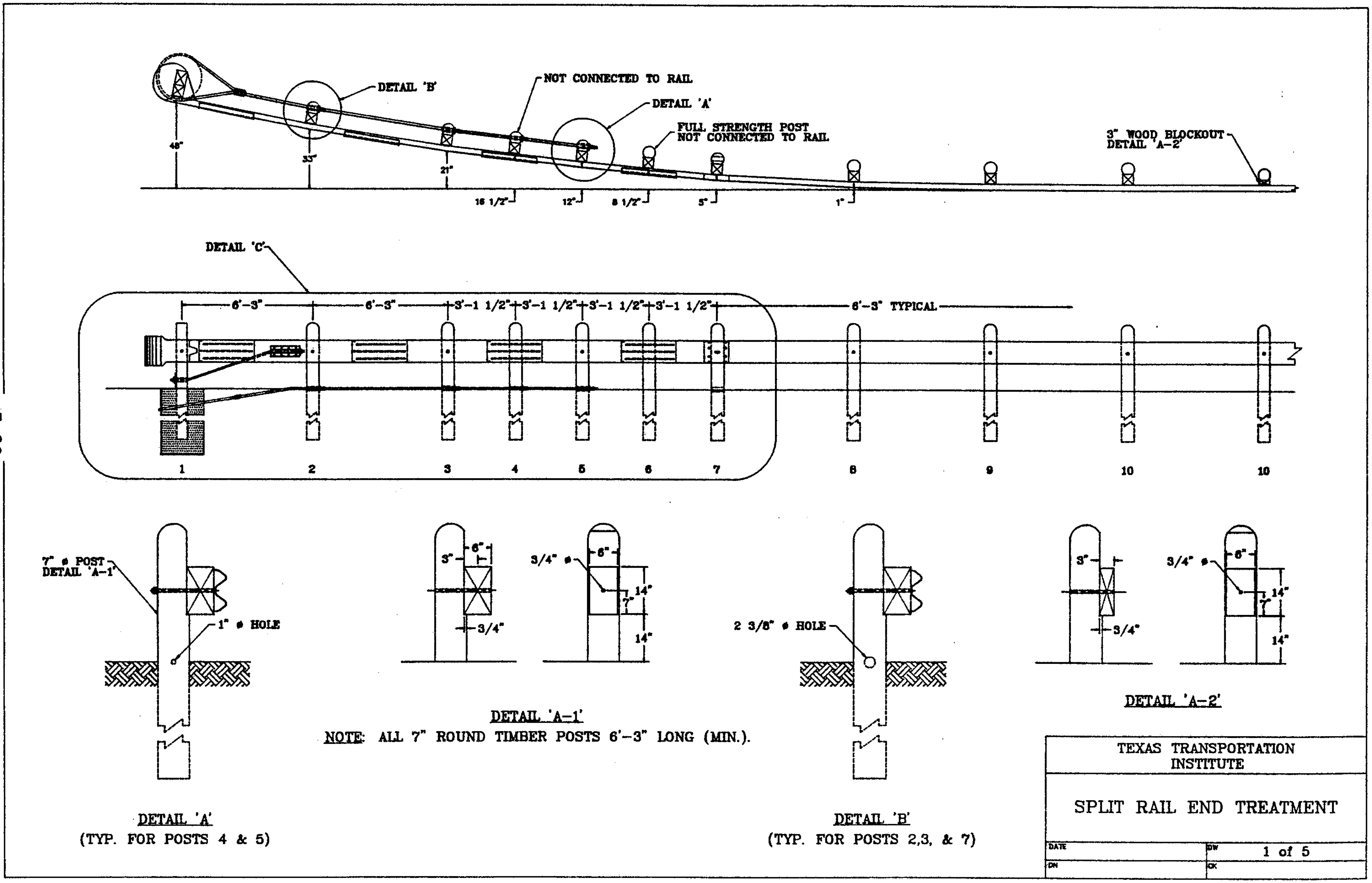

FIGURE E-3. FINAL SPLIT RAIL END TREATMENT DESIGN

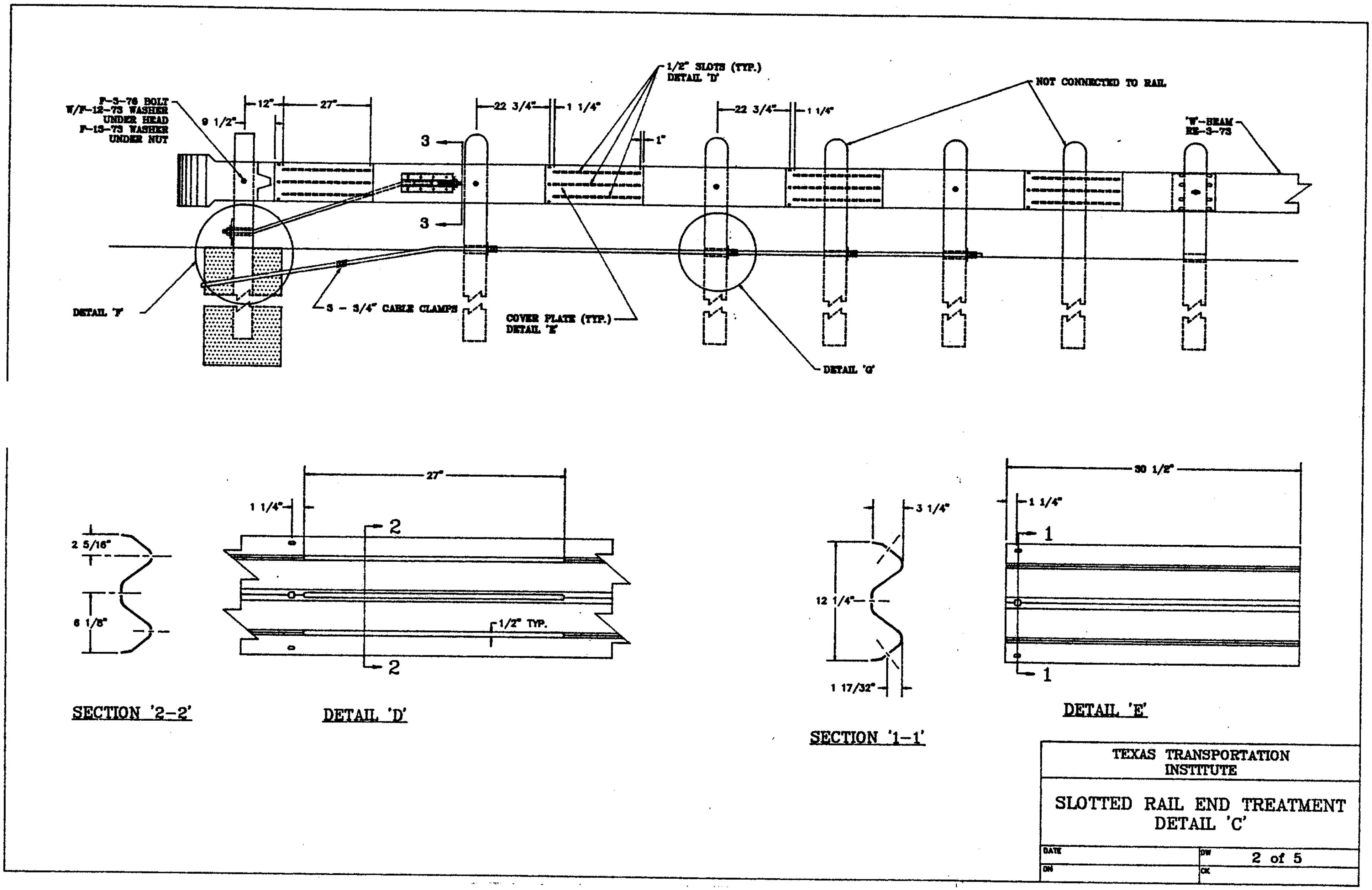

FIGURE E-3. FINAL SPLIT RAIL END TREATMENT DESIGN. (CONTINUED)

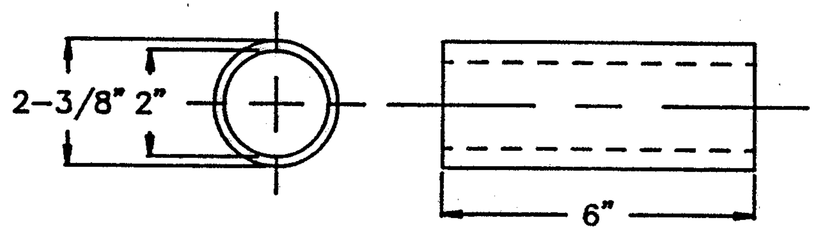

DETAIL 'F-1'

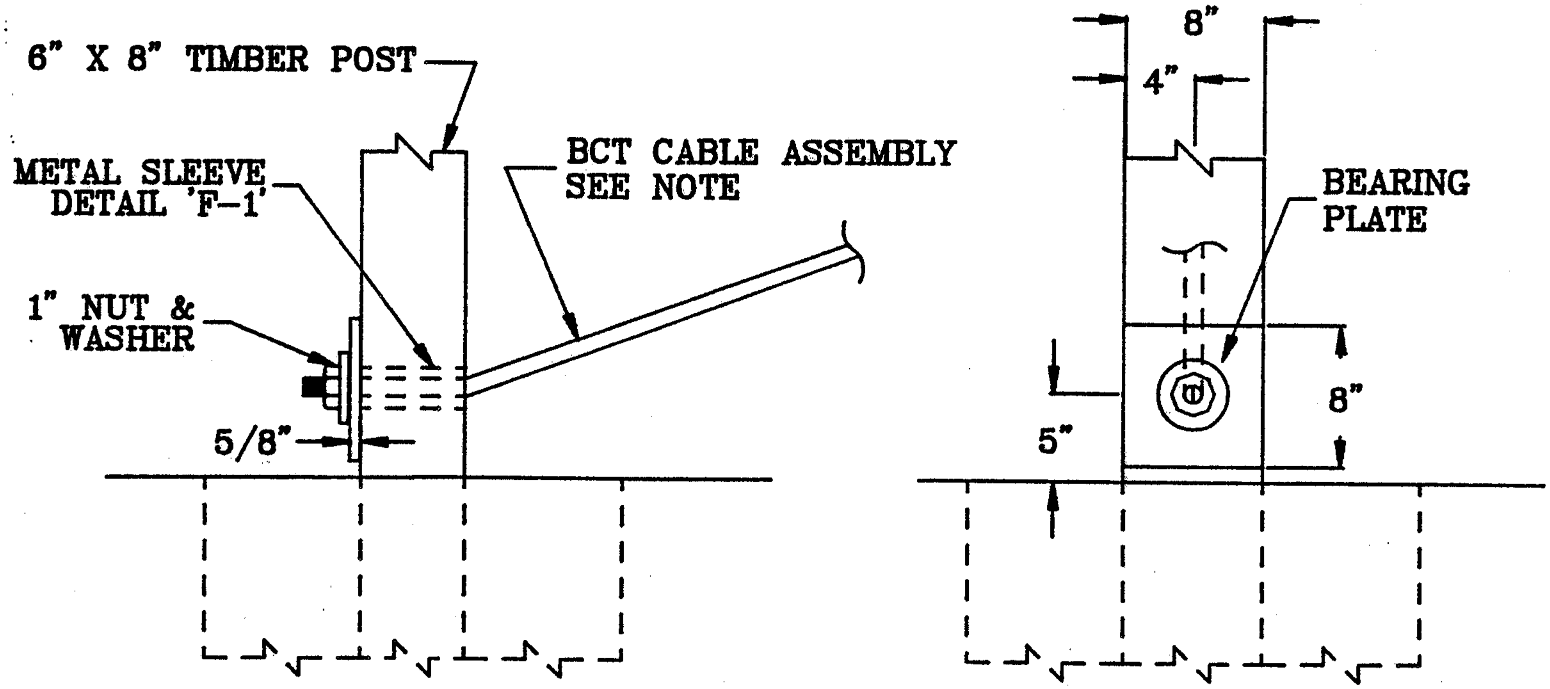

DETAIL 'F'

NOTE: Cable assembly F-37-76 as shown in ARTBA Technical Bulletin No. 268-B

FIGURE E-3. FINAL SPLIT RAIL END TREATMENT DESIGN. (CONTINUED)

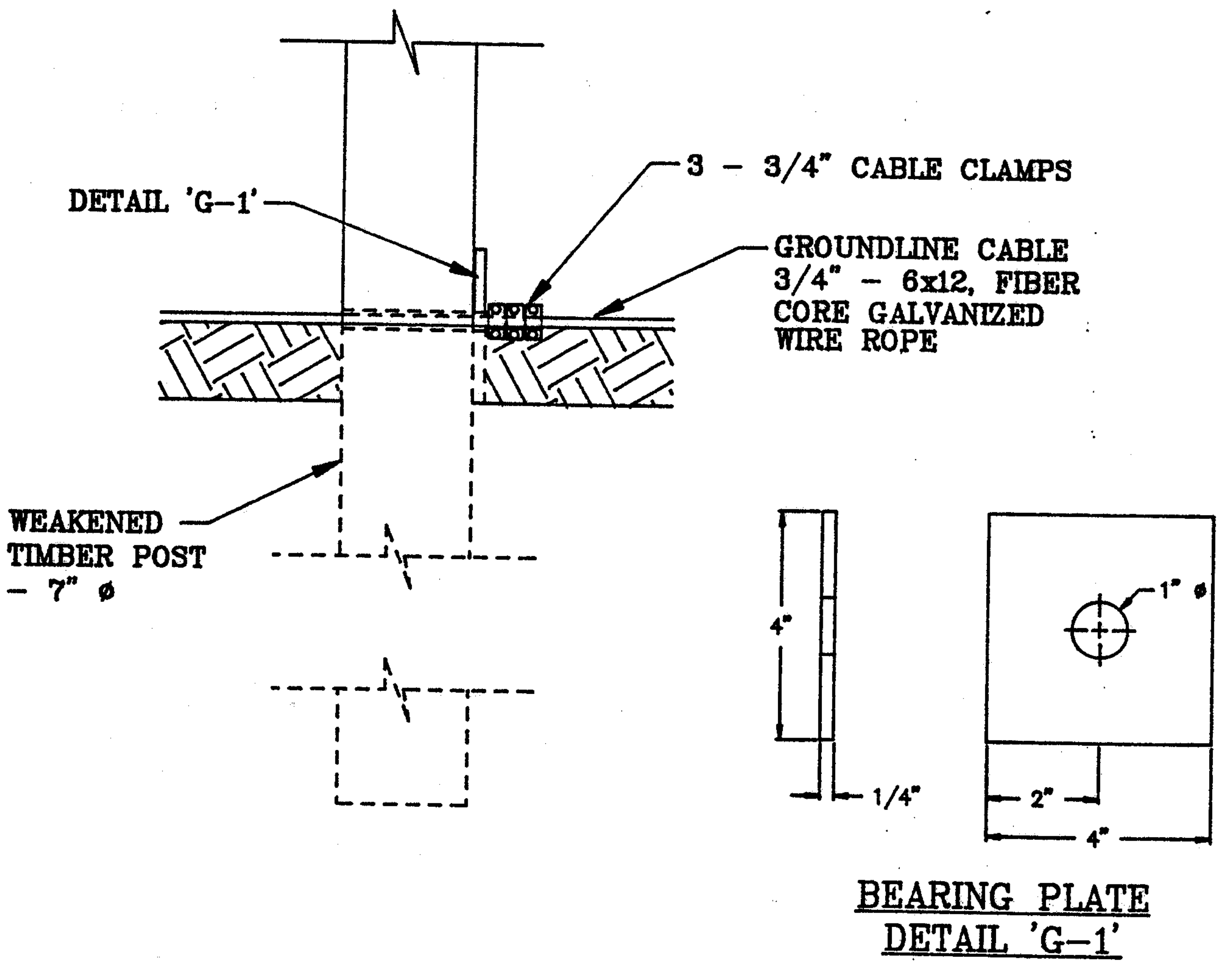

DETAIL 'G'

FIGURE E-3. FINAL SPLIT RAIL END TREATMENT DESIGN. (CONTINUED)

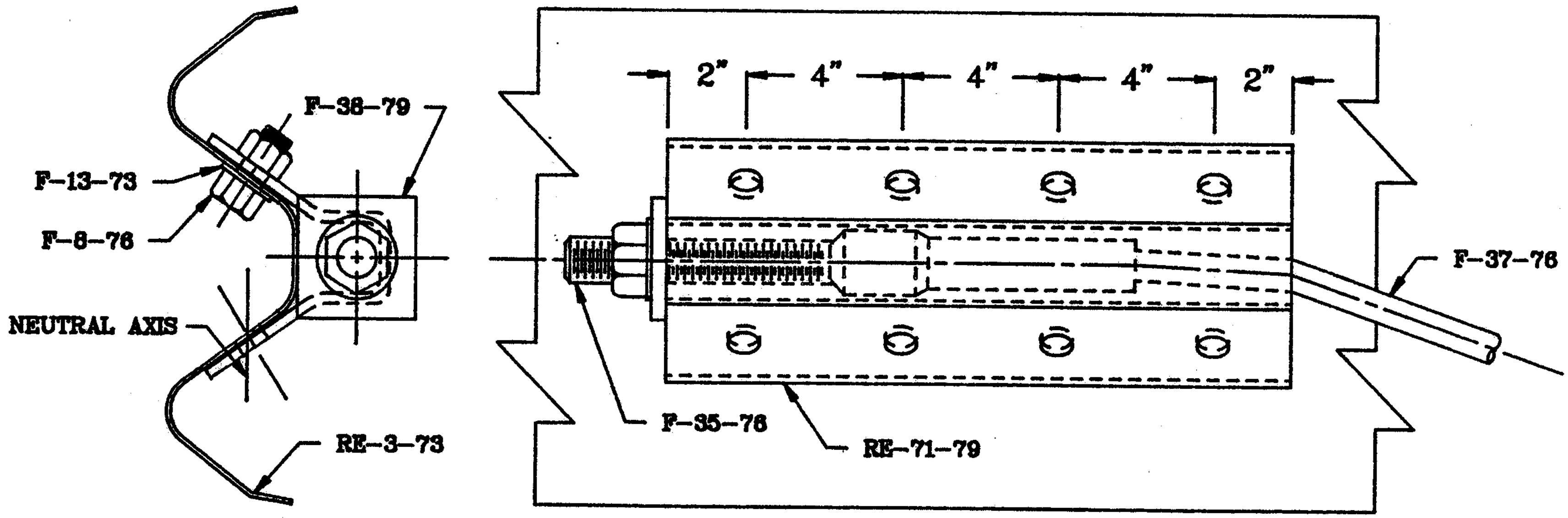

SECTION '3-3'

NOTE: The standard parts referenced to above are shown in ARTBA Technical Bulletin No. 268-B.

FIGURE E-3. FINAL SPLIT RAIL END TREATMENT DESIGN. (CONTINUED)